

**The Heart of the Rugby Football League Athlete: An
Aid to Pre-Participation Cardiac Screening**

Lynsey Claire Forsythe

**A thesis submitted in partial fulfilment of the requirements of Liverpool John
Moores University for the Degree of Doctor of Philosophy**

June 2018

Acknowledgements

I would like to express my sincere gratitude to my Director of Studies, Dr David Oxborough, for his continuous support, guidance, encouragement, time, friendship and sense of humour throughout the PhD process. His enthusiasm and expertise in echocardiography and sports cardiology research has been inspirational and as a fellow clinical cardiac physiologist it has been a privilege to work alongside him. I have learnt so much and could not have asked for a better mentor. Thank you.

Many thanks also go to my supervisor Professor Keith George whose knowledge and guidance has been invaluable. I am so grateful for the research opportunity and thank you for the continuous support, advice and encouragement.

I am indebted to both David and Keith and would not be in this position without them.

Also, thanks to my supervisor Dr Michael Papadakis for the support, constructive feedback and aiding my development as a researcher. Thanks to Professor John Somauroo for his help and support of my project and especially for his work as Consultant Cardiologist for the cardiac screening of all participants. Thanks to Dr David MacIver for an excellent collaboration on the first study of this thesis.

This PhD was matched-funded by LJMU and Cardiac Risk in the Young (CRY). Special thanks go to Dr Steven Cox and CRY for making this research project possible and supporting me throughout. My CRY experience has been fantastic allowing me the unique opportunity to undertake this doctorate whilst providing clinical support on the CRY screening programme. I have met many of the inspirational CRY families and supporters and have gained many new friends and colleagues. Acknowledgements must go to the entire CRY team.

Thanks to all of the participants who took part in this research project and to the rugby football league (RFL) sports medicine and science staff who helped with screening logistics. Thanks to the LJMU cardiac screening team for giving up their free time to support this project. The LJMU technicians must be thanked for endless support and helping with the organisation of equipment especially for mobile screening days.

Thanks also to all of my LJMU postgraduate colleagues and friends who have helped and supported in many ways. A special mention goes to Katie Hesketh for assistance with computer issues and for introducing me to the finer points of Powerpoint and Paint. Thanks to Kirsty Roberts, Ben Brown and Áine Brislane for the many hours of coffee and conversation.

Finally, I would like to thank my wonderful family for all their love and encouragement. This thesis is dedicated to my parents in recognition of their unwavering support throughout my academic and professional endeavours. I could not have done this without you. All my love as always.

Abstract

Pre-participation cardiac screening (PCS) of the athlete has recently become mandatory by many national and international sporting governing bodies and aims to identify those at risk of sudden cardiac death (SCD) from an undiagnosed cardiac condition. The term athletes' heart (AH) describes the physiological adaptation that occurs from chronic exposure to exercise training however, this process can mimic cardiac remodelling caused by pathological conditions such as cardiomyopathy. Transthoracic echocardiography (TTE) plays an integral role during PCS however, differentiation from inherited conditions is often based on a 'one size fits all' interpretation of echocardiographic derived measures. To improve the sensitivity and specificity of echocardiography in PCS it is pertinent to understand normal physiological cardiac adaptation in specific sporting disciplines. This thesis focuses on cardiac structure and function of the elite, male, rugby football league (RFL) athlete with the application of TTE including novel speckle tracking echocardiography (STE). The aims of this thesis were 1) to establish left ventricular (LV) structural and functional indices of the senior RFL athlete using TTE and STE and a mathematical model of the structural-functional relationship; 2) to determine structural and functional indices of the right heart of the senior RFL athlete using TTE and STE; 3) to provide a comparative and holistic, structural and functional assessment of the junior and senior RFL athletic heart using TTE and STE and 4) To assess variation in cardiac parameters across the competitive season in the senior RFL athlete using TTE and STE.

A comprehensive cardiac assessment of the elite RFL athlete was established throughout this thesis. The LV has a predominance for normal LV geometry

irrespective of age or seasonal time point. Mathematical modelling highlights the interaction of divergent effects of left ventricular cavity size (LVIDd) and mean wall thickness (MWT) on LV function to maintain a normal ejection fraction (EF). Significant regional variation in LV STE parameters was apparent including lower apical rotation and twist parameters in senior athletes compared to controls ($8.2 \pm 3.9^\circ$ vs. $11.2 \pm 4.6^\circ$ and 14 ± 4.7 vs $16.1 \pm 4.6^\circ$ respectively) suggesting potential adaptive mechanisms to training. The right ventricle (RV) and right atrium (RA) are larger in athletes compared to controls even after scaling (proximal right ventricular outflow dimension in parasternal long axis (RVOT_{plax}) (23 ± 3 vs. 20 ± 2 mm/(m²)^{0.5}), proximal right ventricular outflow dimension in parasternal short axis (RVOT₁) (24 ± 3 vs. 21 ± 3 mm/(m²)^{0.5}) and RA volume (RAvol) (22 ± 5 vs. 16 ± 4 ml/(m²)^{1.5})). The RVOT and RA are also larger in senior compared to junior athletes (RVOT_{plax} (23 ± 3 vs. 22 ± 3 mm/(m²)^{0.5}, RVOT₁ (24 ± 3 vs. 23 ± 3 mm/(m²)^{0.5} and RAvol (22 ± 5 vs. 21 ± 5 ml/(m²)^{1.5})) suggesting that the right heart is more sensitive to chronic training. Despite significant structural remodelling, RV function in the RFL athlete is normal as assessed by TTE (right ventricular fractional area change (RVFAC) > 33% and STE RV strain (ϵ) < -21%), irrespective of age and time of season. Significant seasonal functional changes were observed with STE as apical rotation (pre-season, $9.8 \pm 4^\circ$; mid-season, $6.1 \pm 2.8^\circ$; end-season, $5.8 \pm 3.2^\circ$ and post-season break, $6.6 \pm 3.1^\circ$) and twist (pre-season, $16.6 \pm 4.7^\circ$; mid-season, $12.6 \pm 4^\circ$; end-season $12.1 \pm 4.5^\circ$ and post-season break, $12.4 \pm 3.5^\circ$) are higher at pre-season than at any other time-point, highlighting physiological variation during the RFL season.

The use of standard and novel echocardiographic techniques have provided further understanding of the normal physiological adaptation of the AH in RFL athletes which may lead to improvements in PCS of this athlete group.

Table of Contents

	Page
Acknowledgements	ii
Abstract	iii
Table of Contents	v
List of Tables	viii
List of Figures	ix
Preface	xi
Abbreviations	xii
Chapter 1 - General Introduction	1
1.1 - Background	2
1.2 - Overarching Aim	3
1.3 - Structure of Thesis	4
Chapter 2 - Literature Review	6
2.1 - Sudden Cardiac Death and Related Conditions	7
2.2 - Pre-Participation Cardiac Screening	10
2.2.1 - The Role of Echocardiography in PCS	11
2.2.2 - The Grey Area between Physiology and Pathology - The Diagnostic Dilemma	13
2.3 - Cardiac Mechanics and Speckle Tracking Echocardiography	16
2.3.1 - Myocardial Architecture	16
2.3.2 - Speckle Tracking Echocardiography	17
2.3.3 - The Rationale for Speckle Tracking Echocardiography	22
2.4 - Exercise Induced Cardiac Remodelling	23
2.5 - The Athletic Heart Phenotype	26
2.5.1 - Conventional Echocardiography and the Left Ventricle	26
2.5.2 - The Relationship between Left Ventricular Structure and Function	31
2.5.3 - Speckle Tracking Echocardiography and the Left Ventricle	32
2.5.4 - Conventional Echocardiography and the Right Ventricle	39
2.5.5 - Speckle Tracking Echocardiography and the Right Ventricle	42
2.5.6 - Conventional Echocardiography and the Atria	45
2.5.7 - Age Related Variation	46
2.5.8 - Seasonal Related Variation in the Athlete's Heart	48
2.6 - Conclusion	51
Chapter 3 - General Methods	54
3.1 - Preliminary information	55
3.1.1 - Ethics Approval	55
3.1.2 - Population	55
3.2 - Study Design and Procedures	57
3.2.1 - Anthropometry	57

3.2.2 - Blood Pressure	57
3.2.3 - Electrocardiography	57
3.2.4 - Echocardiography	57
3.3 - Conventional Echocardiography	58
3.3.1 - Two-Dimensional Left Ventricular Assessment	59
3.3.2 - Two-Dimensional Right Ventricular Assessment	63
3.3.3 - Two-Dimensional Left Atrial Assessment	67
3.3.4 - Two-Dimensional Right Atrial Assessment	69
3.4 - M-Mode	70
3.5 - Doppler	71
3.6 - Tissue Doppler Imaging	72
3.7 - Speckle Tracking Echocardiography	73
3.7.1 - Left Ventricular Longitudinal Mechanics	74
3.7.2 - Left Ventricular Circumferential and Radial Mechanics	78
3.7.3 - Left Ventricular Twist Mechanics	83
3.7.4 - Right Ventricular Longitudinal Mechanics	85
3.8 - Scaling to Body Size	86
3.9 - Data Management	86
Chapter 4 - The Relationship between Left Ventricular Structure and Function in the Elite Rugby Football League Athlete as determined by Conventional Echocardiography and Myocardial Strain Imaging	87
4.1 - Introduction	88
4.2 - Methods	89
4.2.1 - Study Population and Design	89
4.2.2 - Procedures	90
4.2.3 - Mathematical Model	90
4.2.4 - Statistical Analysis	91
4.3 - Results	92
4.4 - Discussion	111
4.5 - Limitations	114
4.6 - Conclusion	115
Chapter 5 - The Right Heart of the Elite Senior Rugby Football League Athlete	116
5.1 - Introduction	117
5.2 - Methods	118
5.2.1 - Study Population and Design	118
5.2.2 - Procedures	119
5.2.3 - Statistical Analysis	119
5.3 - Results	120
5.3.1 - Right Ventricular Structure and Function	120
5.3.2 - Right Atrial Structure and Functional Volumes	127
5.4 - Discussion	128
5.4.1 - Right Ventricular Structure	129
5.4.2 - Right Ventricular Function	130
5.4.3 - Right Atrial Structure and Function	132
5.5 - Limitations	132
5.6 - Conclusion	133
Chapter 6 - The Athletic Heart Phenotype of the Rugby Football League Athlete: A Comparative Study of Senior and Junior Athlete	134

6.1 - Introduction	135
6.2 - Methods	136
6.2.1 - Study Population and Design	136
6.2.2 - Procedures	137
6.2.3 - Statistical analysis	137
6.3 - Results	138
6.3.1 - Left Ventricle	138
6.3.2 - Right Ventricle	155
6.3.3 - Left Atrium	160
6.3.4 - Right Atrium	161
6.4 Discussion	162
6.4.1 - Left Heart	162
6.4.2 - Right Heart	165
6.4.3 - Implications	167
6.5 - Limitations	167
6.6 - Conclusion	167
Chapter 7 - Cardiac Structure and Function in the Elite Senior Rugby League Athlete during the Competitive Season	169
7.1 - Introduction	170
7.2 - Methods	171
7.2.1 - Study Population and Design	171
7.2.2 - Procedures	173
7.2.3 - Statistical Analysis and Standardisation of STE Data	173
7.3 - Results	174
7.3.1 - Left Ventricle	175
7.3.2 - Right Ventricle and atria	187
7.4 - Discussion	192
7.4.1 - Cardiac Structure	193
7.4.2 - Cardiac Function	194
7.5 - Limitations	198
7.6 - Conclusion	198
Chapter 8 - General Discussion	200
8.1 - Aims of thesis	201
8.2 - Brief Summary of Findings	201
8.3 - Overarching Issues and Implications for PCS	203
8.3.1 - The Structural-Functional Relationship	203
8.3.2 - The Impact of Athlete Age	207
8.3.3 - The Impact of Seasonal Variation	208
8.4 - Future Research	209
8.5 - Conclusions	210
References	211
Appendix 1 - Ethics Approval Letters	233
Appendix 2 - Participant PCS documentation	236

List of Tables

	Page
2.1 - Relevant LV STE athlete studies from the literature	37
2.2 - Relevant RV STE athlete studies from the literature	44
4.1 - Echocardiographic parameters of the left ventricle	95
4.2 - Global Left ventricular ϵ , SR and Twist	97
4.3 - Bivariate Correlation	99
4.4 - Regional Longitudinal ϵ and SR	105
4.5 - Regional Circumferential ϵ and SR	107
4.6 - Regional radial ϵ and SR	108
5.1 - Demographics	120
5.2 - Echocardiographic parameters of the right ventricle	122
5.3 - Global and regional right ventricular ϵ and SR	125
5.4 - Right ventricular bivariate correlation	127
5.5 - Echocardiographic parameters of the right atrium	128
6.1 - LV structure and function	139
6.2 - Global LV ϵ , SR and twist	142
6.3 - STE parameters and LV correlations	144
6.4 - Regional Longitudinal ϵ and SR	150
6.5 - Regional Circumferential ϵ and SR	152
6.6 - Regional Radial ϵ and SR	154
6.7 - RV structure and function	156
6.8 - Global and regional RV longitudinal ϵ and SR	158
6.9 - STE parameters and RV correlations	159
6.10 - Left atrial parameters	160
6.11 - Right atrial parameters	161
7.1 - Demographics	175
7.2 - Seasonal echocardiographic parameters of the left ventricle	176
7.3 - Global Left ventricular ϵ , SR and Twist	178
7.4 - Regional Longitudinal ϵ and SR	182
7.5 - Regional Circumferential ϵ and SR	184
7.6 - Regional Radial ϵ and SR	186
7.7 - Echocardiographic parameters of the Right ventricle	188
7.8 - Global and Regional RV ϵ and SR	189
7.9 - RV Longitudinal Regional Strain and strain Rate	190
7.10 - Echocardiographic parameters of the Left atrium	191
7.11 - Echocardiographic parameters of the Right atrium	192

List of Figures

	Page
2.1 - Strain Schematic	19
2.2 - Representation of the principal LV myocardial deformations	21
2.3 - Classification of sports	25
2.4 - Summary of ventricular remodelling during sustained exercise training	27
2.5 - Left ventricular geometry according to relative wall thickness and left ventricular mass	28
3.1 - Parasternal long axis view demonstrating LVIDd	59
3.2 - Parasternal long axis view demonstrating LVIDs	60
3.3 - Biplane LV volume and Ejection Fraction. a, 4 chamber LVEDV; b, 4 chamber LVESV; c, 2 chamber LVEDV; d, 2 chamber LVESV.	61
3.4 - Parasternal short axis view demonstrating basal LV wall thickness. a, antero-septum; b, lateral; c, posterior; d, infero-septum.	62
3.5 - Parasternal short axis view demonstrating mid LV wall thickness. a, antero-septum; b, lateral; c, posterior; d, infero-septum.	62
3.6 - Parasternal long axis view demonstrating RVOTplax	63
3.7 - Parasternal short axis view demonstrating RVOT1	64
3.8 - Parasternal short axis view demonstrating RVOT2	64
3.9 - Apical 4 Chamber view demonstrating RVD1, RVD2 and RVD3	65
3.10 - Subcostal view demonstrating RVFW	65
3.11 - Apical 4 Chamber view demonstrating RV and LV dimensions for RV:LV ratio	66
3.12 - Right ventricular diastolic and systolic area	66
3.13 - Parasternal long axis view demonstrating LA diameter	67
3.14 - Biplane LAvoles; a, Apical 4 chamber and b, Apical 2 chamber	68
3.15 - Biplane LApreA; a, Apical 4 chamber and b, Apical 2 chamber	68
3.16 - Biplane LAvoled; a, Apical 4 chamber and b, Apical 2 chamber	68
3.17 - Apical 4 chamber view demonstrating right atrial area	69
3.18 - Apical 4 chamber view demonstrating RA volume. a, RAvoles; b, RAvolpreA; c, RAvoled	70
3.19 - M-Mode - TAPSE	71
3.20 - Mitral inflow pulsed wave Doppler	72
3.21 - Pulsed Wave TDI. a, infero-septal S', E' and A'; b, lateral S', E' and A'	73
3.22 - Pulsed Wave RV TDI - RV S', RV E' RV A'	73
3.23 - Apical 4 chamber longitudinal STE. a, Longitudinal ϵ curves; b, Longitudinal SR curves	75
3.24 - Apical 2 chamber longitudinal STE. a, Longitudinal ϵ curves; b, Longitudinal SR curves	76
3.25 - Apical long axis longitudinal STE. a, Longitudinal ϵ curves; b, Longitudinal SR curves.	77
3.26 - Longitudinal ϵ and SR model - 18 regional regions	78
3.27 - Basal circumferential STE. a, circumferential ϵ curves; b, circumferential SR curves.	79
3.28 - Mid circumferential STE. a, radial ϵ curves; b, radial SR curves	80
3.29 - Basal radial STE. a, radial ϵ curves; b, radial SR curves	81
3.30 - Mid radial STE. a, radial ϵ curves; b, radial SR curves	82

3.31 - Circumferential and Radial ϵ and SR model -12 myocardial regions	83
3.32 - Apical rotation curves.	84
3.33 - Peak apical and basal rotation and twist.	84
3.34 - RV Longitudinal STE; a, RV longitudinal ϵ curves; b, RV SR curves.	85
4.1 - Left ventricular geometry in RFL athletes and controls according to LV mass index and RWT as described by Lang et al. (2015).	93
4.2a - Regional longitudinal, circumferential and radial ϵ in athletes and controls	101
4.2b - Regional longitudinal, circumferential and radial SRS in athletes and controls	102
4.2c - Regional longitudinal, circumferential and radial SRE in athletes and controls	103
4.2d - Regional longitudinal, circumferential and radial SRA in athletes and controls	104
4.3 - Mathematical modelling of left ventricular contraction	110
5.1 - Percentage of athletes and controls meeting minor and major criteria for ARVC according to Marcus <i>et al.</i> (2010).	124
6.1 - LV geometry in SA and JA (as described by Lang <i>et al.</i> , 2015)	141
6.2a - Regional longitudinal, circumferential and radial ϵ in senior and junior athletes	146
6.2b - Regional longitudinal, circumferential and radial SRS in senior and junior athletes	147
6.2c - Regional longitudinal, circumferential and radial SRE in senior and junior athletes	148
6.2d - Regional longitudinal, circumferential and radial SRA in senior and junior athletes	149
7.1 - Cardiac rotation and twist during the RFL season	180
8.1 - Twist in the RFL athlete and response to training stimulus	209

Preface

Chapter 4 has resulted in a jointly authored peer reviewed publication;

Forsythe, L., MacIver, D. H., Johnson, C., George, K., Somauroo, J., Papadakis, M., Brown, B., Qasem, M. and Oxborough, D. 2018. The relationship between left ventricular structure and function in the elite rugby football league athlete as determined by conventional echocardiography and myocardial strain imaging. *International Journal of Cardiology*, 261, 211–217.

Selected parts of the literature review have contributed to another jointly authored peer reviewed publication (in review).

Forsythe, L., George, K. and Oxborough D. 2018. Speckle Tracking Echocardiography for the Assessment of Athletes' Heart: Is it Ready for Daily Practice? *Current Treatment Options in Cardiovascular Medicine*, In review.

The data from this thesis has also contributed to other jointly authored peer reviewed publications (one in review).

Johnson, C., Forsythe, L., Somauroo, J., Papadakis, M., George, K. and Oxborough, D. 2018. Cardiac structure and function in elite Native Hawaiian and Pacific Islander Rugby Football League athletes: an exploratory study. *International Journal of Cardiovascular Imaging*, 34, 725-534.

Oates, S., George, K., Forsythe, L., Somauroo, J., Papadakis, M. and Oxborough, D. 2018. Scaling to produce size independent indices of echocardiographic derived aortic root dimensions in elite Rugby Football League players. *International Journal of Cardiology*, In review.

Abbreviations

A = Peak Late Mitral Diastolic Velocity

A' = Peak Late Diastolic Myocardial Velocity

ACC = American College of Cardiology

AH = Athletes' Heart

AHA = American Heart Association

ARVC = Arrhythmogenic Right Ventricular Cardiomyopathy

ASE = American Society of Echocardiography

AU = Arbitrary Unit

AVC = Aortic Valve Closure

BP = Blood Pressure

BSA = Body Surface Area

CW = Continuous Wave Doppler

DCM = Dilated Cardiomyopathy

E = Peak Early Mitral Diastolic Velocity

E' = Peak Early Diastolic Myocardial Velocity

ECG = Electrocardiogram

EF = Ejection Fraction

ESC = European Society of Cardiology

GCS = Global Circumferential Strain

GLS = Global Longitudinal Strain

GRS = Global Radial Strain

HCM = Hypertrophic Cardiomyopathy

HR = Heart Rate

JA = Junior Athlete

LA = Left Atrium

LAd = Left Atrial Internal Linear Dimension

LAboo = Left Atrial Booster Volume

LAcon = Left Atrial Conduit Volume

LArès = Left Atrial Reservoir Volume

LAvol = Left Atrial Volume

LAvol_{ed} = Left Atrial Volume at End Diastole

LAvoles = Left Atrial Volume at End Systole
LAvolpreA = Left Atrial Volume Pre Atrial Contraction
LV = Left Ventricle
LVEDV = Left Ventricular End Diastolic Volume
LVESV = Left Ventricular End Systolic Volume
LVH = Left Ventricular Hypertrophy
LVIDd = Left Ventricular Internal Diastolic Dimension
LVISd = Left Ventricular Internal Systolic Dimension
LVOT = Left Ventricular Outflow Tract
MWT = Mean Wall Thickness
Max WT = Maximum Wall Thickness
PCS = Pre-Participation Cardiac Screening
PLAX = Parasternal Long Axis
PSAX = Parasternal Short Axis
PVC = Pulmonary Valve Closure
PW = Pulsed Wave Doppler
RA = Right Atrium
RAa = Right Atrial Area
RAvol = Right Atrial Volume
RAvolboo = Right Atrial Booster Volume
RAvolcon = Right Atrial Conduit Volume
RAvoled = Right Atrial Volume at End Diastole
RAvoles = Right Atrial Volume at End Systole
RAvolpreA = Right Atrial Volume Pre Atrial Contraction
RAvolres = Right Atrial Reservoir Volume
RFL = Rugby Football League
ROI = Region of Interest
RPE = Rating of Perceived Exertion
RV = Right Ventricle
RV ϵ = Right Ventricular Strain
RVA' = Right Ventricular Late Diastolic Myocardial Velocity
RVD₁ = Basal Right Ventricular Cavity Dimension

RVD₂ = Mid Right Ventricular Cavity Dimension
RVD₃ = Right Ventricular Length
RVDa = Right Ventricular End Diastolic Area
RVE' = Right Ventricular Early Diastolic Myocardial Velocity
RVFAC = Right Ventricular Fractional Area Change
RVOT = Right Ventricular Outflow Tract
RVS' = Right Ventricular Systolic Myocardial Velocity
RVSa = Right Ventricular End Systolic Area
RVSRA = Right Ventricular Late Diastolic Strain Rate
RVSRE = Right Ventricular Early Diastolic Strain Rate
RVSRS = Right Ventricular Systolic Strain Rate
RVOT_{plax} = Proximal Right Ventricular Outflow Dimension in Parasternal Long Axis
RVOT₁ = Proximal Right Ventricular Outflow Dimension in Parasternal Short Axis
RVOT₂ = Distal Right Ventricular Outflow Dimension in Parasternal Short Axis
RWT = Relative Wall Thickness
 ε = Strain
S' = Peak Systolic Myocardial Velocity
SA = Senior Athlete
SADS = Sudden Arrhythmic Death Syndrome
SCA = Sudden Cardiac Arrest
SCD = Sudden Cardiac Death
SD = Standard Deviation
SR = Strain Rate
SRA = Late Diastolic Strain Rate
SRE = Early Diastolic Strain Rate
SRS = Systolic Strain Rate
STE = Speckle Tracking Echocardiography
SV = Stroke Volume
TAPSE = Tricuspid Annular Plane Systolic Excursion
TDI = Tissue Doppler Imaging
TTE = Transthoracic Echocardiography

Chapter 1

General Introduction

1.1 Background

Athlete pre-participation cardiac screening (PCS) is recommended by the European Society of Cardiology (ESC) and the American Heart Association (AHA) which has led to national and international sporting governing bodies introducing mandatory PCS for their athletes (Mont *et al.*, 2016). Sudden cardiac death (SCD) in athletes is a rare occurrence, with a prevalence reported as 1 in 40,000 to 1 in 80,000 (Harmon *et al.*, 2014) however SCD in any young person has devastating and widespread consequences. PCS aims to reduce the risk of SCD by identifying athletes with previously undiagnosed, inherited cardiac conditions which would predispose them to an increased risk of SCD.

Echocardiography is an integral part of PCS with many professional sporting organisations requiring the technique to be used as a primary investigation (Mont *et al.*, 2017) to assess cardiac structure and function. A landmark echocardiographic study by Morganroth *et al.* (1975) reported dichotomous cardiac adaptation in endurance and resistance trained athletes from which a number of athlete echocardiographic studies followed. It is widely accepted that athletic training results in a number of structural and electrical changes in the heart, however, much debate still exists over the dichotomous adaptation proposed by Morganroth *et al.* (1975). The athletes' heart (AH) phenotype can mimic cardiac muscle disease or cardiomyopathy and therefore it is imperative to understand normal physiological adaptation in various athlete groups.

Advances in echocardiography and the development of novel echocardiographic techniques and technology is improving our understanding of normal physiological adaptation. Speckle tracking echocardiography (STE) is being increasingly used in

athlete research (Beaumont *et al.*, 2017, D'Ascenzi *et al.*, 2016a) but is not currently routinely used during PCS. STE analysis can be applied to all cardiac chambers with the advantage of providing both global and regional functional assessment in addition to measurements from the standard echocardiographic assessment. STE also has the potential to aid in the elucidation of the normal physiological mechanisms of cardiac remodelling in the athlete.

1.1 Overarching Aim

The overarching aim of this thesis is to provide a comprehensive cardiac assessment of the elite, male rugby football league (RFL) athlete using both standard 2D echocardiography and STE. PCS is mandatory for RFL athletes competing in the European based Super-league and it is pertinent to understand physiological adaptation and cardiac parameters in this group to help inform clinical decisions during PCS. This comprehensive approach to assessment of physiological adaptation in RFL athletes by the use of novel STE along with standard echocardiography may aid PCS especially in the differential diagnosis of athletes where cardiac parameters overlap with criteria for pathological disease. There are limited comprehensive studies of the AH phenotype in junior athletes but there is evidence to suggest that exercise induced cardiac remodelling exists in junior athletes (McClean *et al.*, 2017) and, as PCS is conducted in athletes between the ages of 14-35 years, awareness of how physiological adaptation differs between junior and senior athletes is imperative. The timing of PCS in the competitive season is not standardised and there is some evidence that echocardiographic parameters can vary throughout the sporting season (D'Ascenzi *et al.*, 2015a) due to altered training and competition workloads. This may have important consequences for PCS and especially long-term serial assessments of athletes.

This overarching aim allows a number of specific aims:

- 1) To establish left ventricular structural and functional indices of the senior RFL athlete using TTE and STE and mathematically model the structural-functional relationship.
- 2) To determine structural and functional indices of the right heart of the senior RFL athlete using TTE and STE.
- 3) To provide a comparative and holistic structural and functional assessment of all cardiac chambers in the junior and senior RFL athlete using TTE and STE.
- 4) To assess variation in cardiac parameters across the competitive season in the senior RFL athlete using TTE and STE.

1.2 Structure of Thesis

Following this general introduction the literature review describes firstly SCD and the role of PCS in helping minimise the risk of SCD in athletes. The review then develops to provide a focus on the use and importance of echocardiography in PCS and the future potential of the addition of STE to PCS. Comprehensive cardiac assessment involving 2D echocardiography and STE in athletes is lacking. Limited attention has been paid to the impact of age or seasonal variation on AH and these factors have helped to provide a sound rationale for the studies contained within this thesis.

Chapter 3 contains the general methods pertaining to all the studies in this thesis. Implications for PCS are discussed throughout this thesis with Chapter 4 beginning the empirical studies focusing on the left ventricle of the RFL athlete with emphasis on the structural-functional relationship. Chapter 5 is related to the right heart of the RFL athlete and any overlap with pathology. Chapters 6 and 7 reflect studies of the holistic heart with chapter 6 concerned with age of the RFL athlete and this

comparative study addresses the AH phenotype in senior and junior RFL athletes. Chapter 7 describes the heart of the senior RFL athlete across the competitive season reflecting seasonal cardiac variation in relation to training load.

The thesis comes to its natural conclusion with chapter 8 containing a general discussion of findings from all of the studies with a discussion on the overarching issues and implications for PCS. Future research is also considered with the chapter terminating in an overall conclusion to the thesis as a whole.

Chapter 2

Literature Review

Selected parts of this literature review have been published:

Forsythe, L., George, K. and Oxborough D. (2018). Speckle Tracking Echocardiography for the Assessment of Athletes' Heart: Is it Ready for Daily Practice? Current Treatment Options in Cardiovascular Medicine. Doi: 10.1007/s11936-018-0677-0.

2.1 Sudden cardiac death and related conditions

Sudden cardiac death (SCD) in a young person, especially those who are seemingly healthy with no previous symptoms, is a tragic and devastating event that generates significant levels of concern from both the medical and wider communities. It has been suggested that 6 % of all SCD in young people (14 to 35 years) occur in competitive athletes (Marijon *et al.*, 2011). The underlying aetiology is often related to an inherited cardiac condition such as myocardial disease including hypertrophic cardiomyopathy (HCM), arrhythmogenic right ventricular cardiomyopathy (ARVC) and dilated cardiomyopathy (DCM) (Mont *et al.*, 2017). In some cases of SCD an obvious cause is not found and the death is attributed to sudden arrhythmic death syndrome (SADS) (Finocchiaro *et al.*, 2016). Conditions linked to SADS include the ion channel diseases / ion channelopathies such as Brugada syndrome, Long QT syndrome, catecholaminergic polymorphic VT (CPVT) or congenital accessory pathways like Wolfe Parkinson White syndrome (Merghani *et al.*, 2013). Cardiomyopathies and ion channelopathies are considered arrhythmogenic cardiac conditions which can precipitate the malignant tachyarrhythmias ventricular tachycardia and ventricular fibrillation (Mont *et al.*, 2017) which can lead to sudden cardiac arrest (SCA) and SCD. While many deaths remain unexplained, many will have been found to have had underlying, potentially detectable cardiovascular disease (Mont *et al.*, 2017). The most common cardiomyopathies associated with SCD are HCM and ARVC and DCM and can often be detectable using current diagnostic pathways (Sharma *et al.*, 2017). HCM mainly affects the left ventricle (LV) and has a prevalence of 1/500 of the general sedentary population (Maron *et al.*, 1995) but prevalence is lower in the athletic population. One study of over 3000 British elite athletes reported a prevalence of 1/1500 (Basavarajaiah *et al.*, 2008) and a similar prevalence has been reported from

the Italian screening experience supporting the theory that more severely affected individuals are likely to have been selected out due to impaired cardiovascular performance (Corrado *et al.*, 2008). Athlete deaths where HCM is implicated predominantly occur in intermittent power/speed sports such as soccer, American Football and basketball (Wilson *et al.*, 2011). HCM is a primary myocardial disorder when an autosomal dominant pattern of inheritance characterised by left ventricular hypertrophy (LVH) in the absence of abnormal loading conditions (Maron, 2002). Mutations in sarcomeric contractile proteins are associated with LVH and there is histological evidence of myocardial disarray and fibrosis with a predilection for potentially fatal arrhythmias (Merghani *et al.*, 2013). Although some individuals may be symptomatic, often SCD can be the first clinical manifestation occurring without warning (Maron, 2002). ARVC has been reported to have a prevalence of 1/1000 in the population (Gemayel *et al.*, 2001) and is generally regarded as a genetically determined myocardial degenerative disease (Sheppard, 2012). It is caused by mutations in genes coding for cardiac desmosomal proteins which are thought to lead to myocyte detachment and an abnormal repair process resulting in fibrofatty replacement of the myocardium (Basso *et al.*, 2009). Macroscopic appearances include right ventricular (RV) dilatation, dysfunction and aneurysmal formation often with associated LV involvement (Marcus *et al.*, 2010, Chandra *et al.*, 2013, Merghani *et al.*, 2013). Dilated cardiomyopathy (DCM) is defined by the presence of LV or biventricular dilatation and systolic dysfunction in the absence of abnormal loading conditions or sufficient coronary artery disease to cause global systolic impairment (Pinto *et al.*, 2016). DCM has a prevalence of 1/2500 population and incidence of DCM related SCD in athletes has been reported to be in region of 2-11% (Sheppard, 2012). DCM is more common in males and females and can be both inherited and non-

inherited and is believed to be inherited in 20-48% of cases (Sheppard, 2012). There are thought to be over 50 disease related genes and it is possible for an interaction between genetic and non-genetic causes whereby the interaction of environmental factors for example may exacerbate the DCM phenotype (Pinto *et al.*, 2016). Autosomal dominant forms of the disease are caused by mutations in cytoskeletal, sarcomeric protein / Z band, nuclear membrane and intercalated disc gene proteins (Sheppard, 2012). DCM encompasses a broad range of genetic and acquired disorders that manifest as a spectrum of electrical, structural and functional abnormalities that change with time (Pinto *et al.*, 2016) where a combination of diagnostic tools are needed for clinical diagnosis.

Although SCD in athletes is rare, approximately 1 in 40,000 to 1 in 80,000 (Harmon *et al.*, 2014), athletes are at greater risk of SCA and SCD if they have an undetected underlying condition due to the increased cardiac and physiological demands of sport especially at elite level (Schmied and Borjesson, 2014). Consequently, there is a 2.8 fold increase in risk of SCD in athletes harbouring quiescent cardiovascular abnormalities (Corrado *et al.*, 2003). Exercise exacerbates the pathophysiological changes and a 5 fold increase in risk of SCD in ARVC has been reported during competitive sports when compared to sedentary activity (Corrado *et al.*, 2003).

ARVC has been reported to account for approximately 4 % of SCD in the athletic population (Maron *et al.*, 2007). However more recent results from a UK regional registry of SCD in athletes reported that SADS was documented as the cause of death in 42% cases. Myocardial diseases represented 40% deaths (including idiopathic left ventricular hypertrophy (LVH) plus or minus fibrosis (16%), ARVC (13%) and HCM (6%) (Finocchiaro *et al.*, 2016). Differentiation between physiological adaptation and pathological maladaptation is crucial as elite athletic performance can co-exist with

inherited cardiac disease. In some cases differentiating normal physiological cardiac adaptation to exercise from pathological cardiac disease can pose a significant dilemma for the clinician / diagnostician.

2.2 Pre-Participation Cardiac Screening

Intensive exercise training and sporting competition is believed to act as a trigger for ventricular arrhythmias leading to sudden cardiac arrest and/or death in predisposed individuals (Corrado *et al.*, 2005). In view of this, there is now a growing awareness for the need for pre-participation cardiac screening (PCS) for sports participation to identify those at risk of SCD from a previously undiagnosed cardiac condition (Mont *et al.*, 2017). The European Society of Cardiology (ESC) advocate the use of a screening health questionnaire and a 12-lead electrocardiogram (ECG) for all competitive athletes with any individual presenting with potential abnormalities, symptoms or a family history of cardiomyopathy subsequently referred for further investigation (Corrado *et al.*, 2005).

Whilst there has been agreement in the medical profession on the justification of PCS in the identification and subsequent safeguarding of at risk athletes, the protocol has remained controversial (Corrado *et al.*, 2005, Maron *et al.*, 2015). The ESC recommends personal history, physical examination and a resting 12 lead ECG at a minimum (Corrado *et al.*, 2005) whilst the American Heart Association (AHA) / American College of Cardiology (ACC) (Maron *et al.*, 2015) do not recommend the inclusion of ECG. This ultimately impacts upon the sensitivity, specificity and cost effectiveness of the screening programme (Mont *et al.*, 2017), however, a recent meta-analysis has demonstrated the most effective strategy for screening for cardiovascular disease in athletes is with ECG (Harmon *et al.*, 2015). Current International guidelines

for the interpretation of the athletes' ECG have been developed recently (Sharma *et al.*, 2017) which are likely to improve sensitivity, specificity and cost effectiveness of ECG based athletic screening.

2.2.1 The Role of Echocardiography in PCS

An athlete with an abnormal ECG, family history of SCD or cardiovascular symptoms will require further cardiac investigation and one of the key investigations is echocardiography. Many sporting federations mandate cardiac screening and require echocardiography as a standard part of the primary screening protocol. These include the Federation Internationale de Football Association (FIFA), Union of European Football Associations (UEFA), Union Cycliste International (UCI), Federation Internationale de Motocyclisme and the Federation Internationale de l'Automobile (Mont *et al.*, 2017). 2D transthoracic echocardiography (TTE) is used in the assessment of the AH aiding the determination of physiological adaptation compared to pathological in borderline cardiac phenotypes. TTE is a routine, non-invasive investigation providing both structural and functional information simultaneously making it an extremely useful imaging tool in this setting. Echocardiography has been used to develop understanding of the physiological limits of adaptation to exercise with much work already performed in this area (Pelliccia *et al.*, 1999, Pluim *et al.*, 2000, Whyte *et al.*, 2004, Utomi *et al.*, 2013, Finocchiaro *et al.*, 2017, D'Ascenzi, *et al.*, 2017a).

The use of systematic TTE alongside the 12-lead ECG has not provided increased diagnostic value in the diagnosis of cardiomyopathies compared to ECG alone and is not clinically or cost effective (Sheikh *et al.*, 2014, Riding *et al.*, 2015) although TTE is recommended as the primary follow up investigation to an abnormal screening

(Riding *et al.*, 2015) for primary screening protocols that do not mandate the use of TTE. If used systematically it is believed that it may increase the rate of false positive screening given the grey zone overlap between physiology and pathology (Papadakis *et al.*, 2011, Gati *et al.*, 2013, Zaidi *et al.*, 2013). We need to be conscious of the sporting federations who mandate TTE in the screening protocol and for that reason we need to have greater insight into normal structural and functional athletic adaptation and this improved knowledge may in turn help to improve the sensitivity and specificity of the technique allowing TTE to be more cost effective and included more often as a primary screening tool. The use of TTE however, onsite, at the time of initial screening reduced referral rates by 40-60 % and has a significant positive impact on cost, efficient use of resources and time until the athlete is cleared for competition (Anderson *et al.*, 2014, Mont *et al.*, 2017).

Some of the best evidence for the use of echocardiography in athletes has been in the differential diagnosis of HCM (Sheikh *et al.*, 2015). Coronary artery anomalies are reported to cause SCD in 12-33% athletes (Chandra *et al.*, 2013) as a consequence of impairment in coronary blood flow due to an abnormal ostium of the anomalous vessel compression of the anomalous artery and/or coronary spasm (Basso *et al.*, 2000). Identification of coronary artery anomalies is another important use for echocardiography in PCS and something which cannot be done by ECG screening alone. Differential diagnosis with echocardiography remains a difficult task in athletes (La Gerche *et al.*, 2013) and despite recent echocardiographic research in AH there are no international guidelines / consensus for echocardiographic protocol or normal ranges. The acquisition and interpretation of TTE in athletes follows guidelines created for the use in the normal population (Lang *et al.*, 2015, Rudski *et al.*, 2010). The British Society of Echocardiography (BSE) in association with Cardiac Risk in

the Young (CRY) has recently produced a joint policy document providing guidance on the role of echocardiography in the cardiac screening of sports participants (Oxborough *et al.*, 2018) which suggests performing standard echocardiographic protocol with additional image acquisition in the parasternal short axis to visualise the coronary ostia and for improved accuracy of LV wall thickness measurements. It is also recommended that attention be paid to the type and amount of athletic activity as this can influence the AH phenotype and algorithms are presented to aid interpretation of the athlete's echocardiogram in the absence of normal LV and RV geometry (Oxborough *et al.*, 2018). Advancing our understanding of echocardiography would improve sensitivity and specificity of echocardiography in PCS, like has happened with ECG.

2.2.2 The grey area between physiology and pathology - the diagnostic dilemma

As the heart of the athlete remodels in response to sustained exercise training there is evidence for chronic enlargement of the cardiac chambers and some evidence of reduced function (Pluim *et al.*, 2000, Utomi *et al.*, 2013). It is apparent that cardiac morphology may mimic the pathological changes observed in some cardiac diseases making the differentiation of physiological and pathological remodelling a diagnostic challenge (Maron and Pelliccia, 2006). This overlap between physiology and pathology has been termed the 'grey area' (Maron, 2003) and reflects an area of diagnostic uncertainty. In order to reduce SCD in athletes and to improve the accuracy of PCS it is essential to understand the normal structure and function of the AH including the differences between sporting disciplines and to provide normative values and ranges for specific cardiac parameters. It has been reported that some athletes demonstrate extreme adaptation with LV wall thicknesses of 12-15mm (Pelliccia *et*

al., 1991, Basavarajaiah *et al.*, 2008). LVH may develop as part of normal physiological adaptation but may also mimic HCM (Pelliccia *et al.*, 1991, Basavarajaiah *et al.*, 2008). However, it is thought that physiological hypertrophy is homogenous throughout the LV and is associated with concomitant chamber enlargement with normal indices of diastolic function. The recent finding that LV fibrosis and idiopathic LVH has an increasing link to SCD in athletes (Finocchiaro *et al.*, 2016) suggests differential diagnosis of LVH in the athletes' heart may be even more difficult than first thought. An increased wall thickness raises suspicion of disease however individuals with LV fibrosis may also have normal wall thickness. It is therefore of great importance that any athletes identified to have abnormalities during PCS examination, history taking or ECG undergo further and thorough cardiac diagnostic investigations.

In contrast marked phenotypes of HCM can present with asymmetric LVH, small chamber size and impaired diastolic function. An LV end diastolic dimension (LVIDd) of >55mm is not a common observation in HCM patients but an LVIDd of this size is common in athletes (Chandra *et al.*, 2013). In this regard, some athletes with HCM have been found to exhibit wall thickness of ≥ 16 mm and non-concentric patterns of LVH often with associated ECG abnormalities (pathological T wave inversion) (Sheikh *et al.*, 2015). However, 14% of athletes in this study had milder phenotypes of HCM placing them within the diagnostic grey zone. In these athletes, a LV cavity LVIDd of ≤ 51 mm favoured HCM diagnosis (Sheikh *et al.*, 2015). This adds to the clinical dilemma as athletes with a mild phenotype HCM often have larger cavities and normal indices of diastolic function compared to HCM in sedentary population. In some athletes within the grey zone, conventional echocardiographic parameters alone are insufficient to differentiate HCM from physiological LVH and should be

complemented with additional structural and functional assessments to minimise risk of false reassurance (Sheikh *et al.*, 2015). Reduced left ventricular (LV) systolic function as measured by ejection fraction (EF) has been observed in endurance athletes (Abergel *et al.*, 2004) and whilst this can be explained by athletic adaptation whereby a large ventricle and slow heart rate generates an adequate stroke volume requiring minimal contractility at rest, an enlarged LV and reduced EF can also be indicative pathology including the potentially life threatening condition DCM.

ARVC is an equally challenging diagnosis in the athletic population especially as early in disease there is a concealed phase where the heart may appear morphologically normal (Chandra *et al.*, 2013). Minor ECG abnormalities and infrequent VE's alongside subtle changes in RV structure may be the only manifestations and often overlap with physiological adaptation (Corrado *et al.*, 1997, Chandra *et al.*, 2013). The majority of current data on normal limits of RV size has been derived from normal individuals (Lang *et al.*, 2015, Rudski *et al.*, 2010) whilst we accept that the RV can be dilated in athletes there are no international guidelines for normal athletic ranges. Data from endurance athletes (Oxborough *et al.*, 2012a) shows that 28 % of athletes have RVOT values greater than proposed major echocardiographic structural criteria for ARVC (Marcus *et al.*, 2010). A greater degree of adaptation has been demonstrated at the RV inflow compared to the outflow which may be a useful marker supporting athletic adaptation (Oxborough *et al.*, 2012a, Zaidi *et al.*, 2013). This is supported by a more recent study where the ratio of RV inflow to outflow tract (an index of symmetric remodelling) does not change regardless of extent of RV remodelling. The authors therefore suggested that disproportionate enlargement of the RVOT is unlikely to represent physiological RV adaptation (D'Ascenzi *et al.*, 2017b). One important manifestation of ARVC is the presence of regional wall motion abnormalities and

hence the detection of functional abnormalities would favour a diagnosis of ARVC (Marcus *et al.*, 2010, Basso *et al.*, 2009, Chandra *et al.*, 2013).

TTE is an integral part of PCS and due to advances in technology, novel echocardiographic techniques have been developed which offer the potential of increasing the sensitivity and specificity of echocardiography during cardiac assessment of the athlete, PCS and differential diagnosis.

2.3 Cardiac Mechanics and Speckle Tracking Echocardiography

2.3.1 Myocardial architecture

Regional variations in fibre arrangement exist within ventricular mass both between and within the individual ventricles (Greenbaum *et al.*, 1981) and this is an important consideration for the assessment of cardiac function. Torrent-Guasp determined a helical heart structure and identified a helical ventricular myocardial band to explain functional motion (Torrent-Guasp *et al.*, 2001). Further work has revealed a complex 3-dimensional network of myocytes in a matrix of fibrous tissue (Ho and Nihoyannopoulos, 2006). Each myocyte is joined to another at the ends as well as its side branches forming myofibres and despite a predominant longitudinal orientation of myofibres (Ho and Nihoyannopoulos, 2006), circumferential and also obliquely running fibres form a helical spiral from base to apex (Wu *et al.*, 2006). Helical fibres are contained both within the LV free wall and the septum which during systole leads to the production of longitudinal strain when the reciprocal oblique spirals thicken and coil. A wrap of transverse fibres at the LV base (Kocica *et al.* 2006) allows for the production of circumferential strain (Rushmer *et al.*, 1953, Sallin *et al.*, 1969, Buckberg and Hoffman, 2014). During systole there is also a twisting ‘wringing’ motion of the ventricle as the LV apex rotates anticlockwise whilst the base rotates

clockwise creating twist deformation originating from the dynamic interaction of oppositely wound endocardial and epicardial fibre helices (Notomi *et al.*, 2005).

The RV free wall is thin in comparison to the LV and composed of longitudinal and transverse fibres (Ho and Nihoyannopoulos, 2006, Buckberg and Hoffman, 2014). RV structure and function is defined by the helical ventricular myocardial band with longitudinal shortening the major contributor to overall RV performance with equal contributions from the free wall and the interventricular septum. During systole the septal helical fibres twist and shorten the longitudinal axis of the RV as the wrap around transverse fibres constrict or compress to cause the ‘bellows’ motion (Buckberg and Hoffman, 2014).

The assessment of mechanical activation of the complex biventricular fibre orientation is difficult using conventional echocardiographic methods (Sengupta *et al.*, 2006a) but more novel echocardiographic techniques have been introduced to address the problems of assessing myocardial contraction and relaxation in different planes and regions of the heart.

2.3.2 Speckle Tracking Echocardiography

The concept of strain (ϵ) and strain rate (SR) as measures of myocardial mechanical properties were first introduced by Mirsky and Parmley (1973) who used deformation to study the elastic properties of the myocardium. Myocardial ϵ is a dimensionless index describing myocardial deformation or fractional change in length of a myocardial segment, expressed as a percentage whilst SR is the rate of change in length, a time derivative of the ϵ signal expressed in sec^{-1} (Mirsky and Parmley 1973). Developments in the echocardiographic use of ϵ and SR measurements have followed (Sutherland *et al.*, 1994, Heimdal *et al.*, 1998) and has allowed valuable and

discriminating indices of regional and global ventricular function to be discerned which do not suffer from tethering and translational artefact with the use of speckle tracking echocardiography (STE) also allowing for angle independent analysis of myocardial function (Andersen *et al.*, 2004, Korinek *et al.*, 2005, Marwick *et al.*, 2006), an advantage over TDI ϵ imaging.

Myocardial deformation can be measured by STE from the continuous frame by frame tracking of a small image block of 'natural acoustic markers' in grey scale ultrasound images which form interference patterns (speckled) within myocardial tissue (Reisner *et al.*, 2004). Speckles are the result of constructive and destructive interference of ultrasound backscattered from structures smaller than the ultrasound wavelength (Leitman *et al.*, 2004, Pirat *et al.*, 2008). The appearance of these acoustic markers are considered stable myocardial footprints over the short period between subsequent image frames with change in position assumed to follow tissue motion (Korinek *et al.*, 2005). Tracking is based on searching the new location of the marker in the subsequent frame (Korinek *et al.*, 2005) using block matching algorithm (Hein *et al.*, 1993, Behar *et al.*, 2004). The calculation of ϵ and SR is made from the displacement and displacement rate of each marker (Korinek *et al.*, 2005). This process is repeated for all frames through the cardiac cycle to produce a 2D displacement curve for each point in the myocardium to identify local shortening, thickening and lengthening of the myocardium as a measure of LV regional and global function (Amundsen *et al.*, 2006). Deformation can be measured in longitudinal, circumferential and radial planes of LV motion and can be used in the assessment of LV rotation and twist (Reisner *et al.*, 2004 D'Hooge *et al.*, 2000, Notomi *et al.*, 2005, Korinek *et al.*, 2005, Helle-Valle *et al.*, 2005, Marwick *et al.*, 2006). STE has been validated in comparison with tagging harmonic phase cardiac magnetic resonance and sonomicrometry (Amundsen *et al.*,

2006, Korinek *et al.*, 2007). Positive ϵ values are consigned to lengthening, thickening or clockwise rotation and negative values are consigned to shortening, thinning or anticlockwise rotation. A schematic of the basic principles of ϵ and SR is shown in Figure 2.1 (Yip *et al.*, 2003).

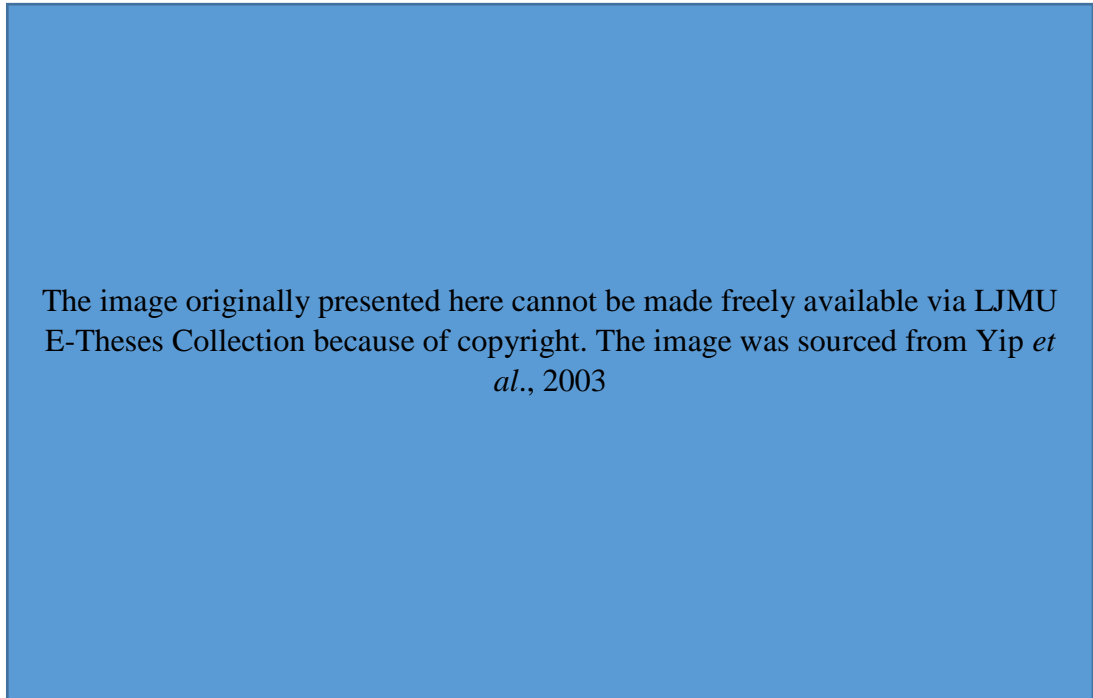


Figure 2.1 Strain Schematic. Strain is a measure of tissue deformation, defined as the change in length (L_1-L_0) normalised to the initial length (L_0) of the region of interest. If the initial length of a myocardial segment is 10cm, shortening to 8cm indicates a ϵ of -20% or lengthening the segment to 12 cm indicates a ϵ of +20%. No change in length suggests 0% ϵ . The rate at which these changes occur is SR (Yip *et al.*, 2003).

Longitudinal ϵ assesses apex to base myocardial deformation by longitudinal fibre shortening (Figure 2.2) with longitudinal mechanics predominantly governed by the subendocardial layer. Greater ϵ values are observed towards the apex and this can be explained by the oblique left and right handed helical segments that converge to form an anatomical vortex of double helical loop (Buckberg *et al.*, 2008).

Circumferential ϵ measures the change in length along the circumference of the myocardium or shortening of the mid wall circumferential fibres (Figure 2.2)

(Sengupta *et al.*, 2006b, Sengupta *et al.*, 2006a) with the magnitude of circumferential ϵ during ejection exceeding that of longitudinal ϵ . Longitudinal and circumferential ϵ have shown a small base to apex gradient so successive shortening ϵ is higher at apical and mid segments compared to the base (Sengupta *et al.*, 2006b).

Radial ϵ is a measure of the change in length between endocardium and epicardium and is analogous to percentage thickening (Figure 2.2). Continuum mechanics would suggest that shortening in the longitudinal and circumferential direction results in thickening in the radial direction for conservation of mass however LV wall thickening is not a result of simple shortening of individual myocytes but an effect of shearing groups of myocytes across one another. This cardiac shearing deformation amplifies the shortening of myocytes into increases in radial wall thickening to create a normal LVEF (Covell, 2008, Mor-Avi *et al.*, 2011). Radial thickening is therefore due to the interaction between the two oblique helical muscle wraps as well as the circumferential muscle fibres (Ammar *et al.*, 2012).

LV rotation refers to myocardial motion around the long axis of the LV and is assessed at basal and apical level (Figure 2.2). LV twist is the result of two helical fibre geometries were the subendocardial fibres arranged in a right handed helix and the subepicardial fibres arranged in a left handed shorten concurrently during ejection (Ashikaga *et al.*, 2009, Covell, 2008, Sengupta *et al.*, 2006a, Mor-Avi *et al.*, 2011). Whilst the subendocardial region contributes predominantly to the longitudinal mechanics of the LV, the midwall and the subepicardium contribute predominantly to the rotational movement. (Sengupta *et al.*, 2006a). During ejection this results in global anti clockwise LV rotation near the apex and clockwise rotation near the base and the absolute base to apex difference in rotation is referred to as net twist which is expressed in degrees. The twisting and shearing of the subendocardial fibres deform

the matrix and results in storage of potential energy with the subsequent recoil of twist (untwist) associated with the release of restoring forces which contribute to diastolic function and facilitate early LV filling (Notomi *et al.*, 2005, Sengupta *et al.*, 2008, Ashikaga *et al.*, 2009).

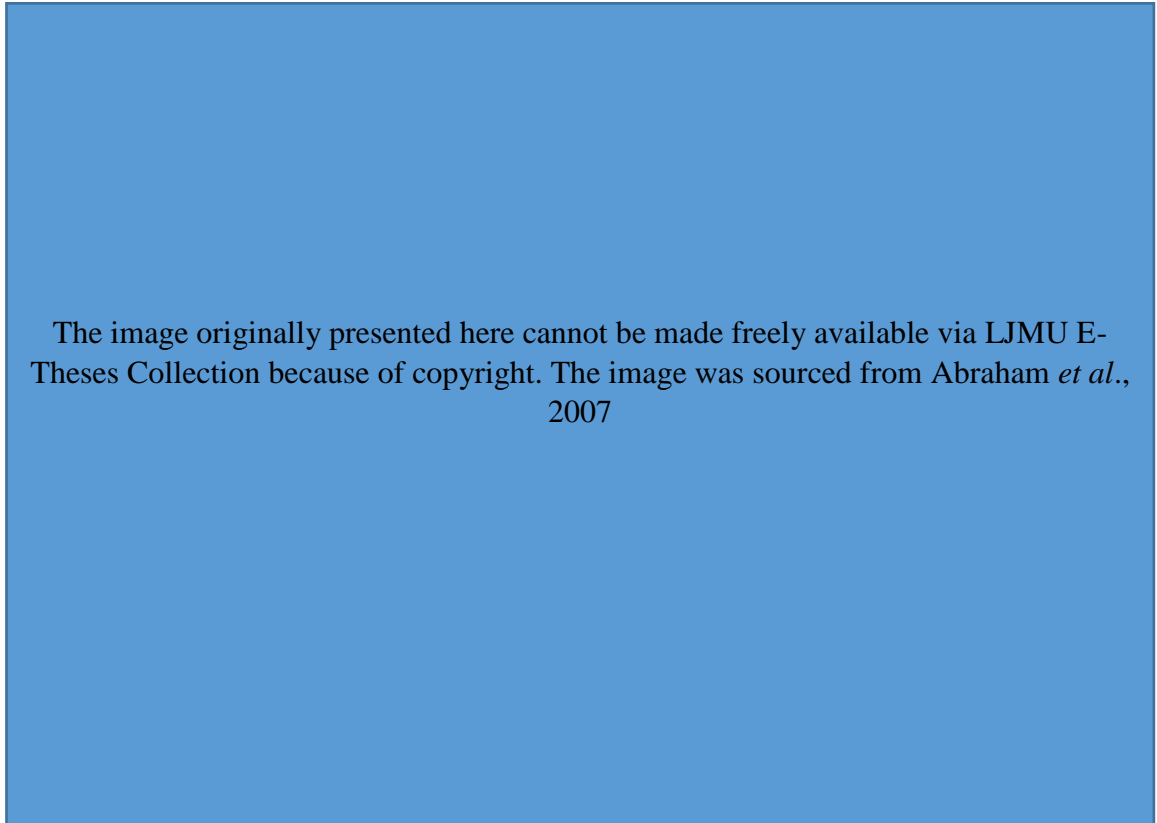


Figure 2.2 Representation of the principal LV myocardial deformations. A: Longitudinal (LONG), B: circumferential (CIRC) and radial (RAD), C: Rotation and Twist at the apex and base. The direction of motion in systole is indicated by solid arrows and in diastole by dashed arrows (Abraham *et al.*, 2007).

Due to the dominance of longitudinal and oblique myocardial fibres in the RV free wall (Ho and Nihoyannopoulos, 2006) longitudinal RV ϵ can be measured by STE with measurements previously found to have acceptable reproducibility (Teske *et al.*, 2008, Oxborough *et al.*, 2012b). Peak RV ϵ is expressed as a mean of the basal, mid and apical segmental ϵ with normal RV ϵ parameters showing a base to apex gradient with highest values observed at the apex (Rudski *et al.*, 2010).

SR measures the time course of deformation and appears to be a correlate of rate of change in pressure (dP/dt), a parameter that is used to reflect contractility (Marwick, 2006). Peak systolic SR is the parameter that is closest to measuring local contractile function in clinical cardiology as it is relatively volume independent and less pressure dependent than ϵ (Abraham *et al.*, 2007). ϵ is more akin to regional EF (Marwick, 2006) and as peak systolic ϵ is also volume dependent it does not reflect contractile function as well (Abraham *et al.*, 2007). As with EF, an increase in preload is associated with an increase in ϵ and an increase in afterload is associated with a reduction of ϵ and in contrast SR is considered to be a less load dependent measure than ϵ (Marwick, 2006). Despite a relationship with contractility, SR however can be limited by signal noise and relatively low frame rates (Smiseth *et al.*, 2016). Systolic SR (SRS), early diastolic SR (SRE) and late diastolic SR (SRA) can be assessed both globally and regionally in longitudinal, circumferential and radial planes of motion.

2.3.3 The Rationale for Speckle Tracking Echocardiography

Standard echocardiographic global functional assessment is limited by the perception that normal and abnormal LV EF equates to normal and abnormal systolic function respectively. This may not always be the case and has been highlighted by recent studies of pathological hypertension in patients diagnosed with heart failure with normal EF (HFNEF). HFNEF patients have by definition normal EF where systolic function and contractility have been assumed to be normal (MacIver and Townsend, 2008). There is however a paradox with reduced longitudinal, circumferential and radial ϵ with normal absolute radial thickening in these patients with a normal EF can be explained by an increased diastolic wall thickness (MacIver, 2011, MacIver and Dayer, 2012). The terms EF and LV function are not synonymous and in the context of increased wall thickness, normal absolute radial thickening results in normal EF

with the illusion of normal pump function (MacIver and Dayer, 2012). The assessment of cardiac mechanics can be an important addition to any examination, particularly in those individuals with variable cardiac morphology. Longitudinal function appears to precede radial dysfunction in many pathological models (Nesto *et al.*, 1987) which has contributed to the adoption of ϵ imaging in the early detection of sub-clinical LV dysfunction as well as being a prognostic indicator (Plana *et al.*, 2014, Tops *et al.*, 2017, Biering-Sørensen *et al.*, 2017). Current clinical practice guidelines for management of HCM (Elliott *et al.*, 2014) include ϵ echocardiography for evaluating longitudinal function in early disease as this can be depressed before development of a HCM phenotype in gene positive family members (Elliott *et al.*, 2014, Smiseth *et al.*, 2016). Decreased longitudinal ϵ has also been observed in DCM patients compared to controls (Okada *et al.*, 2012) and decreased RV longitudinal ϵ has been observed in ARVC (Teske *et al.*, 2009a). With altered ϵ indices being reported in cardiomyopathy patients (Smiseth *et al.*, 2016) the use of STE in cardiac disease highlights the possibility of STE improving the diagnostic capability of echocardiography in the AH. When we consider that many athletes have marked structural remodelling and given that functional abnormalities are likely to be subtle at an early stage, the addition of STE may improve the sensitivity and specificity of echocardiography in PCS. It is also important to note that the relationship of EF to longitudinal function and cardiac size in a physiological model of adaptation is currently unknown.

2.4 Exercise Induced Cardiac Remodelling

Haemodynamic changes that occur during exercise constitute the primary stimulus for exercise induced cardiac remodelling however these can vary across different sporting disciplines. Despite the overlap in some sporting disciplines, exercise activity can be divided into two principal physiological forms (Weiner and Baggish, 2012).

Dynamic (isotonic) exercise commonly referred to as endurance exercise results in a marked increase in oxygen consumption, cardiac output, heart rate, stroke volume and systolic blood pressure resulting in a volume challenge for the heart. This is often associated with a moderate increase in mean arterial blood pressure and reduction in diastolic pressure and total peripheral vascular resistance resulting in an increased contractile state (Mitchell *et al.*, 2005). This form of exercise underlies activities including long distance running, cycling, rowing and swimming and involves sustained elevations in cardiac output (Weiner and Baggish, 2012).

Static (isometric) exercise commonly referred to as strength training results in a small increase in oxygen consumption, cardiac output and HR usually without significant change in stroke volume. The associated marked increases in systolic, diastolic and mean arterial pressure without significant change in total peripheral vascular resistance exercise and has been proposed to cause an increased pressure challenge on the left ventricle resulting in an increased contractile state (Mitchell *et al.*, 2005). This type of exercise underlies power sports such as weightlifting, track and field throwing events and involves short but intense bouts of increased peripheral vascular resistance (Weiner and Baggish, 2012).

Most sports actually require a combination of both types of activity and a matrix of classification of sports (Figure 2.3) has been developed to categorise sports by level of intensity of dynamic and static exercise generally required to perform that sport during competition (Levine *et al.*, 2015).

The image originally presented here cannot be made freely available via LJMU E-Theses Collection because of copyright. The image was sourced from Levine *et al.*, 2015

Figure 2.3 Classification of sports based on peak static and dynamic components achieved during competition. * Danger of bodily collision. † Increased risk if syncope occurs. (Levine *et al.*, 2015).

Repeated exposure to increases in volume and/or pressure results in chronic cardiovascular adaptations leading to changes in myocardial structure and function in athletes (Sharma, 2003. Baggish and Wood, 2011). The extent and magnitude of phenotypical expression of AH is multifactorial and includes not only sporting discipline but the athlete's demographic profile including their gender, body size, ethnicity and age (Baggish and Wood, 2011, Brown *et al.*, 2017). Importantly, cardiac adaptations associated with normal physiological adaptation to exercise in response to a chronic exercise stimulus can regress with a period of detraining (Sharma, 2003).

2.5 The Athletic Heart Phenotype

2.5.1 *Conventional Echocardiography and the Left Ventricle*

Early echocardiographic studies of the AH focused on the LV with Morganroth *et al.*, (1975) describing a dichotomous theory of cardiac adaptation in athletes depending on the type of exercise performed and is now known as the Morganroth hypothesis. Endurance athletes (Swimmers) exhibited eccentric left ventricular hypertrophy (LVH), a balanced increase in wall thickness and cavity size, characterised by an increased left ventricular internal dimension (LVIDd) and left ventricular mass with minor changes in wall thickness. According to Morganroth *et al.* (1975), resistance / strength trained athletes (wrestlers) exhibited concentric hypertrophy, an increase in wall thickness with normal cavity size, characterised by increased LV mass and wall thickness without changes in LVIDd (Morganroth *et al.*, 1975) however this limb of the dichotomy has been challenged and the nature of cardiac adaptation relating to different sporting disciplines has been the subject of recent research. Characteristics of eccentric and concentric hypertrophy in response to exercise training can be seen in figure 2.4.

The image originally presented here cannot be made freely available via LJMU E-Theses Collection because of copyright. The image was sourced from Weiner and Baggish, 2012

Figure 2.4 Summary of ventricular remodelling during sustained exercise training highlighting the sport-specific nature of exercise induced cardiac remodelling (Weiner and Baggish, 2012).

The assessment of LVH in AH is pertinent and the echocardiographic assessment must include accurate and reliable measurements of LVIDd, wall thickness leading to the subsequent calculation of LV mass. LV geometry should be determined using the combination of LV mass and relative wall thickness (RWT) or wall to chamber ratio. RWT is calculated by summing the basal septal and posterior wall thickness in diastole and dividing into the LVIDd. According to published guidelines (Lang *et al.*, 2015) LV geometry should be reported as ‘normal’, ‘concentric remodelling’ (increased RWT >0.42 , normal LV mass), ‘concentric hypertrophy’ (increased RWT

>0.42, increased LV mass) or ‘eccentric hypertrophy’ (normal RWT, increased LV mass) (Figure 2.5).

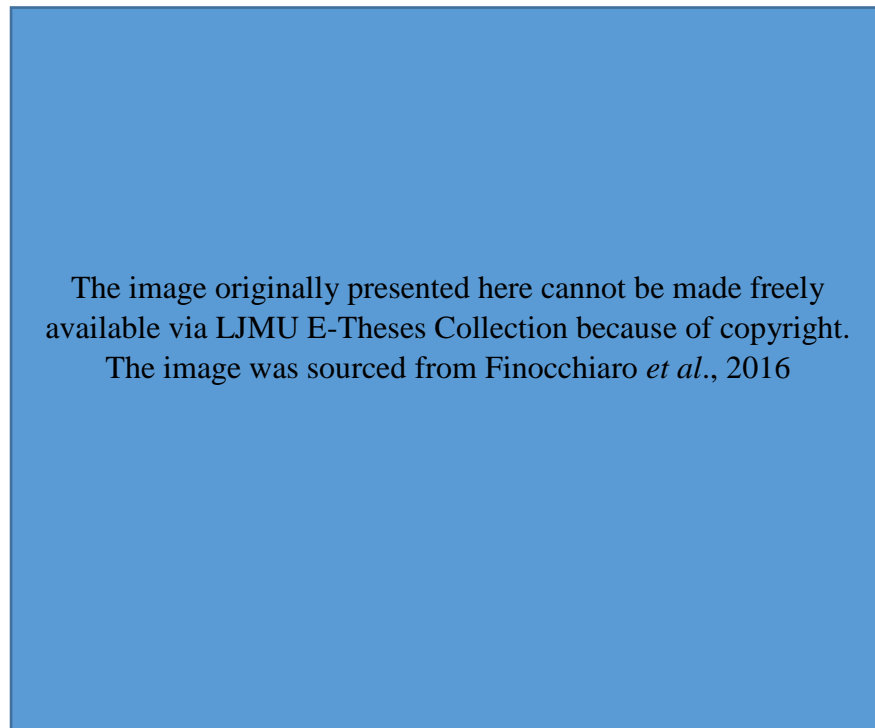


Figure 2.5 Left ventricular geometry according to relative wall thickness and left ventricular mass (Finocchiaro *et al.*, 2016, adapted from Lang *et al.*, 2015).

There is robust evidence supporting the presence of eccentric LVH in endurance athletes (Pluim *et al.*, 2000) with most of the knowledge of upper limits of physiological adaptation coming mainly from endurance based athletes (Pelliccia *et al.*, 1991, Nagashima *et al.*, 2003). In a longitudinal study concentric LVH was observed after 3 to 6 months of resistance training (Baggish *et al.*, 2008a) however the evidence for concentric LVH in resistance trained athletes has been queried by cross-sectional (Haykowsky *et al.*, 2000a, Kinoshita *et al.*, 2003) and longitudinal data sets (Haykowsky *et al.*, 2000b, Spence *et al.*, 2011). The lack of evidence of concentric LVH in resistance trained athletes (Haykowsky *et al.*, 2000a) is one of the main controversies (Utomi *et al.*, 2013) with growing evidence to refute the existence of true physiological concentric hypertrophy (Utomi *et al.*, 2014). It has been suggested

that the stimulus for concentric remodelling may not occur during heavy resistance exercise due to simultaneous valsalva manoeuvre during this type of exercise. Valsalva manoeuvre was not found to be associated with increased LV end systolic wall stress during leg press resistance exercise and therefore there may be absence of a real afterload pressure stimulus (Haykowsky *et al.*, 2001). Given that the magnitude of eccentric hypertrophy resulting from endurance exercise is more pronounced than concentric hypertrophy associated with strength training (Spence *et al.*, 2011), dynamic exercise appears to be the primary stimulus for adaptation which appears to be quantitatively greater in endurance training compared to resistance training (Utomi *et al.*, 2013). Concentric hypertrophy is less likely therefore based on these studies.

In more recent studies increases in LV cavity size were found in endurance athletes but concentric remodelling and concentric hypertrophy were not observed in the resistance trained athletes (Spence *et al.*, 2011, Utomi *et al.*, 2013). Utomi *et al.*, (2013) observed greater wall thickness in resistance athletes compared to controls but no difference compared to endurance athletes. Whilst the cavity dimension was larger in resistance athletes compared to controls, it was smaller compared to endurance athletes supporting the notion that this may in fact just be a lower degree of eccentric adaptation (Utomi *et al.*, 2013). Pluim *et al.* (2000) reported an increased RWT with resistance training and whilst Utomi *et al.* (2013) found a minimally increased RWT in resistance athletes but this was within normal range (Lang *et al.*, 2015) and not meaningfully different between groups (Utomi *et al.*, 2013). A further and more recent study by Utomi *et al.* (2014) described a predominance of normal LV geometry in both endurance and resistance trained athletes and highlights the importance of scaling for body size. There is an established association between body size and cardiac morphology (George *et al.*, 2001) but often indexing was found to be inconsistently

or inappropriately applied (Utomi *et al.*, 2013, Utomi *et al.*, 2014). The introduction of appropriate scaling may help to reduce the debate around resistance trained athletes. The findings of Utomi *et al.* (2013) are important as they show that whilst there are increases in wall thickness and chamber dimensions they do not fall within the pathological range for cardiomyopathy. The majority of studies show no differences in systolic function at rest between resistance and endurance athletes as measured by EF (Utomi *et al.*, 2013). Whilst studies have found increased SV in endurance athletes, due to increased cavity dimensions, most studies suggest that LVEF is normal in athletes (Pluim *et al.*, 2000, Utomi *et al.*, 2013, Utomi *et al.*, 2014) however limited reports of reduced LV systolic function do exist (Abergel *et al.*, 2004). Some differences in diastolic function have been reported between endurance and resistance athletes as both LV E/A and LV E' were greater in endurance athletes than controls (Utomi *et al.*, 2013) and supernormal filling in athletes has been demonstrated before (Claessens *et al.*, 2001, D'andrea *et al.*, 2002, D'Ascenzi *et al.*, 2011), however these changes are often dependent on the parameter assessed and whilst improved diastolic filling has been observed in athletes at rest this finding is not consistent (George *et al.*, 2010). In a further study no changes were observed for diastology between resistance and endurance athletes (Utomi *et al.*, 2014). Studies report no difference in systolic and diastolic measurements by TDI (Baggish *et al.*, 2008a, Utomi *et al.*, 2014) however higher longitudinal systolic and diastolic velocities have been found in a study of endurance athletes compared to controls, interestingly with no change in EF (Florescu *et al.*, 2010). Differences observed in these studies may be related to inconsistent approach to scaling (Utomi *et al.*, 2014). Lack of scaling for body size or inconsistent methods of scaling also makes the comparison of results between studies more difficult. Echocardiographic indices can also be affected by volume load (Burns

et al., 2010a) and high intensity training (Banks *et al.*, 2010) therefore assessment should be made when the athlete is in the hydrated state and has refrained from exercise at least 6 hours.

2.5.2 The Relationship between Left Ventricular Structure and Function

Despite the literature regarding LV morphology and deformation in the AH there is no evidence to suggest the mechanisms behind the increased LV wall thickness, cavity size and LV mass and the maintenance of normal LV function. Some recent work on increases in LVH in pathological hypertension and LV function has been reported (MacIver, 2011) and the models of structure and function mechanisms reported may prove useful in understanding physiological adaptation of the LV in AH. Mathematical modelling of LV contraction has shown EF is determined by both myocardial shortening and diastolic wall thickness were augmented radial wall thickening may overestimate EF (MacIver, 2011). Mathematical modelling can assess effects of peak systolic wall strain and end diastolic wall thickness on EF and modelling suggests a near linear relationship between absolute wall thickening and EF suggesting that EF is determined predominantly by absolute wall thickening rather than relative wall thickness or strain (MacIver, 2011). More recently the paradox of reduced myocardial shortening in presence of preserved EF has been explained mathematically through geometric factors where EF can be constant for a large variation in shortening (Stokke *et al.*, 2017). Alterations in LV geometry may compensate for reduced shortening and measurement of EF may not accurately reflect overall ventricular systolic function. Longitudinal shortening may potentially be a more sensitive marker of systolic dysfunction which typically affects the subendocardial region first and if circumferential shortening is also reduced involving circumferential fibres in the

midwall may suggest transmural dysfunction (Stokke *et al.*, 2017). The authors therefore suggest that strain measurements reflect systolic function better than EF in patients with pathological LVH but preserved EF. Mathematical modelling has not been used to assess the relationship between structure and function in the physiologically remodelled AH but given the results from mathematical studies and the conclusion that ϵ is a better measurement of LV systolic function in patients with pathological LVH and normal EF it is a very interesting concept and will be explored in this research. STE may have the potential to reveal early sub-clinical markers of disease that may aid diagnosis during PCS.

2.5.3 Speckle Tracking Echocardiography and the Left Ventricle

LV global longitudinal strain (GLS) is the most frequently reported deformation parameter in clinical and athlete studies (Pelliccia *et al.*, 2017) and it is now considered a more sensitive measure of systolic function than EF in the identification sub-clinical LV dysfunction (Smiseth *et al.*, 2016). Recent meta-analyses and systematic reviews have highlighted a number of STE studies in athletes in comparison to controls, athletes of different sports and patients with cardiac disease (Beaumont *et al.*, 2017, D'Ascenzi *et al.*, 2016a). The findings are heterogeneous with some studies demonstrating higher GLS in athletes compared to controls (Vitarelli *et al.*, 2013, Simsek *et al.*, 2013) others showing no differences (Utomi *et al.*, 2014), Stefani *et al.*, 2009, Nottin *et al.*, 2009) and lower values in the athlete (Kansal *et al.*, 2011, Caselli *et al.*, 2015). This disparity is likely a consequence of a variation in LV structure secondary to the training type and volume. Variable ϵ parameters were found when assessing different sporting disciplines which were subsequently normalised following indexing for LV end diastolic volume (Oxborough *et al.*, 2016). In addition, a recent publication demonstrates a clear relationship between LV morphology, strain

and ejection fraction (Forsythe *et al.*, 2018). Female athletes have also been found to have higher GLS than male athletes (Giraldeau *et al.*, 2015) suggesting further research is also needed in STE and gender differences. In a longitudinal training study of athletes (soccer, basketball and volleyball) involved in an 18 week training study, only a mild increase in GLS, associated with HR and LV size, was observed despite significant increases in LV mass, LVIDd and systolic volume (D'Ascenzi *et al.*, 2015a). Recent European guidelines (Pelliccia *et al.*, 2017) demonstrate that GLS in the general population, can be variable, as in athletes, and the current normal GLS range has been reported as -16% to -22% with a mean of -20%.

When considering the differentiation from pathology, a study of athletes, controls and hypertensive patients (Cappelli *et al.*, 2010) demonstrated a significantly lower GLS in hypertension patients with other studies demonstrating similar findings (Galderisi *et al.*, 2010). These studies highlight the potential of STE and a reduction in GLS as an early sign of LV dysfunction. Patients with HCM have been found to have lower GLS compared to controls (Soullier *et al.*, 2012) with Kansal *et al.* (2011) and Butz *et al.* (2011) demonstrating lower GLS in HCM patients compared to athletes. In a study of dilated cardiomyopathy (DCM) patients, decreased GLS was observed even in the setting of normal EF highlighting the potential of GLS as an early marker of DCM and in serial assessment of systolic function (Okada *et al.*, 2012). The reduction in GLS in hypertensive, DCM and HCM patients has prognostic significance suggesting a maladaptive association with cardiovascular pathology and therefore offers potential in the differentiation of these conditions from AH. STE may therefore improve the sensitivity and specificity for the differentiation of cardiomyopathy identifying subtle structural-functional alterations. Based on this the European guidelines suggest that GLS of less than -15% may be indicative of myocardial disease

(Pelliccia *et al.*, 2017). The likelihood of pathology is raised when a low GLS is seen alongside increases in relative wall thickness and/or significant LV dilatation (Kansal *et al.*, 2011, D'Ascenzi *et al.*, 2016a).

There are few studies reporting global circumferential strain (GCS) and radial strain (GRS) in athletes. From existing studies, Nottin *et al.* (2008) reported little or no differences in circumferential ϵ but observed lower peak apical radial ϵ during systole in cyclists compared to controls. No differences in GCS or GRS were reported in a study of sedentary and trained subjects (Donal *et al.*, 2011) and likewise no differences in GCS and GRS were reported in athletes from different sporting categories (endurance, strength, mixed) compared to controls (Vitarelli *et al.*, 2013). Szauder *et al.* (2015) however reported that bodybuilders have lower GCS than marathon runners which is also supported by data from Utomi *et al.* (2014). The recent meta-analysis (Beaumont *et al.*, 2017) concluded that there are no differences in GCS between athletes and controls but when categorised for sporting type, resistance athletes have lower values creating a diagnostic quandary in those athletes involved with this specific training stimulus.

GCS and GRS was found to be similar between controls, rowers and early hypertensive patients (Galderisi *et al.*, 2010). Patients with HCM have been found to have lower values of LV longitudinal and radial strains and increased circumferential strains compared to controls (Soullier *et al.*, 2012). In a study of STE between soccer players, HCM patients and controls, radial strains were significantly higher in athletes than controls, but compared to HCM patients athletes had higher values of radial and circumferential ϵ (Richard *et al.*, 2007) meaning therefore that a disproportionate shift in mechanics may provide additional differential utility.

Few studies have examined comprehensive regional STE data across longitudinal, circumferential and radial planes (Baggish *et al.*, 2008b, Forsythe *et al.*, 2018) but heterogeneity in ϵ has been reported in all planes and is likely related to physiological structural remodelling. Knowledge of normal physiological regional adaptation may add additional relevant information when investigating abnormal global parameters. Further studies of regional assessment in all cardiac planes of motion in athletes involved in a range of sporting disciplines would provide valuable information in this regard.

Intra-observer reliability of LV ϵ has been previously reported as good to very good with intraclass correlation coefficient (ICC) values of 0.714 - 0.807. Radial ϵ however was inferior in terms of coefficients of variation (CoV) at 19% (Oxborough *et al.*, 2012b). Left ventricular ϵ data from a range of studies based on athletes' of different sporting disciplines is summarised in table 2.1.

LV twist from helically orientated fibres is a key component of myocardial performance and can be determined by STE. The technique has been found to be concordant with torsion measurements from tagged MRI studies in patients with a variety of cardiac pathologies (Notomi *et al.*, 2005). In a number of studies twist and apical rotation has been found to be lower in endurance (cyclists) compared to strength (weightlifters) athletes and controls despite any difference in longitudinal ϵ (Santoro *et al.*, 2014a). Similarly twist and apical rotation was lower in rugby football league (RFL) athletes compared to controls and associated with an increase in basal rotation and no change in longitudinal ϵ (Forsythe *et al.*, 2018). Also in an exploratory study, lower twist and apical rotation were observed in native Hawaiian and Pacific Island RFL athletes compared to Caucasian counterparts, suggesting there may also be significant ethnic differences (Johnson *et al.*, 2018). Lower apical rotation and twist

has been observed in amateur swimmers of different ages (16-48 years) with higher longitudinal ϵ compared to controls (Santoro *et al.*, 2015). Similarly, lower values of twist have reported in soccer players (Zócalo *et al.*, 2008) and cyclists compared to controls (Nottin *et al.*, 2008). The reduction in twist appears to be predominantly driven by reduced apical rotation and it has been reported that the LV apex may be more dependent on sympathetic activity than the LV base (Nottin *et al.*, 2008). This equivocal finding may be related to training induced sympatho-vagal balance and could be interpreted as a functional reserve to aid oxygen and substrate delivery to the muscle during exercise (D'Ascenzi *et al.*, 2016a). In contrast, higher twist has been exhibited in endurance (marathon runners) and mixed trained (martial arts) athletes compared to controls (Vitarelli *et al.*, 2013) and further evidence of higher twist in resistance athletes compared to controls was reported by Beaumont *et al.* (2017). Whilst the evidence suggests that twist appears to be lower in endurance athletes, some data would suggest an increase in twist in resistance athletes is a normal phenomenon. There are few longitudinal studies assessing LV twist but there is evidence of a phasic phenomenon in twist parameters. In rowers, following 3 months of training twist was higher than baseline but after 39 months, twist was lower suggesting both acute and chronic exercise effects on this parameter (Weiner *et al.*, 2015).

LV twist was found to be increased in hypertension patients compared to controls with no difference between athletes and controls (Cappelli *et al.*, 2010) but in contrast twist has been also been found to be similar in athletes, controls and newly diagnosed hypertensive patients (Galderisi *et al.*, 2010). The authors suggested that an increase in twist with pathology and a preserved EF could be an early indicator of systolic dysfunction as the LV compensates for a reduction in longitudinal function in pathological LVH (Santoro *et al.*, 2014b) and may therefore twist may have some

diagnostic value in the PCS setting. No differences in twist, apical or basal rotation parameters were observed in a study between athletes, HCM patients and controls (Kovacs *et al.*, 2014). However despite this, peak twist occurred after aortic valve closure exclusively in HCM patients suggesting a late, lower and slower untwist may be able to differentiate from pathology. In contrast, untwist was higher in elite athletes occurring earlier and faster. Untwist and untwist rate correlated with E/A ratio and the early diastolic phase was the most discernible component of the cardiac cycle (Kovacs *et al.*, 2014). Similarly, Pacileo *et al.* (2011) have demonstrated prolonged LV twist in cardiomyopathies. These studies indicate the potential clinical benefit of twist and untwist in differential diagnosis, not only by the use of peak values but also through a temporal assessment. Peak basal and apical rotation have demonstrated quite high variability whilst torsion had low variability and excellent agreement intraclass correlation coefficient (ICC) of 0.940 and coefficients of variation (CoV) of 10% (Oxborough *et al.*, 2012b). Twist data from a range of studies based on athletes of different disciplines is summarised in table 2.1.

Table 2.1 Relevant LV STE athlete studies from the literature (Table adapted from Pelliccia *et al.*, 2017 and Beaumont *et al.*, 2017)

STE	Author	Year	n	Sporting Discipline	ϵ / Twist
LV Longitudinal	Nottin <i>et al</i>	2008	16	Cyclists	-19.2 ± 1.9 %
	Cappelli <i>et al</i>	2010	50	Endurance Athletes	-18.4 ± 3 %
	Galderisi <i>et al</i>	2010	22	Rowers	-22.2 ± 2.7 %
	Donal <i>et al</i>	2011	18	Cyclists	-17.0 ± 1.3 %
	Simsek <i>et al</i>	2013	22	Marathon Runners	-22.3 ± 2.2 %
	Simsek <i>et al</i>	2013	24	Wrestlers	-21.8 ± 1.7 %
	Vitarelli <i>et al</i>	2013	35	Marathon Runners	-21.7 ± 2.6 %
	Vitarelli <i>et al</i>	2013	35	Power Lifters	-22.5 ± 2.4 %
	Vitarelli <i>et al</i>	2013	35	Martial Artists	-21.6 ± 2.2 %
	Caselli <i>et al</i>	2014	200	Olympic Athletes	-18.1 ± 2.2 %
	Santoro <i>et al</i> (a)	2014	33	Cyclists	-16.5 ± 1.7 %
	Santoro <i>et al</i> (a)	2014	36	Weight-Lifters	-16.6 ± 2.1 %
	Santoro <i>et al</i> (b)	2014	45	Water Polo Players	-19.2 ± 5.0 %
	Szaunder <i>et al</i>	2015	24	Ultra-marathon Runners	-19.4 ± 3.4 %

	Szauder <i>et al</i> Santoro <i>et al</i>	2015 2015	14 125	Body Builders Swimmers	-23.3 ± 2.1 % -20.4 ± 2.5 %
LV Circumferential	Galderisi <i>et al</i> Donal <i>et al</i> Vitarelli <i>et al</i> Vitarelli <i>et al</i> Vitarelli <i>et al</i> Szauder <i>et al</i> Szauder <i>et al</i>	2010 2011 2013 2013 2013 2015 2015	22 18 35 35 35 24 14	Rowers Cyclists Marathon Runners Power Lifters Martial Artists Ultra-marathon Runners Body Builders	-17.7 ± 2.5 % -17.4 ± 3.3 % -22.9 ± 3.3 % -24.1 ± 2.7 % -22.6 ± 3.6 % -26.6 ± 3.8 % -22.4 ± 4.3 %
LV Radial	Nottin <i>et al</i> Galderisi <i>et al</i> Donal <i>et al</i> Vitarelli <i>et al</i> Vitarelli <i>et al</i> Vitarelli <i>et al</i> Szauder <i>et al</i> Szauder <i>et al</i>	2008 2010 2011 2013 2013 2013 2015 2015	16 22 18 35 35 35 24 14	Cyclists Rowers Cyclists Marathon Runners Power Lifters Martial Artists Ultra-Marathon Runners Body Builders	42.2 ± 11.2 % 47.6 ± 19.1 % 38.7 ± 7.8 % 46.9 ± 9.4 % 49.6 ± 8.5 % 47.5 ± 8.7 % 42.5 ± 5.5 % 44.2 ± 8.2 %
LV Twist	Nottin <i>et al</i> Galderisi <i>et al</i> Vitarelli <i>et al</i> Vitarelli <i>et al</i> Vitarelli <i>et al</i> Kovacs <i>et al</i> Santoro <i>et al</i> (a) Santoro <i>et al</i> (a) Santoro <i>et al</i> (b) Santoro <i>et al</i>	2008 2010 2013 2013 2013 2014 2014 2014 2014 2015	16 22 35 35 35 28 33 36 45 125	Cyclists Rowers Marathon Runners Power Lifters Martial Artists Kayak, Canoe and Rowers Cyclists Weight-Lifters Water Polo Players Swimmers	6.0 ± 1.8° 9.2 ± 2.0° 21.5 ± 5.2° 15.8 ± 4.5° 20.8 ± 5.4° 6.4 ± 2.1° 6.2 ± 1.1° 12.0 ± 2.1° 8.8 ± 3.6° 9.0 ± 3.8°

Whilst comprehensive SR data in athletes is less frequently reported there have been reports of increased variability in SR indices compared to ϵ , with radial SR performing least favourably (Oxborough *et al.*, 2012b). An increase in SRS associated with an increase in GLS has been reported in both endurance and power athletes compared to controls (Simsek *et al.* 2013) but in contrast, athletes of endurance disciplines exhibited lower GLS with lower SRS and SRE (Caselli *et al.*, 2015). A finding of lower peak longitudinal ϵ in resistance athletes compared to endurance athletes has been associated with lower longitudinal SRE and SRA in resistance athletes compared to controls. In the same study, a lower basal circumferential ϵ in resistance athletes

compared to endurance athletes was associated with lower basal circumferential SRS (Utomi *et al.*, 2014). The heterogeneous findings and lack of normative ranges for both adults and athletes have led to under reporting of reporting of global and regional SR parameters in STE studies. SR together with ϵ have a potential use in differentiation between physiology and pathology and have been used in assessment of cardiomyopathy patients to detect regional myocardial impairment despite normal EF. ϵ and SR alterations have been suggested to represent mechanical adaptation to subclinical systolic abnormalities (Pacileo *et al.*, 2011). ϵ and SR have been reported to be reduced in HCM patients even in the absence of myocardial fibrosis on cardiac magnetic resonance imaging (Yang *et al.*, 2003) and before development of increased wall thickness (Elliott *et al.*, 2014).

2.5.4 Conventional Echocardiography and the Right Ventricle

Fewer studies have addressed the impact of chronic exercise exposure on the right heart however RV cardiac adaptation to exercise has been reported to be due to increased preload and a disproportionate load compared to the LV (La Gerche *et al.*, 2011). The RV responds to endurance training with a balanced increase in mass and volume, maintaining a constant mass to volume ratio, consistent with eccentric hypertrophy (Arbab-Zadeh *et al.*, 2014). RV adaptation has been found to be greater in athletes involved in sports with a high dynamic component such as rowing and cycling and soccer and little evidence of significant RV adaptation in resistance based athletes (D'Andrea *et al.*, 2013). This may be explained by the fact that the pulmonary circulation and right side of the heart are shielded from the exercise induced stress of systemic hypertension by the mitral valve (Weiner and Baggish 2012). There is no current evidence to suggest that athletes develop RV concentric hypertrophy.

Similarly to the LV, there appears to be eccentric hypertrophy of the RV, which has led to suggestions that endurance based remodelling is a balanced biventricular phenomenon (Scharhag *et al.*, 2002). Recent echocardiographic studies by Oxborough *et al* (2012a) and D'Andrea *et al.* (2013) have demonstrated larger RV cavities, and inflow and outflow dimensions in endurance athletes compared to resistance athletes with RV chamber sizes in resistance athletes reported to be similar to sedentary controls (D'andrea *et al*, 2013). An increased RV:LV ratio reported in endurance athletes suggests that remodelling however may be unequal (Oxborough *et al.*, 2012a) and a 12 month study reported RV eccentric hypertrophy and progressive increases in RV:LV ratio in response to high dynamic training again suggesting disproportionate loading as a stimulus for more marked RV dilatation (Arbab-Zadeh *et al.*, 2014). There are few studies of the RV in resistance athletes (Utomi *et al.*, 2013) but in a 6 month study by Spence *et al.* (2011) no increases in RV cavity dimensions were seen in participants completing a period of resistance training (Spence *et al.*, 2011). These findings produce a diagnostic dilemma in the differentiation of physiological remodelling as although the RV outflow is generally larger than the normal population the RV inflow is generally dilated to a greater degree (Oxborough *et al.*, 2012a). Increased RV size has been observed in endurance athletes compared to controls and RV inflow higher in endurance than resistance athletes (Utomi *et al.*, 2015). In a large study of Olympic athletes (D'Ascenzi *et al.*, 2017b) RV remodelling was assessed in a variety of sporting disciplines characterised into skill, power, mixed and endurance sports. Approximately one third (32%) of athletes presented with RV dimensions exceeding reference normal values (Marcus *et al.*, 2010, Rudski *et al.*, 2010, D'Ascenzi *et al.*, 2017b) with 4% of these meeting major task force criteria (Marcus *et al.*, 2010) for ARVC. Endurance sport was found to be associated with the largest

RV dimensions despite increases in the other disciplines and this was reported to be due to the extent of haemodynamic overload associated with type of sport. A symmetric remodelling of the RV was witnessed with the RV inflow to outflow ratio remaining unchanged across different disciplines (D'Ascenzi *et al.*, 2017b). ARVC patients often present with increased RVOT compared to RV inflow (Bauce *et al.*, 2010) so RVOT size may be an appropriate criterion to help distinguish AH from ARVC. Disproportionate RVOT enlargement is unlikely to represent physiological remodelling and a balanced biventricular enlargement was seen in athletes of all disciplines measured by RV:LV ratio (D'Ascenzi *et al.*, 2017b). A recent meta-analysis of normative RV values for athletes of different sporting disciplines has been performed (D'Ascenzi *et al.*, 2017a). Athletes were divided into 4 groups – endurance, strength, mixed and combined. Combined athletes (including triathlon, rowing and canoeing) showed a greater extent of RV remodelling including RV areas and basal and mid cavity diameter. Strength athletes had the lowest areas and diameters however RVOT did not vary between groups (D'Ascenzi *et al.*, 2017a). $RVOT_{plax}$ and $RVOT_1$ in athletes in the cohort were larger than normal references values however when indexed or BSA whilst the RVOT in athletes was greater than that for minor ARVC criteria but RVOT was in normal limits when considering major ARVC criteria (D'Ascenzi *et al.*, 2017a). Thus the authors suggest comparisons to ARVC major criteria to reduce false positive results in athletes and they confirm that the current RV guidelines (Rudski *et al.*, 2010) cannot be used for athlete population (D'Ascenzi *et al.*, 2017a).

A critical step in the differential diagnosis of RV remodelling is in the assessment of RV function. ARVC often results in systolic impairment in function either regional or global (Marcus *et al.*, 2010). It is therefore important to assess RV function by a

number methods including tricuspid plane systolic excursion (TAPSE), RV fractional area change (RVFAC), RV tissue Doppler velocities. Despite changes in RV morphology RV systolic function as measured by RVFAC and TDI S' remain largely unchanged in athletes of different discipline (D'Ascenzi *et al.*, 2017b). Little attention has been paid to appropriate scaling of RV cardiac parameters and similarly to the LV, appropriate scaling could aid interpretation of the athletes heart (Utomi *et al.*, 2015) especially in differential diagnosis. In the study by D'Ascenzi *et al.* (2017b) lower RVFAC has been observed in in all groups except the mixed exercise group and whilst other functional parameters did not change between groups this confirms the uncertainties of applying only RVFAC to functional assessment. This slight reduction in RVFAC has been proposed as a possible physiological adaptation to training (D'Ascenzi, *et al.*, 2017b) however in contrast no differences in RV function were observed between endurance and resistance athletes and controls (Utomi *et al.*, 2015).

2.5.5 Speckle Tracking Echocardiography and the Right Ventricle

Normal resting RV ϵ parameters in endurance athletes (Oxborough *et al.*, 2012a) have been reported to fall within the reported normal population range (-18 to -39%) (Rudski *et al.*, 2010). In contrast there are reports of a higher global RV ϵ in top level rowers compared to sedentary controls (Esposito *et al.*, 2014). Conversely, lower RV ϵ has been reported in elite endurance athletes compared to controls, specifically in those athletes with an associated dilated RV cavity. This was due to lower basal strain, (Teske *et al.*, 2009b) a finding that was reproduced in a subsequent study but with the additional finding of an increase in apical segment strain (La Gerche *et al.*, 2012). A normal base to apex ϵ gradient has been observed (Teske *et al.*, 2009b, La Gerche *et al.*, 2012) and whilst this gradient was also observed by Utomi *et al.* (2015) no regional differences in RV ϵ were found in this study. Studies also report no differences in RV

ϵ between endurance and strength based athletes (Pagourelas *et al.*, 2013, Utomi *et al.*, 2015). Lower RV ϵ has been observed in endurance (marathon runners), strength (power lifters) and mixed trained athletes (Martial arts) with increases observed with exercise (Vitarelli *et al.*, 2013). In a seasonal study, despite increases in RV size in basketball and volleyball players during the season, RV function and global RV ϵ did not change. However there were some regional changes with RV apical ϵ increasing from pre-season to end season (D'Ascenzi *et al.*, 2016b). It is clear that, similarly to the LV, RV longitudinal ϵ is variable and may well be related to RV enlargement / geometry (Qasem *et al.*, 2018). Global RV ϵ rarely falls outside of normal range but the regional changes at the apex and base may compound the diagnostic differentiation particularly as regional abnormalities have been identified in asymptomatic patients who are carriers of genetic mutations for ARVC (Teske *et al.*, 2009a). Recent studies reporting RV ϵ values for athletes' of different sporting disciplines are summarised in table 2.2.

Table 2.2 Relevant RV STE athlete studies from the literature (Table adapted from Pelliccia *et al.*, 2017)

STE	Author	Year	n	Sporting Discipline	ϵ
RV Longitudinal	Teske <i>et al</i> (b)	2009	58	Endurance Athletes	$-28.5 \pm 2.9 \%$
	Teske <i>et al</i> (b)	2009	63	Olympic Endurance Athletes	$-27.6 \pm 3.1 \%$
	Oxborough <i>et al</i> (a)	2012	102	Endurance Athletes	$-27.0 \pm 6.0 \%$
	Pagourelas <i>et al</i>	2013	80	Endurance Athletes	$-23.1 \pm 3.7 \%$
	Pagourelas <i>et al</i>	2013	28	Strength Athletes	$-25.1 \pm 3.2 \%$
	Esposito <i>et al</i>	2014	40	Rowers	$-29.1 \pm 4.1 \%$
	D'Ascenzi <i>et al</i> (a)	2016	29	Mixed Sport Disciplines	$-28.7 \pm 4.9 \%$ (pre-season)
					$-29.2 \pm 4.1 \%$ (mid-season)
$-30.0 \pm 3.7 \%$ (end-season)					

Peak systolic RV ϵ is significantly reduced in ARVC patients compared to controls and RV STE has been used to identify regional wall abnormalities in patients making STE superior to conventional echocardiography in identifying the disease (Teske *et al.*, 2009a). Compared to the LV, there are limited RV STE studies in athletes and there is a lack of universally accepted cut-off values (Pelliccia *et al.*, 2017). A recent and large meta-analysis of RV structure and function in ARVC (Qasem *et al.*, 2016) also concluded that RV ϵ is significantly lower in ARVC patients compared to controls with a range of RV ϵ in controls of -27 to -31% and in ARVC patients of -13 to -21%. A cut-off for pathology of -21% was therefore suggested.

Basal RV ϵ and SRS have been found to be reduced in endurance athletes compared to controls (La Gerche *et al.*, 2012) similar to a finding by Teske *et al* (2009b) who reported reduced basal RV ϵ and SRS in athletes with a dilated RV. In contrast similar ϵ values were found between athletes and non-athletes but increased global SRS in resistance athletes (Pagourelas *et al.*, 2013). A more recent study also reported no differences in ϵ and SRS between endurance and resistance athletes and controls

(Utomi *et al.*, 2015). RV ϵ and SRS imaging is being increasingly used to objectively quantify regional RV dysfunction (Pelliccia *et al.*, 2017) especially as ϵ and SRS indices have been found to be lower in all regional segments of the RV wall in ARVC patients compared to controls (Teske *et al.*, 2009a). Excellent reproducibility has been observed for RV ϵ , intraclass correlation coefficient (ICC) of 0.834 and coefficients of variation (CoV) of 7%. RV SR has been found to be more variable with generally acceptable ICC and CoV (Oxborough *et al.*, 2012b).

2.5.6 Conventional Echocardiography and the Atria

There is limited data pertaining to the left and especially the right atrium in the assessment of the athletes' heart. Left atrial (LA) enlargement has been described in athletes engaged in high dynamic training (Pelliccia *et al.*, 2005, McClean *et al.*, 2015). In a study of professional footballers morphological and functional LA remodelling was induced by dynamic training with increases in reservoir (maximal filling) and conduit (passive emptying) volumes but stable active (active emptying/booster) volumes. There was a regression in LA remodelling with de-training (D'Ascenzi *et al.*, 2015c). McClean *et al.* (2015) also report that LA size is consistently larger throughout the cardiac cycle associated with high dynamic training and similarly RA enlargement due to this type of exercise has also been observed supporting the previously reported concept of 'bi-atrial' hypertrophy of the myocardium (Utomi *et al.*, 2013). Chronic high dynamic training also contributed to LA and RA function with improvements in volumetric flow. There were increased functional volumes in the LA and RA with high dynamic, high static athletes who showed higher passive and active emptying volumes compared with low dynamic, high static athletes and controls whilst also demonstrating a larger reservoir for pulmonary venous return during LV contraction and isovolumetric relaxation

(McClellan *et al.*, 2015). There is some evidence to suggest that LA dilatation seen in chronic athletic adaptation leads to increased prevalence of atrial fibrillation (Turagam *et al.*, 2012, La Gerche and Schmied, 2013). Atrial enlargement is a manifestation in many cardiac diseases so differential diagnosis will be important in some cases, however, these conditions are more likely to manifest with a decrease in reservoir and conduit volumes and an increase in active pump volume to compensate for increased LV filling pressures (D'Ascenzi *et al.*, 2015c). Increased RA size has been documented in endurance and strength based athletes with the biggest increases found in endurance athletes (D'Andrea *et al.*, 2013, D'Ascenzi *et al.*, 2017b).

Echocardiography is very useful in cardiac assessment of athletes heart however due to the controversies and debate around normal cardiac adaptation to endurance and resistance exercise the potential for mis-diagnosis in athletes should not be overlooked (La Gerche *et al.*, 2013). When the complex anatomy of the heart is considered it is more apparent why the additional use of novel echocardiographic techniques may aid cardiac assessment in athletes.

2.5.7 Age Related Variation

PCS is aimed at athletes aged 14-35 years however much less attention has been paid to cardiac evaluation in adolescents in comparison to senior athletes. Recently, a large systematic review of SCD in a general athletic population reported the mean age at death to be 17 years (Harmon *et al.*, 2014) supporting the need for understanding the cardiac adaptation to training of this group in order to support PCS in this population. There is no current universally accepted consensus as to the impact of the athletes age on the classification of normal/abnormal findings (Harmon *et al.*, 2014). There are only a few studies in adolescent athletes (Sharma *et al.*, 1999, Sharma *et al.*, 2002,

George *et al.*, 2001 Makan *et al.*, 2005, Sheikh *et al.*, 2013) and LV cavity and wall thicknesses have been found to be increased compared to controls but less pronounced compared to senior athletes, likely reflecting the lack of physical maturity and fewer cumulative training hours (Makan *et al.*, 2005, Sharma *et al.*, 2002, Sheikh *et al.*, 2013). The RV and atria in adolescent athletes have received less attention than the LV although both have been shown to increase in size throughout adolescence (George *et al.*, 2001). Increases in left atrial size have been documented in adolescent soccer players (D'ascenzi *et al.*, 2012) and increased bi-atrial and RV size has been reported in pre-adolescent athletes (D'Ascenzi *et al.*, 2016c, D'Ascenzi *et al.*, 2017c).

Conventional measures of LV systolic function have been demonstrated to be similar between sedentary young individuals, junior athletes, sedentary older individuals and master athletes (Makan *et al.*, 2005, Sharma *et al.*, 2002). LV diastolic function has been demonstrated to be supernormal (Claessens *et al.*, 2001, D'Ascenzi *et al.*, 2011) or normal in the elite athlete (Pluim *et al.*, 2000, Sharma and Maron, 2002) however the impact of the athletes' age has not been studied.

Information regarding mechanical function in junior athletes is limited (De Luca *et al.*, 2011, Simsek *et al.*, 2013) but from what we know of cardiac mechanics in adult athletes it would seem pertinent to describe similar functional data in a junior athletic population. Whilst there are few studies of age related difference in STE, a study of young and old athletes and controls (Donal *et al.*, 2011) longitudinal, circumferential and radial ϵ was found to be similar at rest but longitudinal ϵ was greater during exercise in younger athletes compared to older athletes and young and old controls. In this study there were no differences in EF despite some ϵ differences during exercise and EF was concluded to be a poor measure of contractile function (Donal *et al.*, 2011). Again this highlights the dangers of only using one global, functional parameter

in cardiac assessment and the potential of STE. LV twist in a non-athletic population has been reported to increase from early to advancing age, commonly due to greater apical rotation (Notomi *et al.*, 2006, Van Dalen *et al.*, 2008, Kaku *et al.*, 2014) but the training effect on twist parameters in adolescents is unknown.

2.5.8 Seasonal Related Variation

Most large studies of AH are cross sectional in design studies with much less focus on longitudinal or seasonal studies. Variation in cardiac adaptation has been associated with progression of the competitive sporting season (D'Ascenzi *et al.*, 2015a) and is an important consideration when undertaking a serial athlete assessments during PCS to ensure accurate and reproducible measurements. It is as yet undetermined as to whether conducting PCS at different time points in the competitive athletic season would make a difference to the outcome of PCS. The theory that there may be a seasonal difference stems from the different training strategies and training loads at different times of the season. There are limited echocardiographic longitudinal studies relating to dynamic cardiac adaptation over time or due to varying training intensities (D'Ascenzi *et al.*, 2015, Baggish *et al.*, 2008a, Fagard *et al.*, 1983, Abergel *et al.*, 2004, Csajági *et al.*, 2015, Weiner *et al.*, 2015). Changes in cardiac adaptation in non-chronically trained athletes after structured exercise training have been described (Baggish *et al.*, 2008a, Spence *et al.*, 2011) and LV cavity dilatation has been observed in elite Tour de France cyclists over a period of years associated with reduced LV wall thickness and a reduction in LVEF in some participants (Abergel *et al.*, 2004). Cardiac adaptation within the competitive season has been reported in competitive cyclists with a decreased LV wall thickness and a slight decrease in LV systolic function in the resting season (Fagard *et al.*, 1983) and in elite male soccer players increased LV mass was observed within the competitive season with regression reported with

detraining (D'Ascenzi *et al.*, 2015a, Cabanelas *et al.*, 2012). Increased LV mass and wall thickness has been observed in elite adolescent swimmers in the endurance phase of training but without change in LV mass index (Csajági *et al.*, 2015).

In one study of RV adaptation across during the competitive season (D'Ascenzi *et al.*, 2016b) in basketball and volleyball players, RV size was found to increase during the season as measured by RV basal and mid end diastolic cavity dimensions and RV area. However interestingly RVOT did not change across the season. Standard measures of RV systolic and diastolic function did not change (D'Ascenzi *et al.*, 2016b).

Scarce longitudinal studies of STE exist regarding the timing or extent of training induced adaptation over longer periods of time (D'Ascenzi *et al.*, 2016a) and fully comprehensive studies are lacking. In an exercise training study, subjects assigned to either endurance or resistance training, LV longitudinal strain did not change from baseline despite changes in LV mass and volumes (Spence *et al.*, 2011). As well as being limited, previous longitudinal cardiac mechanics studies show mixed results (D'Ascenzi *et al.*, 2015b, Baggish *et al.*, 2010, Weiner *et al.*, 2015, Baggish *et al.*, 2008b, Weiner *et al.*, 2010). In a study of athletes (soccer, basketball and volleyball) involved in an 18 week training study only a mild increase in global longitudinal LV ϵ , associated with HR and LV size, was observed despite significant increases in LV mass, LVIDd and systolic volume (D'Ascenzi *et al.*, 2015b). Echo performed pre and post 90 days of endurance training in rowers found that whilst LVEF remained unchanged there were changes in other indicators of systolic function (Baggish *et al.*, 2008b). Increases in peak systolic TDI and radial and longitudinal ϵ in all segments with a base to apex gradient. Circumferential ϵ increased in LV free wall but decreased in regions adjacent to RV possibly secondary to RV adaptation (Baggish *et al.*, 2008b).

Importantly these functional systolic changes were not detected by conventional echocardiographic measurements (Baggish *et al.*, 2008b).

A phasic response to cardiac remodelling has been reported in competitive rowers. In the acute augmentation phase of exercise training (90 days) an increase in twist was reported. Follow up of these athletes at 39 months revealed a regression of twist following the chronic phase of adaptation (Weiner *et al.*, 2015). These rowers were however university athletes and not elite athletes therefore it is not known if this would be the same result in elite athletes.

Despite increases in RV size in basketball and volleyball players during the season, RV function and global RV ϵ did not change. There were however some regional changes RV apical ϵ increasing from pre-season to end season (D'Ascenzi *et al.*, 2016b). This is relevant as regional abnormalities have been identified in asymptomatic patients who are carriers of genetic mutations for ARVC (Teske *et al.*, 2009a) therefore a knowledge of seasonal variation in RV deformation is important for timing of PCS.

LA volumes have been assessed in soccer players in pre-season, mid-season, end season and post detraining period (D'Ascenzi *et al.*, 2015c) and LA volumes were found to be significantly increased at mid and end season compared to pre-season. Echocardiographic studies pre and post 16 weeks of training in female volleyball athletes reported increases in both LA and RA volume index with the authors concluding that bi-atrial remodelling occurs in a model of volume rather than pressure overload (D'Ascenzi *et al.*, 2014).

There is a lack of studies concerned with the comprehensive cardiac assessment of the holistic heart during the competitive season and future studies may help elude to

possible mechanisms of cardiac adaptation to exercise and may have important consequences for PCS.

2.6 Conclusion

It is apparent from this review that much variation exists in the assessment of AH and cardiac parameters in athletes and in order to effectively carry out PCS or cardiac investigation in athletes it is pertinent to understand cardiac structure and function in athletes from individual sports by considering each sporting discipline separately. The emphasis of this thesis is on the characterisation of the male, Rugby Football League (RFL) athletic heart phenotype. RFL is a high intensity collision sport completed over 80 minutes and rugby sits in the centre of the classification of sports (Levine *et al.*, 2015) and RFL athletes therefore provide an excellent model for assessment of the athletes' heart due to the concomitant dynamic and static components of the sport and the mixed resistance and endurance components of their training programmes. To our knowledge there are no comprehensive studies of athletic cardiac adaptation in the RFL athlete. PCS is mandatory for RFL athletes competing in the professional Super-league and the recent occurrence of high profile SCD of athletes in the sport suggest the need for detailed cardiac investigation to gain knowledge and understanding of the normal phenotype of physiological cardiac adaptation of these athletes. It is essential during PCS of athletes that normal physiology can be discerned from potentially life threatening pathological conditions related to SCD.

The subsequent chapters of this thesis focus on the structural and functional assessment of the heart of the RFL athlete using standard 2D TTE and by novel assessment of cardiac mechanics utilising STE. Including STE in echocardiographic assessment will give a greater understanding of cardiac adaptation in RFL athletes and

help to relate structural with functional adaptation. It will provide a unique and comprehensive set of sport specific echocardiographic data for RFL athletes.

Whilst the development of normative cardiac parameters for athletes in specific sports will aid PCS, STE although not currently, routinely used in PCS protocols has the potential to become an important diagnostic tool in PCS differential diagnosis. The potential of STE in the assessment of patients with cardiac disease alongside emerging understanding of the structure and functional relationships in pathology has helped to build the rationale for chapter 4; a cross-sectional study of structure and function of the LV in senior RFL athletes using novel mathematical modelling to investigate the structure-function relationship and chapter 5; a cross sectional study of the RV in senior RFL athletes. Evidence suggests increasing RV size in athletes overlaps with ARVC criteria and in order to differentially diagnose between physiology and pathology accurate functional assessment is key. STE therefore provides an important functional assessment with the ability to measure both global and regional function and may be able to detect sub-clinical dysfunction. However this will only be possible in the future if normative physiological STE parameters are developed. Junior/adolescent athletes are also involved in PCS despite limited comprehensive cardiac assessment in this age group. This provides the rationale for chapter 6; a comparative study of cardiac parameters across all chambers of the heart in senior and junior athletes using TTE and STE. Although study design in this thesis is largely cross sectional in nature, given the limited comprehensive assessment of cardiac variation associated with the competitive season and the importance that this might have for timing of PCS, the rationale for chapter 7 was developed; the investigation of seasonal cardiac variation in senior RFL athletes.

Data presented in this research will help to inform normal physiological adaptation to exercise in RFL athletes and may aid clinical decisions in those athletes where cardiac parameters fall into an area of diagnostic uncertainty, the ‘grey area’, between what is considered normal physiological athletic adaptation and pathological cardiac disease.

Chapter 3

General Methods

The general methods chapter describes procedures common to studies within this thesis. Any alternate methods are described in the relevant study chapter. This section contains preliminary information and details of specific echocardiographic procedures.

3.1 Preliminary information

3.1.1 *Ethics Approval*

The studies that are included in this thesis gained full ethics approval from Liverpool John Moores University (LJMU) ethics committee (approval number 11/SPS/045) and the Health Research Authority (HRA) (approval number 16/L0/2245). (See Appendix 1 for ethics approval documentation).

3.1.2 *Population*

Male volunteers aged between 14-35 years participated in these studies and included rugby football league (RFL) athletes and age and gender matched sedentary controls. Participant information sheets were provided to all volunteers and full informed written consent was obtained from all participants before data collection commenced. Participants also completed a cardiac screening questionnaire which documented participant demographics, previous medical history and any current medication, previous cardiac history or cardiac symptoms and any medication and any family history of cardiac disease. Training history of all participants was also recorded (See Appendix 2 for documentation).

Inclusion criteria for RFL athletes

- Male

- Elite (professional athlete at national or international level) rugby football league players aged between 14 and 35 years
- Participating in structured physical training for a minimum of 10 hours per week

Exclusion criteria for RFL athletes

- History of hypertension, valve disease, Ischaemic heart disease, diabetes, respiratory disease, endocrine disease, liver disease or renal disease.
- Smoker
- Age <14 and >35 years
- Taking long-term medication
- Undertakes less than 10 hours per week of structured physical training.

Inclusion criteria for sedentary controls

- Male
- Sedentary individuals aged between 14-35 years
- Participating in physical training for no more than 3 hours per week

Exclusion criteria for sedentary controls

- History of hypertension, valve disease, Ischaemic heart disease, diabetes, respiratory disease, endocrinal disease, liver disease or renal disease.
- Smoker
- Age <18 and >35 years
- Taking long-term medication
- Undertakes more than 3 hours of organised physical training per week

3.2 Study Design and Procedures

Unless otherwise stated, testing was carried out during one single visit. Athlete testing was performed either at individual RFL club facilities or at LJMU cardiovascular laboratory. All control participants procedures were carried out in LJMU cardiovascular laboratory. All participants had been asked to refrain from exercise for at least 6 hours prior to testing.

3.2.1 Anthropometry

A routine standard anthropometric assessment was performed including body mass (Seca supra 719, Hannover, Germany) and height measurements (Seca 217, Hannover, Germany) to allow for determination of body surface area (BSA) (Mosteller, 1987) and indexing of cardiac parameters to body size.

3.2.2 Blood Pressure

Standard resting systolic and diastolic blood pressure (BP) was recorded in a seated position (Dinamap pro, GE Medical, Horten, Norway) after a period of 5 minutes resting quietly.

3.2.3 Electrocardiography

A resting 12-Lead Electrocardiogram (ECG) was acquired using commercially available equipment (CardioExpress SL6, Spacelabs Healthcare, Washington US) and interpreted in accordance with current International screening guidelines (Sharma *et al.*, 2017).

3.2.4 Echocardiography

Transthoracic echocardiography (TTE) is a standard, widely used non-invasive clinical diagnostic procedure which is used to assess cardiac structure and function.

Different echocardiographic modalities form part of a standard transthoracic echocardiogram. 2D, M-mode, Doppler and Tissue Doppler imaging (TDI) taken together provide a non-invasive assessment of cardiac structure and function. One of the more novel echocardiographic techniques is STE, a particular focus of this thesis, which may add diagnostic value to the cardiac function assessment (Mor-Avi et al., 2011).

All echocardiographic images were acquired using a commercially available ultrasound system (Vivid Q, GE Medical, Horten, Norway) with a 1.5-4 MHz phased array transducer. Two experienced sonographers were used to acquire images due to a large number of participants per session and a limited window of opportunity for testing. All images were acquired with the participant lying in the left lateral decubitus position using a systematic approach and in adherence to ASE guidelines (Lang et al., 2015). A full study was obtained using harmonic imaging with all the standard images and assessment from parasternal long axis (PLAX), parasternal short axis (PSAX), apical 4 chamber, 3 chamber and 2 chamber windows. Subcostal images and suprasternal images were also recorded. Images were stored as a raw digital imaging and communications in medicine (DICOM) format and exported to an offline workstation (Echopac, Version 7.0, GE Healthcare, Horten, Norway) for subsequent analysis. Measurements were made in accordance with ASE guidelines (Lang et al., 2015, Rudski et al., 2010).

3.3 Conventional Echocardiography

The acquisition technique described above was a common feature between the different echocardiographic modalities: 2D; M-mode; Doppler and Tissue Doppler imaging. Echocardiographic parameters were obtained from parasternal and apical

acoustic windows with all settings including gain, sector width, depth, frequency, frame rate, sector angle and focal point optimised to obtain maximum signal to noise ratio to provide optimal endocardial delineation. Structural and functional assessment was performed on all four cardiac chambers: left ventricle (LV); right ventricle (RV); left atrium (LA) and right atrium (RA).

3.3.1 Two-Dimensional Left Ventricular Assessment

Linear internal measurements of the LV cavity were measured in PLAX. Measurements were made perpendicular to the LV axis at the level of or just below the mitral valve leaflet tips. Left ventricular internal diastolic dimension (LVIDd) was measured at the point where the cavity was at its biggest (Figure 3.1) and left ventricular internal systolic volume (LVIDs) at the point where the cavity was at its smallest (Figure 3.2). This method aids the perpendicular orientation to the ventricular long axis (Lang *et al.*, 2015). Linear measurements were also indexed for BSA to allow comparison of participants of different body sizes.

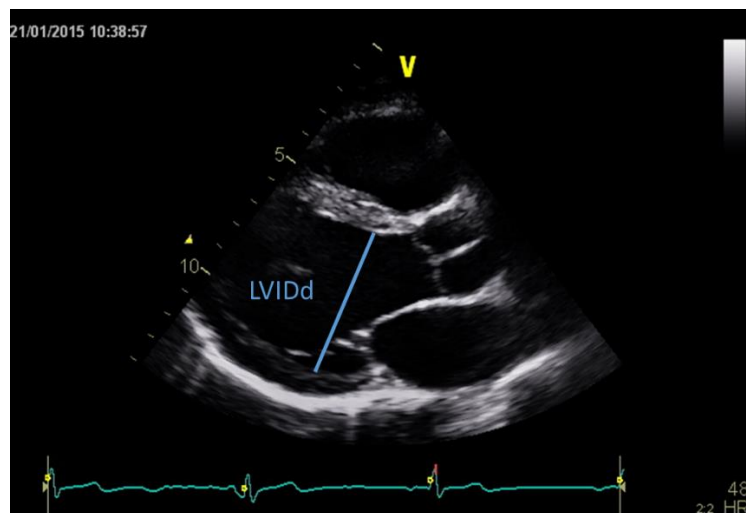


Figure 3.1 Parasternal long axis view demonstrating LVIDd

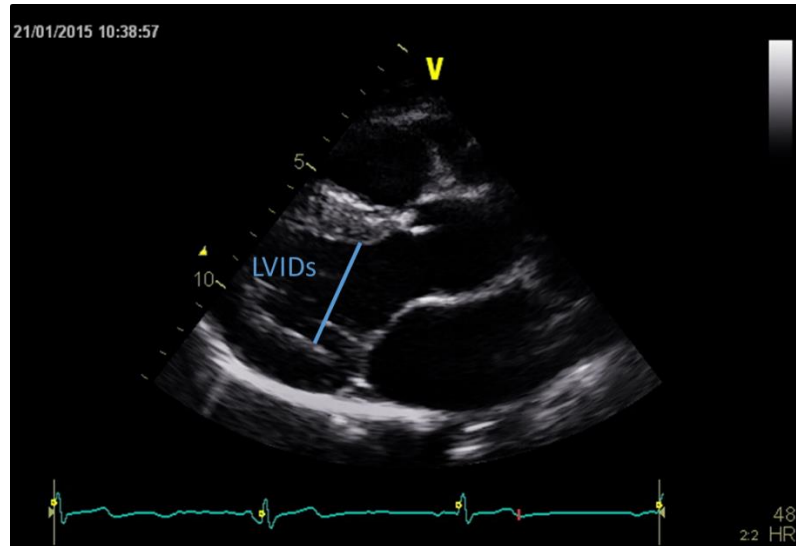


Figure 3.2 Parasternal long axis view demonstrating LVIDs

LV volumes were calculated using the Simpson's Biplane summation of discs method – the recommended method for assessment of LV 2D volumes (Lang *et al.*, 2015). This was achieved by tracing the LV internal myocardial border (blood tissue interface) of both the apical 4-chamber and 2-chamber images, in both diastole and systole to give the LV end diastolic volume (LVEDV) and LV end systolic volume (LVESV) respectively and the resulting systolic ejection fraction (EF) as a percentage (Figure 3.3). LV stroke volume (SV) is also determined by this method. LV length was also measured and determined from this technique as the length from the midpoint of the contour line between the mitral valve leaflets to the apex.

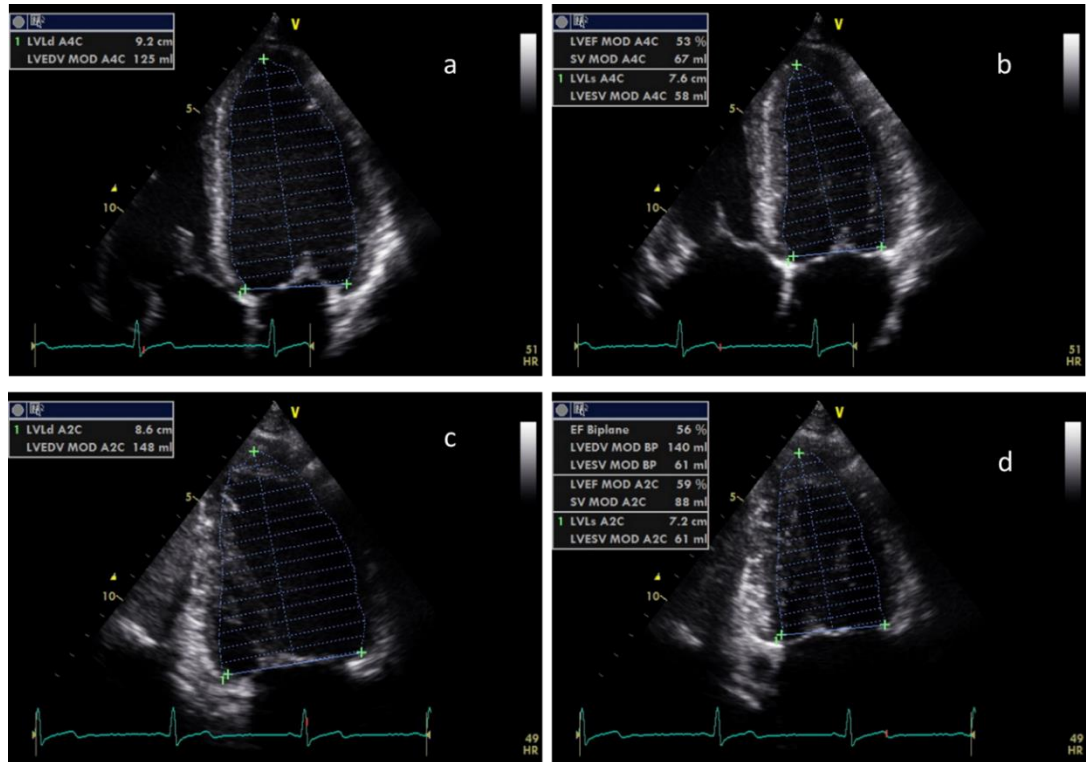


Figure 3.3 Biplane LV volume and Ejection Fraction. a, 4 chamber LVEDV; b, 4 chamber LVESV; c, 2 chamber LVEDV; d, 2 chamber LVESV.

The standard method of measuring wall thickness (Lang *et al.*, 2015) is in PLAX during diastole. However due to the heterogeneous phenotype expression in pathological LVH, a range of measurements of LV wall thickness across the length of the ventricle were made (Wigle *et al.*, 1985). Four linear measurements were taken from the LV anteroseptum, inferoseptum, posterior wall and lateral wall at both the PSAX basal (Figure 3.4) and mid-level (Figure 3.5) at end diastole. The mean wall thickness (MWT) was calculated from the average of the 8 segments. The maximum wall thickness (Max WT) was also determined as an absolute value.

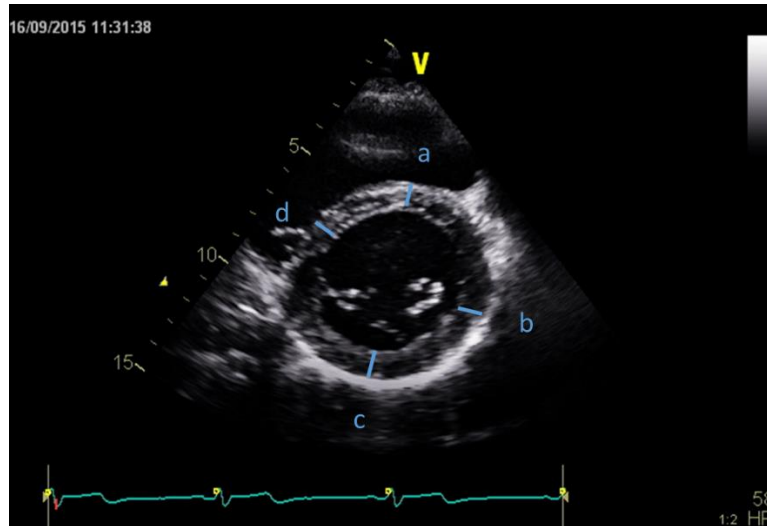


Figure 3.4 Parasternal short axis view demonstrating basal LV wall thickness. a, antero-septum; b, lateral; c, posterior; d, infero-septum.

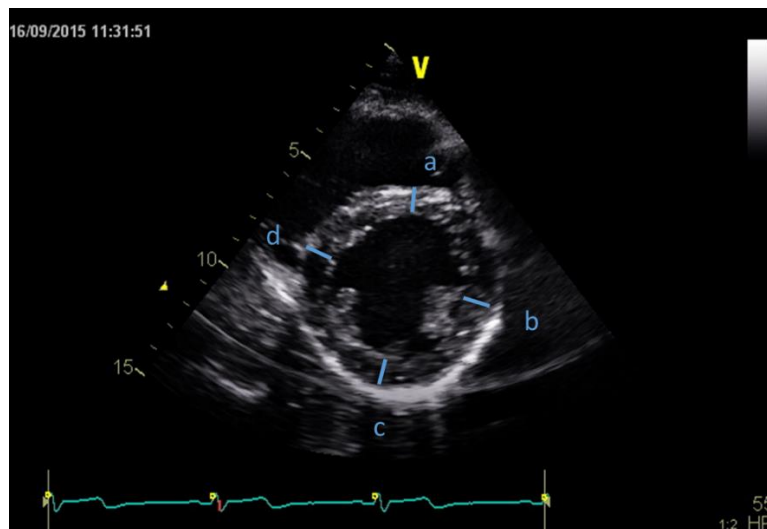


Figure 3.5 Parasternal short axis view demonstrating mid LV wall thickness. a, antero-septum; b, lateral; c, posterior; d, infero-septum.

LV geometry was determined by relative wall thickness (RWT) and LV mass. RWT was calculated by summing basal antero-septal and posterior wall thicknesses measured in diastole and dividing by the LVIDD. The linear method was also used for determination of LV mass. LV mass was determined using the ASE corrected equation (Lang *et al.*, 2015). A geometric formula is used to calculate the volume of LV

myocardium and the volume is then converted to mass (g) by multiplying the volume of myocardium by the myocardial density.

$$\text{LV mass} = 0.8 \times 1.04 \times ((\text{IVSd} + \text{LVIDd} + \text{PWTd})^3 - \text{LVIDd}^3) + 0.6\text{g}$$

The absolute LV mass (g) was indexed for body surface area (LVMI g/m^2) and for height raised to the power of 2.7 (Lang *et al.*, 2015).

$$\text{LV mass index (linear for BSA)} (\text{g}/\text{m}^2) = \text{LV mass} / \text{BSA}$$

$$\text{LV mass index (linear for height}^{2.7}) (\text{g}/\text{m}^2) = \text{LV mass} / \text{Height}^{2.7}$$

3.3.2 Two-Dimensional Right Ventricular Assessment

The RV outflow dimensions were measured from the parasternal images at end diastole. Proximal RV outflow dimension in PLAX ($\text{RVOT}_{\text{plax}}$) was measured from the anterior RV wall to the inter-ventricular septal – aortic junction at end diastole where the RVOT is at its biggest (Figure 3.6). Proximal RV outflow dimension in PSAX (RVOT_1) was measured in the PSAX aortic valve level view from the anterior RV wall to the aortic valve at end diastole (Figure 3.7). Distal RV outflow dimension in PSAX (RVOT_2) was measured transversally just proximal to the pulmonary valve at end diastole (Figure 3.8).

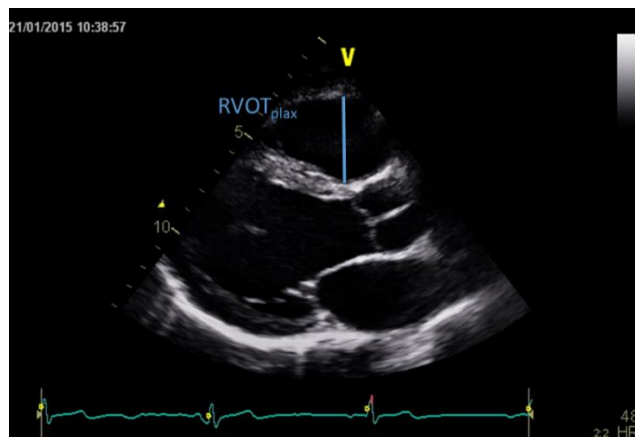


Figure 3.6 Parasternal long axis view demonstrating $\text{RVOT}_{\text{plax}}$

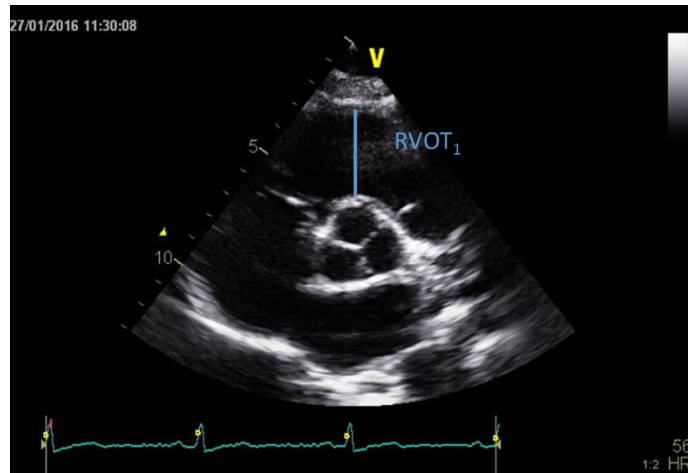


Figure 3.7 Parasternal short axis view demonstrating RVOT₁

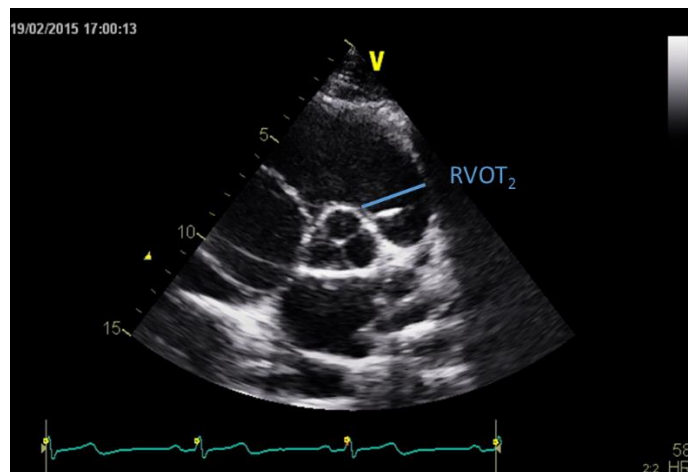


Figure 3.8 Parasternal short axis view demonstrating RVOT₂

The RV inflow measurements were made at end diastole from the RV focused apical 4 chamber view using a lateral or medial transducer orientation. The image was obtained with the LV apex at the centre of the sector, whilst displaying the largest RV basal diameter and avoiding foreshortening. Care was taken to avoid opening of the LVOT in the 5 chamber view (Rudski *et al.*, 2010). The maximal transversal RV dimension (RVD₁) was measured at basal RV inflow. The mid transversal RV dimension (RVD₂) was measured in the middle third of RV inflow halfway between

the RVD1 and the apex at papillary muscle level. The length of the RV (RVD₃) was measured from apex to base at the level of the tricuspid annulus (Figure 3.9). The RV free wall thickness (RVFW) was measured from the subcostal image (Figure 3.10) with zoom on the RV mid wall taking care to avoid papillary muscle and trabeculation (Rudski *et al.*, 2010). The RV:LV ratio was determined using measurements of the RV and LV base taken from the apical 4 chamber image at end diastole (Figure 3.11).

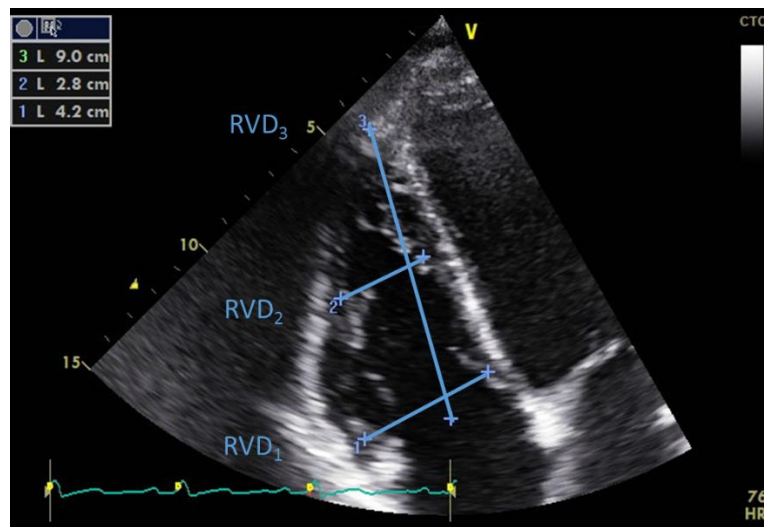


Figure 3.9 Apical 4 Chamber view demonstrating RVD₁, RVD₂ and RVD₃

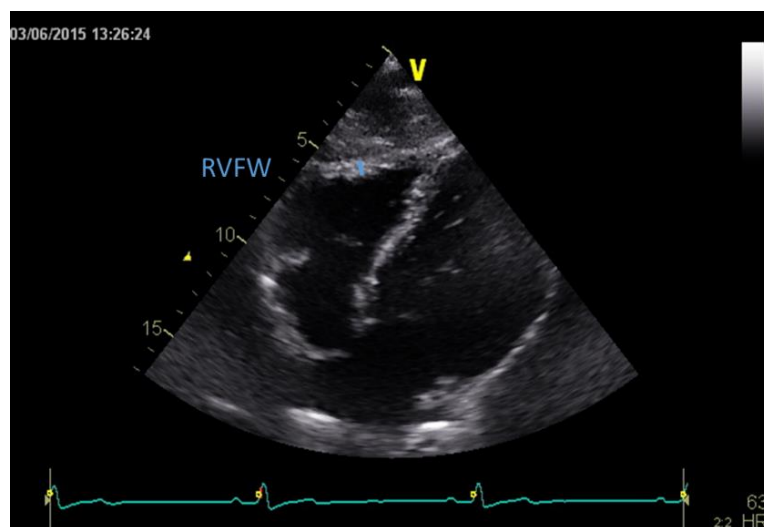


Figure 3.10 Subcostal view demonstrating RVFW

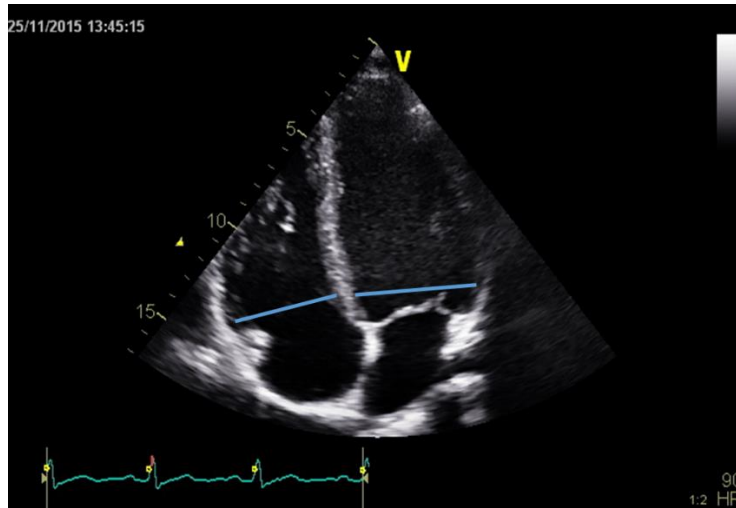


Figure 3.11 Apical 4 Chamber view demonstrating RV and LV dimensions for RV:LV ratio

RV area was measured from the RV focused imaged. The RV area was traced at both end diastole (RVDa) and end systole (RVSa) by tracing the internal endocardial border from the lateral tricuspid annulus, along the free wall to the apex then down the interventricular septum to the medial tricuspid annulus (Figure 3.12). The RV fractional area change (RVFAC) was estimated from the following equation:

$$\text{RVFAC (\%)} = ((\text{RVDa} - \text{RVSa}) / \text{RVDa}) \times 100$$

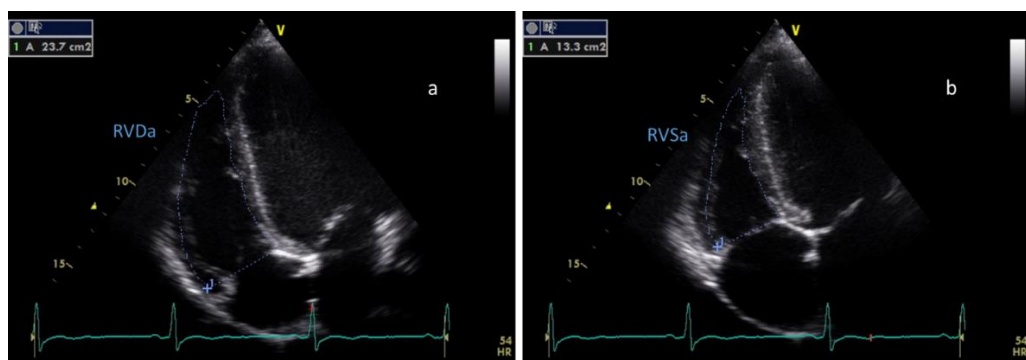


Figure 3.12 Right Ventricular diastolic and systolic area

3.3.3 Two-Dimensional Left Atrial Assessment

The LA internal linear dimension (LAd) was made in the PLAX view at end systole just prior to valve opening from the anterior to the posterior LA perpendicular to the aortic root long axis.

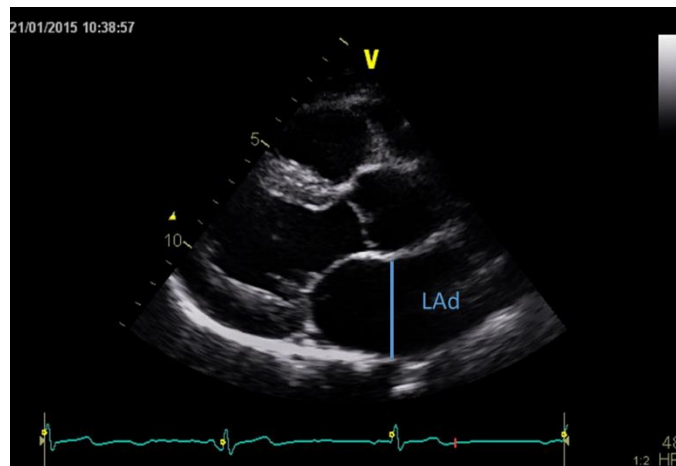


Figure 3.13 Parasternal long axis view demonstrating LA diameter

The disc summation technique was used to measure biplane LA Volume (LAvol). LAvol at end systole (LAvoles) was measured in both the apical 4 chamber and 2 chamber images at end systole (averaged volume of the two planes), by tracing the LA inner border from septal annulus around to posterior annulus avoiding pulmonary veins and LA appendage (Figure 3.14). Volume measurements were made in the same way pre-atrial contraction (LAvolpreA) and at end diastole (LAvoled) and the average determined (Figures 3.15 and 3.16 respectively). From these measurements, LA functional volumes were measured as previously described (Ogawa *et al.*, 2009, McClean *et al.*, 2015). These include, LA reservoir volume (LAres), the blood volume from pulmonary venous return during systole, which is defined as the difference between LAvoles and LAvoled. LA conduit volume (LAcon) represents the volume of blood moving from LA to LV during early ventricular diastole and is defined as the

difference between LV SV (from LV Biplane Simpsons method) and LAres. The LA atrial booster volume (LABoo) describes the LA active emptying volume and is defined as the difference between LAVolpreA and LAVoled. The functional LAcon:LABoo ratio was also determined. Measurements were indexed for BSA (Lang *et al.*, 2015).

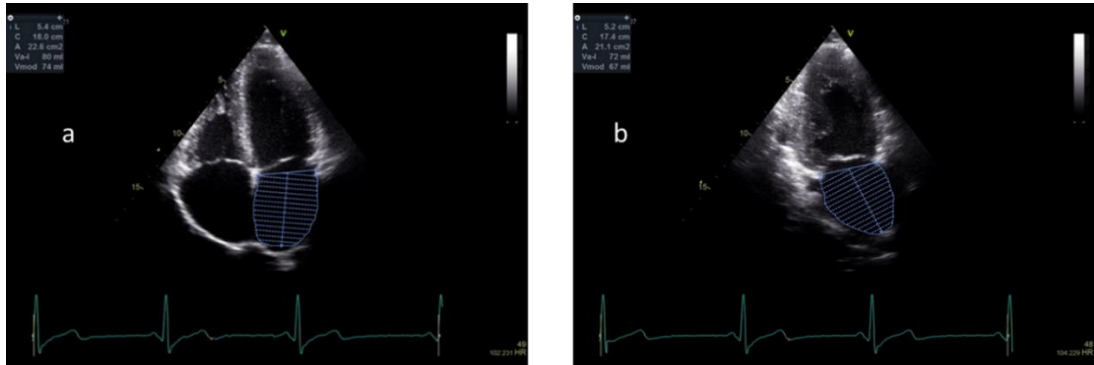


Figure 3.14 Biplane LAvoles; a, Apical 4 chamber and b, Apical 2 chamber

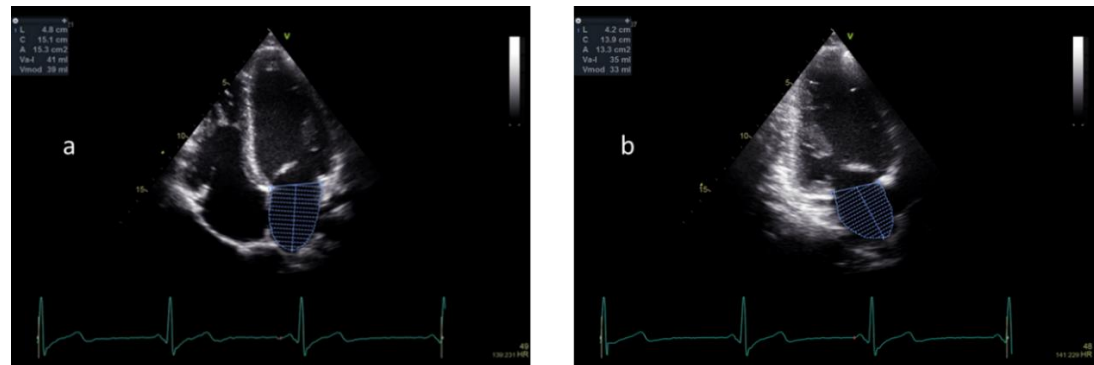


Figure 3.15 Biplane LAPreA; a, Apical 4 chamber and b, Apical 2 chamber

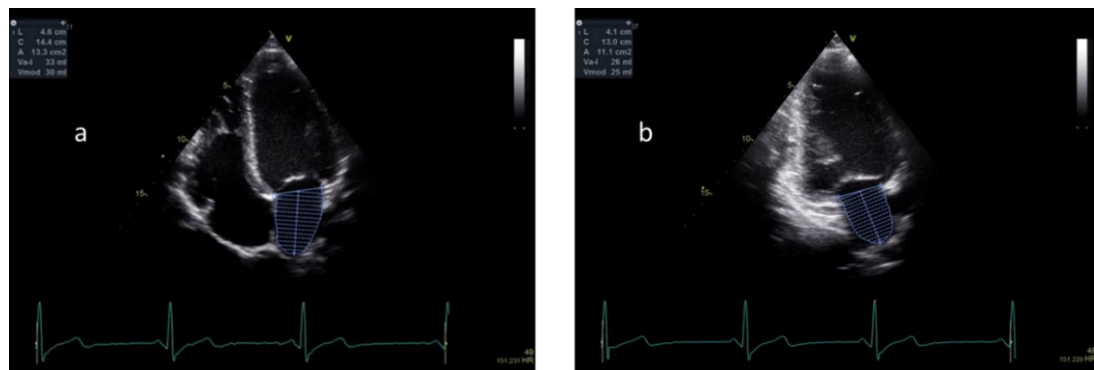


Figure 3.16 Biplane LAVoled; a, Apical 4 chamber and b, Apical 2 chamber

3.3.4 Two-Dimensional Right Atrial Assessment

The right atrial area (RAa) (Figure 3.17) and end systolic volume (RAvoles) was measured from the apical 4 chamber view at end systole (just before valve opening) by tracing the RA inner border excluding the area under the tricuspid leaflets. The disc summation technique was used to measure RAvoles. Volume measurements were made in the same way at pre-atrial contraction (RAvolpreA) and at end diastole (RAvoled) (Figure 3.18). From these measurements, RA functional volumes were measured as previously described (Ogawa *et al.*, 2009, McClean *et al.*, 2015). These include, RA reservoir volume (RAres), the blood volume from pulmonary venous return during systole, which is defined as the difference between RAvoles and RAvoled. RA conduit volume (RAcon) represents the volume of blood moving from RA to RV during early ventricular diastole and is defined as the difference between LV SV and RAres. The RA atrial booster volume (RAboo) describes the RA active emptying volume and is defined as the difference between RAvolpreA and RAvoled. The functional RAcon:RAboo ratio was also determined. Measurements were indexed for BSA (Rudski *et al.*, 2010, Lang *et al.*, 2015).

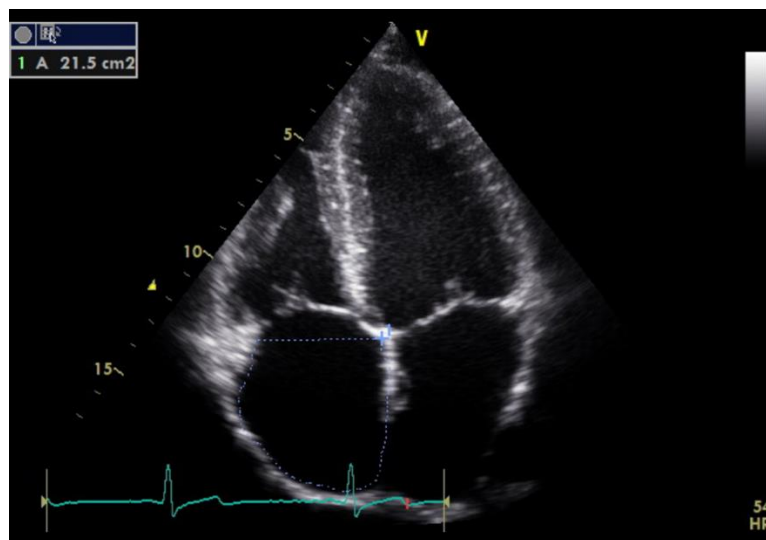


Figure 3.17 Apical 4 Chamber view demonstrating right atrial area

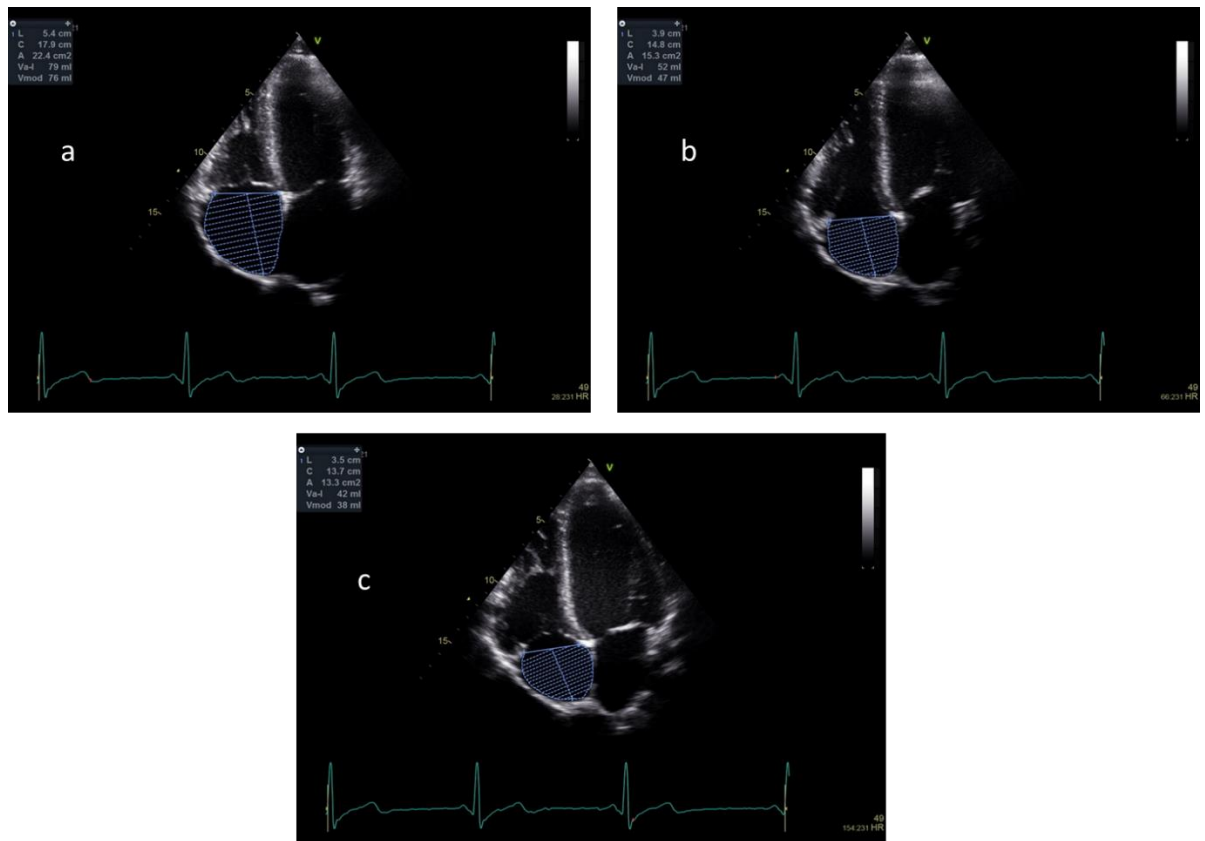


Figure 3.18 Apical 4 Chamber view demonstrating RA volume. a, RAVoles; b, RAVolpreA; c, RAVoled

3.4 M-Mode

M-Mode is a time motion display of the ultrasound beam in a single plane through the heart. M-mode images were recorded in the left heart by placing the cursor through the tips of the aortic valve and the tips of the mitral valve. Whilst these were not used for linear measurements they were a useful addition to valve assessment. M-mode in the right heart was used for longitudinal systolic function assessment, the tricuspid annular plane systolic excursion (TAPSE). The cursor was placed through the tricuspid annulus to measure the amount of longitudinal movement and was measured at peak systole (Figure 3.19). Care was taken to align the beam with the direction of the tricuspid lateral annulus in the apical 4 chamber view (Rudski *et al.*, 2010).

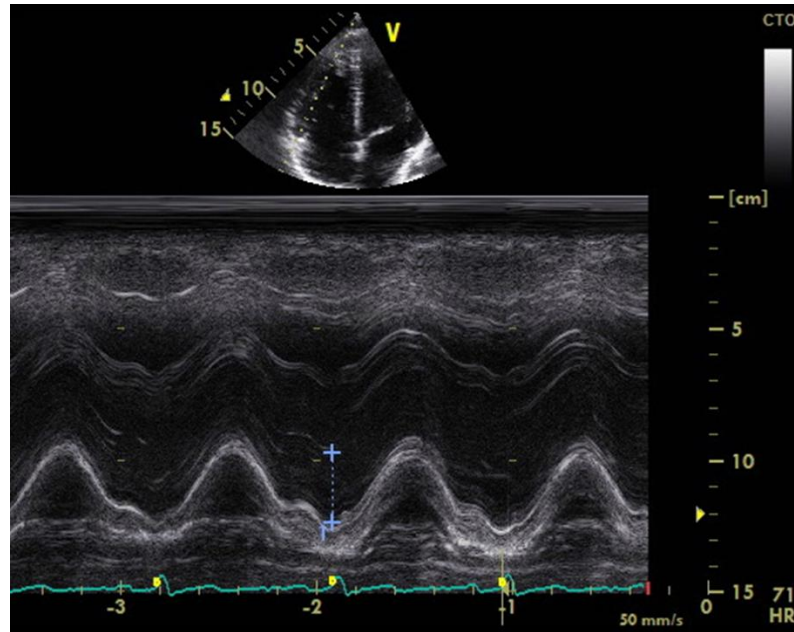


Figure 3.19 M-Mode - TAPSE

3.5 Doppler

Doppler echocardiography has two uses: Detection and quantification of normal and disturbed flow velocities. The Doppler principle states that the frequency of reflected ultrasound is altered by a moving target, such as red blood cells (Quiñones *et al.*, 2002) and this technique is used to assess blood flow velocity using red blood cells as the moving target. Doppler echocardiography consists of 3 modalities, Continuous wave (CW), Pulsed wave (PW) and colour Doppler imaging. Blood inflow and outflow of the LV and RV was assessed using a combination of methods and pressure gradients across valves were also measured. Diastolic assessment of LV function is very important in the screening process and involves assessment of LV filling pressures. Mitral inflow velocities were assessed from the apical 4 chamber image (Figure 3.20). The sample volume on the cursor was placed in the LV at the mitral valve leaflet tips. From the resultant PW trace, the peak mitral early (E) and late (A) diastolic velocities

were assessed along with the E/A ratio and deceleration time (Nagueh *et al.*, 2016 Lang *et al.*, 2015).

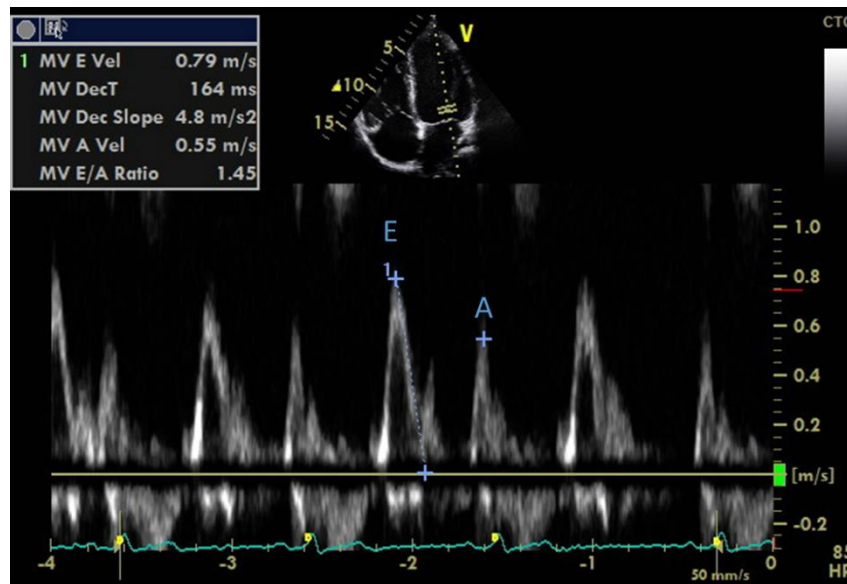


Figure 3.20 Mitral Inflow Pulsed Wave Doppler

3.6 Tissue Doppler Imaging

The Doppler principle can also be used to assess the velocity of the myocardial tissue. In this case the moving target is the myocardial tissue (Quiñones *et al.*, 2002). The apical four chamber view was optimised to ensure the longitudinal movement of the infero-septum and lateral wall of the LV was aligned with the ultrasound beam. The peak early (E'), and late (A') diastolic myocardial velocities along with the peak systolic (S') myocardial velocity were recorded at each site and averaged values also recorded. The PW sample volume was placed in the basal tissue just above the annulus of the mitral valve on both the infero-septal and lateral walls (Figure 3.21). In the case of the RV, the apical four-chamber view was modified to allow correct alignment with the ultrasound beam. The PW sample volume was placed in the basal tissue just above the tricuspid annulus (Figure 3.22). The Peak diastolic early E', late diastolic A' and systolic S' velocities were recorded. TDI was used a measure of systolic and diastolic

longitudinal function and TDI and Doppler measurements together were used for a comprehensive LV diastolic function assessment (Nagueh *et al.*, 2016, Lang *et al.*, 2015). To account for chamber size, average values LV TDI values were indexed for LV length (S' index, E' index and A' index) as previously recommended (Batterham *et al.*, 2008). RV TDI data was indexed RV length (by dividing by RVD₃) to provide RVS' index, RVE' index and RVA' index) (Popovic *et al.*, 2005).

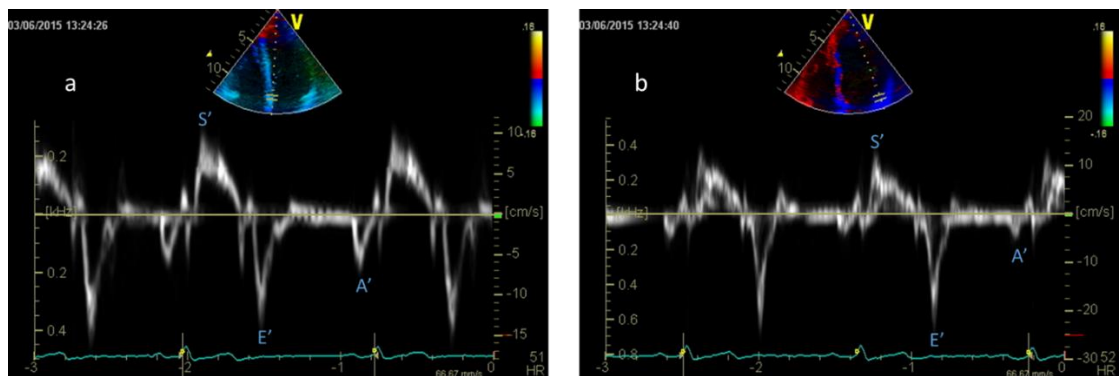


Figure 3.21 Pulsed Wave TDI. a, infero-septal S', E' and A'; b, lateral S', E' and A'

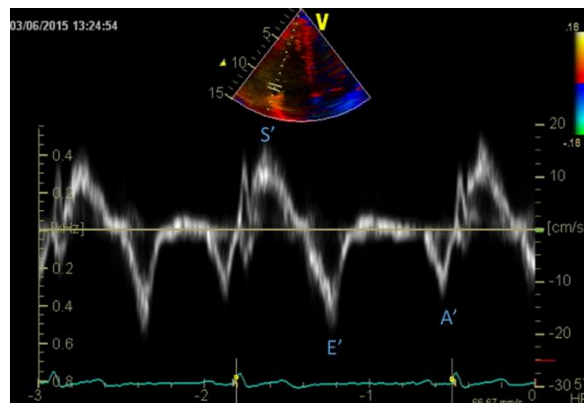


Figure 3.22 Pulsed Wave RV TDI – RV S', RV E' RV A'

3.7 Speckle Tracking Echocardiography

For the assessment of LV ϵ and SR both 2D parasternal short axis and apical images were assessed. In both PSAX and apical orientations the frame rates were maximised and between acceptable levels of >40 and <90 frames per second. The LV cross section

was as circular as possible (Notomi *et al.*, 2005). The analysis software includes increased averaging capabilities that improve signal to noise ratio (Modesto *et al.*, 2006) as well as the ability to automatically grade the quality of the tracking as either acceptable or unacceptable and segments were excluded from the analysis if the software considered them unacceptable and/or the operator observed inappropriate tracking during the analysis process. A region of interest (ROI) was applied LV images ensuring alignment with the endocardium and epicardium. Optimisation of the ROI ensured that the whole of the myocardium was encompassed.

3.7.1 Left Ventricular Longitudinal Mechanics

Longitudinal ϵ and SR was assessed using the apical 4 chamber, apical long axis and 2 chamber images. The focal point was positioned at the level of the mitral valve (Mor-Avi *et al.*, 2011, Lang *et al.*, 2015). The AVC time was set by the user using the aortic CW Doppler trace. In the 4 chamber image the ROI was traced around the myocardium from basal infero-septum to basal lateral wall. In the apical long axis image, the ROI was traced around the LV from basal posterior wall to basal antero-septum and in the 2 chamber view the ROI was traced around the LV from the basal inferior wall to the basal anterior wall.

Each apical image provided 6 segments including basal, mid and apical segments from which ϵ , systolic strain rate (SRS), early diastolic strain rate (SRE) and late diastolic strain rate (SRA) were measured (Figures 3.23-3.25).

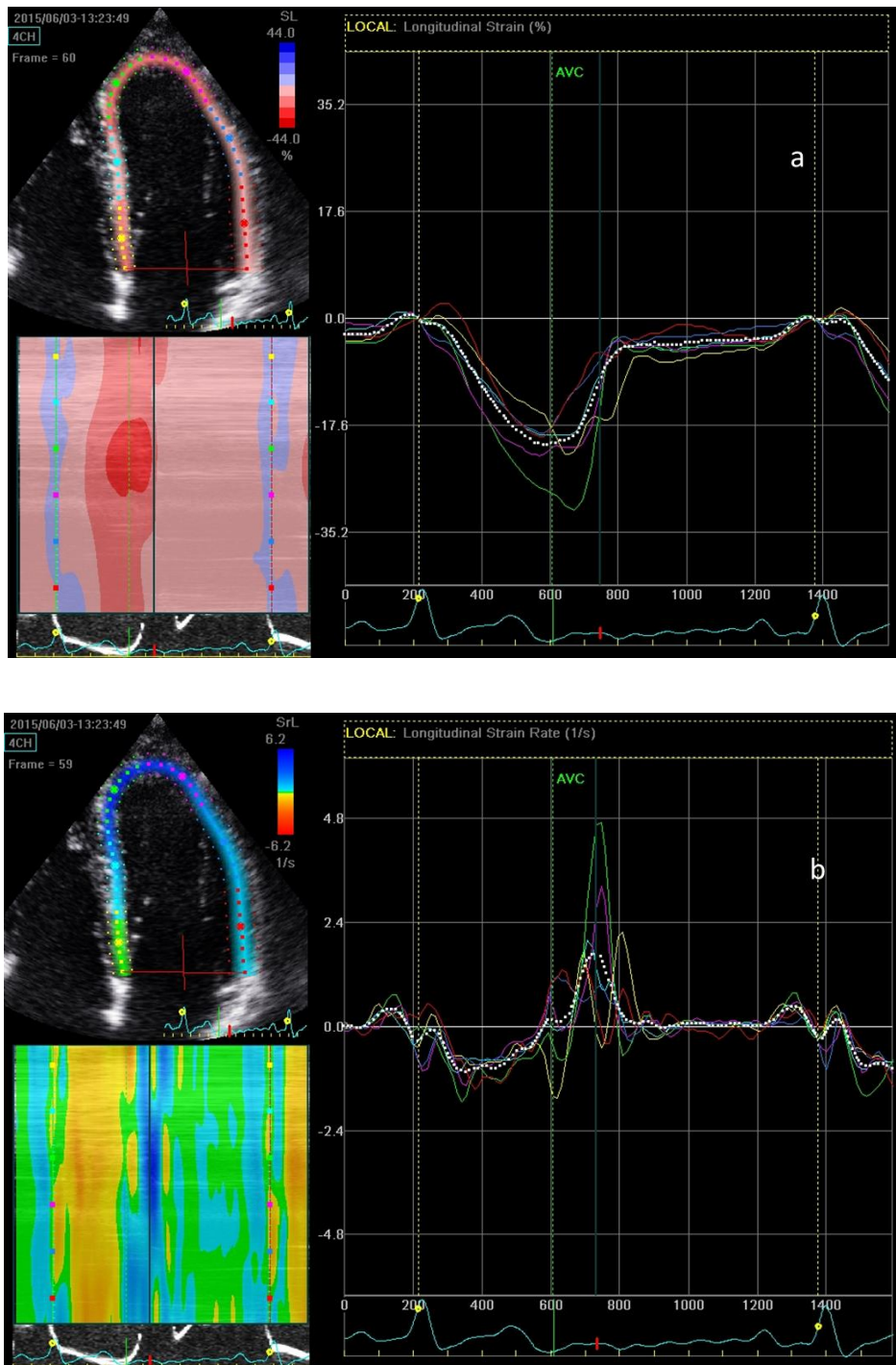


Figure 3.23 Apical 4 chamber longitudinal STE. a, Longitudinal ϵ curves; b, Longitudinal SR curves.

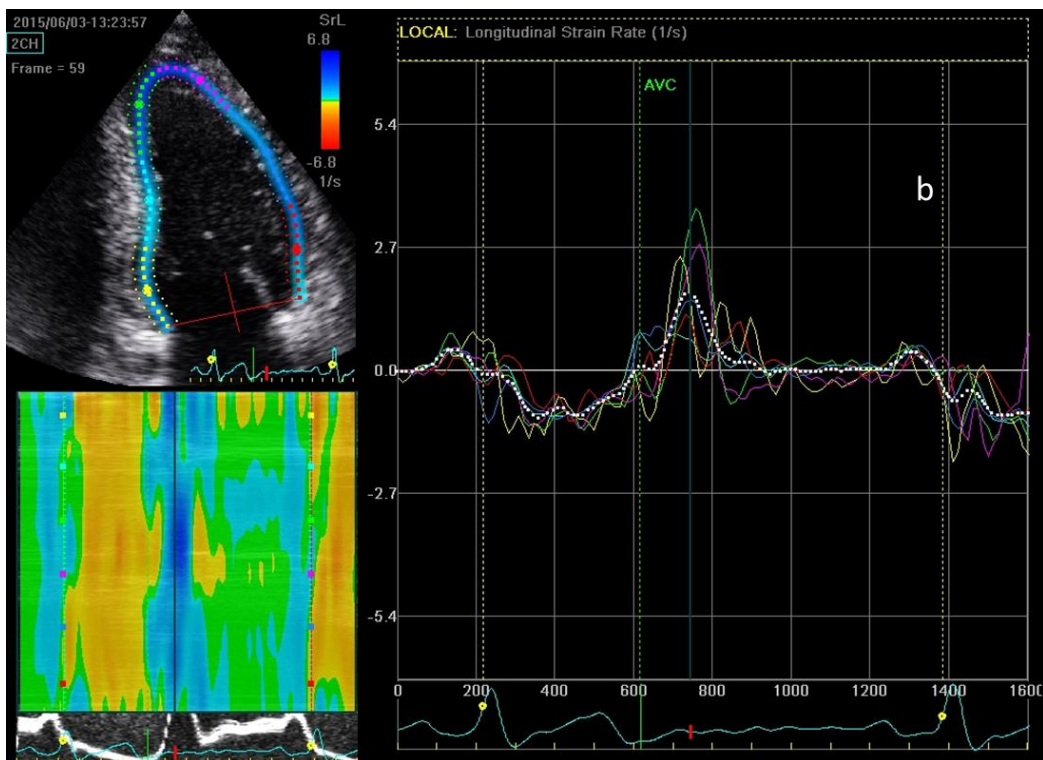
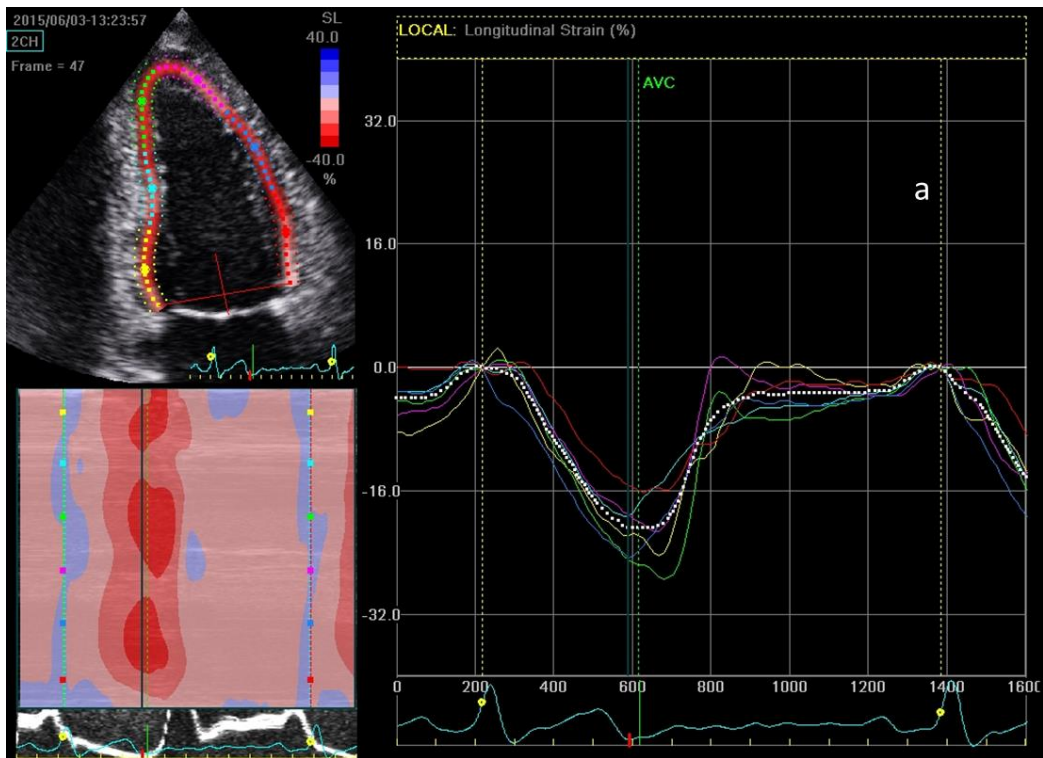


Figure 3.24 Apical 2 chamber longitudinal STE. a, Longitudinal ϵ curves; b, Longitudinal SR curves.

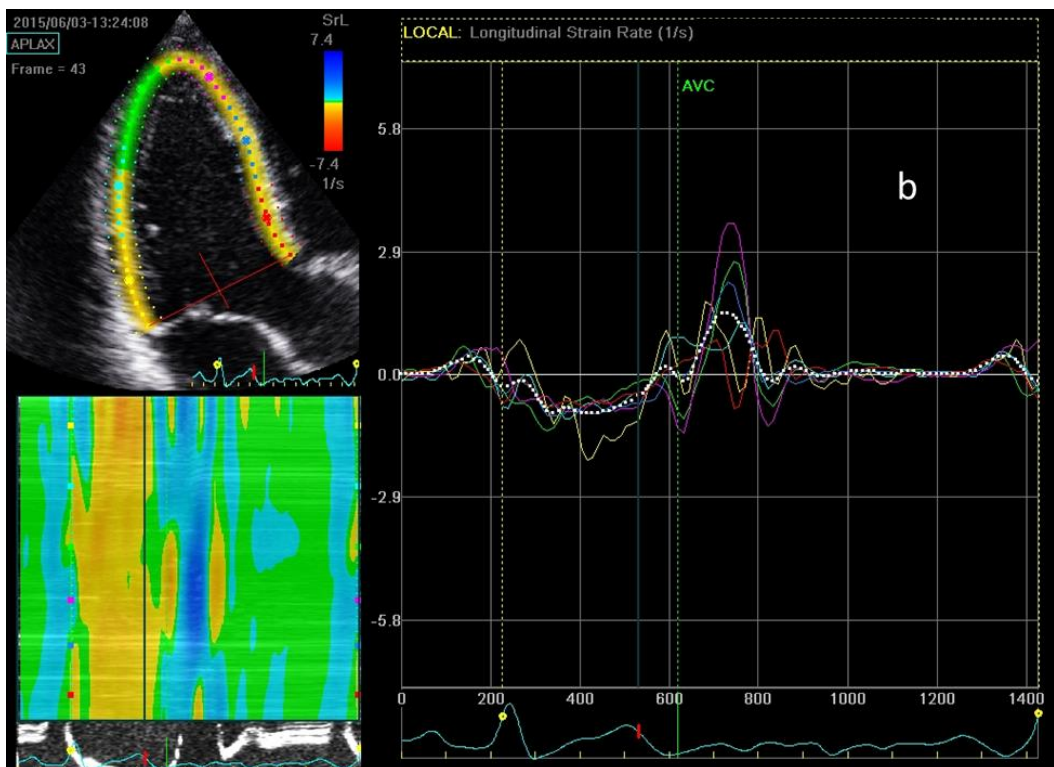
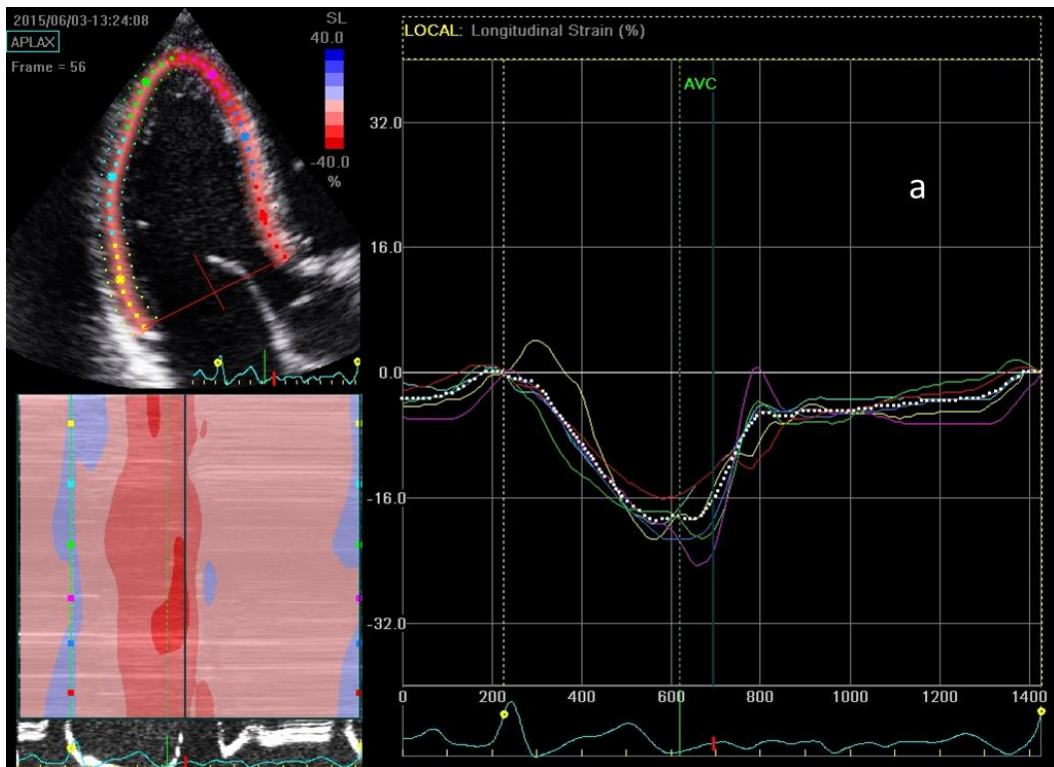


Figure 3.25 Apical long axis longitudinal STE. a, Longitudinal ϵ curves; b, Longitudinal SR curves.

All regional values were recorded and a mean value of all the acceptable segments was presented as a global parameter of LV longitudinal function. Regional data was presented by a bullseye diagram (Figure 3.26).

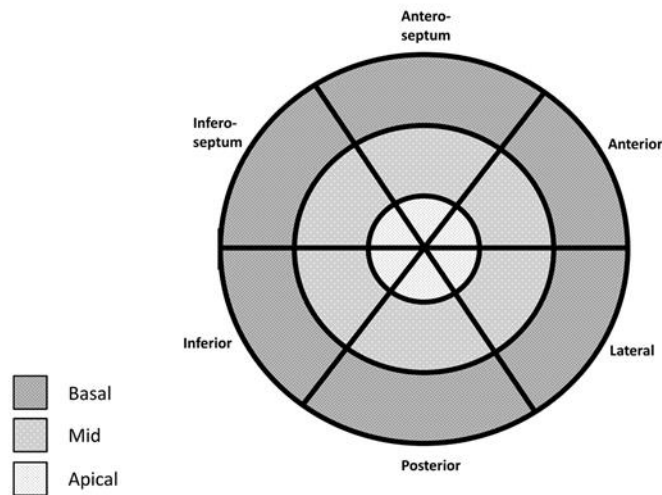


Figure 3.26: Longitudinal ϵ and SR model – 18 regional regions.

3.7.2 Left Ventricular Circumferential and Radial Mechanics

Circumferential and radial ϵ and SR were obtained from the LV PSAX image at both basal level (mitral valve) and mid-level (papillary muscle). The focal point was positioned close to the centre of the LV cavity to produce optimum beam width and to reduce the effect of divergence. The aortic valve closure (AVC) time was set by the user. Circumferential ϵ and SR at basal and mid-level is shown in Figures 3.27 and 3.28 respectively. Radial ϵ and SR at basal and mid-level is shown in Figures 3.29 and 3.30 respectively.

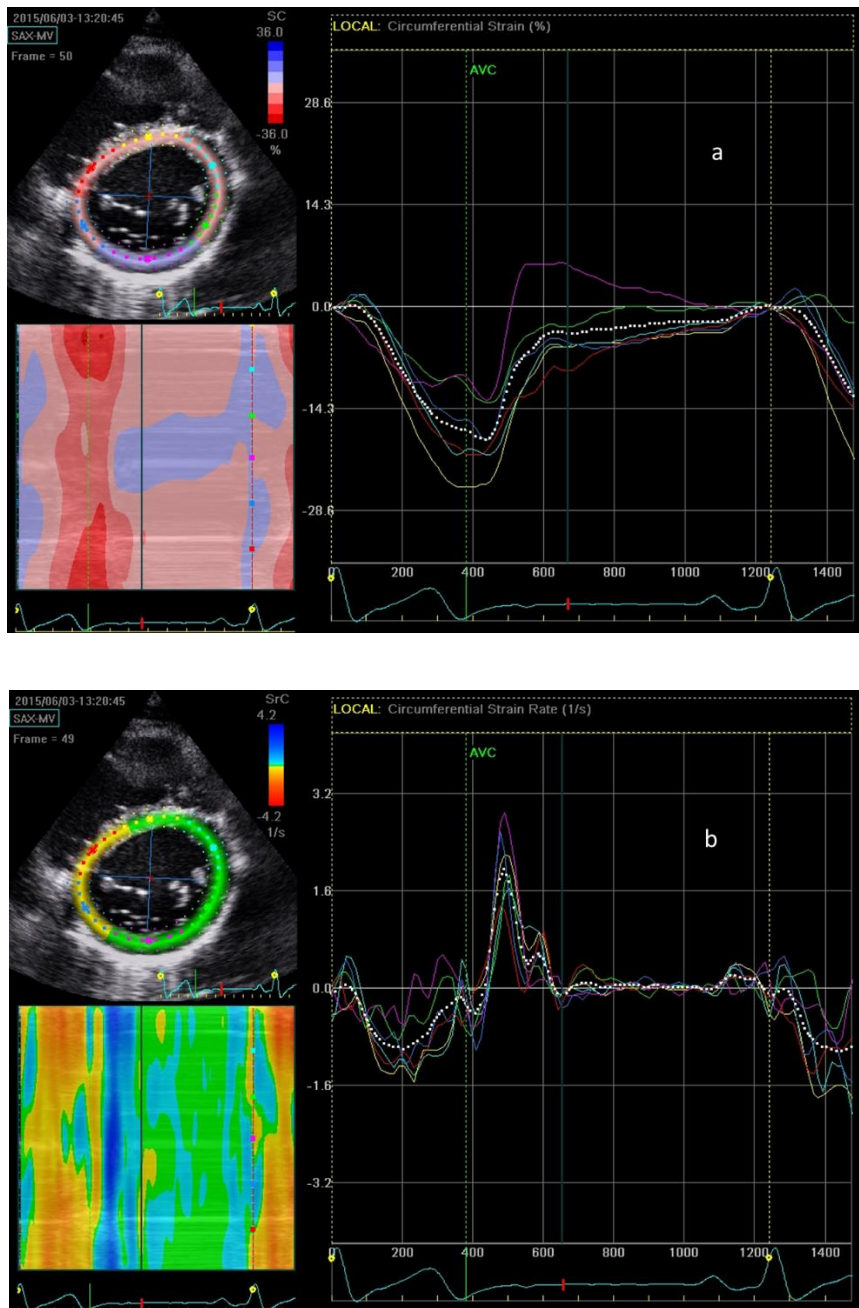


Figure 3.27 Basal circumferential STE. a, circumferential ϵ curves; b, circumferential SR curves.

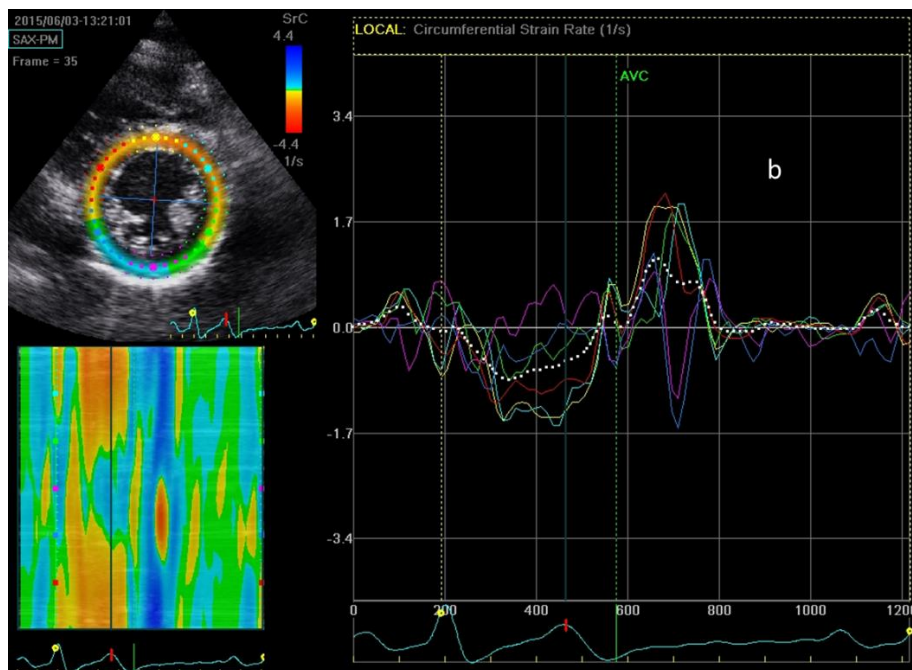
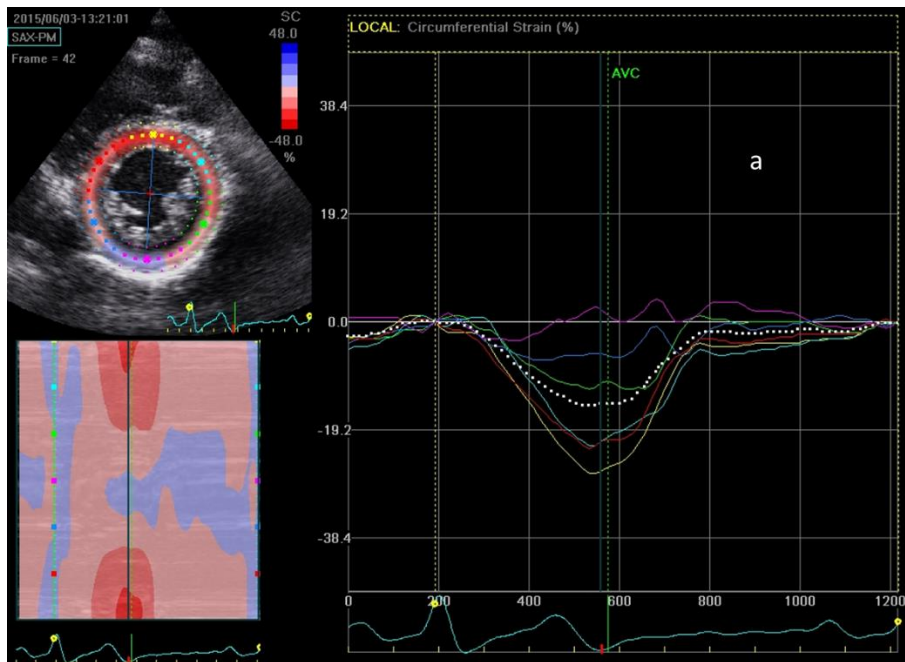


Figure 3.28 Mid circumferential STE. a, radial ϵ curves; b, radial SR curves

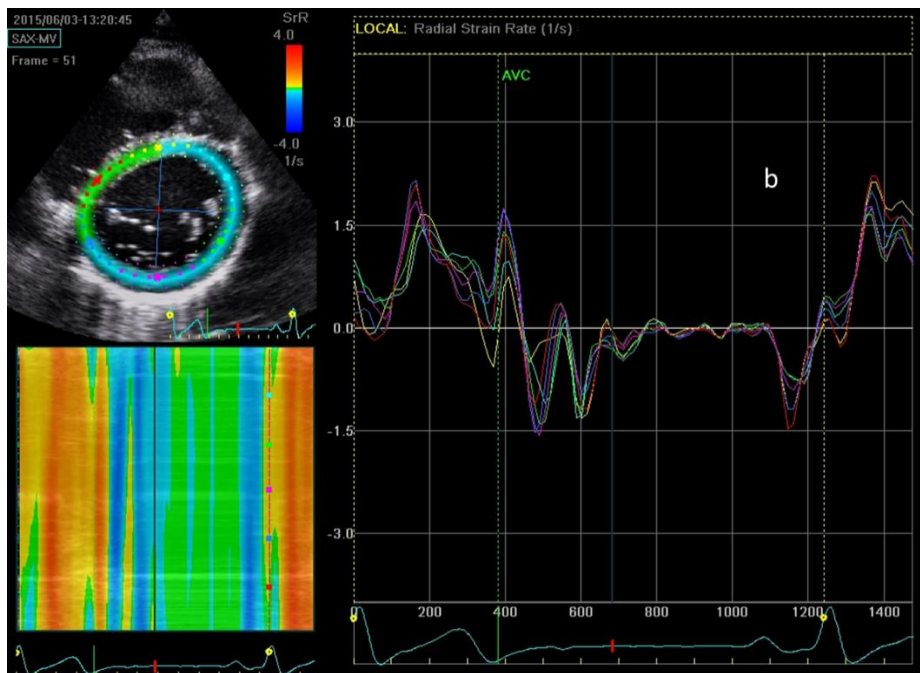
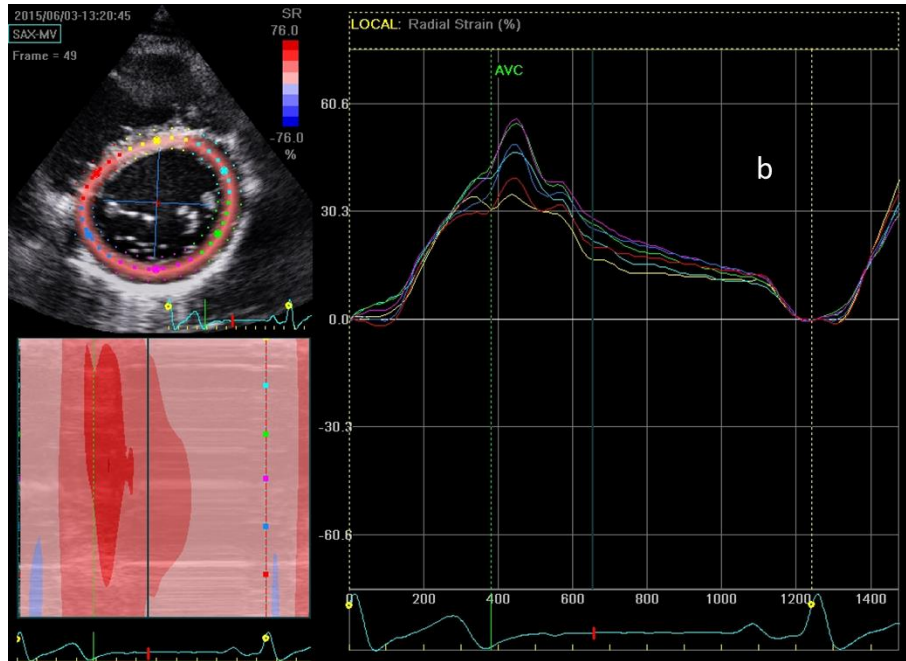


Figure 3.29 Basal radial STE. a, radial ϵ curves; b, radial SR curves

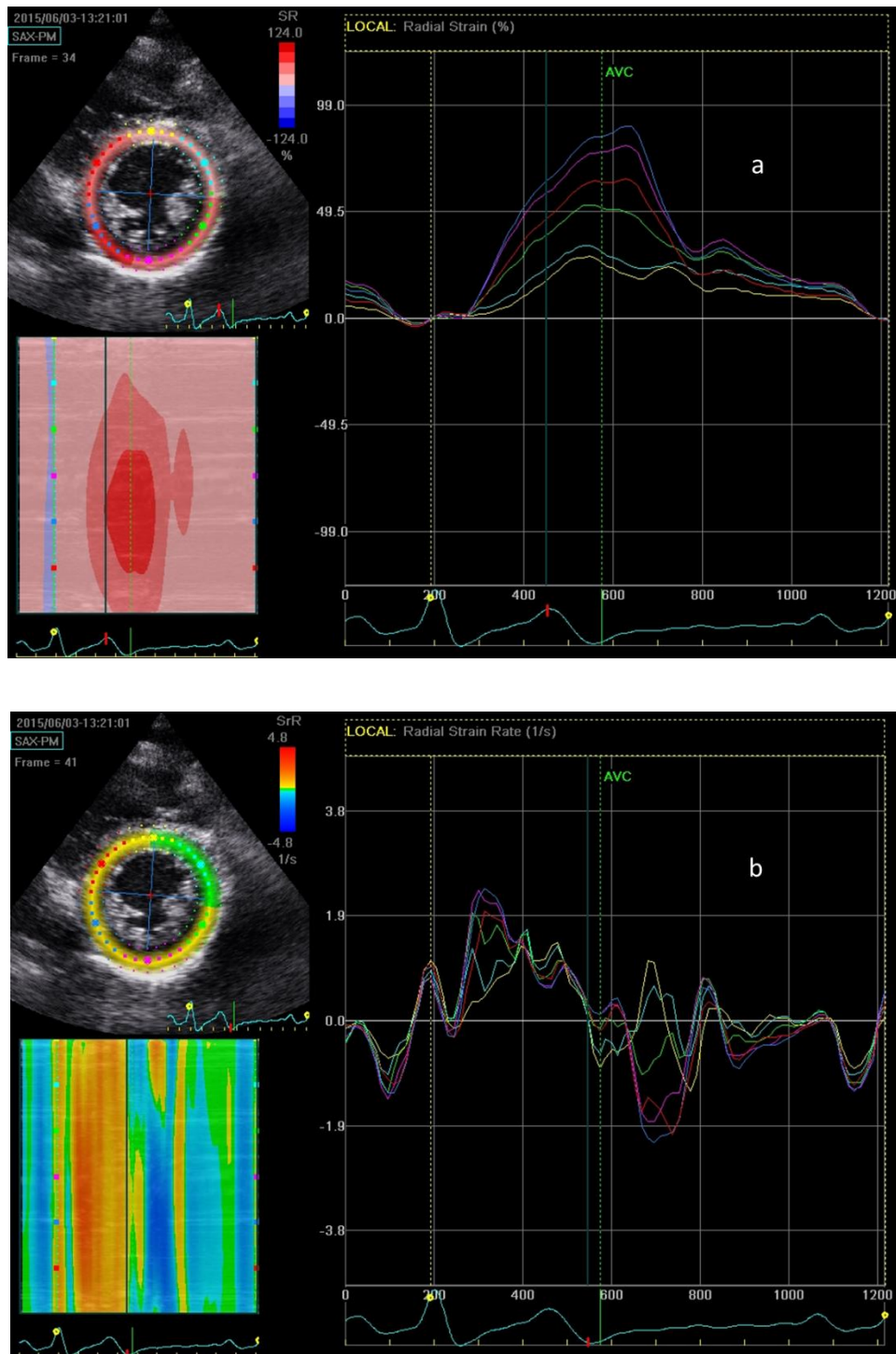


Figure 3.30 Mid radial STE. a, radial ϵ curves; b, radial SR curves

The PSAX orientations include 6 segments – inferoseptum, anteroseptum, anterior, lateral, posterior and inferior walls. Peak radial and circumferential ϵ and SRS, SRE and SRA data were recorded for each of the 6 segments of both basal and mid-levels. A mean of all 6 segments was used in analysis of parameters at each level and average

global circumferential and global radial ϵ and SR parameters were calculated from the 12 segmental basal and mid values (Figure 3.31).

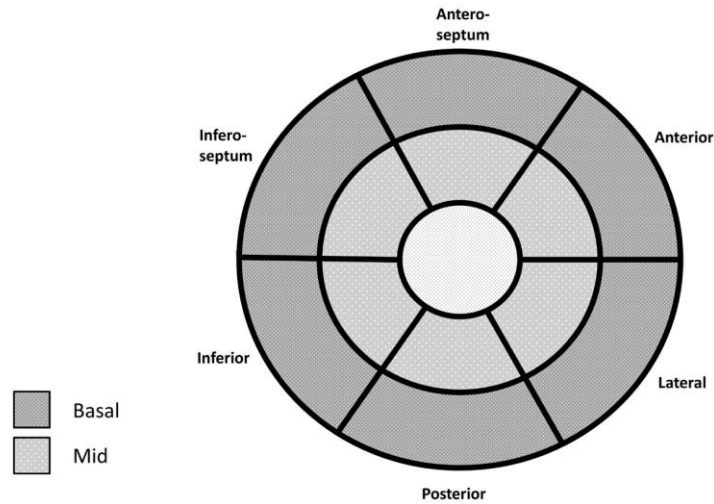


Figure 3.31 Circumferential and Radial ϵ and SR model -12 myocardial regions.

3.7.2 Left Ventricular Twist Mechanics

The twist of the LV was analysed by tracking the rotation of the myocardium in the PSAX basal and PSAX apical image. A PSAX apical image was defined as the level just above the point of systolic cavity obliteration with no evidence of papillary muscle (Notomi *et al.*, 2005). Apical rotation and rotation rate was determined by the same tracking procedure as for the basal level (Figure 3.32). Twist was calculated as the net difference between peak basal and peak apical rotation (Figure 3.33) (Park *et al.*, 2008, Burns *et al.*, 2010b).

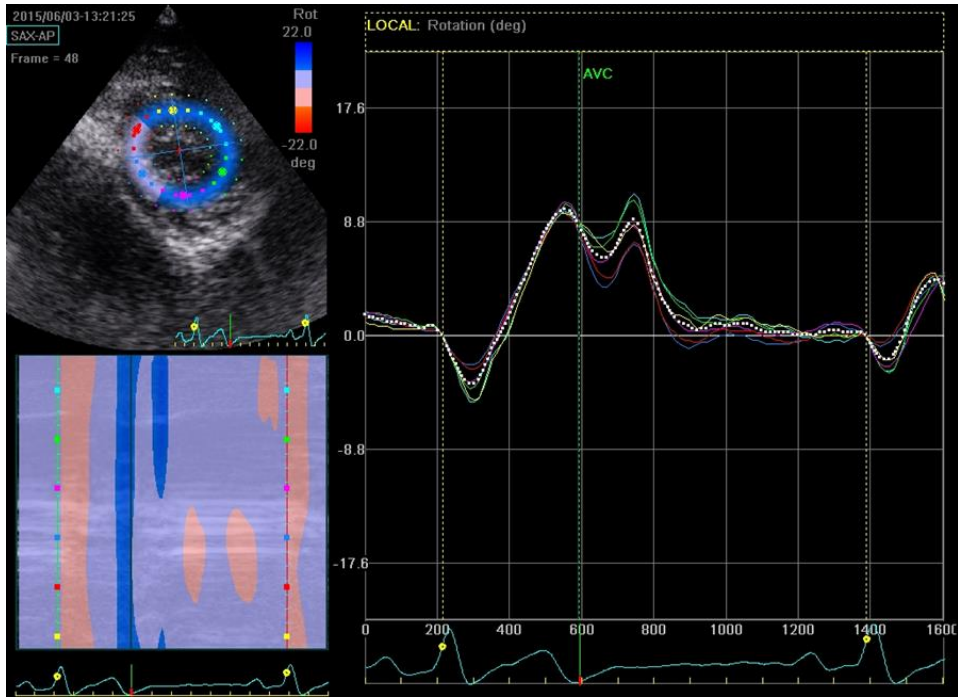


Figure 3.32 Apical rotation curves.

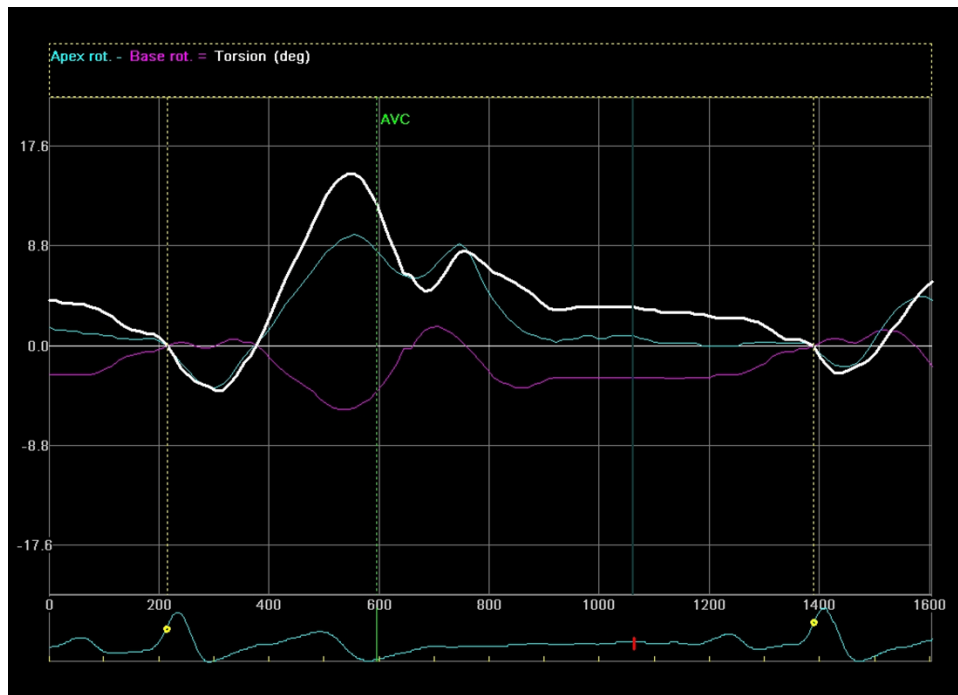


Figure 3.33 Peak apical and basal rotation and twist.

3.7.4 Right Ventricular Longitudinal Mechanics

The assessment of the RV ϵ and SR was achieved using the RV focused apical image. The focal point was placed mid cavity. The Pulmonary valve closure (PVC) time was set by the user using the pulmonary CW Doppler trace and the ROI was traced along the lateral free wall from base to apex (Figure 3.34). The subsequent tracking analysis produced global RV ϵ , SR, SRE and SRA values averaged from 3 myocardial segments - basal, mid and apical (Mor Avi *et al.*, 2011, Korinek *et al.*, 2005, Lang *et al.*, 2015).

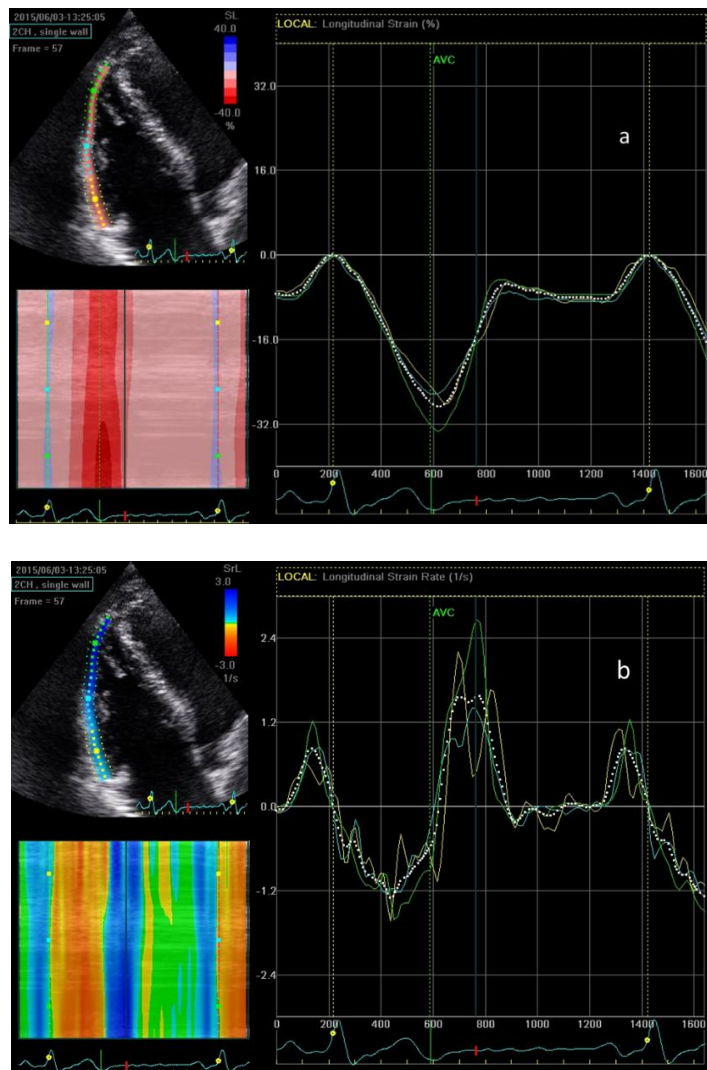


Figure 3.34 RV Longitudinal STE; a, RV longitudinal ϵ curves; b, RV SR curves.

3.8 Scaling to Body Size

All structural indices were scaled allometrically to BSA based on the principle of geometrical similarity (Batterham *et al.*, 1999). Linear dimensions were scaled to $BSA^{0.5}$, areas directly to BSA and volumes to $BSA^{1.5}$. LV mass was also scaled to $height^{2.7}$ (Daniels *et al.*, 1995).

3.9 Data Management

Study data were collected and managed using REDCAP electronic data capture tools hosted at Liverpool John Moores University (Harris *et al.*, 2009). REDCAP (Research Electronic Data Capture) is a secure, web-based application designed to support data capture for research studies providing 1) an intuitive interface for validated data entry; 2) audit trails for tracking data manipulation and export procedures; 3) automated export procedures for seamless data downloads to common statistical packages; and 4) procedures for importing data from external sources.

Chapter 4

The Relationship between Left Ventricular Structure and Function in the Elite Rugby Football League Athlete as determined by Conventional Echocardiography and Myocardial Strain Imaging

Chapter 4 has resulted in a jointly authored peer reviewed publication;

Forsythe, L., MacIver, D. H., Johnson, C., George, K., Somauroo, J., Papadakis, M., Brown, B., Qasem, M. and Oxborough, D. 2018. The relationship between left ventricular structure and function in the elite rugby football league athlete as determined by conventional echocardiography and myocardial strain imaging. *International Journal of Cardiology*, 261, 211–217.

4.1 Introduction

Recent studies have demonstrated changes in LV geometry (Utomi *et al.*, 2013, Finocchiaro *et al.*, 2016) with functional adaptation (Baggish *et al.*, 2008b) across sporting disciplines. It is appropriate that screening strategies should be tailored to the population being screened (Lavie and Harmon, 2016) and it is therefore pertinent to establish the LV phenotype in RFL athletes. Echocardiography is routinely used in the assessment of AH and more recently STE has been implemented to describe chamber mechanics (Beaumont *et al.*, 2017). Previous data on LV mechanics is variable due to heterogeneous study design, methods and/or athlete populations with differentiation from inherited conditions often being based on a ‘one size fits all’ interpretation of echocardiographic derived measures and with little consideration of body size.

The relationships between LV geometry and EF have been extensively investigated in pathological hypertrophy (Maciver *et al.*, 2015, Rodrigues *et al.*, 2016) whilst the association in a physiological model, such as AH, remains incompletely understood. Since the interrelationship between ventricular wall thickness, cavity dimension and EF is complicated, a better comprehension of the relationship between the thickness of the LV wall, EF and ϵ has been aided using mathematical modelling (MacIver, 2011, Maciver *et al.*, 2015). Using intuition alone to assess the effects of multiple changes in structure and geometry may lead to incorrect interpretation. Mathematical modelling helps to eliminate confounding factors and quantifies the individual effects of geometric and physiological changes. The understanding provided by modelling studies has now been applied to hypertensive hypertrophic ventricular disease (Rodrigues *et al.*, 2016). It has been shown that using mathematical modelling (MacIver *et al.*, 2015) and confirmed observational clinical data, that increasing LV

wall thickness and/or myocardial ϵ independently leads to increased EF (Rodrigues *et al.*, 2016). Similar findings have been seen in hypertrophic cardiomyopathy where the combination of reduced myocardial ϵ and increased wall thickness results in a normal or even increased EF (MacIver and Clark, 2016). In contrast, athletes tend to have greater wall thickness and dimensions yet have similar EF compared with controls (Utomi *et al.*, 2014).

This study focusses on the LV to provide an in-depth assessment of the structural and functional characteristics of this chamber in the elite RFL athlete to aid PCS and differential diagnosis where the LV is implicated. The primary aims of this study are to (1) establish the LV phenotype in elite male RFL athletes using standard 2D, Doppler, tissue Doppler, ϵ and strain rate (SR), STE; and (2) mathematically model the association between LV size, EF and ϵ in a physiological model of hypertrophy.

4.2 Methods

4.2.1 Study population and design

Following approval by the ethics committee of Liverpool John Moores University, 139 elite, RFL Super-League athletes aged 24 ± 4 years (range 19-34) and 52 sedentary control subjects 22 ± 3 years (range 20–35) provided written informed consent to participate in the study. Athlete data was collected as part of mandatory PCS. Athletes participated in more than 10 hours structured exercise training per week and healthy controls engaged in less than 3 hours recreational activity per week. Participants completed a medical questionnaire to document any cardiovascular symptoms, family history of SCD or other cardiovascular history and abstained from exercise training or recreational activity for at least 6 hours prior to the investigation. Participants were allowed to take food and water *ad libitum* but were restricted from alcohol

consumption 24 hours prior. A cross-sectional study was employed and data acquired in a resting state at a single testing session. Screening results were reported by a sports cardiologist with clinical referrals made for any participant requiring further cardiac evaluation. Further evaluation in cases of suspected pathology provided no evidence of cardiac disease, therefore all participants remained in the study.

4.2.2 Procedures

Anthropometric assessment included height (Seca 217, Hannover, Germany) and body mass (Seca supra 719, Hannover, Germany) measurements with BSA calculated as previously described (Mosteller 1987). BP was assessed with an automated sphygmomanometer (Dinamap 300, GE Medical systems, USA). A resting 12-Lead ECG was recorded (CardioExpress SL6, Spacelabs Healthcare, Washington US). All echocardiographic acquisition and analysis of the LV was undertaken as described in chapter 3.

4.2.3 Mathematical Model

In order to calculate the independent effects of LV cavity size, mural thickness and contractile ϵ on EF, a mathematical model of LV contraction was used as previously described (MacIver, 2011, Maciver *et al.*, 2015). The mathematical model has recently been validated using echocardiography (Stokke *et al.*, 2017). The LV geometry was modelled using a two-layer with an ellipsoidal (prolate spheroidal) shape. The total mid-wall volume (intra-ventricular volume plus inner shell volume) was obtained and the volumes of the outer and inner shells were then calculated. The diastolic external and internal ventricular volumes were then obtained using the area-length method (Dodge and Baxley, 1969), and the total myocardial volume derived from the difference. The mid-wall short-axis diameter and LV length were reduced, so that

myocardial longitudinal ϵ and mid-wall circumferential ϵ were the same, to simulate systole and the new mid-wall volume was derived. Myocardial volume was assumed to be conserved therefore allowing the internal end-systolic volume to be calculated by subtracting the total muscle volume from the external end-systolic volume. The end-diastolic LV length was held constant and the end-diastolic MWT, end-diastolic diameter and myocardial ϵ were adjusted to include the range found in both the athlete and control groups. The systolic and diastolic left ventricular volumes were calculated as described above and EF calculated.

4.2.4 Statistical Analysis

Study data were collected and managed using REDCAP electronic data capture tools hosted at Liverpool John Moores University (Harris *et al.*, 2009). All echocardiographic data are presented as mean \pm SD and ranges. Statistical analyses were performed using a commercially available software package (SPSS, Version 23.0 for Windows, Illinois, USA). Variables were analysed between athletes and controls using independent t-tests with a P value < 0.05 considered statistically significant.

Where significant differences in global ϵ , SR and TDI between groups were found, a bivariate Pearson's correlation was performed against appropriate structural measures and HR. Where significant correlations were found multi-linear regression was undertaken to determine the relative contribution of each parameter on the dependent variable.

4.3 Results

Data are presented as mean \pm standard deviation (SD). Athletes were significantly older ($P = 0.001$) than controls (24 ± 4 vs. 22 ± 3 years). Height (1.82 ± 0.06 vs. 1.78 ± 0.06 m), weight (96 ± 11 vs. 78 ± 9 kg) and BSA (2.20 ± 0.15 vs. 1.96 ± 0.13 m²) were all significantly ($P < 0.001$) higher in the athlete group whilst HR was significantly ($P < 0.001$) lower in the athlete group (56 ± 10 vs. 69 ± 9 beats.min⁻¹). BP was 131/69 and 129/74 mmHg in the athlete and control groups respectively. There was no significant difference in systolic BP between groups but diastolic BP was significantly lower in athletes ($P < 0.001$).

Conventional LV structural and functional indices are presented in Table 4.1. All absolute and scaled LV structural indices were significantly larger ($P < 0.05$) in the athlete group compared to the control group. RWT was not significantly different between groups. LV geometry was assessed in all participants highlighting a predominance for normal geometry with 1.4 % and 0.7% of athletes having eccentric hypertrophy and concentric remodelling respectively. None of the athletes exhibited concentric hypertrophy. The entire control group presented with normal geometry (Figure 4.1)

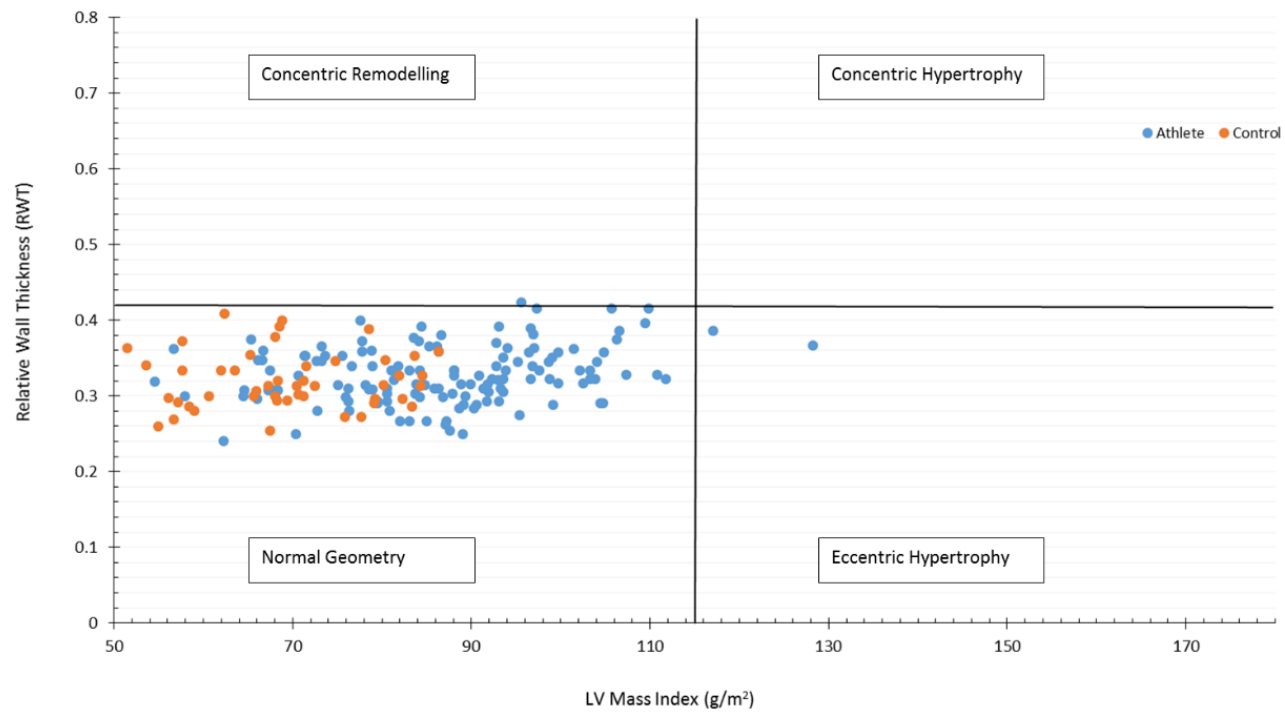


Figure 4.1 Left ventricular geometry in RFL athletes and controls according to LV mass index and RWT as described by Lang *et al.* (2015). RWT = relative wall thickness

There was no significant difference in EF or septal S' between groups. However lateral S' and average S' were significantly lower in the athlete group ($P < 0.001$ and $= 0.001$ respectively). E wave velocity was similar between groups but A velocity was significantly lower ($P < 0.001$) in athletes resulting in a higher E/A ratio ($P = 0.002$). Septal E', A' and lateral A' were significantly lower in the athlete group ($P = 0.027$, 0.003 and 0.016 respectively) and hence average E' and A' were also significantly lower ($P = 0.028$ and 0.020). Indexed S', E' and A' were significantly lower ($P < 0.001$) in the athlete group

Table 4.1 Echocardiographic parameters of the left ventricle

	Athlete Mean \pm SD (Range)	Control Mean \pm SD (Range)	P value
LVIDd (mm)	56 \pm 4 (47 - 63)	50 \pm 4 (40 - 56)	<0.001*
LVIDd index (mm/(m²)^{0.5})	37 \pm 2 (31 - 43)	35 \pm 3 (30 - 40)	<0.001*
LVIDs (mm)	38 \pm 3 (28 - 48)	34 \pm 3 (28 - 40)	<0.001*
LVIDs index (mm/(m²)^{0.5})	26 \pm 2 (19 - 31)	25 \pm 2 (20 - 29)	0.017*
MWT (mm)	9 \pm 1 (7-11)	8 \pm 1 (6-9)	<0.001*
Max WT (mm)	10 \pm 1 (8 - 12)	8 \pm 1 (7 - 10)	<0.001*
RWT	0.33 \pm 0.04 (0.24 - 0.42)	0.32 \pm 0.04 (0.25 - 0.41)	0.205
LV Mass (g)	191 \pm 31 (112 - 279)	132 \pm 24 (81 - 187)	<0.001*
LV Mass index (g/(m²)^{2.7})	38 \pm 7 (24 - 63)	28 \pm 6 (15 - 39)	<0.001*
LV mass index (g/m²)	87 \pm 13 (55 - 128)	67 \pm 11 (42 - 86)	<0.001*
LV Length (mm)	97 \pm 5 (84 - 111)	87 \pm 6 (70 - 99)	<0.001*
LVEDV (ml)	157 \pm 25 (105 - 228)	105 \pm 20 (55 - 148)	<0.001*
LVEDV (ml/(m²)^{1.5})	48 \pm 7 (33 - 65)	38 \pm 8 (22 - 51)	<0.001*
LVESV (ml)	65 \pm 13 (40 - 108)	43 \pm 9 (24-59)	<0.001*
LVESV (ml/(m²)^{1.5})	20 \pm 4 (13-30)	16 \pm 4 (9-23)	<0.001*
SV (ml)	92 \pm 16 (60-136)	62 \pm 12 (30-90)	<0.001*
EF (%)	59 \pm 4 (48 - 70)	59 \pm 3 (54 - 68)	0.466
E Velocity (m/s)	0.79 \pm 0.15 (0.47 - 1.15)	0.82 \pm 0.15 (0.49 - 1.19)	0.307
A Velocity (m/s)	0.41 \pm 0.10 (0.24 - 0.69)	0.49 \pm 0.10 (0.31 - 0.81)	<0.001*
E:A Ratio	2.01 \pm 0.54 (0.84 - 3.83)	1.75 \pm 0.47 (0.78 - 2.91)	0.002*
Medial S' (cm/s)	9 \pm 1 (8 - 13)	9 \pm 1 (7 - 13)	0.228
Medial E' (cm/s)	13 \pm 2 (9 - 18)	13 \pm 3 (9 - 21)	0.027*
Medial A' (cm/s)	7 \pm 2 (4-12)	8 \pm 2 (5-12)	0.003*

Lateral S' (cm/s)	11 ± 2 (8 - 18)	13 ± 3 (7 - 19)	<0.001*
Lateral E' (cm/s)	18 ± 3 (11 - 27)	19 ± 4 (8 - 28)	0.084
Lateral A' (cm/s)	7 ± 2 (3 - 13)	8 ± 2 (3 - 16)	0.016*
Average S' (cm/s)	10 ± 1 (8 - 15)	11 ± 2 (8 - 16)	0.001*
Average E' (cm/s)	16 ± 2 (11 - 21)	16 ± 3 (9 - 24)	0.028*
Average A' (cm/s)	7 ± 2 (4 - 12)	8 ± 2 (6 - 11)	0.02*
Average S' index ((cm/s)/cm)	1.06 ± 0.15 (0.73 - 1.61)	1.28 ± 0.24 (0.87 - 1.79)	<0.001*
Average E' Index ((cm/s)/cm)	1.61 ± 0.24 (1.09 - 2.41)	1.89 ± 0.33 (1.18 - 2.73)	<0.001*
Average A' index ((cm/s)/cm)	0.72 ± 0.17 (0.40 - 1.32)	0.90 ± 0.19 (0.57 - 1.43)	<0.001*
Average E/E'	5.14 ± 0.96 (3.03 - 9.33)	5.07 ± 1.01 (3.29 - 7.50)	0.649

* Denotes P < 0.05

Global LV ϵ , SR and twist data are presented in Table 4.2. There was no statistically significant difference between groups for global longitudinal, circumferential or radial peak ϵ . The respective time to peak ϵ (P < 0.001) was significantly increased in the athlete group across all planes of contraction. Longitudinal SRS, SRE, SRA (P = 0.01, < 0.001 and 0.011 respectively), circumferential SRS, SRE, SRA (P = 0.08, < 0.001 and 0.023 respectively) and radial SRS, SRE, SRA (P = <0.001, <0.001 and 0.019 respectively) were lower in the athlete group. Significant differences between groups were observed for LV rotational parameters with higher basal rotation (P = 0.030), lower apical rotation (P < 0.001) and lower twist (P = 0.010) exhibited in the athlete group compared to the control group.

Table 4.2 Global Left ventricular ϵ , SR and Twist

	Athlete mean \pm SD (Range)	Control mean \pm SD (Range)	P Value
LV Longitudinal			
Global ϵ (%)	-19.8 \pm 1.9 (-15.5 to -24.5)	-19.4 \pm 1.8 (-15.8 to -25.0)	0.240
Time to Peak ϵ (s)	0.37 \pm 0.03 (0.30 - 0.44)	0.35 \pm 0.03 (0.27 - 0.43)	<0.001*
SRS (s⁻¹)	-0.96 \pm 0.10 (-0.72 to -1.31)	-1.02 \pm 0.15 (-0.81 to -1.41)	0.01*
SRE (s⁻¹)	1.41 \pm 0.23 (0.75 - 2.00)	1.56 \pm 0.24 (1.02 - 2.15)	<0.001*
SRA (s⁻¹)	0.61 \pm 0.13 (0.28 - 1.00)	0.66 \pm 0.13 (0.40 - 0.99)	0.011*
LV Circumferential			
Global ϵ (%)	-18.7 \pm 2.5 (-12.6 to -24.9)	-19 \pm 2.4 (-13.9 to -25.0)	0.458
Time to Peak ϵ (s)	0.37 \pm 0.03 (0.28 - 0.45)	0.35 \pm 0.03 (0.28 - 0.43)	<0.001*
SRS (s⁻¹)	-1.06 \pm 0.15 (-0.72 to -1.60)	-1.14 \pm 0.22 (-0.80 to -1.72)	0.008*
SRE (s⁻¹)	1.51 \pm 0.33 (0.77 - 2.59)	1.72 \pm 0.32 (1.09 - 2.54)	<0.001*
SRA (s⁻¹)	0.42 \pm 0.13 (0.21 - 0.84)	0.47 \pm 0.17 (0.22 - 1.11)	0.023*
LV Radial			
Global ϵ (%)	46.8 \pm 11.2 (25.1 - 72.7)	50.1 \pm 9.0 (32.3 - 68.3)	0.059
Time to Peak ϵ (s)	0.41 \pm 0.04 (0.26 - 0.52)	0.38 \pm 0.04 (0.29 - 0.50)	<0.001*
SRS (s⁻¹)	1.57 \pm 0.28 (1.03 - 2.38)	1.90 \pm 0.43 (1.16 - 3.12)	<0.001*
SRE (s⁻¹)	-1.94 \pm 0.44 (-1.08 to -4.08)	-2.39 \pm 0.61 (-1.59 to -4.26)	<0.001*
SRA (s⁻¹)	-0.95 \pm 0.39 (-0.31 to -2.76)	-1.12 \pm 0.54 (-0.30 to -2.47)	0.019*
LV Rotation			
Basal rotation (°)	-6.23 \pm 2.94 (-11.97 - 0)	-5.21 \pm 2.47 (-11.19 - 0)	0.030*
Apical rotation (°)	8.22 \pm 3.86 (0.87 - 22.75)	11.22 \pm 4.59 (1.51 - 22.66)	<0.001*
Twist (°)	14.0 \pm 4.7 (3.0 - 28.1)	16.1 \pm 4.9 (6.9 - 26.5)	0.010*

* Denotes P < 0.05

There were significant correlations between HR, MWT, LVIDd, LV length and global SR parameters across both groups (Table 4.3). Increased HR correlated with higher SR, whilst increased structural indices correlated with lower SR's. Following multi-linear regression, HR ($\beta = -0.003$, $P < 0.001$) and MWT ($\beta = 0.020$, $P = 0.039$) accounted for 16% of the variance in longitudinal SRS. HR ($\beta = 0.007$, $P = 0.001$) and MWT ($\beta = -0.061$, $P = 0.033$) accounted for 11% of the variance in circumferential SRE, whilst HR ($\beta = -0.013$, $P < 0.001$) and MWT ($\beta = 0.120$, $P = 0.006$) also accounted for 15% of the variance in radial SRE. HR ($\beta = 0.011$, $P < 0.001$) and LVIDd ($\beta = -0.019$, $P = 0.001$) accounted for 25% of the variance in radial SRS and HR ($\beta = 0.003$, $P = 0.001$) and LV length ($\beta = -0.003$, $P = 0.024$) accounted for 15% of the variance in longitudinal SRA. MWT ($\beta = -0.099$, $P < 0.001$) was a significant independent contributor to longitudinal SRE and apical rotation accounting for 19% and 10% of the variance respectively. MWT is also independently correlated to LV twist ($R = -0.170$, $P = 0.021$). HR also correlated with medial, lateral and average A' ($R = 0.311$, $P < 0.001$, $R = 0.349$, $P < 0.001$ and $R = 0.390$, $P < 0.001$). There was no correlation between HR and TDI medial, lateral or average E'.

Table 4.3 Bivariate Correlation

STE Parameter	Parameters correlated	R value	P value
Longitudinal Time to Peak ϵ	HR	-0.662	<0.001*
	MWT	0.286	<0.001*
	LVIDd	0.351	<0.001*
	LV Length	0.281	<0.001*
Longitudinal SRS	HR	-0.377	<0.001*
	MWT	0.257	<0.001*
	LV Length	0.245	0.001*
Longitudinal SRE	MWT	-0.419	<0.001*
	LVIDd	-0.197	0.007*
	LV Length	-0.286	<0.001*
Longitudinal SRA	HR	0.355	<0.001*
	LVIDd	-0.211	0.004*
	LV Length	-0.309	<0.001*
Circumferential Time to Peak ϵ	HR	-0.590	<0.001*
	LVIDd	0.348	<0.001*
	LV Length	0.279	<0.001*
Circumferential SRS	HR	-0.345	<0.001*
	LVIDd	0.153	0.037*
	LV Length	0.200	0.006*
Circumferential SRE	HR	0.299	<0.001*
	MWT	-0.240	<0.001*
	LV Length	-0.211	0.004*
Circumferential SRA	HR	0.305	<0.001*
Radial Time to Peak ϵ	HR	-0.520	<0.001*
	MWT	0.166	0.023*
	LVIDd	0.262	<0.001*
	LV Length	0.250	0.001*
Radial SRS	HR	0.455	<0.001*
	MWT	-0.246	0.001*
	LVIDd	-0.398	<0.001*
	LV Length	-0.320	<0.001*
Radial SRE	HR	-0.342	<0.001*
	MWT	0.292	<0.001*
	LVIDd	0.300	<0.001*
	LV Length	0.258	<0.001*
Radial SRA	HR	-0.399	<0.001*
	LVIDd	0.288	<0.001*
	LV Length	0.235	0.001*
Apical Rotation	HR	0.195	0.008*
	MWT	-0.280	<0.001*
	LVIDd	-0.235	0.001*
Torsion	MWT	-0.170	0.021*

* Denotes $P < 0.05$

Regional LV longitudinal, circumferential and radial ϵ and SR data is presented in Figure 4.2 and Tables 4.4-4.6. Regional heterogeneity was most prominent within longitudinal SRS (P = 0.049), circumferential SRE (P = 0.008), circumferential SRA (P = 0.011), radial SRS (P = 0.009) and radial SRE (P = 0.049).

a

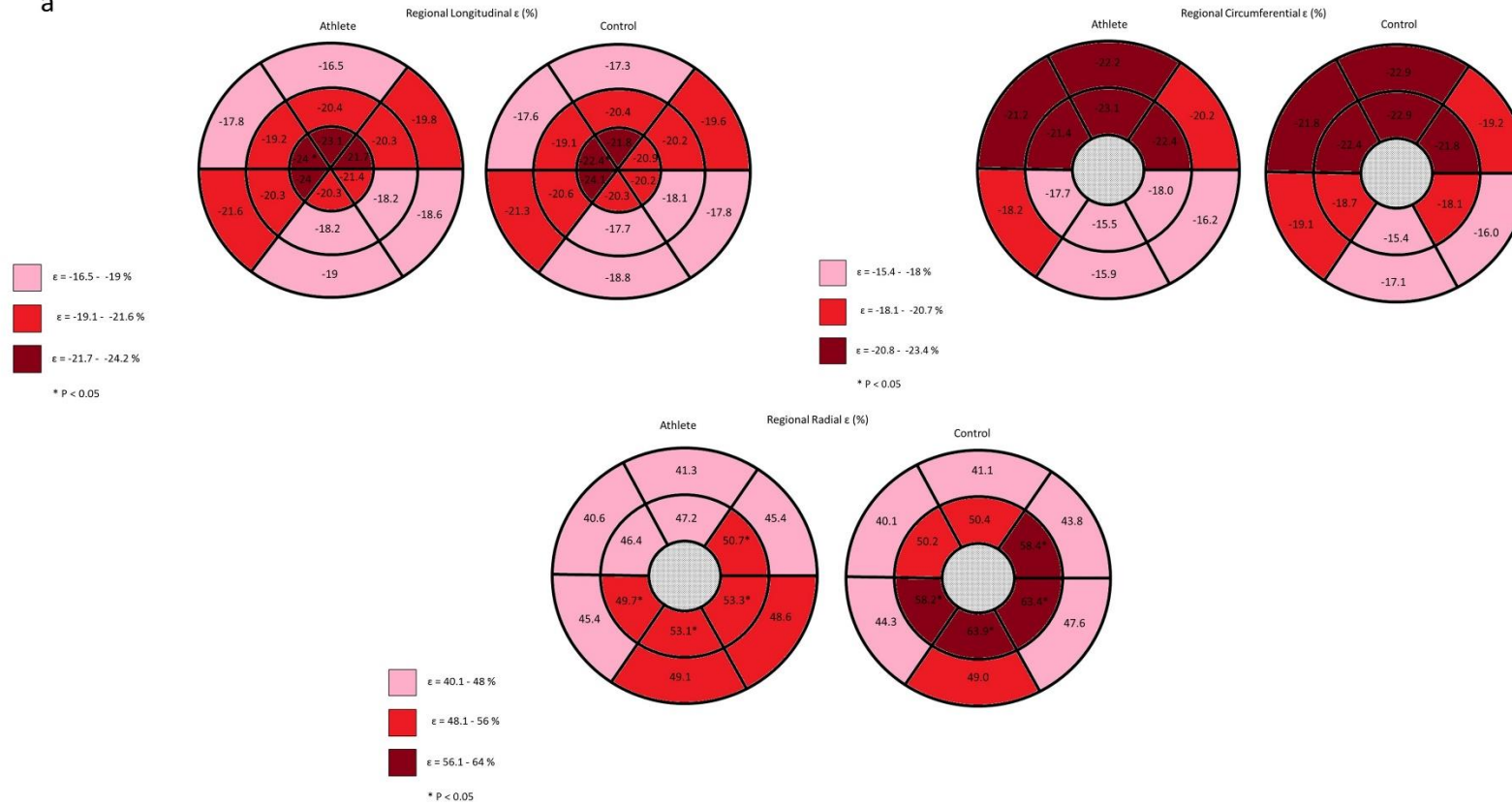


Figure 4.2a Regional longitudinal, circumferential and radial ϵ in athletes and controls

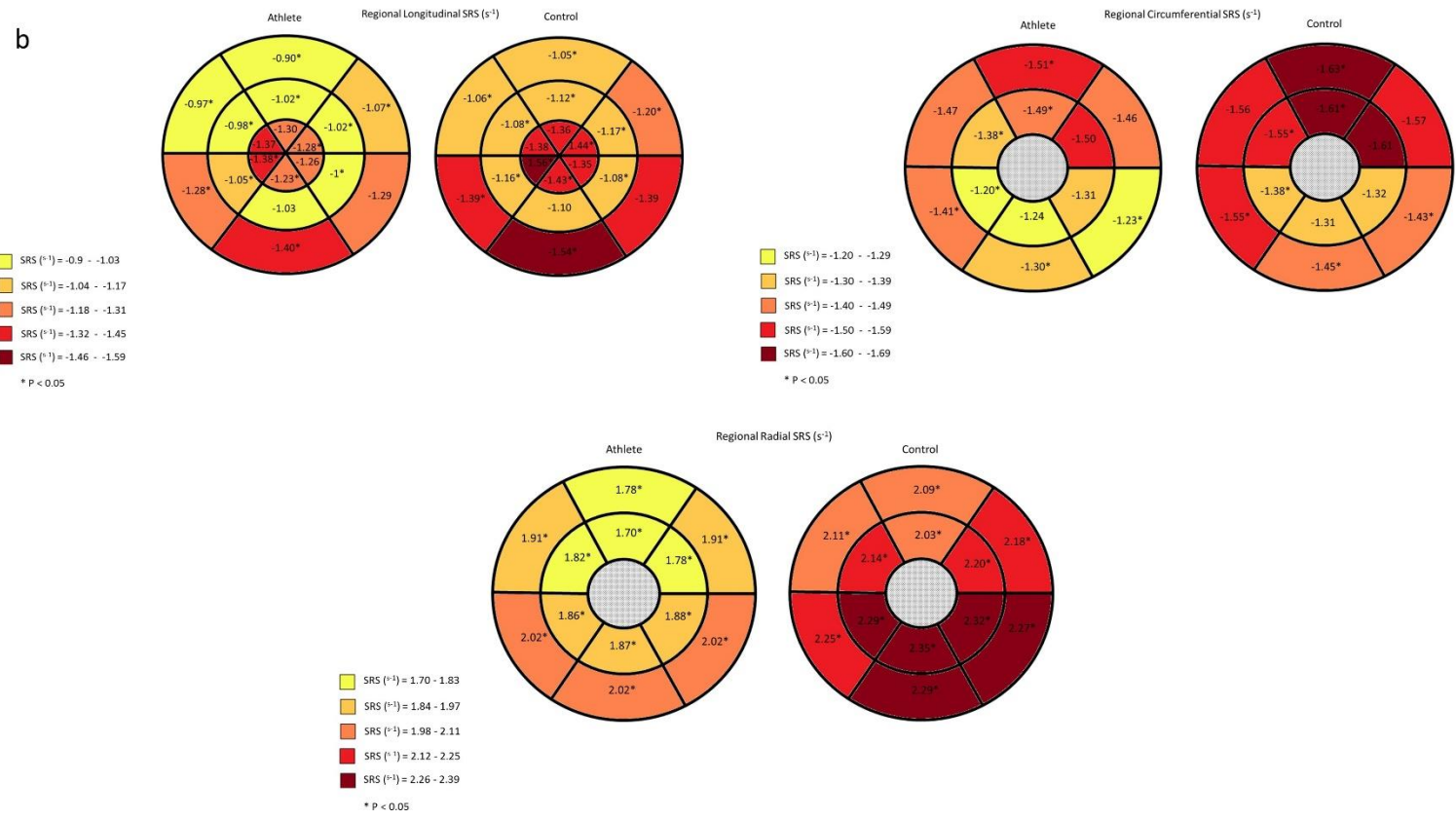


Figure 4.2b Regional longitudinal, circumferential and radial SRS in athletes and controls

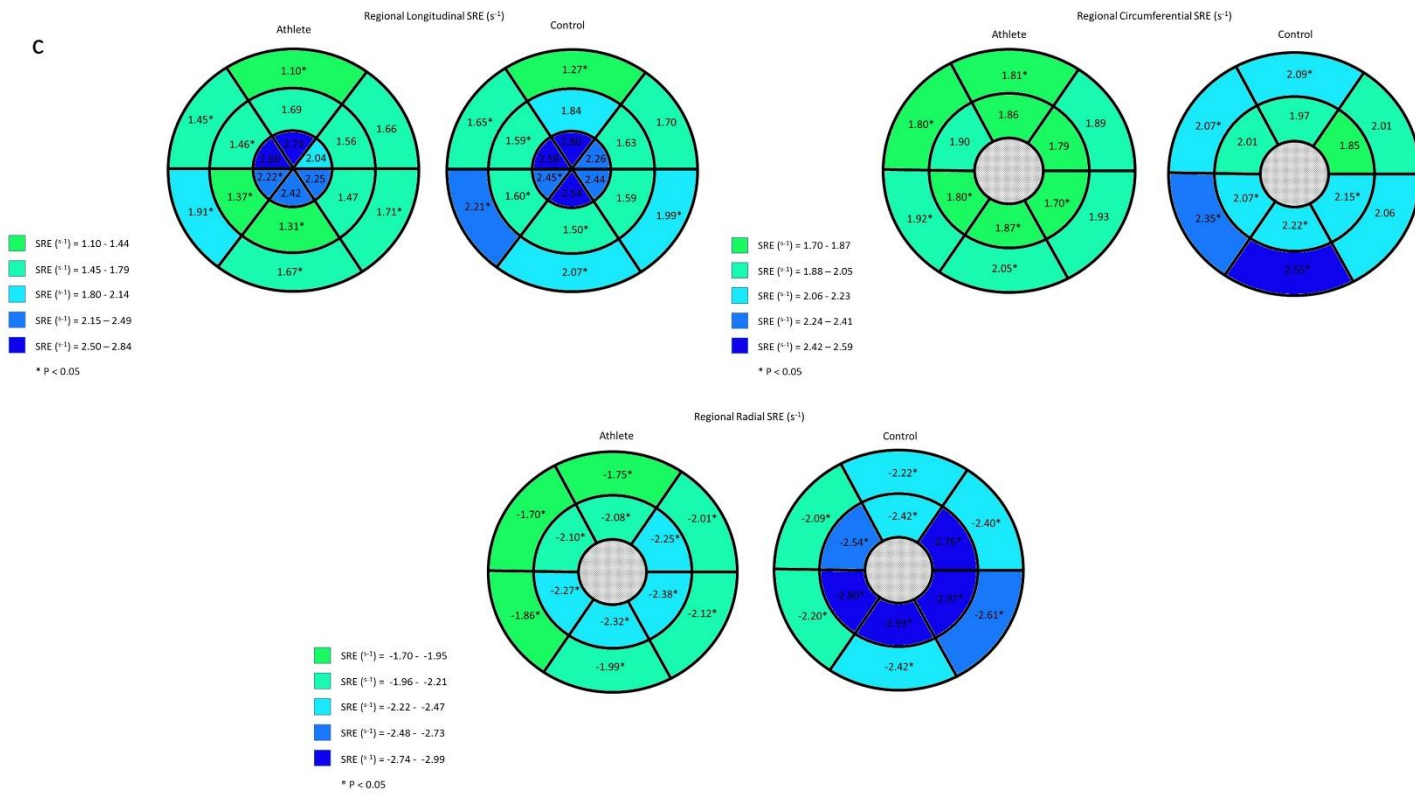


Figure 4.2c Regional longitudinal, circumferential and radial SRE in athletes and controls

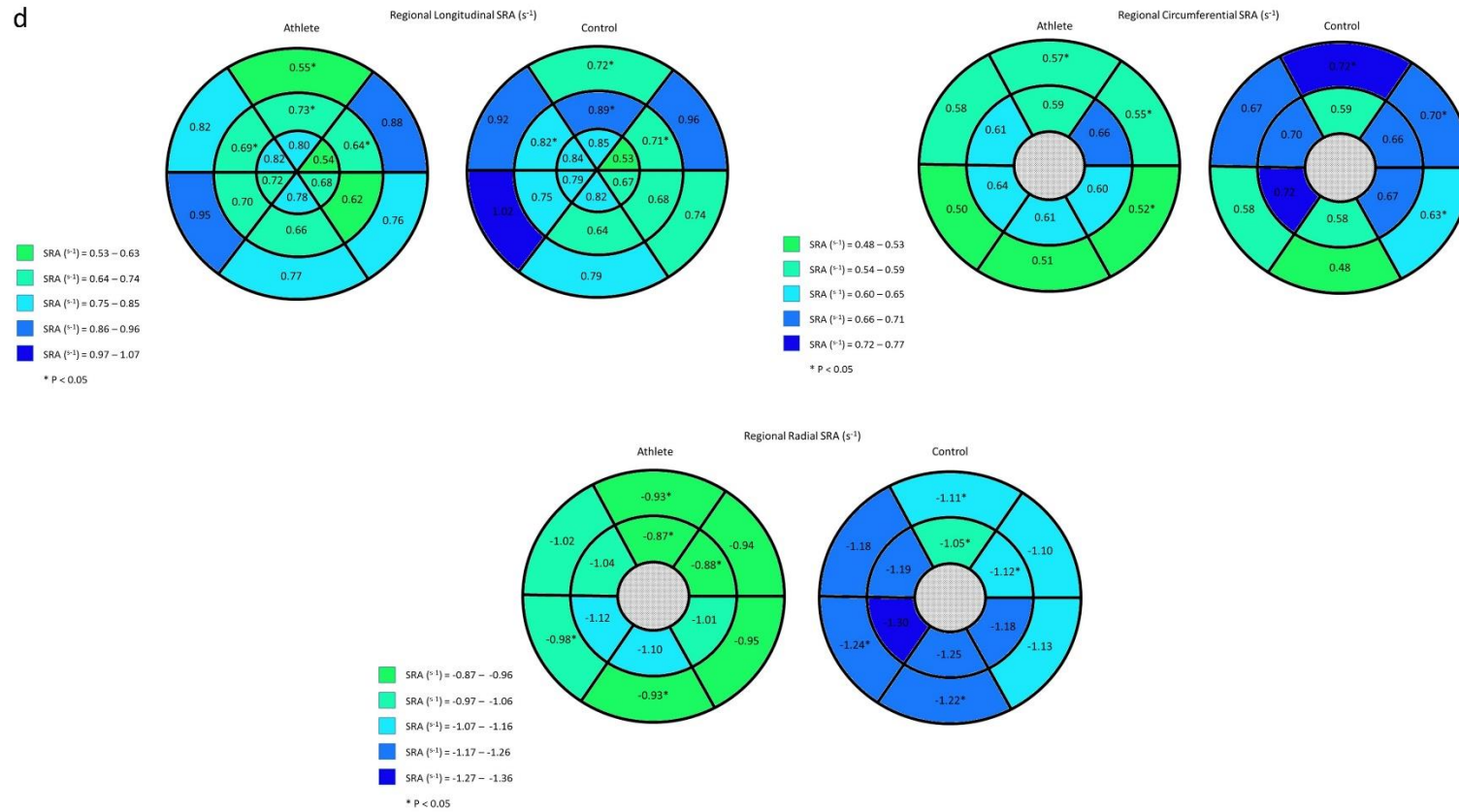


Figure 4.2d Regional longitudinal, circumferential and radial SRA in athletes and controls

Table 4.4 Regional Longitudinal ϵ and SR

	Athlete Mean \pm SD	Control Mean \pm SD	P Value
Longitudinal ϵ			
Basal Infero-septal ϵ (%)	-17.8 \pm 2.1	-17.6 \pm 2.7	0.603
Mid Infero-septal ϵ (%)	-19.2 \pm 2.3	-19.1 \pm 2.6	0.972
Apical Infero-septal ϵ (%)	-24.0 \pm 4.1	-22.4 \pm 3.9	0.018*
Apical Lateral ϵ (%)	-21.4 \pm 4.4	-20.2 \pm 4.2	0.080
Mid Lateral ϵ (%)	-18.2 \pm 2.9	-18.1 \pm 2.4	0.770
Basal Lateral ϵ (%)	-18.6 \pm 3.7	-17.8 \pm 3.0	0.145
Basal Inferior ϵ (%)	-21.6 \pm 3.2	-21.3 \pm 3.5	0.673
Mid Inferior ϵ (%)	-20.3 \pm 2.8	-20.6 \pm 2.4	0.514
Apical Inferior ϵ (%)	-24.0 \pm 4.2	-24.1 \pm 3.6	0.862
Apical Anterior ϵ (%)	-21.7 \pm 4.8	-20.9 \pm 6.2	0.332
Mid Anterior ϵ (%)	-20.3 \pm 3.1	-20.2 \pm 3.1	0.928
Basal Anterior ϵ (%)	-19.8 \pm 3.4	-19.6 \pm 3.1	0.787
Basal Posterior ϵ (%)	-19.0 \pm 4.2	-18.8 \pm 3.1	0.705
Mid Posterior ϵ (%)	-18.2 \pm 3.5	-17.7 \pm 2.5	0.390
Apical Posterior ϵ (%)	-20.3 \pm 6.2	-20.3 \pm 3.1	0.983
Apical Antero-septal ϵ (%)	-23.1 \pm 5.0	-21.8 \pm 4.8	0.128
Mid Antero-septal ϵ (%)	-20.4 \pm 3.0	-20.4 \pm 2.9	0.967
Basal Antero-septal ϵ (%)	-16.5 \pm 2.9	-17.3 \pm 2.9	0.116
Longitudinal SRS			
Basal Infero-septal SRS (s^{-1})	-0.97 \pm 0.18	-1.06 \pm 0.21	0.007*
Mid Infero-septal SRS (s^{-1})	-0.98 \pm 0.14	-1.08 \pm 0.21	<0.001*
Apical Infero-septal SRS (s^{-1})	-1.37 \pm 0.31	-1.38 \pm 0.34	0.916
Apical Lateral SRS (s^{-1})	-1.26 \pm 0.30	-1.35 \pm 0.37	0.083
Mid Lateral SRS (s^{-1})	-1.00 \pm 0.22	-1.08 \pm 0.23	0.025*
Basal Lateral SRS (s^{-1})	-1.29 \pm 0.31	-1.39 \pm 0.33	0.057
Basal Inferior SRS (s^{-1})	-1.28 \pm 0.26	-1.39 \pm 0.42	0.042*
Mid Inferior SRS (s^{-1})	-1.05 \pm 0.16	-1.16 \pm 0.21	<0.001*
Apical Inferior SRS (s^{-1})	-1.38 \pm 0.28	-1.56 \pm 0.33	<0.001*
Apical Anterior SRS (s^{-1})	-1.28 \pm 0.29	-1.44 \pm 0.44	0.004*
Mid Anterior SRS (s^{-1})	-1.02 \pm 0.20	-1.17 \pm 0.23	<0.001*
Basal Anterior SRS (s^{-1})	-1.07 \pm 0.31	-1.20 \pm 0.42	0.020*
Basal Posterior SRS (s^{-1})	-1.40 \pm 0.32	-1.54 \pm 0.34	0.007*
Mid Posterior SRS (s^{-1})	-1.03 \pm 0.21	-1.10 \pm 0.27	0.074
Apical Posterior SRS (s^{-1})	-1.23 \pm 0.31	-1.43 \pm 0.39	<0.001*
Apical Antero-septal SRS (s^{-1})	-1.30 \pm 0.34	-1.36 \pm 0.31	0.280
Mid Antero-septal SRS (s^{-1})	-1.02 \pm 0.17	-1.12 \pm 0.21	0.001*
Basal Antero-septal SRS (s^{-1})	-0.90 \pm 0.20	-1.05 \pm 0.29	<0.001*
Longitudinal SRE			
Basal Infero-septal SRE (s^{-1})	1.45 \pm 0.38	1.65 \pm 0.39	0.001*
Mid Infero-septal SRE (s^{-1})	1.46 \pm 0.32	1.59 \pm 0.33	0.021*
Apical Infero-septal SRE (s^{-1})	2.60 \pm 0.81	2.58 \pm 0.73	0.920

Apical Lateral SRE (s ⁻¹)	2.25 ± 0.79	2.44 ± 0.75	0.150
Mid Lateral SRE (s ⁻¹)	1.47 ± 0.38	1.59 ± 0.34	0.051
Basal Lateral SRE (s ⁻¹)	1.71 ± 0.51	1.99 ± 0.63	0.002*
Basal Inferior SRE (s ⁻¹)	1.91 ± 0.61	2.21 ± 0.61	0.003*
Mid Inferior SRE (s ⁻¹)	1.37 ± 0.28	1.60 ± 0.35	<0.001*
Apical Inferior SRE (s ⁻¹)	2.22 ± 0.65	2.45 ± 0.72	0.029*
Apical Anterior SRE (s ⁻¹)	2.04 ± 0.67	2.26 ± 0.84	0.072
Mid Anterior SRE (s ⁻¹)	1.56 ± 0.36	1.63 ± 0.39	0.247
Basal Anterior SRE (s ⁻¹)	1.66 ± 0.46	1.70 ± 0.54	0.586
Basal Posterior SRE (s ⁻¹)	1.67 ± 0.59	2.07 ± 0.70	<0.001*
Mid Posterior SRE (s ⁻¹)	1.31 ± 0.34	1.50 ± 0.48	0.003*
Apical Posterior SRE (s ⁻¹)	2.42 ± 0.65	2.54 ± 0.60	0.238
Apical Antero-septal SRE (s ⁻¹)	2.73 ± 0.91	2.80 ± 0.91	0.635
Mid Antero-septal SRE (s ⁻¹)	1.69 ± 0.46	1.84 ± 0.44	0.057
Basal Antero-septal SRE (s ⁻¹)	1.10 ± 0.35	1.27 ± 0.36	0.004*
Longitudinal SRA			
Basal Infero-septal SRA (s ⁻¹)	0.82 ± 0.32	0.92 ± 0.36	0.054
Mid Infero-septal SRA (s ⁻¹)	0.69 ± 0.18	0.82 ± 0.21	<0.001*
Apical Infero-septal SRA (s ⁻¹)	0.82 ± 0.27	0.84 ± 0.23	0.608
Apical Lateral SRA (s ⁻¹)	0.68 ± 0.27	0.67 ± 0.27	0.811
Mid Lateral SRA (s ⁻¹)	0.62 ± 0.23	0.68 ± 0.25	0.133
Basal Lateral SRA (s ⁻¹)	0.76 ± 0.35	0.74 ± 0.42	0.791
Basal Inferior SRA (s ⁻¹)	0.95 ± 0.32	1.02 ± 0.34	0.165
Mid Inferior SRA (s ⁻¹)	0.70 ± 0.21	0.75 ± 0.21	0.158
Apical Inferior SRA (s ⁻¹)	0.72 ± 0.27	0.79 ± 0.29	0.147
Apical Anterior SRA (s ⁻¹)	0.54 ± 0.22	0.53 ± 0.24	0.842
Mid Anterior SRA (s ⁻¹)	0.64 ± 0.20	0.71 ± 0.23	0.037*
Basal Anterior SRA (s ⁻¹)	0.88 ± 0.37	0.96 ± 0.37	0.207
Basal Posterior SRA (s ⁻¹)	0.77 ± 0.33	0.79 ± 0.35	0.727
Mid Posterior SRA (s ⁻¹)	0.66 ± 0.23	0.64 ± 0.22	0.616
Apical Posterior SRA (s ⁻¹)	0.78 ± 0.33	0.82 ± 0.24	0.442
Apical Antero-septal SRA (s ⁻¹)	0.80 ± 0.35	0.85 ± 0.28	0.365
Mid Antero-septal SRA (s ⁻¹)	0.73 ± 0.24	0.89 ± 0.18	<0.001*
Basal Antero-septal SRA (s ⁻¹)	0.55 ± 0.22	0.72 ± 0.23	<0.001*

* Denotes P < 0.05

Table 4.5 Regional Circumferential ϵ and SR

	Athlete Mean \pm SD	Control Mean \pm SD	P Value
Circumferential ϵ			
Basal Antero-septal ϵ (%)	-22.2 \pm 4.7	-22.9 \pm 5.0	0.383
Basal Anterior ϵ (%)	-20.2 \pm 5.6	-19.2 \pm 6.3	0.254
Basal Lateral ϵ (%)	-16.2 \pm 5.9	-16.0 \pm 6.2	0.885
Basal Posterior ϵ (%)	-15.9 \pm 6.2	-17.1 \pm 5.7	0.230
Basal Inferior ϵ (%)	-18.2 \pm 5.6	-19.1 \pm 5.3	0.318
Basal Infero-septal ϵ (%)	-21.2 \pm 5.1	-21.8 \pm 4.6	0.418
Mid Antero-septal ϵ (%)	-23.1 \pm 4.2	-22.9 \pm 4.3	0.769
Mid Anterior ϵ (%)	-22.4 \pm 5.4	-21.8 \pm 5.5	0.489
Mid Lateral ϵ (%)	-18.0 \pm 5.3	-18.1 \pm 6.0	0.885
Mid Posterior ϵ (%)	-15.5 \pm 5.2	-15.4 \pm 6.0	0.932
Mid Inferior ϵ (%)	-17.7 \pm 4.1	-18.7 \pm 4.0	0.133
Mid Infero-septal ϵ (%)	-21.4 \pm 4.4	-22.4 \pm 4.8	0.186
Circumferential SRS			
Basal Antero-septal SRS (s^{-1})	-1.51 \pm 0.35	-1.63 \pm 0.40	0.037*
Basal Anterior SRS (s^{-1})	-1.46 \pm 0.45	-1.57 \pm 0.52	0.160
Basal Lateral SRS (s^{-1})	-1.23 \pm 0.41	-1.43 \pm 0.49	0.005*
Basal Posterior SRS (s^{-1})	-1.30 \pm 0.45	-1.45 \pm 0.48	0.047*
Basal Inferior SRS (s^{-1})	-1.41 \pm 0.31	-1.55 \pm 0.36	0.009*
Basal Infero-septal SRS (s^{-1})	-1.47 \pm 0.35	-1.56 \pm 0.38	0.143
Mid Antero-septal SRS (s^{-1})	-1.49 \pm 0.31	-1.61 \pm 0.33	0.022*
Mid Anterior SRS (s^{-1})	-1.50 \pm 0.36	-1.61 \pm 0.46	0.082
Mid Lateral SRS (s^{-1})	-1.31 \pm 0.38	-1.32 \pm 0.41	0.858
Mid Posterior SRS (s^{-1})	-1.24 \pm 0.39	-1.31 \pm 0.44	0.280
Mid Inferior SRS (s^{-1})	-1.20 \pm 0.34	-1.38 \pm 0.36	0.002*
Mid Infero-septal SRS (s^{-1})	-1.38 \pm 0.31	-1.55 \pm 0.34	0.001*
Circumferential SRE			
Basal Antero-septal SRE (s^{-1})	1.81 \pm 0.57	2.09 \pm 0.56	0.003*
Basal Anterior SRE (s^{-1})	1.89 \pm 0.64	2.01 \pm 0.79	0.288
Basal Lateral SRE (s^{-1})	1.93 \pm 0.78	2.06 \pm 0.76	0.295
Basal Posterior SRE (s^{-1})	2.05 \pm 0.80	2.55 \pm 0.89	<0.001*
Basal Inferior SRE (s^{-1})	1.92 \pm 0.66	2.35 \pm 0.69	<0.001*
Basal Infero-septal SRE (s^{-1})	1.80 \pm 0.60	2.07 \pm 0.77	0.011*
Mid Antero-septal SRE (s^{-1})	1.86 \pm 0.53	1.97 \pm 0.49	0.234
Mid Anterior SRE (s^{-1})	1.79 \pm 0.60	1.85 \pm 0.45	0.557
Mid Lateral SRE (s^{-1})	1.70 \pm 0.61	2.15 \pm 0.85	<0.001*
Mid Posterior SRE (s^{-1})	1.87 \pm 0.71	2.22 \pm 0.93	0.007*
Mid Inferior SRE (s^{-1})	1.80 \pm 0.56	2.07 \pm 0.61	0.004*
Mid Infero-septal SRE (s^{-1})	1.90 \pm 0.59	2.01 \pm 0.63	0.280
Circumferential SRA			

Basal Antero-septal SRA (s ⁻¹)	0.57 ± 0.29	0.72 ± 0.37	0.002*
Basal Anterior SRA (s ⁻¹)	0.55 ± 0.32	0.70 ± 0.34	0.008*
Basal Lateral SRA (s ⁻¹)	0.52 ± 0.28	0.63 ± 0.44	0.039*
Basal Posterior SRA (s ⁻¹)	0.51 ± 0.30	0.48 ± 0.30	0.534
Basal Inferior SRA (s ⁻¹)	0.50 ± 0.28	0.58 ± 0.40	0.160
Basal Infero-septal SRA (s ⁻¹)	0.58 ± 0.33	0.67 ± 0.36	0.084
Mid Antero-septal SRA (s ⁻¹)	0.59 ± 0.28	0.59 ± 0.26	0.905
Mid Anterior SRA (s ⁻¹)	0.66 ± 0.34	0.66 ± 0.30	0.960
Mid Lateral SRA (s ⁻¹)	0.60 ± 0.27	0.67 ± 0.34	0.189
Mid Posterior SRA (s ⁻¹)	0.61 ± 0.31	0.58 ± 0.35	0.644
Mid Inferior SRA (s ⁻¹)	0.64 ± 0.32	0.72 ± 0.38	0.149
Mid Infero-septal SRA (s ⁻¹)	0.61 ± 0.31	0.70 ± 0.34	0.103

* Denotes P < 0.05

Table 4.6 Regional Radial ϵ and SR

	Athlete Mean ± SD	Control Mean ± SD	P Value
Radial ϵ			
Basal Antero-septal ϵ (%)	41.3 ± 16.2	41.1 ± 14.0	0.931
Basal Anterior ϵ (%)	45.4 ± 16.1	43.8 ± 15.7	0.542
Basal Lateral ϵ (%)	48.6 ± 17.4	47.6 ± 16.0	0.730
Basal Posterior ϵ (%)	49.1 ± 18.5	49.0 ± 14.4	0.961
Basal Inferior ϵ (%)	45.4 ± 17.4	44.3 ± 13.8	0.698
Basal Infero-septal ϵ (%)	40.6 ± 15.4	40.1 ± 13.1	0.844
Mid Antero-septal ϵ (%)	47.2 ± 14.7	50.4 ± 14.4	0.188
Mid Anterior ϵ (%)	50.7 ± 15.5	58.4 ± 16.3	0.003*
Mid Lateral ϵ (%)	53.3 ± 17.0	63.4 ± 16.1	<0.001*
Mid Posterior ϵ (%)	53.1 ± 18.5	63.9 ± 16.1	<0.001*
Mid Inferior ϵ (%)	49.7 ± 17.9	58.2 ± 16.2	0.003*
Mid Infero-septal ϵ (%)	46.4 ± 15.4	50.2 ± 14.4	0.131
Radial SRS			
Basal Antero-septal SRS (s ⁻¹)	1.78 ± 0.47	2.09 ± 0.57	<0.001*
Basal Anterior SRS (s ⁻¹)	1.91 ± 0.46	2.18 ± 0.61	0.001*
Basal Lateral SRS (s ⁻¹)	2.02 ± 0.51	2.27 ± 0.65	0.005*
Basal Posterior SRS (s ⁻¹)	2.02 ± 0.57	2.29 ± 0.70	0.008*
Basal Inferior SRS (s ⁻¹)	2.02 ± 0.59	2.25 ± 0.74	0.027*
Basal Infero-septal SRS (s ⁻¹)	1.91 ± 0.53	2.11 ± 0.65	0.030*
Mid Antero-septal SRS (s ⁻¹)	1.70 ± 0.41	2.03 ± 0.61	<0.001*
Mid Anterior SRS (s ⁻¹)	1.78 ± 0.42	2.20 ± 0.71	<0.001*
Mid Lateral SRS (s ⁻¹)	1.88 ± 0.45	2.32 ± 0.64	<0.001*
Mid Posterior SRS (s ⁻¹)	1.87 ± 0.48	2.35 ± 0.64	<0.001*
Mid Inferior SRS (s ⁻¹)	1.86 ± 0.46	2.29 ± 0.63	<0.001*
Mid Infero-septal SRS (s ⁻¹)	1.82 ± 0.38	2.14 ± 0.64	<0.001*

Radial SRE			
Basal Antero-septal SRE (s ⁻¹)	-1.75 ± 0.58	-2.22 ± 0.86	<0.001*
Basal Anterior SRE (s ⁻¹)	-2.01 ± 0.63	-2.40 ± 0.87	0.001*
Basal Lateral SRE (s ⁻¹)	-2.12 ± 0.76	-2.61 ± 0.99	<0.001*
Basal Posterior SRE (s ⁻¹)	-1.99 ± 0.75	-2.42 ± 1.00	0.002*
Basal Inferior SRE (s ⁻¹)	-1.86 ± 0.63	-2.20 ± 0.85	0.003*
Basal Infero-septal SRE (s ⁻¹)	-1.70 ± 0.56	-2.09 ± 0.77	<0.001*
Mid Antero-septal SRE (s ⁻¹)	-2.08 ± 0.82	-2.42 ± 0.82	0.015*
Mid Anterior SRE (s ⁻¹)	-2.25 ± 0.83	-2.76 ± 0.86	<0.001*
Mid Lateral SRE (s ⁻¹)	-2.38 ± 0.77	-2.97 ± 0.96	<0.001*
Mid Posterior SRE (s ⁻¹)	-2.32 ± 0.75	-2.93 ± 0.97	<0.001*
Mid Inferior SRE (s ⁻¹)	-2.27 ± 0.75	-2.80 ± 0.93	<0.001*
Mid Infero-septal SRE (s ⁻¹)	-2.10 ± 0.78	-2.54 ± 0.89	0.001*
Radial SRA			
Basal Antero-septal SRA (s ⁻¹)	-0.93 ± 0.46	-1.11 ± 0.63	0.036*
Basal Anterior SRA (s ⁻¹)	-0.94 ± 0.55	-1.10 ± 0.68	0.109
Basal Lateral SRA (s ⁻¹)	-0.95 ± 0.55	-1.13 ± 0.77	0.077
Basal Posterior SRA (s ⁻¹)	-0.93 ± 0.58	-1.22 ± 0.77	0.006*
Basal Inferior SRA (s ⁻¹)	-0.98 ± 0.54	-1.24 ± 0.63	0.006*
Basal Infero-septal SRA (s ⁻¹)	-1.02 ± 0.90	-1.18 ± 0.63	0.225
Mid Antero-septal SRA (s ⁻¹)	-0.87 ± 0.50	-1.05 ± 0.62	0.037*
Mid Anterior SRA (s ⁻¹)	-0.88 ± 0.47	-1.12 ± 0.69	0.007*
Mid Lateral SRA (s ⁻¹)	-1.01 ± 0.48	-1.18 ± 0.71	0.064
Mid Posterior SRA (s ⁻¹)	-1.10 ± 0.52	-1.25 ± 0.73	0.112
Mid Inferior SRA (s ⁻¹)	-1.12 ± 0.56	-1.30 ± 0.74	0.087
Mid Infero-septal SRA (s ⁻¹)	-1.04 ± 0.55	-1.19 ± 0.63	0.100

* Denotes P < 0.05

The mathematical model demonstrated that as MWT increased from 7 to 18 mm predicted an increase in EF (Figure 4.3). As myocardial ϵ improved from -15 % to -19 % also predicted an increasing EF. As LVIDd increased from 40 to 60 mm, however, the EF decreased. Furthermore, the combination of an increase in MWT combined with an elevated EDV, as seen in the athletes, led to a normalisation of EF.

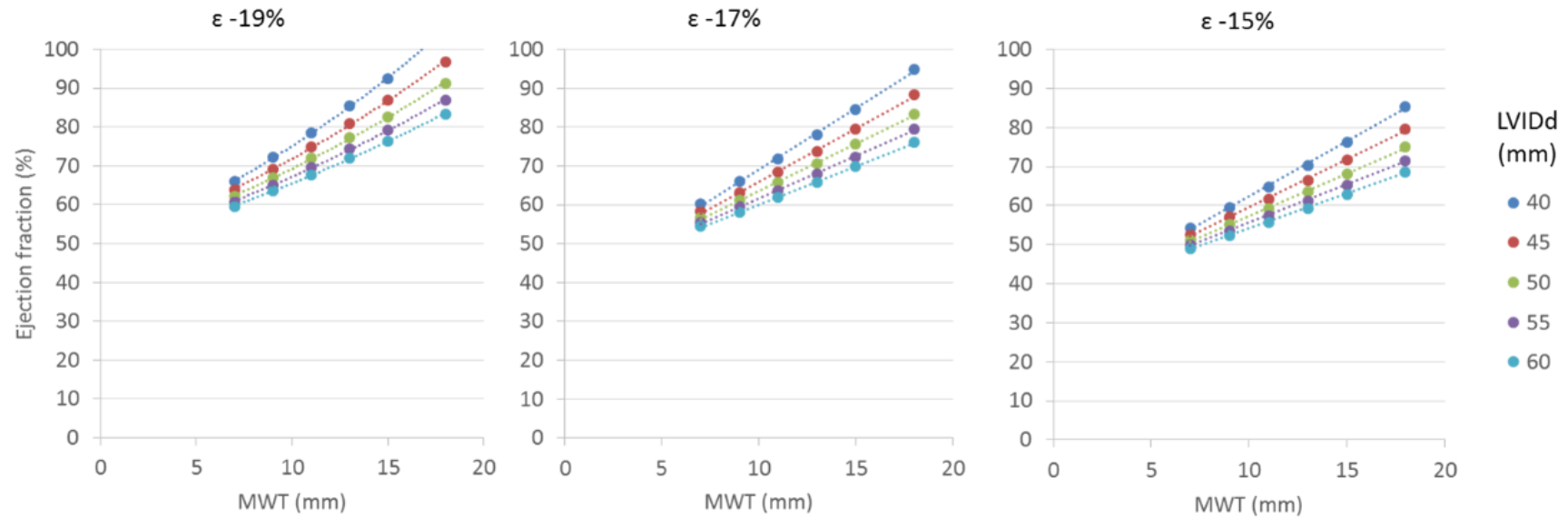


Figure 4.3 Mathematical modelling of left ventricular contraction. As ϵ decreases, ejection fraction decreases. The opposing effects of increased MWT and increased LVIDd results in a normalisation of ejection fraction.

4.4 Discussion

The main findings of this study are: (1) Absolute and scaled values for LV chamber size and wall thickness are increased in RFL athletes whilst indexed TDI, SR, apical rotation and twist are lower in RFL athletes compared to sedentary controls; (2) EF is maintained which is likely due to the interaction of divergent effects of LVIDd and MWT on LV function.

Absolute and indexed LV structural parameters are increased in elite RFL athletes consistent with previous studies (Pluim *et al.*, 2000, Utomi *et al.*, 2013). Utomi *et al.* (2014) described a predominance of normal LV geometry in both endurance and resistance trained athletes, a pattern seen in this study of RFL athletes who were engaged in structured training and competition and had a history of long-term chronic exposure to training. None of the athletes exhibited concentric LVH in contrast to a study by Finocchiaro *et al.*, (2017) who reported that 12% of male athletes demonstrated concentric remodelling/LVH, rising to 15 % for males competing in dynamic sports. The natural progression of LV geometric changes are not completely understood within populations (Oktay *et al.*, 2016) however studies have shown that abnormal LV geometry can be detrimental and has been associated with increased morbidity and mortality risk (Lavie *et al.*, 2014) thereby supporting the inclusion of LV geometry assessment in athlete echocardiographic screening.

No significant differences in longitudinal, circumferential and radial ϵ were observed between groups similar to previous findings (Beaumont *et al.*, 2017). Previously, athletes with the most marked LV remodelling were found to have similar longitudinal ϵ patterns as those with normal LV dimensions (Caselli *et al.*, 2015) and in groups of untrained subjects assigned to either endurance or resistance training LV longitudinal

ϵ did not change despite changes in LV mass and volumes (Spence *et al.*, 2011). During an 18 week intensive training programme in competitive athletes engaged in team sports, there was an increase in global longitudinal ϵ with an increase in LV cavity size, suggesting a reduction in longitudinal ϵ is not associated with physiological adaptation (D'Ascenzi *et al.*, 2015b). Our data would suggest that a reduction in global longitudinal, circumferential and radial ϵ is not a normal, physiological training adaptation. Lower SR was observed in RFL athletes and has been observed previously in athletes' (Caselli *et al.*, 2015). Regional heterogeneity was observed for both ϵ and SR, the latter demonstrating most variation, both within and between groups which suggests this may be a normal finding in adults possibly due to regional curvature and myocardial architecture differences (Marwick *et al.*, 2009) and/or a non-uniform contractile stress across the LV (MacIver and Clark, 2016). The decreased regional SR in athletes may be a normal physiological adaptation to exercise and likely reflects a combination of lower HR and larger LV dimensions. Speculatively, with increased MWT, the LV may reach the same required deformation or EF at a slower rate due to an increased number of myofibrils, or in other words, a similar wall tension and intraventricular pressure can be generated or released at a slower speed. An increase in MWT and a reduced contractile stress may result in the same contractile force (MacIver and Townsend, 2008).

Twist contributes to LV function by storing additional potential energy which is released to increase early diastolic suction, with the recoil inducing a rapid reduction of LV pressure leading to early diastolic filling (Sengupta *et al.*, 2008). Weiner *et al.* (2010) have previously highlighted that apical rotation is the primary determinant of peak systolic LV torsion. In the current study increased basal rotation and decreased apical rotation and twist in the athlete group is in part related to increased MWT and

we can speculate that there may be some reduction in mechanical function or more simply this may be an adaptive training response to create a 'reserve' for the onset of exercise as previously suggested (Doucende *et al.*, 2010). Zocalo *et al* (2007) reported reduced twist in soccer players and Nottin *et al* (2008) reported reduced twist in elite cyclists mainly driven by a reduction in apical rotation. Stöhr *et al.* (2012) also reported significantly lower LV apical rotation at rest and during submaximal exercise in individuals with high aerobic fitness, however this could not be explained by LV wall thickness or HR. A phasic response to cardiac remodelling has been reported in competitive rowers where in the acute phase of exercise training (90 days) an increase in apical rotation and twist was reported; however follow up at 39 months following the chronic phase of adaptation revealed a regression in both apical rotation and twist (Weiner *et al.*, 2015). It is possible that reduced apical rotation and twist is a normal physiological response to chronic exercise training. The LV base rotates in the opposite direction to that of the apex and is significantly lower in magnitude (Sengupta *et al.*, 2006a) with net twist explained on the basis of varying spiral myofibre architecture of these regions (Taber *et al.*, 1996, Sengupta *et al.*, 2006a). With high aerobic fitness, it has been previously speculated that lower apical rotation may be due to a change in LV microstructure with subsequent rearrangement of LV myofibres (Stöhr *et al.*, 2012).

All participants in the current study exhibited normal indices of diastolic function. Indexed and absolute diastolic TDI measures were significantly lower in the RFL athletes compared to controls and were associated with a significantly increased, but normal E/A mitral inflow ratio. Importantly, unlike A', there was a lack of correlation between E' and HR demonstrating that a faster HR in the control population is not responsible for the differences observed. These data may be reflective of differences

in cardiac mechanics between the two groups, in particular reduced apical rotation and twist. A reduction in LV twist would impact the subsequent diastolic recoil, which has implications for diastolic filling (Esch and Warburton, 2009) and may help to explain the reduction in TDI.

LV remodelling in RFL athletes allows for preservation of EF within normal range possibly through an adaptive process involving a balance between the breakdown and rebuilding of myocardial tissue (O’Keefe *et al.*, 2015). Longitudinal ϵ is similar between groups but in the presence of a significantly increased wall thickness, cavity size, and therefore, LV mass. No differences in EF between groups suggests a relationship exists between increased LVIDd and increased MWT to normalise EF for any given ϵ . EF is one of the most commonly used parameters to describe LV systolic function during serial athlete cardiac assessments. Our results are in agreement with Baggish *et al.* (2008b) who concluded that EF alone was unable to account for geometric and functional changes, with lack of sensitivity to track LV function in the presence of significant changes in LV architecture.

4.5 Limitations

From this cross sectional study we cannot determine the timing of exercise induced changes in LV structure and function. The athletes were selected according to sporting discipline and whilst physiological adaptation of the nature observed in RFL athletes is likely similar to athletes of other sports of this type, further application of the model is warranted in athletes involved in a range of sporting disciplines. Genetic factors and seasonal variation should also be considered during cardiac evaluation.

4.6 Conclusion

Despite an increased LV size, there is a predominance for normal LV geometry in RFL athletes, who undertake mixed resistance and endurance based training. Despite normal EF and global ϵ , global SR is lower and there is significant regional ϵ and SR heterogeneity compared to controls. Apical rotation and twist are also significantly lower in the athlete group and it is likely that lower SR and twist mechanics are part of the normal physiological cardiac adaptation in RFL athletes. Normal EF and therefore ϵ , observed in these athletes, is explained by the increase in both MWT and LVIDd. This study suggests that the utilisation of myocardial mechanics in addition to standard functional indices may be beneficial during PCS. A normal or abnormal STE assessment in those RFL athletes presenting with standard LV parameters at or above/below the physiological limits or ranges considered normal for those parameters is likely to aid differential diagnosis.

Chapter 5

The Right Heart of the Elite Senior Rugby Football League Athlete

5.1 Introduction

Although the AH phenotype involves all cardiac chambers, the LV has been the most extensively studied and reported in meta-analyses (Pluim *et al.*, 2000, Utomi *et al.*, 2013) with the impact of remodelling on the RV and RA having received less attention (Zaidi *et al.*, 2013, D'Ascenzi *et al.*, 2013, D'Andrea *et al.*, 2013, Pagourelas *et al.*, 2013, McClean *et al.*, 2015, D'Ascenzi *et al.*, 2017b). This thesis now moves on to characterise the right heart of the RFL athlete as a comprehensive structural and functional assessment of the right heart is also pertinent to PCS. RV enlargement is a common phenotype in AH but is also one of the diagnostic criteria for ARVC (D'Ascenzi *et al.*, 2017a), a condition linked to SCD, thereby creating a diagnostic challenge. Current Task Force criteria for the diagnosis of ARVC have been developed (Marcus *et al.*, 2010) where data was obtained from a patient population with established ARVC, however, this criteria demonstrates poor specificity when applied to a lower risk population, such as athletes (Zaidi *et al.*, 2013).

Echocardiography is utilised in the assessment of the RV during PCS and novel functional assessment techniques including ϵ and SR imaging may assist clinical differentiation between normal physiologic RV adaptation and inherited pathological conditions such as ARVC (Teske *et al.*, 2009a, D'Ascenzi *et al.*, 2016). There is, however, conflicting data defining the magnitude of RV ϵ values in athletes with some studies reporting reduced RV ϵ (Teske *et al.*, 2009b, La Gerche *et al.*, 2012, King *et al.*, 2013) whilst others have reported normal values (Oxborough *et al.*, 2012a, Utomi *et al.*, 2015).

Only a small number of studies have investigated the RA phenotype in athletes (D'Ascenzi *et al.*, 2013, D'Andrea *et al.*, 2013, Pagourelas *et al.*, 2013, McClean *et*

al., 2015) with the consensus being an enlargement reflective of the physiological change in haemodynamic loading conditions (D'Ascenzi *et al.*, 2013). Whilst RA enlargement is a recognised manifestation of the AH (Baggish and Wood, 2011) it also occurs in patients with increased filling pressures secondary to RV anomalies and cardiovascular disease (Roca *et al.*, 2015). Enlargement can also be associated with atrial arrhythmias (Müller *et al.*, 2008, Rudski *et al.*, 2010, Calvo *et al.*, 2012) and cardiomyopathy (D'Andrea *et al.*, 2009) and therefore the ability to define normal RA physiology in the athletic population is clinically relevant.

The primary aim of this study was to establish the RV phenotype in elite male RFL athletes using standard 2D, Doppler, TDI, ϵ and SR imaging. The secondary aim was to describe RA structure and function using 2D echocardiography.

5.2 Methods

5.2.1 Study population and design

Following approval from the Ethics Committee of Liverpool John Moores University, 139 elite senior RFL Super-league athletes aged 24 ± 4 years (range 19 - 34) and 52 sedentary control subjects 22 ± 3 years (range 20 - 35) provided written informed consent to participate in the study. Athlete data was collected as part of their mandatory annual PCS. All athletes participated in more than 10 hours structured exercise training per week and controls were healthy individuals who were not involved in structured sport related training, engaging in less than 3 hours recreational activity per week. After a detailed explanation of the testing protocol participants completed a medical questionnaire to document any cardiovascular symptoms, family history of SCD or other cardiovascular history. All participants abstained from exercise training or recreational activity for at least 6 hours prior to the investigation.

They were allowed to take food and water *ad libitum* but were restricted from alcohol consumption 24 hours prior. A cross-sectional study was employed and data was acquired in a resting state at a single testing session. Screening results were reported by a sports cardiologist with clinical referrals made for any participant requiring further cardiac evaluation. On further evaluation no cardiac disease was present in any of the athletes or controls, allowing for all participants to be included in the study.

5.2.2 Procedures

A routine standard anthropometric assessment included height (Seca 217, Hannover, Germany) and body mass (Seca supra 719, Hannover, Germany) measurements with BSA calculated as previously described (Mosteller, 1987). Resting BP was assessed with an automated sphygmomanometer (Dinamap 300, GE Medical systems, USA). A resting 12-Lead ECG was recorded (CardioExpress SL6, Spacelabs Healthcare, Washington US). All echocardiographic acquisition and analysis of the right heart (RV and RA) was undertaken as described in chapter 3.

5.2.3 Statistical Analysis

Study data were collected and managed using REDCAP electronic data capture tools hosted at Liverpool John Moores University (Harris *et al.*, 2009). All echocardiographic data were presented as mean \pm SD and ranges. Statistical analyses were performed using the commercially available software package SPSS (SPSS, Version 23.0 for Windows, Illinois, USA). Variables were analysed between athletes and controls using independent t-tests with $P < 0.05$ was considered statistically significant.

Where group differences were found for RV functional parameters, a bivariate Pearson's correlation was performed to establish the association to appropriate

structural measures and HR. A $P < 0.05$ was considered statistically significant. When multiple significant correlations were found with ε and SR multi-linear regression was undertaken to determine the relative contribution of each parameter on the dependent variable.

5.3 Results

Athletes were older than controls ($P = 0.001$) but within the same age range. Height, weight and BSA were all greater ($P < 0.001$) whilst HR was lower ($P < 0.001$) in the athlete group. There was no difference in systolic BP ($P = 0.413$) but diastolic BP was lower in athletes ($P < 0.001$) (Table 5.1).

Table 5.1 Demographics

	Athlete Mean±SD (Range)	Control Mean±SD (Range)	P value
Age (Years)	24±4 (19-34)	22±3 (20-35)	0.001*
Height (m)	1.82±0.06 (1.62-1.98)	1.78±0.06 (1.65-1.91)	<0.001*
Weight (Kg)	96±11 (75-132)	78±9 (60-107)	<0.001*
BSA (m²)	2.20±0.15 (1.91-2.66)	1.96±0.13 (1.66-2.38)	<0.001*
HR (Beats.min⁻¹)	56±10 (39-83)	69±9 (50-95)	<0.001*
Systolic BP	131±9 (107-155)	129±10 (113-151)	0.413
Diastolic BP	69±7 (53-89)	74±7 (63-90)	<0.001*

* Denotes $P < 0.05$

5.3.1 Right Ventricular Structure and Function

RV standard structural and functional indices are presented in Table 5.2. All absolute measures of RV size including RVWT and the RV : LV ratio were larger ($P < 0.01$) in the athlete compared to the control group. All parameters remained statistically

significant following allometric scaling with exception of RVD₂. 88% of athletes and 38% of controls met RVOT_{plax} dimension criteria for ARVC (Marcus *et al.*, 2010). 78% of athletes and 29% of controls met RVOT₁ dimension criteria for ARVC (Marcus *et al.*, 2010). None of the controls met major ARVC criteria for RVOT₁ compared to 46% of athletes (Figure 5.1). The RVOT₁:RVD₁ ratio was increased in athletes (P = 0.012). TAPSE and RVFAC were not significantly different between groups. Absolute RV systolic and diastolic TDI values - RVS', RVE', RVA' and RV E'/A' ratio were not different between groups however the associated indexed values for RVS', RVE' and RVA' were lower in the athlete group (P = 0.002, < 0.001 and 0.015 respectively).

Table 5.2 Echocardiographic parameters of the right ventricle

	Athlete Mean±SD (Range)	Control Mean±SD (Range)	P Value
RVOT_{PLAX} (mm)	34 ± 4 (21 - 47)	28 ± 4 (20 - 36)	<0.001*
RVOT₁ (mm)	36 ± 5 (22 - 49)	29 ± 4 (19 - 35)	<0.001*
RVOT₂ (mm)	27 ± 3 (19 - 35)	23 ± 2 (18 - 28)	<0.001*
RVD₁ (mm)	44 ± 5 (33 - 60)	39 ± 4 (31 - 47)	<0.001*
RVD₂ (mm)	33 ± 4 (22 - 44)	30 ± 5 (17 - 42)	<0.001*
RVD₃ (mm)	91 ± 8 (72 - 111)	82 ± 7 (71 - 98)	<0.001*
RVD_a (cm²)	30 ± 4 (21 - 41)	22 ± 3 (15 - 29)	<0.001*
RVS_a (cm²)	16 ± 3 (10 - 23)	12 ± 2 (6 - 18)	<0.001*
RVFW (mm)	4 ± 1 (2 - 7)	4 ± 1 (3 - 5)	<0.001*
TAPSE (mm)	24 ± 4 (16 - 33)	23 ± 3 (17 - 32)	0.144
RVOT₁:RVD₁ Ratio	0.81 ± 0.14 (0.52 - 1.23)	0.76 ± 0.11 (0.44 - 0.97)	0.012*
RV:LV Ratio	0.91 ± 0.10 (0.70 - 1.20)	0.82 ± 0.07 (0.66 - 1.01)	<0.001*
RVFAC (%)	46 ± 6 (34 - 61)	47 ± 7 (38 - 64)	0.442
RVOT_{PLAX} (mm/(m²)^{0.5})	23 ± 3 (15 - 30)	20 ± 2 (15 - 25)	<0.001*
RVOT₁ (mm/(m²)^{0.5})	24 ± 3 (15 - 32)	21 ± 3 (14 - 26)	<0.001*
RVOT₂ (mm/(m²)^{0.5})	18 ± 2 (13 - 24)	17 ± 2 (13 - 20)	<0.001*
RVD₁ (mm/(m²)^{0.5})	30±3 (22-38)	28 ± 2 (23 - 34)	<0.001*
RVD₂ (mm/(m²)^{0.5})	22 ± 3 (15 - 30)	21 ± 3 (12 - 29)	0.174
RVD₃ (mm/(m²)^{0.5})	61 ± 5 (47 - 75)	59 ± 5 (49 - 70)	0.04*
RVD_a Index (cm²/m²)	14 ± 2 (9 - 18)	11 ± 2 (7 - 15)	<0.001*
RVS_a Index (cm²/m²)	7 ± 1 (4 - 11)	6 ± 1 (3 - 8)	<0.001*
RVS' (cm/s)	15 ± 2 (6 - 23)	14 ± 2 (10 - 18)	0.581
RVE' (cm/s)	15 ± 3 (7 - 24)	15 ± 3 (9 - 21)	0.502
RVA' (cm/s)	10 ± 3	11 ± 3	0.852

	(5 - 17)	(6 - 18)	
RV E'/A' (cm/s)	1.54 ± 0.44 (0.71 - 3.00)	1.56 ± 0.49 (0.81 - 2.71)	0.775
RVS' index ((cm/s)/cm)	1.61 ± 0.29 (0.61 - 2.44)	1.75 ± 0.26 (1.06 - 2.34)	0.002*
RVE' index ((cm/s)/cm)	1.65 ± 0.32 (0.84 - 2.76)	1.89 ± 0.39 (0.98 - 2.76)	<0.001*
RVA' index ((cm/s)/cm)	1.15 ± 0.33 (0.56 - 2.05)	1.28 ± 0.34 (0.74 - 2.05)	0.015*

* Denotes P < 0.05

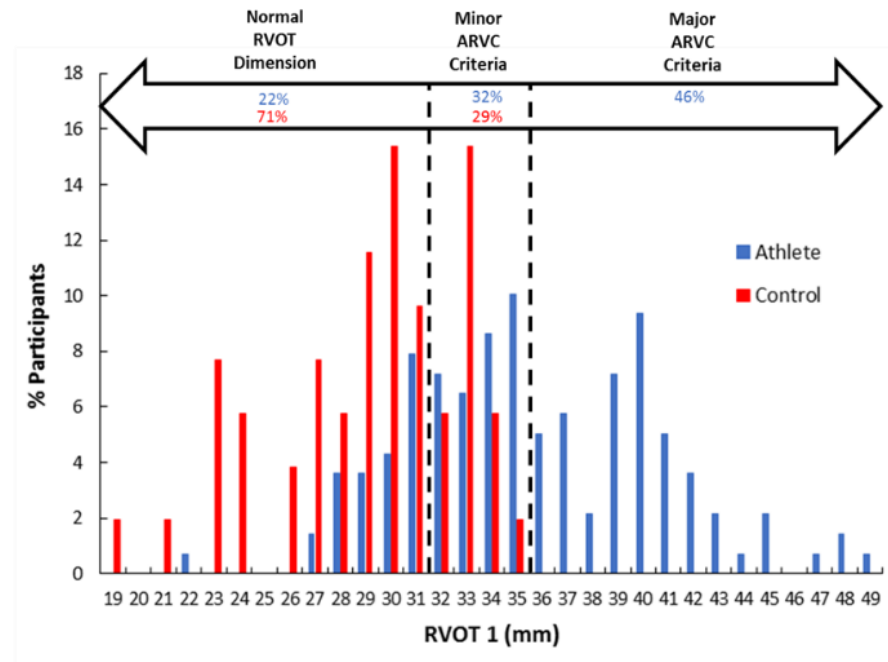
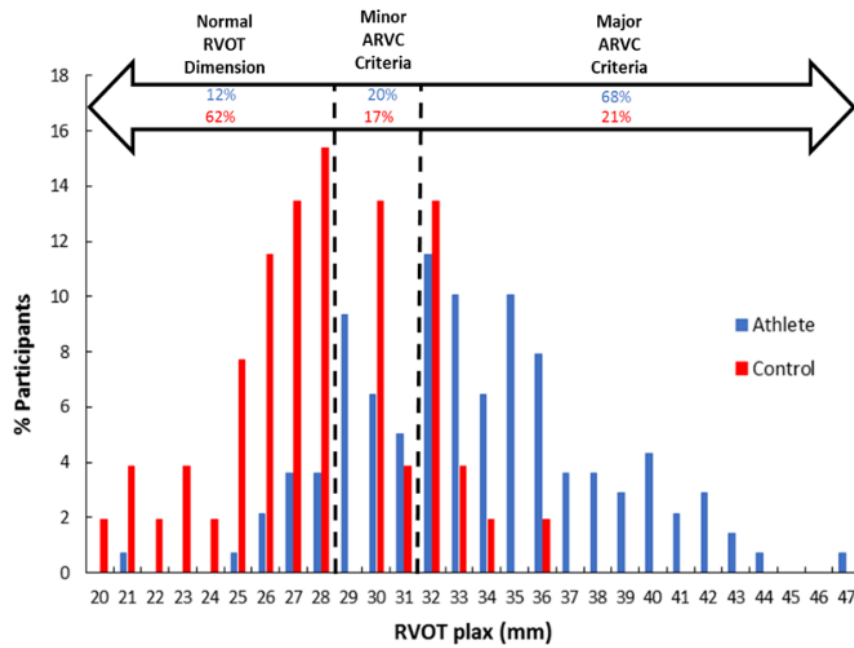


Figure 5.1 Percentage of athletes and controls meeting minor and major criteria for ARVC according to Marcus *et al.* (2010).

Global RV longitudinal ϵ , although lower in athletes, was not statistically significant between groups (Table 5.3). Time to peak ϵ was higher ($P < 0.001$) in the athlete group whilst RVSRS, RVSRE and RVSRA were all lower ($P < 0.001$) in the athlete compared to the control group.

Table 5.3 Global and regional right ventricular ϵ and SR

	Athlete mean \pm SD (Range)	Control mean \pm SD (Range)	P Value
Global RVϵ (%)	-27.2 \pm 3.4 (-18.4 to -40.7)	-28.4 \pm 4.2 (-19.1 to -41.2)	0.053
Time to Peak RV ϵ (s)	0.38 \pm 0.03 (0.31 - 0.46)	0.36 \pm 0.03 (0.31 - 0.44)	<0.001*
RVSRS (s^{-1})	-1.32 \pm 0.22 (-0.77 to -2.19)	-1.48 \pm 0.28 (-0.97 to -2.34)	<0.001*
RVSRE (s^{-1})	1.59 \pm 0.33 (0.79 - 2.67)	1.92 \pm 0.50 (1.11 - 3.26)	<0.001*
RVSRA (s^{-1})	0.89 \pm 0.27 (0.34 - 1.77)	1.09 \pm 0.28 (0.39 - 1.85)	<0.001*
Basal RVϵ (%)	-24.9 \pm 5.4	-26.3 \pm 4.9	0.105
Mid RVϵ (%)	-27.2 \pm 4.1	-28.4 \pm 4.8	0.096
Apical RVϵ (%)	-30.0 \pm 4.3	-31.1 \pm 4.6	0.146
Apex to Base RVϵ gradient (%)	-5.2	-4.8	0.743
Basal RVSRS (s^{-1})	-1.50 \pm 0.41	-1.74 \pm 0.41	<0.001*
Mid RVSRS (s^{-1})	-1.37 \pm 0.27	-1.50 \pm 0.31	0.004*
Apical RVSRS (s^{-1})	-1.58 \pm 0.31	-1.86 \pm 0.43	<0.001*
Basal RVSRE (s^{-1})	2.10 \pm 0.67	2.50 \pm 0.84	0.001*
Mid RVSRE (s^{-1})	1.68 \pm 0.40	2.02 \pm 0.58	<0.001*
Apical RVSRE (s^{-1})	2.07 \pm 0.55	2.22 \pm 0.54	0.081
Basal RVSRA (s^{-1})	1.06 \pm 0.34	1.26 \pm 0.38	0.001*
Mid RVSRA (s^{-1})	0.98 \pm 0.33	1.13 \pm 0.37	0.007*
Apical RVSRA (s^{-1})	1.25 \pm 0.40	1.46 \pm 0.44	0.003*

* Denotes $P < 0.05$

There were no significant differences between groups for RV regional longitudinal ϵ (Table 5.3) and both groups exhibited similar apex to base ϵ gradients (-5%, $P = 0.743$). In the athlete group, all 3 RV wall segments demonstrated lower RVSRS (basal $P < 0.001$, mid $P = 0.004$ and apical $P < 0.001$) and RVSRA (Basal $P = 0.001$, mid P

= 0.007 and apical $P = 0.003$). Basal ($P = 0.001$) and mid segments also demonstrated lower RVSRE ($P < 0.001$) (Table 5.3).

There were significant correlations between SR and HR, RVD_1 and $RVOT_1$ and between TDI index and RVD_1 , RVD_3 and HR (with exception of RVE' index) across both groups (Table 5.4). Following multi-linear regression, HR ($\beta = -0.006$, $P < 0.001$) and RVD_1 ($\beta = 0.008$, $P = 0.014$) accounted for 15% of the variation in RVSRS. HR ($\beta = -0.013$, $P < 0.001$) and RVD_1 ($\beta = 0.016$, $P = 0.030$) accounted for 14% of the variation in RVSRE. HR ($\beta = -0.018$, $P < 0.001$) and $RVOT_1$ ($\beta = -0.014$, $P = 0.012$) accounted for 19% of the variation in RVSRA.

Table 5.4 Right ventricular bivariate correlation

Functional Parameter	Parameters correlated	R value	P value
RV Time to Peak ϵ	HR	-0.583	<0.001*
	RVOT ₁	0.278	<0.001*
	RVD ₁	0.303	<0.001*
	RVD ₃	0.235	0.001*
RVSRS	HR	-0.347	<0.001*
	RVOT ₁	0.220	0.003*
	RVD ₁	0.279	<0.001*
	RVD ₃	0.256	<0.001*
RVSRE	HR	0.203	0.005*
	RVOT ₁	-0.233	0.001*
	RVD ₁	-0.332	<0.001*
	RVD ₃	-0.330	<0.001*
RVSRA	HR	0.193	0.008*
	RVOT ₁	-0.244	0.001*
	RVD ₁	-0.172	0.019*
	RVD ₃	-0.178	0.015*
RVS' index	HR	0.159	0.028*
	RVOT ₁	-0.013	0.858
	RVD ₁	-0.212	0.003*
	RVD ₃	-0.538	<0.001*
RVE' index	HR	0.112	0.124
	RVOT ₁	-0.137	0.059
	RVD ₁	-0.163	0.024*
	RVD ₃	-0.366	<0.001*
RVA' index	HR	0.227	0.002*
	RVOT ₁	-0.113	0.122
	RVD ₁	-0.160	0.027*
	RVD ₃	-0.256	<0.001*

* Denotes $P < 0.05$

5.3.2 RA Structure and Functional Volumes

Absolute RAa, RAvoles, RAvolpreA and RAvoled and their respective indexed values were larger in the athlete group compared to controls ($P < 0.001$). RAvolres, RAvolcon and RAvolboo were larger in the athlete group ($P < 0.001$) (Table 5.5) however con:boo was not different between groups ($P = 0.557$).

Table 5.5 Echocardiographic parameters of the Right Atrium

	Athlete Mean±SD (Range)	Control Mean±SD (Range)	P Value
RAa (cm²)	22 ± 4 (13 - 29)	15 ± 2 (10 - 20)	<0.001*
RAa Index (cm²/m²)	10 ± 1 (6 - 13)	8 ± 1 (5 - 10)	<0.001*
RAvoles (ml)	73 ± 18 (33 - 121)	44 ± 10 (25 - 63)	<0.001*
RAvoles Index (ml/(m²)^{1.5})	22 ± 5 (11 - 35)	16 ± 4 (10 - 24)	<0.001*
RAvolpreA (ml)	49 ± 13 (25 - 92)	28 ± 7 (14 - 45)	<0.001*
RAvolpreA Index (ml/(m²)^{1.5})	15 ± 4 (6 - 27)	10 ± 2 (6 - 16)	<0.001*
RAvoled (ml)	35 ± 10 (15 - 75)	18 ± 5 (7 - 32)	<0.001*
RAvoled Index (ml/(m²)^{1.5})	10 ± 3 (5 - 22)	6 ± 2 (3 - 10)	<0.001*
RAvolres (ml)	39 ± 11 (13 - 77)	26 ± 7 (13 - 44)	<0.001*
RAvolcon (ml)	53 ± 17 (5 - 96)	36 ± 12 (12 - 65)	<0.001*
RAvolboo (ml)	14 ± 5 (5 - 30)	10 ± 3 (4 - 19)	<0.001*
Con : Boo Ratio	4.32 ± 2.65 (0.17 - 16.2)	4.07 ± 2.27 (1.2 - 12.75)	0.557

* Denotes P < 0.05

5.4 Discussion

The main findings of this study are: 1) absolute measures for RV chamber size and wall thickness are greater in RFL athletes compared to sedentary controls. This finding remains following allometric scaling with the exception of RVD₂. There are no differences in the functional parameters RVFAC and RV longitudinal ϵ between groups but TDI index and SR are lower in athletes, which are, in part, associated with lower HR and increased RV chamber size; and 2) all absolute and indexed structural RA parameters are greater in athletes. Whilst functional RA volumes are increased in athletes there is no difference in the relative contribution to diastolic filling.

5.4.1 RV Structure

Larger RV cavities in endurance athletes have been previously demonstrated with increases in both inflow and outflow dimensions (Oxborough *et al.*, 2012a, D'Andrea *et al.*, 2013) however, there are few studies that have assessed the RV in resistance athletes or those involved in mixed training (Utomi *et al.*, 2013). A 6 month resistance exercise training study demonstrated no increase in RV cavity dimensions (Spence *et al.*, 2011) and in a study by D'Andrea *et al.* (2013) RV chamber size in resistance athletes was similar to sedentary controls. The results of the current study in athletes with mixed endurance and resistance training components would suggest that RV structure in the RFL athlete is more akin to that of the endurance athlete with an observed increased RV inflow and outflow dimensions and an increased RV:LV ratio compared to controls. Unequal remodelling and increased RV:LV ratio has been reported previously in endurance athletes (La Gerche *et al.*, 2011, Oxborough *et al.*, 2012a, Arbab-Zadeh *et al.*, 2014) attributable to disproportionate loading on the RV during exercise (La Gerche *et al.*, 2011). The increased RVOT₁:RVD₁ ratio in athletes suggests a lack of proportional enlargement of RV outflow and inflow as RVOT₁ appears to dilate to a greater extent. Differentiation of physiological RV enlargement from ARVC in RFL athletes is pertinent given that 88% and 78% of these meet ARVC structural criteria (Marcus *et al.*, 2010) at RVOT_{plax} and RVOT₁ respectively.

Little attention has been paid to appropriate scaling of RV structural parameters but it is likely to aid interpretation of the RV in AH (Utomi *et al.*, 2015). With appropriate scaling for body size in this study all structural parameters were significantly greater in athletes compared to controls, with the exception of RVD₂. This would suggest that body size alone does not account for the enlarged RV in a RFL athlete.

5.4.2 RV Function

In addition to structural assessment, functional assessment is key when attempting to differentiate physiological RV remodelling from ARVC (Marcus *et al.*, 2010). It is considered best practice to apply a multifactorial approach to functional assessment including the use of TAPSE, RVFAC and RV TDI (Qasem *et al.*, 2016). The current study reports no difference in TAPSE, RVFAC or standard indices of TDI between RFL athletes and controls and therefore the presence of abnormal values should prompt further investigation.

ϵ imaging is advocated in the assessment of RV function (Rudski *et al.*, 2010) and it has been reported that STE ϵ parameters are superior to conventional echocardiographic parameters in aiding the identification of ARVC (Teske *et al.*, 2009a). No difference in longitudinal global RV ϵ was noted between RFL athletes and controls, providing additional support that a reduction in function is not a normal physiological response in RFL athletes. Lower global RV ϵ values have been previously reported in elite endurance athletes due to a reduction in basal function (Teske *et al.*, 2009b), a finding that was reproduced in a subsequent study which also reported increased ϵ in the apical segment (La Gerche *et al.*, 2012). In the current study there was no difference in regional RV ϵ between groups and both RFL athletes and controls exhibit an RV ϵ gradient of 5% from base to apex, suggesting a normal pattern of deformation even with increased RV size in RFL athletes. Other recent studies reported no difference in resting ϵ parameters (Oxborough *et al.*, 2012a) and no differences in global or regional RV deformation in athletes compared to controls (Utomi *et al.*, 2015). Similarly, a study involving both endurance and resistance athletes found few meaningful differences in deformation parameters of the right heart

irrespective of sporting discipline, training volume and physiological remodelling (Pagourelas *et al.*, 2013).

SR and TDI index are largely related to HR and RV dimensions. TDI index is reduced in athletes and despite regional SR showing similar distribution in both RFL athletes and controls, both global and regional SR is lower in athletes. In an endurance training study by Teske *et al.* (2009b) SR values were found to be reduced in basal and mid segments in athletes with marked RV dilatation, whereas athletes without RV dilatation showed no significant difference compared to controls. It was reported that this should be interpreted as a normal finding when evaluating athletes suspected for RV pathology (Teske *et al.*, 2009b). Lower SR in athletes in the current study is also likely to represent normal physiological adaptation to training in the RFL athlete given that ϵ , TDI, RVFAC and TAPSE were not different compared to controls. It has been previously reported that during brief maximal exercise the RV has the capacity to increase contractility to compensate for disproportionate increases in work (La Gerche *et al.*, 2011) and it is reasonable to speculate that reduced SR (aligned to chamber size and HR) may be an adaptation of myocardial contractility to support contractile reserve during exercise. The increased size of the RV would suggest an increased RV mass and number of myofibrils and it is plausible that a greater number of myofibrils (MacIver and Townsend, 2008) may reach the same required deformation at a slower rate, or in other words, a similar wall tension and intraventricular pressure can be generated or released at a slower speed. An increase in RV free wall thickness and a reduced contractile stress may result in the same contractile force.

5.4.3 RA Structure and Function

Increased RA area, volume and indexed volume has been reported in athletes with changes in the RA proportional to those of the RV (D'Ascenzi *et al.*, 2013). McClean *et al* (2015) reported that RA size is consistently larger throughout the cardiac cycle, in athletes with high dynamic training. The data of both studies are supported by the current study. The RA assists RV filling by: 1) acting as a reservoir for venous return; 2) acting as a passive conduit in early diastole; and 3) acting as an active conduit (booster) in late diastole during atrial contraction (Rudski *et al.*, 2010). During all 3 phases of RV filling, functional volumes, RAVolres, RAVolcon and RAVolboo were greater in RFL athletes. This does not infer a functional RA improvement in RFL athletes as no difference in the passive conduit / booster (con:boo) volume ratio was found between groups. Although atrial enlargement appears to be a normal physiological response to dynamic training there is increasing evidence of an association between an AH phenotype and autonomic alterations with atrial arrhythmia (Calvo *et al.*, 2012). As mechanisms of atrial arrhythmia in the athlete are not clearly understood (Calvo *et al.*, 2012, Turagam *et al.*, 2012), the RA is likely to receive more attention in the future.

5.5 Limitations

This is a cross sectional study and hence the timing and development of exercise induced structural and functional adaptation cannot be determined. The athletes were selected according to sporting discipline and these findings may not therefore be representative of all athletes. Genetic factors and seasonal variation should also be considered during cardiac evaluation. There is a significant difference in age between

groups, however the mean difference is small and is not clinically meaningful in view of our understanding of normal echocardiographic ranges.

5.6 Conclusion

This study provides a novel and comprehensive assessment of the right heart in the RFL athlete. RV dimensions are larger in athletes independent of body size, whilst reduced SR and indexed TDI is likely a normal physiological phenomenon in the elite RFL athlete. Despite RA enlargement in RFL athletes there is no evidence in this study of functional RA/RV improvement compared to controls. These normative data may be used to aid differentiation between physiology and pathology during PCS of these athletes.

Chapter 6

The Athletic Heart Phenotype of the Rugby Football League Athlete: A Comparative Study of Senior and Junior Athletes

6.1 Introduction

Chapters 4 and 5 have described important structural and functional relationships in the left and right heart of the senior RFL athlete but how does the cardiac phenotype of the RFL change in relation to age? This is an important issue to address as PCS involves athletes from 14 -35 years.

Most studies of the AH have been focused on adult (senior) athletes with only a few studies in adolescent (junior) athletes (Sharma et al., 1999, Sharma *et al.*, 2002, George *et al.*, 2001, Makan *et al.*, 2005, Sheikh *et al.*, 2013). Left ventricular (LV) cavity enlargement and an increase in wall thickness have been found in junior athletes compared with non-athletic controls but these changes were less pronounced compared to senior athletes, likely due to lack of physical maturity and fewer cumulative training hours (Makan *et al.*, 2005, Sharma et al., 2002, Sheikh *et al.*, 2013). The RV and atria in adolescent athletes have received less attention although both have been shown to increase in size throughout adolescence (George *et al.*, 2001). An increase in left atrial size has been documented in adolescent soccer players (D'ascenzi *et al.*, 2012) and an increased bi-atrial and RV size has been reported in pre-adolescent athletes (D'Ascenzi *et al.*, 2016c, D'Ascenzi *et al.*, 2017c). The assessment of cardiac function in the junior athlete has also received limited attention (De Luca *et al.*, 2011, Simsek *et al.*, 2013). Recent advances in echocardiography, including ϵ and SR imaging have allowed the assessment of cardiac mechanics in senior athletes (D'Ascenzi *et al.*, 2016a, Beaumont *et al.*, 2017) and therefore it is pertinent to describe similar functional data in a junior athletic population. Recently, a large systematic review of SCD in a general athletic population reported the mean age at death to be 17 years (Harmon et al., 2014) supporting the need for PCS in this young population. There is, however, no universally accepted consensus as to the

impact of the athletes age on the classification of normal/abnormal findings (Harmon *et al.*, 2014). The definition of the upper limits of physiological enlargement in AH have been based on echocardiographic studies of adult athletes (Pluim *et al.*, 2000, Makan *et al.*, 2005) and it remains difficult to extrapolate these data to younger athletes (Makan *et al.*, 2005).

Information regarding the upper physiological limits in both junior and senior RFL athletes will aid the differentiation between physiology and pathology.

The aim of this study was to establish and compare the AH phenotype of both junior (14 to 18 years) and senior (19 to 34 years) RFL athletes using a combination of 2D, Doppler, tissue Doppler echocardiography and cardiac mechanics derived from STE.

6.2 Methods

6.2.1 Study population and design

Following approval by the ethics committee of Liverpool John Moores University, 139 elite, RFL senior athletes (SA) aged 24 ± 4 years (range 19 - 34) and 97 RFL junior athletes (JA) 17 ± 1 years (range 14 -18) provided written informed consent to participate in the study. Athlete data was collected as part of mandatory annual pre-participation cardiac screening. All athletes participated in more than 10 hours structured exercise training per week. SA reported a larger number of training years compared to JA (15 ± 5 and 11 ± 2 years respectively) as well as a larger number of training hours per week (20 ± 8 and 13 ± 5 hours respectively). Both groups reported 5 ± 1 training days per week. Following a detailed explanation of the testing protocol participants completed a medical questionnaire to document any cardiovascular symptoms, family history of SCD or other cardiovascular history. All participants abstained from exercise training or recreational activity for at least 6 hours prior to the

investigation. They were allowed to take food and water *ad libitum* but were restricted from alcohol consumption 24 hours prior. A cross-sectional study design was employed and data was acquired in a resting state at a single testing session. Screening results were reported by a sports cardiologist with clinical referrals made for any participant requiring further cardiac evaluation (Sharma *et al.*, 2017). After screening and further evaluation where necessary to exclude underlying cardiac disease, all participants were included in the study.

6.2.2 Procedures

A routine standard anthropometric assessment included height (Seca 217, Hannover, Germany) and body mass (Seca supra 719, Hannover, Germany) measurements with BSA calculated as previously described (Mosteller 1987). BP was assessed with an automated sphygmomanometer (Dinamap 300, GE Medical systems, USA). A resting 12-Lead ECG was recorded (CardioExpress SL6, Spacelabs Healthcare, Washington US). All echocardiographic acquisition and analysis was undertaken as described in chapter 3. Mean apical wall thickness was also determined from two further LV wall measurements taken at the anterior and posterior apex in a modified PSAX LV apical image.

6.2.3 Statistical Analysis

Study data were collected and managed using REDCAP electronic data capture tools hosted at Liverpool John Moores University (Harris *et al.*, 2009). All echocardiographic data were presented as mean \pm SD and ranges. Statistical analyses were performed using commercially available software package SPSS Version 23.0 for Windows (SPSS, Illinois, USA). Variables were analysed between SA and JA using independent T-tests with $P < 0.05$ considered statistically significant. Where

between group differences were observed for ϵ and SR in both the LV and RV, bivariate Pearson's correlation was performed. This included the total study population, to establish any associations with appropriate LV and RV structural measures and HR. A $P < 0.05$ was considered statistically significant. When multiple significant correlations were found, multi-linear regression was undertaken to determine relative contribution of each parameter on the dependent (functional) variable. HR and structural parameters were correlated with each ϵ and SR parameters that was found to be significantly different between groups.

6.3 Results

Height (1.82 ± 0.06 vs. 1.80 ± 0.07 m), weight (96 ± 11 vs. 83 ± 13 kg) and BSA (2.20 ± 0.15 vs. 2.03 ± 0.18 m²) were all larger ($P \leq 0.001$) in SA whilst HR was significantly ($P < 0.001$) lower in SA (56 ± 10 vs. 60 ± 9 beats.min⁻¹) compared to JA. There was no difference in systolic or diastolic BP ($P > 0.05$) between SA and JA ($131/69$ mmHg vs. $130/68$ mmHg, respectively). SA demonstrated a larger number ($P < 0.001$) of training years and training hours per week compared to JA. There were no differences ($P = 0.323$) between groups for number of training days per week.

6.3.1 Left Ventricle

Conventional LV structural and functional indices are presented in Table 6.1. Absolute LVIDd, LVIDs, LVEDV, LVESV and LV length were larger in SA ($P < 0.001$), however, there were no differences in the respective indexed values. MWT ($P < 0.001$), Max WT ($P < 0.001$), and mean apical wall thickness ($P < 0.001$) were larger in SA, however, after allometric scaling only mean apical wall thickness was larger in SA. In addition, RWT was larger in SA ($P = 0.039$). LV mass ($P < 0.001$) and associated indexed values (LVMI g/m², $P = 0.006$; LVMI (g/m²)^{2.7}, $P < 0.001$) were

larger in SA. Figure 6.1 demonstrates LV geometry in all participants highlighting a predominance for normal geometry in both groups. One JA and one SA exhibited concentric remodelling whilst one JA and two SA exhibited eccentric hypertrophy. None of the athletes demonstrated concentric hypertrophy. LVEF was not different between groups and there were no differences in the systolic medial and lateral TDI S'. Diastolic E wave velocity and E:A ratio ($P < 0.001$) were lower in SA. Average E' was lower in SA ($P < 0.001$) and average A' was lower in JA ($P = 0.010$). When indexed for LV length, lower ($P < 0.001$) average E' remained in SA.

Table 6.1 Left Ventricular Structural and Functional Indices

	Senior Mean \pm SD (Range)	Junior Mean \pm SD (Range)	P Value
LVIDd (mm)	56 \pm 4 (47 - 63)	54 \pm 4 (43 - 65)	<0.001*
LVIDd index (mm/(m²)^{0.5})	37 \pm 2 (31 - 43)	38 \pm 2 (31 - 44)	0.304
LVIDs (mm)	38 \pm 3 (28 - 48)	36 \pm 4 (25 - 46)	<0.001*
LVIDs index (mm/(m²)^{0.5})	26 \pm 2 (19-31)	25 \pm 3 (18-31)	0.472
MWT (mm)	9 \pm 1 (7 - 11)	8 \pm 1 (7 - 11)	<0.001*
MWT (mm/m²)^{0.5}	6.0 \pm 0.5 (4.8 - 7.2)	5.9 \pm 0.4 (4.9 - 7.7)	0.191
Max WT(mm)	10 \pm 1 (8 - 12)	9 \pm 1 (8 - 11)	<0.001*
Max WT (mm/m²)^{0.5}	6.6 \pm 0.5 (5.5 - 7.9)	6.6 \pm 0.5 (5.2 - 7.9)	0.405
RWT	0.33 \pm 0.04 (0.24 - 0.42)	0.32 \pm 0.04 (0.22 - 0.47)	0.039*
Mean Apical Wall Thickness (mm)	7 \pm 1 (5 - 10)	6 \pm 1 (5 - 9)	<0.001*
Mean Apical Wall Thickness Index (mm/m²)^{0.5}	4.6 \pm 0.8 (3.3 - 6.7)	4.1 \pm 0.6 (3.1 - 6.3)	<0.001*
LV Mass (g)	191 \pm 31 (112 - 279)	167 \pm 31 (90 - 256)	<0.001*
LV Mass index (g/(m²)^{2.7})	38 \pm 7 (24 - 63)	34 \pm 6 (20 - 55)	<0.001*
LV mass index (g/m2)	87 \pm 13 (55 - 128)	82 \pm 13 (52 - 124)	0.006*

LV Length (mm)	97 ± 5 (84 - 111)	93 ± 5 (80 - 105)	<0.001*
LV Length Index (mm/m²)^{0.5}	65 ± 4 (56 - 78)	66 ± 4 (55 - 73)	0.354
LVEDV (ml)	157 ± 25 (105 - 228)	141 ± 20 (96 - 207)	<0.001*
LVEDV (ml/(m²)^{1.5})	48 ± 7 (33 - 65)	49 ± 7 (34 - 63)	0.136
LVESV (ml)	65 ± 13 (40 - 108)	57 ± 10 (38 - 100)	<0.001*
LVESV (ml/(m²)^{1.5})	20 ± 4 (13 - 30)	20 ± 4 (13 - 31)	0.930
SV (ml)	92 ± 16 (60 - 136)	84 ± 15 (55 - 119)	<0.001*
EF (%)	59 ± 4 (48 - 70)	60 ± 5 (50 - 71)	0.081
E Velocity (m/s)	0.79 ± 0.15 (0.47 - 1.15)	0.93 ± 0.14 (0.56 - 1.25)	<0.001*
A Velocity (m/s)	0.41 ± 0.10 (0.24 - 0.69)	0.41 ± 0.11 (0.25 - 0.94)	0.928
E:A Ratio	2.01 ± 0.54 (0.84 - 3.83)	2.39 ± 0.71 (0.87 - 4.46)	<0.001*
Medial S' (cm/s)	9 ± 1 (8 - 13)	9 ± 1 (7 - 14)	0.227
Medial E' (cm/s)	13 ± 2 (9 - 18)	14 ± 2 (10 - 21)	<0.001*
Medial A' (cm/s)	7 ± 2 (4-12)	7 ± 2 (4-13)	0.004*
Medial E'/A'	1.85 ± 0.55 (0.82 - 4)	2.19 ± 0.64 (0.92 - 4.25)	<0.001*
Lateral S' (cm/s)	11 ± 2 (8 - 18)	12 ± 2 (8 - 19)	0.340
Lateral E' (cm/s)	18 ± 3 (11 - 27)	20 ± 3 (12 - 27)	0.001*
Lateral A' (cm/s)	7 ± 2 (3 - 13)	6 ± 2 (3 - 12)	0.067
Lateral E'/A'	2.99 ± 1.03 (1.08 - 5.75)	3.41 ± 1.04 (1.30 - 6.75)	0.003*
Average S' (cm/s)	10 ± 1 (8 - 15)	10 ± 2 (8 - 15)	0.778
Average E' (cm/s)	16 ± 2 (11 - 21)	17 ± 2 (12 - 23)	<0.001*
Average A' (cm/s)	7 ± 2 (4 - 12)	6 ± 2 (4 - 12)	0.010*
Average E/E'	5.14 ± 0.96 (3.03 - 9.33)	5.62 ± 1.01 (3.00 - 8.44)	<0.001*
Average S' index ((cm/s)/cm)	1.06 ± 0.15 (0.73 - 1.61)	1.10 ± 0.17 (0.77 - 1.69)	0.078
Average E' Index ((cm/s)/cm)	1.61 ± 0.24 (1.09 - 2.41)	1.82 ± 0.26 (1.26 - 2.59)	<0.001*
Average A' index ((cm/s)/cm)	0.72 ± 0.17 (0.40 - 1.32)	0.68 ± 0.16 (0.40 - 1.25)	0.095

* Denotes P < 0.05

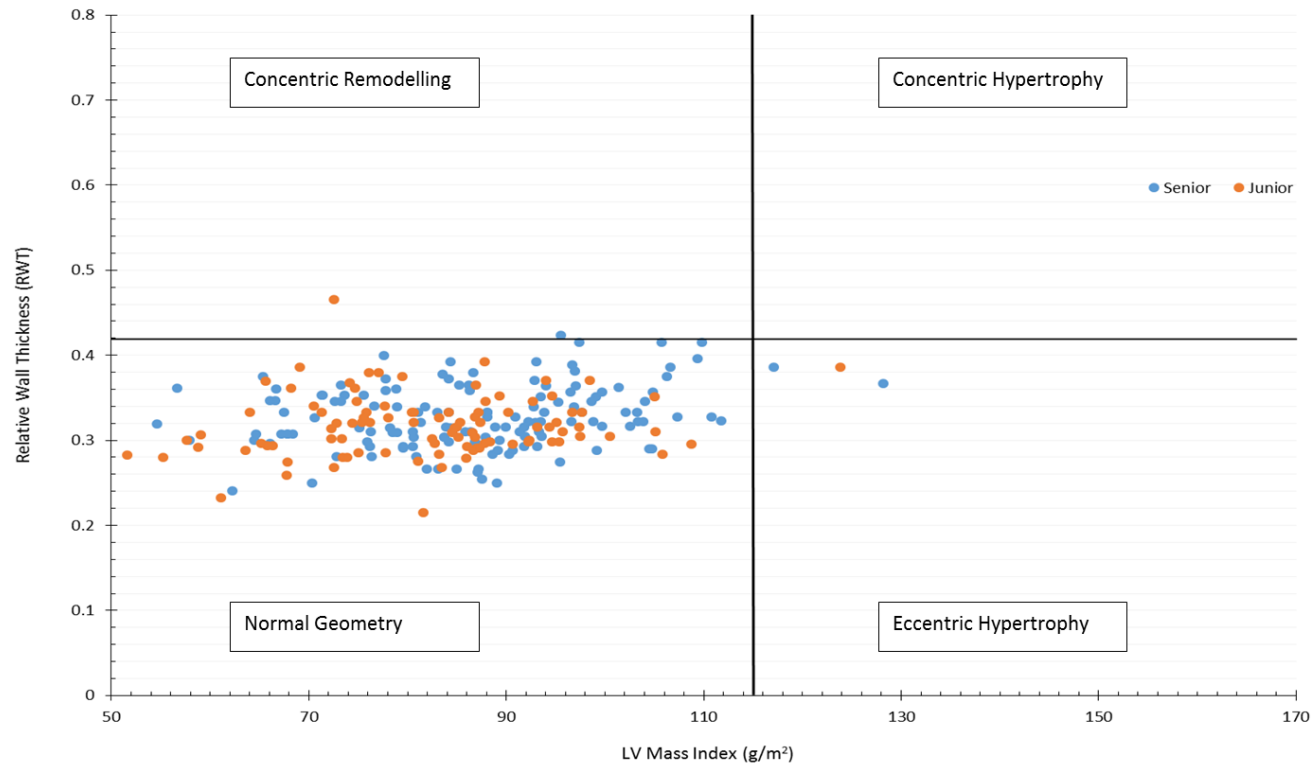


Figure 6.1 LV geometry in SA and JA (as described by Lang *et al.*, 2015)

Global LV ϵ , SR and twist data are presented in Table 6.2. There were no differences between groups for global longitudinal, circumferential, radial peak ϵ , rotation or twist. Global Longitudinal SRS ($P = 0.001$) and SRE ($P < 0.001$) were lower in SA whilst circumferential and radial SRA were lower ($P < 0.001$) in JA.

There were significant correlations of HR and LV structural parameters (MWT, LVIDd and LV length) to global SR parameters that reached significance between SA and JA (Table 6.3). Following multi-linear regression, HR remained as an independent predictor and accounted for 10% of the variance in longitudinal SRS ($\beta = -0.004$, $P < 0.001$). MWT ($\beta = -0.082$, $P < 0.001$), LVIDd ($\beta = -0.010$, $P = 0.020$) and LV length ($\beta = -0.010$, $P < 0.001$) together accounted for 18% of the variance in longitudinal SRE. HR ($\beta = -0.010$, $P < 0.001$), MWT ($\beta = -0.111$, $P < 0.001$) and LVIDd ($\beta = 0.013$, $P = 0.043$) together accounted for 14% of the variance in radial SRA.

Table 6.2 Global LV ϵ , SR and twist parameters

	Senior mean \pm SD (Range)	Junior mean \pm SD (Range)	P Value
LV Longitudinal			
Global ϵ (%)	-19.8 \pm 1.9 (-15.5 to -24.5)	-20.2 \pm 1.9 (-15.0 to -25.3)	0.105
Time to Peak ϵ (s)	0.37 \pm 0.03 (0.30 - 0.44)	0.37 \pm 0.03 (0.29 - 0.43)	0.133
SRS (s^{-1})	-0.96 \pm 0.10 (-0.72 to -1.31)	-1.01 \pm 0.15 (-0.67 to -1.55)	0.001*
SRE (s^{-1})	1.41 \pm 0.23 (0.75 - 2.00)	1.65 \pm 0.23 (1.14 - 2.32)	<0.001*
SRA (s^{-1})	0.61 \pm 0.13 (0.28 - 1.00)	0.57 \pm 0.15 (0.25 - 0.91)	0.104
LV Circumferential			
Global ϵ (%)	-18.7 \pm 2.5 (-12.6 to -24.9)	-19.1 \pm 2.4 (-13.2 to -28.3)	0.330
Time to Peak ϵ (s)	0.37 \pm 0.03 (0.28 - 0.45)	0.36 \pm 0.03 (0.28 - 0.42)	0.008*
SRS (s^{-1})	-1.06 \pm 0.15	-1.09 \pm 0.18	0.224

	(-0.72 to -1.60)	(-0.74 to -1.82)	
SRE (s⁻¹)	1.51 ± 0.33 (0.77 - 2.59)	1.59 ± 0.29 (0.88 - 2.45)	0.064
SRA (s⁻¹)	0.42 ± 0.13 (0.21 - 0.84)	0.33 ± 0.10 (0.15 - 0.71)	<0.001*
LV Radial			
Global ε (%)	46.8 ± 11.2 (25.1 - 72.7)	44.2 ± 10.9 (17.2 - 73.0)	0.095
Time to Peak ε (s)	0.41 ± 0.04 (0.26 - 0.52)	0.40 ± 0.04 (0.31 - 0.50)	0.305
SRS (s⁻¹)	1.57 ± 0.28 (1.03 - 2.38)	1.52 ± 0.30 (0.82 - 2.40)	0.208
SRE (s⁻¹)	-1.94 ± 0.44 (-1.08 to -4.08)	-2.04 ± 0.48 (-1.07 to -3.37)	0.097
SRA (s⁻¹)	-0.95 ± 0.39 (-0.31 to -2.76)	-0.75 ± 0.30 (-0.23 to -1.53)	<0.001*
LV Rotation			
Basal rotation (°)	-6.23 ± 2.94 (-11.97 - 0)	-5.83 ± 3.36 (-13.94 - 0)	0.363
Apical rotation (°)	8.22 ± 3.86 (0.87 - 22.75)	8.60 ± 3.64 (2.08 - 20.15)	0.484
Twist (°)	14.02 ± 4.73 (2.96 - 28.05)	13.96 ± 4.85 (4.67 - 24.66)	0.937

* Denotes P < 0.05

Table 6.3 LV correlation

STE Parameter	Parameters Correlated	R Value	P Value
Longitudinal SRS	HR	-0.317	<0.001*
	MWT	-0.027	0.693
	LVIDd	0.138	0.040*
	LV Length	0.153	0.022*
Longitudinal SRE	HR	0.096	0.154
	MWT	-0.315	<0.001*
	LVIDd	-0.245	<0.001*
	LV Length	-0.311	<0.001*
Circumferential SRA	HR	0.107	0.112
	MWT	0.113	0.092
	LVIDd	0.124	0.064
	LV Length	0.121	0.071
Radial SRA	HR	-0.278	<0.001*
	MWT	-0.198	0.003*
	LVIDd	0.158	0.018*
	LV Length	-0.062	0.359

* Denotes $P < 0.05$

Regional LV longitudinal, circumferential and radial ϵ and SR data is presented in Figure 6.2 and Tables 6.4-6.6. Differences observed between groups for regional SR reflects the differences observed with global SR between groups. Lower longitudinal SRS values were seen in some basal, mid and apical regions in SA ($P < 0.05$). Differences in diastolic SR were also observed with predominantly lower longitudinal SRE values in SA ($P < 0.05$) and predominantly lower circumferential and radial SRA values in JA ($P < 0.05$).

Other regional differences ($P < 0.05$) were observed, not reflected by global mechanical data, including lower longitudinal ϵ in some apical segments in SA with regional radial ϵ predominantly lower at the base in JA athletes. Lower circumferential and radial SRS values were seen at mid-level and base respectively in JA. A few regions exhibited lower basal circumferential and radial SRE in SA along and some longitudinal mid and apical segments recorded lower SRA values in JA. Care is

warranted with multiple comparison effect and statistical artefact and it is possible that these data may simply reflect a few random differences.

a

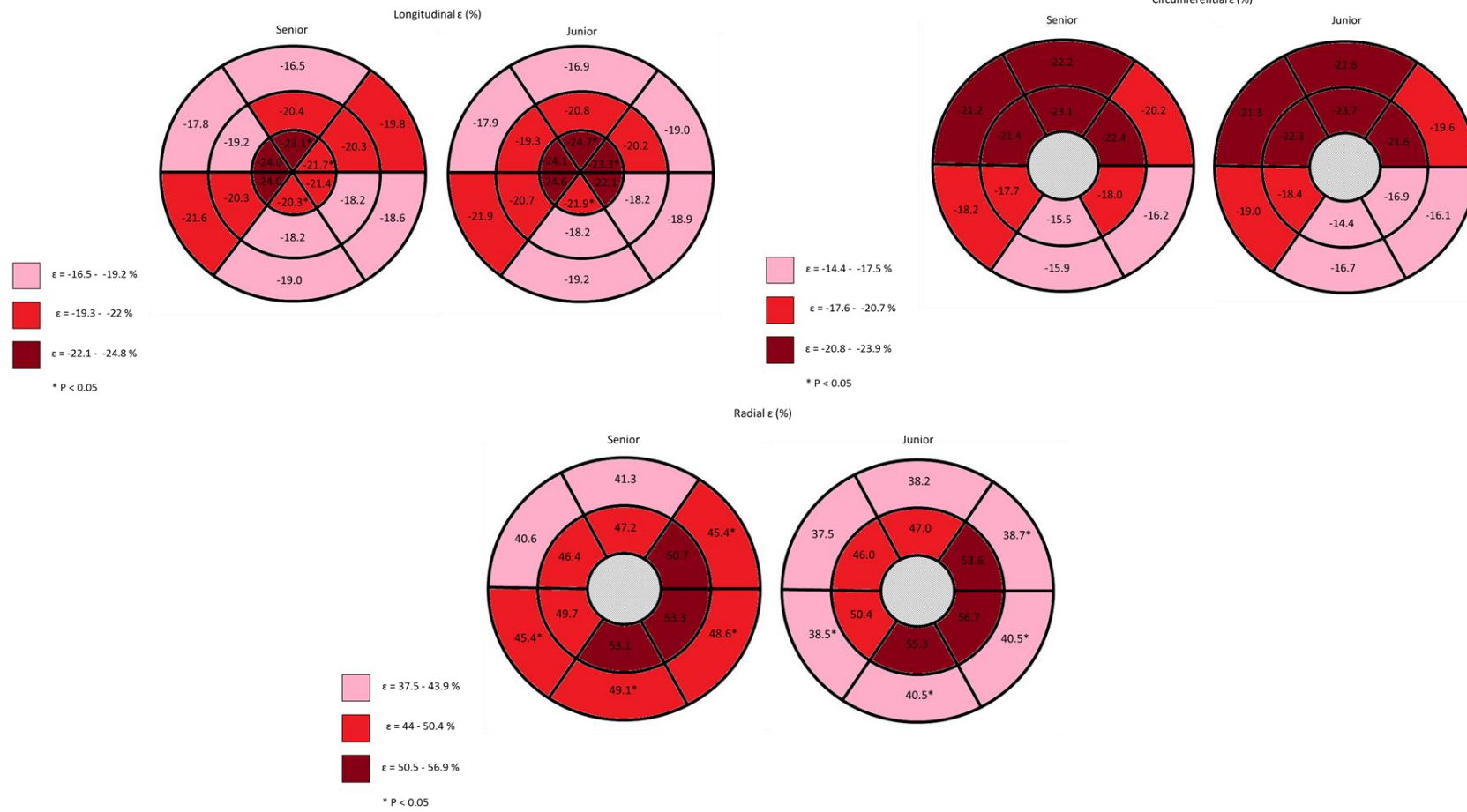


Figure 6.2a Regional longitudinal, circumferential and radial ϵ in senior and junior athletes

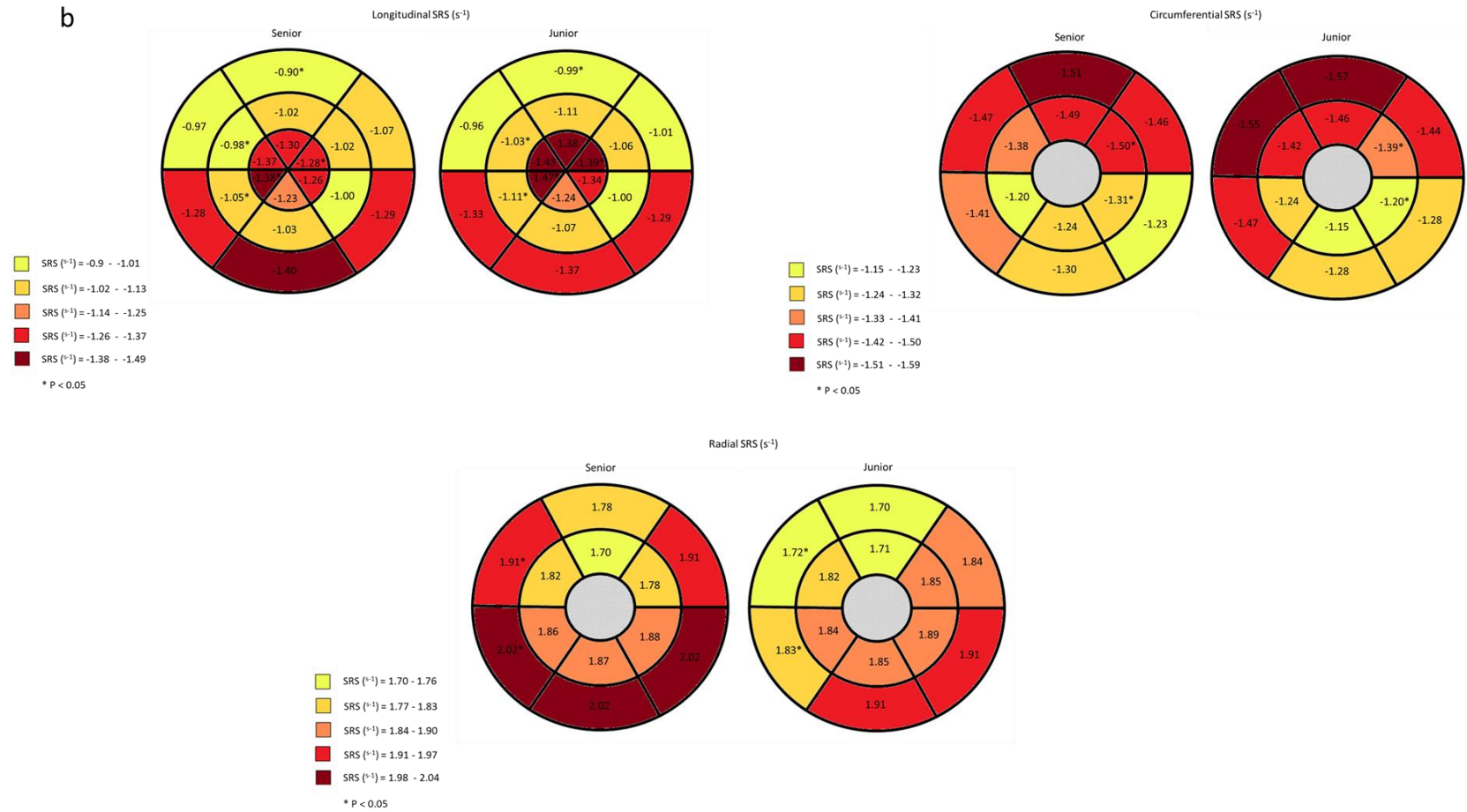


Figure 6.2b Regional longitudinal, circumferential and radial SRS in senior and junior athletes

C

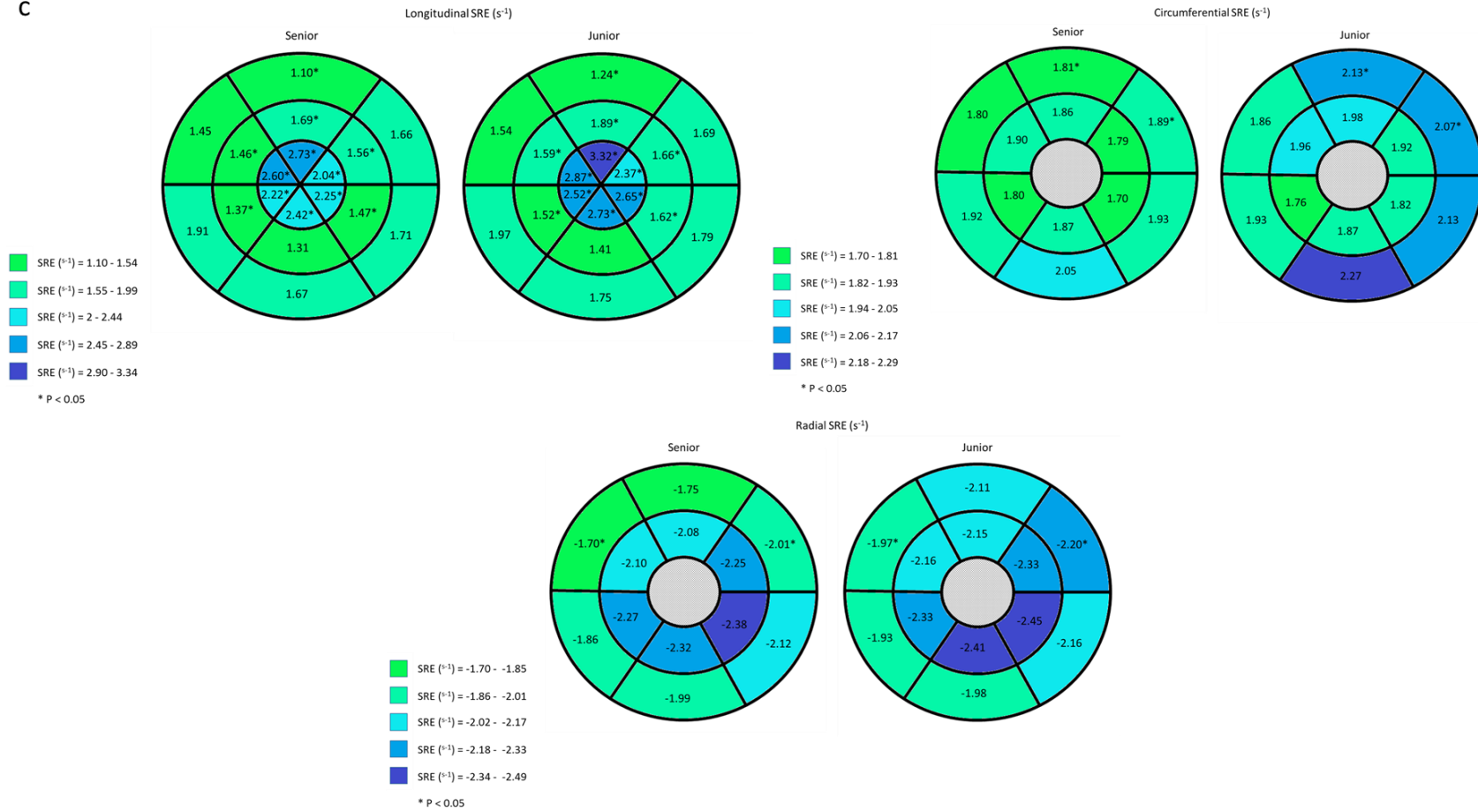


Figure 6.2c Regional longitudinal, circumferential and radial SRE in senior and junior athletes

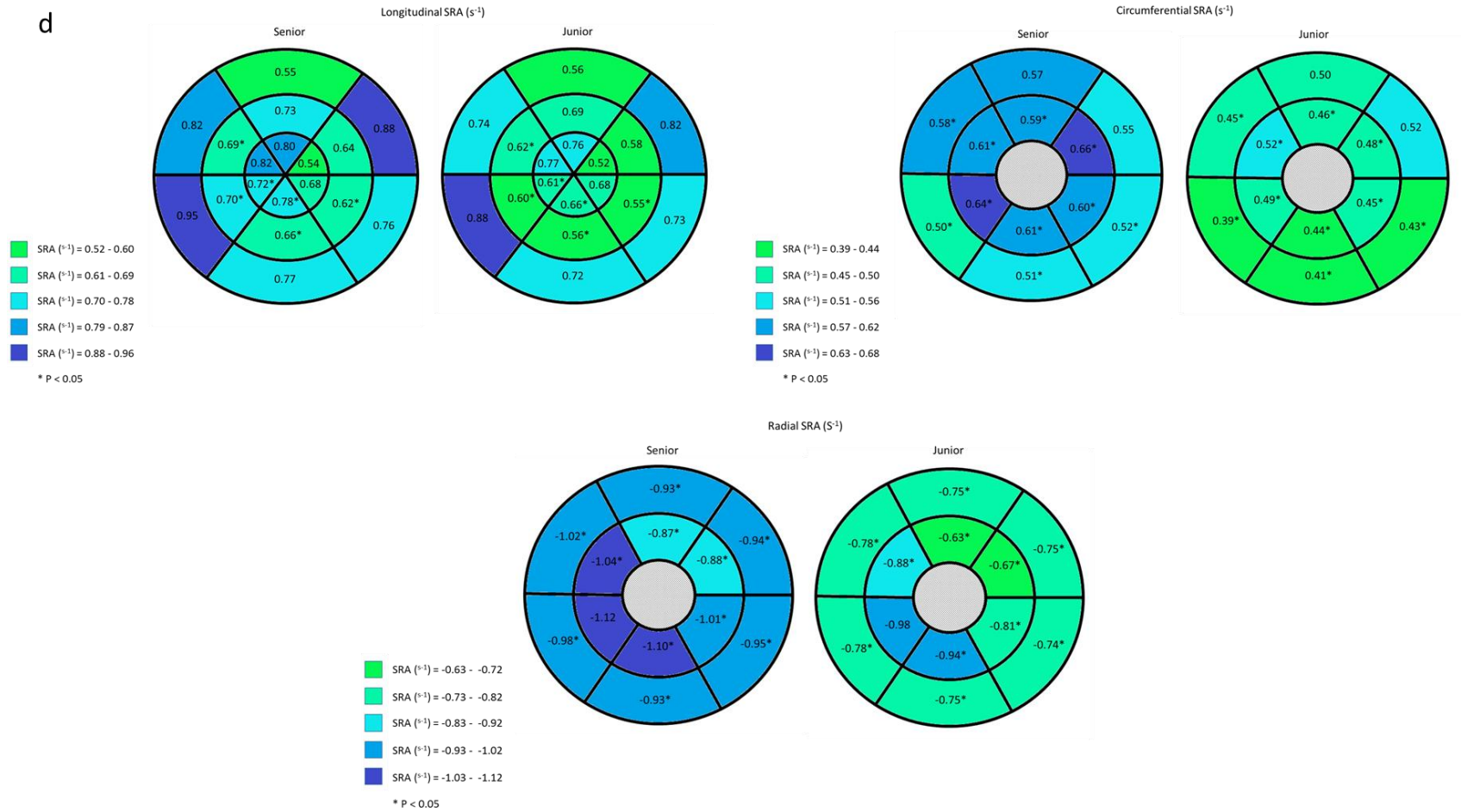


Figure 6.2d Regional longitudinal, circumferential and radial SRA in senior and junior athletes.

Table 6.4 Longitudinal Regional ϵ and SR

	Senior Mean \pm SD	Junior Mean \pm SD	P Value
Longitudinal ϵ			
Basal Infero-septal ϵ (%)	-17.8 \pm 2.1	-17.9 \pm 2.2	0.904
Mid Infero-septal ϵ (%)	-19.2 \pm 2.3	-19.3 \pm 2.3	0.554
Apical Infero-septal ϵ (%)	-24.0 \pm 4.1	-24.1 \pm 4.4	0.795
Apical Lateral ϵ (%)	-21.4 \pm 4.4	-22.1 \pm 4.3	0.213
Mid Lateral ϵ (%)	-18.2 \pm 2.9	-18.2 \pm 2.7	0.866
Basal Lateral ϵ (%)	-18.6 \pm 3.7	-18.9 \pm 3.1	0.549
Basal Inferior ϵ (%)	-21.6 \pm 3.2	-21.9 \pm 3.3	0.489
Mid Inferior ϵ (%)	-20.3 \pm 2.8	-20.7 \pm 2.5	0.295
Apical Inferior ϵ (%)	-24.0 \pm 4.2	-24.6 \pm 4.3	0.294
Apical Anterior ϵ (%)	-21.7 \pm 4.8	-23.3 \pm 5.3	0.021*
Mid Anterior ϵ (%)	-20.3 \pm 3.1	-20.2 \pm 3.8	0.948
Basal Anterior ϵ (%)	-19.8 \pm 3.4	-19.0 \pm 3.3	0.093
Basal Posterior ϵ (%)	-19.0 \pm 4.2	-19.2 \pm 2.6	0.780
Mid Posterior ϵ (%)	-18.2 \pm 3.5	-18.2 \pm 2.3	0.953
Apical Posterior ϵ (%)	-20.3 \pm 6.2	-21.9 \pm 3.7	0.028*
Apical Antero-septal ϵ (%)	-23.1 \pm 5.0	-24.7 \pm 4.1	0.010*
Mid Antero-septal ϵ (%)	-20.4 \pm 3.0	-20.8 \pm 2.5	0.124
Basal Antero-septal ϵ (%)	-16.5 \pm 2.9	-16.9 \pm 2.7	0.392
Longitudinal SRS			
Basal Infero-septal SRS (s^{-1})	-0.97 \pm 0.18	-0.96 \pm 0.29	0.831
Mid Infero-septal SRS (s^{-1})	-0.98 \pm 0.14	-1.03 \pm 0.19	0.022*
Apical Infero-septal SRS (s^{-1})	-1.37 \pm 0.31	-1.43 \pm 0.39	0.217
Apical Lateral SRS (s^{-1})	-1.26 \pm 0.30	-1.34 \pm 0.36	0.074
Mid Lateral SRS (s^{-1})	-1.00 \pm 0.22	-1.00 \pm 0.29	0.976
Basal Lateral SRS (s^{-1})	-1.29 \pm 0.31	-1.29 \pm 0.27	0.868
Basal Inferior SRS (s^{-1})	-1.28 \pm 0.26	-1.33 \pm 0.30	0.239
Mid Inferior SRS (s^{-1})	-1.05 \pm 0.16	-1.11 \pm 0.18	0.004*
Apical Inferior SRS (s^{-1})	-1.38 \pm 0.28	-1.47 \pm 0.33	0.038*
Apical Anterior SRS (s^{-1})	-1.28 \pm 0.29	-1.39 \pm 0.39	0.014*
Mid Anterior SRS (s^{-1})	-1.02 \pm 0.20	-1.06 \pm 0.21	0.205
Basal Anterior SRS (s^{-1})	-1.07 \pm 0.31	-1.01 \pm 0.32	0.198
Basal Posterior SRS (s^{-1})	-1.40 \pm 0.32	-1.37 \pm 0.31	0.583
Mid Posterior SRS (s^{-1})	-1.03 \pm 0.21	-1.07 \pm 0.18	0.174
Apical Posterior SRS (s^{-1})	-1.23 \pm 0.31	-1.24 \pm 0.27	0.801
Apical Antero-septal SRS (s^{-1})	-1.30 \pm 0.34	-1.38 \pm 0.34	0.066
Mid Antero-septal SRS (s^{-1})	-1.02 \pm 0.17	-1.11 \pm 0.24	0.181
Basal Antero-septal SRS (s^{-1})	-0.90 \pm 0.20	-0.99 \pm 0.26	0.006*
Longitudinal SRE			
Basal Infero-septal SRE (s^{-1})	1.45 \pm 0.38	1.54 \pm 0.40	0.066
Mid Infero-septal SRE (s^{-1})	1.46 \pm 0.32	1.59 \pm 0.31	0.006*
Apical Infero-septal SRE (s^{-1})	2.60 \pm 0.81	2.87 \pm 0.97	0.021*

Apical Lateral SRE (s ⁻¹)	2.25 ± 0.79	2.65 ± 0.86	0.001*
Mid Lateral SRE (s ⁻¹)	1.47 ± 0.38	1.62 ± 0.40	0.008*
Basal Lateral SRE (s ⁻¹)	1.71 ± 0.51	1.79 ± 0.52	0.238
Basal Inferior SRE (s ⁻¹)	1.91 ± 0.61	1.97 ± 0.63	0.489
Mid Inferior SRE (s ⁻¹)	1.37 ± 0.28	1.52 ± 0.33	<0.001*
Apical Inferior SRE (s ⁻¹)	2.22 ± 0.65	2.52 ± 0.71	0.001*
Apical Anterior SRE (s ⁻¹)	2.04 ± 0.67	2.37 ± 0.80	0.001*
Mid Anterior SRE (s ⁻¹)	1.56 ± 0.36	1.66 ± 0.39	0.045*
Basal Anterior SRE (s ⁻¹)	1.66 ± 0.46	1.69 ± 0.55	0.714
Basal Posterior SRE (s ⁻¹)	1.67 ± 0.59	1.75 ± 0.55	0.313
Mid Posterior SRE (s ⁻¹)	1.31 ± 0.34	1.41 ± 0.45	0.058
Apical Posterior SRE (s ⁻¹)	2.42 ± 0.65	2.73 ± 0.74	0.001*
Apical Antero-septal SRE (s ⁻¹)	2.73 ± 0.91	3.32 ± 1.01	<0.001*
Mid Antero-septal SRE (s ⁻¹)	1.69 ± 0.46	1.89 ± 0.45	0.003*
Basal Antero-septal SRE (s ⁻¹)	1.10 ± 0.35	1.24 ± 0.36	0.005*
Longitudinal SRA			
Basal Infero-septal SRA (s ⁻¹)	0.82 ± 0.32	0.74 ± 0.28	0.057
Mid Infero-septal SRA (s ⁻¹)	0.69 ± 0.18	0.62 ± 0.19	0.011*
Apical Infero-septal SRA (s ⁻¹)	0.82 ± 0.27	0.77 ± 0.28	0.183
Apical Lateral SRA (s ⁻¹)	0.68 ± 0.27	0.68 ± 0.27	0.992
Mid Lateral SRA (s ⁻¹)	0.62 ± 0.23	0.55 ± 0.20	0.020*
Basal Lateral SRA (s ⁻¹)	0.76 ± 0.35	0.73 ± 0.34	0.612
Basal Inferior SRA (s ⁻¹)	0.95 ± 0.32	0.88 ± 0.37	0.116
Mid Inferior SRA (s ⁻¹)	0.70 ± 0.21	0.60 ± 0.19	<0.001*
Apical Inferior SRA (s ⁻¹)	0.72 ± 0.27	0.61 ± 0.25	0.002*
Apical Anterior SRA (s ⁻¹)	0.54 ± 0.22	0.52 ± 0.25	0.575
Mid Anterior SRA (s ⁻¹)	0.64 ± 0.20	0.58 ± 0.21	0.068
Basal Anterior SRA (s ⁻¹)	0.88 ± 0.37	0.82 ± 0.37	0.232
Basal Posterior SRA (s ⁻¹)	0.77 ± 0.33	0.72 ± 0.30	0.219
Mid Posterior SRA (s ⁻¹)	0.66 ± 0.23	0.56 ± 0.19	0.002*
Apical Posterior SRA (s ⁻¹)	0.78 ± 0.33	0.66 ± 0.22	0.003*
Apical Antero-septal SRA (s ⁻¹)	0.80 ± 0.35	0.76 ± 0.29	0.341
Mid Antero-septal SRA (s ⁻¹)	0.73 ± 0.24	0.69 ± 0.21	0.310
Basal Antero-septal SRA (s ⁻¹)	0.55 ± 0.22	0.56 ± 0.29	0.939

* Denotes P < 0.05

Table 6.5 Circumferential Regional ϵ and SR

	Senior Mean \pm SD	Junior Mean \pm SD	P Value
Circumferential ϵ			
Basal Antero-septal ϵ (%)	-22.2 \pm 4.7	-22.6 \pm 5.9	0.543
Basal Anterior ϵ (%)	-20.2 \pm 5.6	-19.6 \pm 5.4	0.368
Basal Lateral ϵ (%)	-16.2 \pm 5.9	-16.1 \pm 6.8	0.910
Basal Posterior ϵ (%)	-15.9 \pm 6.2	-16.7 \pm 7.0	0.357
Basal Inferior ϵ (%)	-18.2 \pm 5.6	-19.0 \pm 5.9	0.349
Basal Infero-septal ϵ (%)	-21.2 \pm 5.1	-21.3 \pm 5.5	0.884
Mid Antero-septal ϵ (%)	-23.1 \pm 4.2	-23.7 \pm 4.9	0.363
Mid Anterior ϵ (%)	-22.4 \pm 5.4	-21.6 \pm 4.9	0.294
Mid Lateral ϵ (%)	-18.0 \pm 5.3	-16.9 \pm 5.1	0.106
Mid Posterior ϵ (%)	-15.5 \pm 5.2	-14.4 \pm 5.4	0.133
Mid Inferior ϵ (%)	-17.7 \pm 4.1	-18.4 \pm 4.0	0.206
Mid Infero-septal ϵ (%)	-21.4 \pm 4.4	-22.3 \pm 6.6	0.232
Circumferential SRS			
Basal Antero-septal SRS (s^{-1})	-1.51 \pm 0.35	-1.57 \pm 0.4	0.272
Basal Anterior SRS (s^{-1})	-1.46 \pm 0.45	-1.44 \pm 0.39	0.692
Basal Lateral SRS (s^{-1})	-1.23 \pm 0.41	-1.28 \pm 0.39	0.346
Basal Posterior SRS (s^{-1})	-1.30 \pm 0.45	-1.28 \pm 0.49	0.758
Basal Inferior SRS (s^{-1})	-1.41 \pm 0.31	-1.47 \pm 0.37	0.156
Basal Infero-septal SRS (s^{-1})	-1.47 \pm 0.35	-1.55 \pm 0.41	0.151
Mid Antero-septal SRS (s^{-1})	-1.49 \pm 0.31	-1.46 \pm 0.32	0.498
Mid Anterior SRS (s^{-1})	-1.50 \pm 0.36	-1.39 \pm 0.35	0.024*
Mid Lateral SRS (s^{-1})	-1.31 \pm 0.38	-1.20 \pm 0.32	0.020*
Mid Posterior SRS (s^{-1})	-1.24 \pm 0.39	-1.15 \pm 0.37	0.074
Mid Inferior SRS (s^{-1})	-1.20 \pm 0.34	-1.24 \pm 0.32	0.388
Mid Infero-septal SRS (s^{-1})	-1.38 \pm 0.31	-1.42 \pm 0.33	0.353
Circumferential SRE			
Basal Antero-septal SRE (s^{-1})	1.81 \pm 0.57	2.13 \pm 0.68	<0.001*
Basal Anterior SRE (s^{-1})	1.89 \pm 0.64	2.07 \pm 0.69	0.047*
Basal Lateral SRE (s^{-1})	1.93 \pm 0.78	2.13 \pm 0.83	0.076
Basal Posterior SRE (s^{-1})	2.05 \pm 0.80	2.27 \pm 0.91	0.055
Basal Inferior SRE (s^{-1})	1.92 \pm 0.66	1.93 \pm 0.62	0.907
Basal Infero-septal SRE (s^{-1})	1.80 \pm 0.60	1.86 \pm 0.71	0.522
Mid Antero-septal SRE (s^{-1})	1.86 \pm 0.53	1.98 \pm 0.64	0.153
Mid Anterior SRE (s^{-1})	1.79 \pm 0.60	1.92 \pm 0.67	0.143
Mid Lateral SRE (s^{-1})	1.70 \pm 0.61	1.82 \pm 0.70	0.168
Mid Posterior SRE (s^{-1})	1.87 \pm 0.71	1.87 \pm 0.79	0.993
Mid Inferior SRE (s^{-1})	1.80 \pm 0.56	1.76 \pm 0.56	0.586
Mid Infero-septal SRE (s^{-1})	1.90 \pm 0.59	1.96 \pm 0.62	0.495
Circumferential SRA			

Basal Antero-septal SRA (s ⁻¹)	0.57 ± 0.29	0.50 ± 0.25	0.059
Basal Anterior SRA (s ⁻¹)	0.55 ± 0.32	0.52 ± 0.29	0.457
Basal Lateral SRA (s ⁻¹)	0.52 ± 0.28	0.43 ± 0.26	0.015*
Basal Posterior SRA (s ⁻¹)	0.51 ± 0.30	0.41 ± 0.22	0.009*
Basal Inferior SRA (s ⁻¹)	0.50 ± 0.28	0.39 ± 0.23	0.002*
Basal Infero-septal SRA (s ⁻¹)	0.58 ± 0.33	0.45 ± 0.22	0.001*
Mid Antero-septal SRA (s ⁻¹)	0.59 ± 0.28	0.46 ± 0.23	0.001*
Mid Anterior SRA (s ⁻¹)	0.66 ± 0.34	0.48 ± 0.24	<0.001*
Mid Lateral SRA (s ⁻¹)	0.60 ± 0.27	0.45 ± 0.22	<0.001*
Mid Posterior SRA (s ⁻¹)	0.61 ± 0.31	0.44 ± 0.24	<0.001*
Mid Inferior SRA (s ⁻¹)	0.64 ± 0.32	0.49 ± 0.25	<0.001*
Mid Infero-septal SRA (s ⁻¹)	0.61 ± 0.31	0.52 ± 0.24	0.019*

* Denotes P < 0.05

Table 6.6 Radial Regional ϵ and SR

	Senior Mean \pm SD	Junior Mean \pm SD	P Value
Radial ϵ			
Basal Antero-septal ϵ (%)	41.3 \pm 16.2	38.2 \pm 15.3	0.151
Basal Anterior ϵ (%)	45.4 \pm 16.1	38.7 \pm 13.8	0.002*
Basal Lateral ϵ (%)	48.6 \pm 17.4	40.5 \pm 17.7	0.001*
Basal Posterior ϵ (%)	49.1 \pm 18.5	40.5 \pm 19.1	0.001*
Basal Inferior ϵ (%)	45.4 \pm 17.4	38.5 \pm 17.2	0.004*
Basal Infero-septal ϵ (%)	40.6 \pm 15.4	37.5 \pm 16.0	0.148
Mid Antero-septal ϵ (%)	47.2 \pm 14.7	47.0 \pm 13.9	0.937
Mid Anterior ϵ (%)	50.7 \pm 15.5	53.6 \pm 16.7	0.186
Mid Lateral ϵ (%)	53.3 \pm 17.0	56.7 \pm 16.7	0.152
Mid Posterior ϵ (%)	53.1 \pm 18.5	55.3 \pm 16.7	0.376
Mid Inferior ϵ (%)	49.7 \pm 17.9	50.4 \pm 17.7	0.773
Mid Infero-septal ϵ (%)	46.4 \pm 15.4	46.0 \pm 16.6	0.845
Radial SRS			
Basal Antero-septal SRS (s^{-1})	1.78 \pm 0.47	1.70 \pm 0.54	0.257
Basal Anterior SRS (s^{-1})	1.91 \pm 0.46	1.84 \pm 0.53	0.276
Basal Lateral SRS (s^{-1})	2.02 \pm 0.51	1.91 \pm 0.61	0.163
Basal Posterior SRS (s^{-1})	2.02 \pm 0.57	1.91 \pm 0.57	0.148
Basal Inferior SRS (s^{-1})	2.02 \pm 0.59	1.83 \pm 0.54	0.015*
Basal Infero-septal SRS (s^{-1})	1.91 \pm 0.53	1.72 \pm 0.51	0.010*
Mid Antero-septal SRS (s^{-1})	1.70 \pm 0.41	1.71 \pm 0.46	0.215
Mid Anterior SRS (s^{-1})	1.78 \pm 0.42	1.85 \pm 0.51	0.276
Mid Lateral SRS (s^{-1})	1.88 \pm 0.45	1.89 \pm 0.43	0.243
Mid Posterior SRS (s^{-1})	1.87 \pm 0.48	1.85 \pm 0.41	0.786
Mid Inferior SRS (s^{-1})	1.86 \pm 0.46	1.84 \pm 0.42	0.685
Mid Infero-septal SRS (s^{-1})	1.82 \pm 0.38	1.82 \pm 0.42	0.992
Radial SRE			
Basal Antero-septal SRE (s^{-1})	-1.75 \pm 0.58	-2.11 \pm 0.61	0.174
Basal Anterior SRE (s^{-1})	-2.01 \pm 0.63	-2.20 \pm 0.74	0.041*
Basal Lateral SRE (s^{-1})	-2.12 \pm 0.76	-2.16 \pm 0.93	0.756
Basal Posterior SRE (s^{-1})	-1.99 \pm 0.75	-1.98 \pm 0.87	0.923
Basal Inferior SRE (s^{-1})	-1.86 \pm 0.63	-1.93 \pm 0.74	0.456
Basal Infero-septal SRE (s^{-1})	-1.70 \pm 0.56	-1.97 \pm 0.63	0.001*
Mid Antero-septal SRE (s^{-1})	-2.08 \pm 0.82	-2.15 \pm 0.75	0.534
Mid Anterior SRE (s^{-1})	-2.25 \pm 0.83	-2.33 \pm 0.84	0.491
Mid Lateral SRE (s^{-1})	-2.38 \pm 0.77	-2.45 \pm 0.80	0.488
Mid Posterior SRE (s^{-1})	-2.32 \pm 0.75	-2.41 \pm 0.73	0.387
Mid Inferior SRE (s^{-1})	-2.27 \pm 0.75	-2.33 \pm 0.74	0.527
Mid Infero-septal SRE (s^{-1})	-2.10 \pm 0.78	-2.16 \pm 0.74	0.518
Radial SRA			

Basal Antero-septal SRA (s ⁻¹)	-0.93 ± 0.46	-0.75 ± 0.43	0.003*
Basal Anterior SRA (s ⁻¹)	-0.94 ± 0.55	-0.75 ± 0.40	0.004*
Basal Lateral SRA (s ⁻¹)	-0.95 ± 0.55	-0.74 ± 0.44	0.002*
Basal Posterior SRA (s ⁻¹)	-0.93 ± 0.58	-0.75 ± 0.45	0.011*
Basal Inferior SRA (s ⁻¹)	-0.98 ± 0.54	-0.78 ± 0.43	0.003*
Basal Infero-septal SRA (s ⁻¹)	-1.02 ± 0.90	-0.78 ± 0.40	0.024*
Mid Antero-septal SRA (s ⁻¹)	-0.87 ± 0.50	-0.63 ± 0.34	<0.001*
Mid Anterior SRA (s ⁻¹)	-0.88 ± 0.47	-0.67 ± 0.37	0.001*
Mid Lateral SRA (s ⁻¹)	-1.01 ± 0.48	-0.81 ± 0.40	0.001*
Mid Posterior SRA (s ⁻¹)	-1.10 ± 0.52	-0.94 ± 0.42	0.013*
Mid Inferior SRA (s ⁻¹)	-1.12 ± 0.56	-0.98 ± 0.45	0.051
Mid Infero-septal SRA (s ⁻¹)	-1.04 ± 0.55	-0.88 ± 0.45	0.024*

* Denotes P < 0.05

6.3.2 Right Ventricle

RV standard structural and functional indices are presented in Table 6.7. Absolute values for RVOT_{plax}, RVOT₁, RVOT₂, RVD₁, RVD₂, RVD₃ and RVDA are all larger in SA (P < 0.001, < 0.001, 0.001, < 0.001, = 0.008, < 0.001 respectively). When these parameters were indexed only RVOT_{plax} and RVOT₁ were larger in SA (P = 0.013, P = 0.005). RV:LV ratio was not different between groups. TAPSE was higher in SA (P = 0.035) but there was no difference in RVFAC or RVS'. RVE' was not different between groups but when indexed for RV length was lower in SA. RV E'/A' ratio was lower (P < 0.001) in SA.

Table 6.7 Right Ventricular Structural and Functional Indices

	Senior Mean \pm SD (Range)	Junior Mean \pm SD (Range)	P Value
RVOT_{plax} (mm)	34 \pm 4 (21 - 47)	31 \pm 4 (21 - 44)	<0.001*
RVOT_{plax} (mm/(m²)^{0.5})	23 \pm 3 (15 - 30)	22 \pm 3 (16 - 31)	0.013*
RVOT₁ (mm)	36 \pm 5 (22 - 49)	33 \pm 5 (22 - 42)	<0.001*
RVOT₁ (mm/(m²)^{0.5})	24 \pm 3 (15 - 32)	23 \pm 3 (16 - 29)	0.005*
RVOT₂ (mm)	27 \pm 3 (19 - 35)	25 \pm 3 (20 - 39)	0.001*
RVOT₂ (mm/(m²)^{0.5})	18 \pm 2 (13 - 24)	18 \pm 2 (13 - 27)	0.290
RVD₁ (mm)	44 \pm 5 (33 - 60)	42 \pm 4 (33 - 52)	<0.001*
RVD₁ (mm/(m²)^{0.5})	30 \pm 3 (22 - 38)	30 \pm 3 (23 - 39)	0.597
RVD₂ (mm)	33 \pm 4 (22 - 44)	31 \pm 4 (23 - 40)	0.008*
RVD₂ (mm/(m²)^{0.5})	22 \pm 3 (15 - 30)	22 \pm 3 (16 - 30)	0.875
RVD₃ (mm)	91 \pm 8 (72 - 111)	87 \pm 8 (66 - 108)	<0.001*
RVD₃ (mm/(m²)^{0.5})	61 \pm 5 (47 - 75)	61 \pm 5 (45 - 78)	0.778
RVDa (cm²)	30 \pm 4 (21 - 41)	28 \pm 4 (21 - 37)	0.002*
RVDa (cm²/m²)	14 \pm 2 (9 - 18)	14 \pm 2 (11 - 19)	0.061
RVSa (cm²)	16 \pm 3 (10 - 23)	15 \pm 3 (11 - 23)	0.119
RVSa Index (cm²/m²)	7 \pm 1 (4 - 11)	8 \pm 1 (5 - 11)	0.012*
TAPSE (mm)	24 \pm 4 (16 - 33)	23 \pm 4 (16 - 32)	0.035*
RV:LV Ratio	0.91 \pm 0.10 (0.70 - 1.20)	0.89 \pm 0.08 (0.69 - 1.09)	0.183
RVFAC (%)	46 \pm 6 (34 - 61)	45 \pm 6 (33 - 59)	0.154
RV S' (cm/s)	15 \pm 2 (6 - 23)	15 \pm 2 (8 - 20)	0.937
RV E' (cm/s)	15 \pm 3 (7 - 24)	16 \pm 3 (7 - 27)	0.161
RV A' (cm/s)	10 \pm 3 (5 - 17)	10 \pm 3 (4 - 19)	0.045*
RV E'/A' (cm/s)	1.54 \pm 0.44 (0.71 - 3.00)	1.82 \pm 0.77 (0.44 - 4.50)	<0.001*

RV S' index ((cm/s)/cm)	1.61 ± 0.29 (0.61 - 2.44)	1.68 ± 0.25 (1.04 - 2.34)	0.051
RV E' index ((cm/s)/cm)	1.65 ± 0.32 (0.84 - 2.76)	1.80 ± 0.40 (0.81 - 2.90)	0.001*
RV A' index ((cm/s)/cm)	1.15 ± 0.33 (0.56 - 2.05)	1.10 ± 0.37 (0.51 - 2.22)	0.333

* Denotes $P < 0.05$

Global and regional RV ϵ and SR data are presented in Table 6.8. Global RV ϵ was lower in SA compared to JA ($P = 0.013$). No difference in time to peak RV ϵ was observed between groups. Both RV SRS and RV SRE were lower ($P = 0.002$ and $P < 0.001$ respectively) in SA but there was no difference in RV SRA between groups.

There were significant correlations of HR, and RV structural parameters (RVOT₁, RVOT₂, RVD₁, RVD₂ and RVD₃) to global RV mechanical parameters that reached significance between SA and JA (Table 6.9). Following multi-linear regression, HR ($\beta = -0.006$, $P < 0.001$) and RVD₂ ($\beta = 0.009$, $P = 0.007$) together accounted for 11% of the variance in RV SRS. RVOT₂ ($\beta = -0.020$, $P = 0.005$) and RVD₁ ($\beta = -0.015$, $P = 0.003$) together accounted for 9% of the variance in RV SRE. There were no correlations observed between HR and RV structural parameters and RV ϵ .

Table 6.8 RV Longitudinal Global and Regional ϵ and SR

	Senior Mean \pm SD	Junior Mean \pm SD	P Value
Global			
Global ϵ (%)	-27.2 \pm 3.4 (-18.36 to -40.73)	-28.3 \pm 3.0 (-20.7 to -36.0)	0.013*
Time to Peak ϵ (s)	0.38 \pm 0.03 (0.31 - 0.46)	0.38 \pm 0.03 (0.32 - 0.44)	0.102
SRS (s^{-1})	-1.32 \pm 0.22 (-0.77 to -2.19)	-1.41 \pm 0.23 (-0.99 to -2.04)	0.002*
SRE (s^{-1})	1.59 \pm 0.33 (0.79 - 2.67)	1.81 \pm 0.35 (1.17 - 3.14)	<0.001*
SRA (s^{-1})	0.89 \pm 0.27 (0.34 - 1.77)	0.86 \pm 0.26 (0.32 - 1.35)	0.460
Regional			
Basal RV ϵ (%)	-24.9 \pm 5.4	-25.9 \pm 4.5	0.154
Mid RV ϵ (%)	-27.2 \pm 4.1	-27.8 \pm 3.6	0.343
Apical RV ϵ (%)	-30.0 \pm 4.3	-31.5 \pm 4.3	0.016*
RV apex to base ϵ gradient (%)	-5.18	-5.62	0.627
Basal RV SRS (s^{-1})	-1.50 \pm 0.41	-1.56 \pm 0.37	0.260
Mid RV SRS (s^{-1})	-1.37 \pm 0.27	-1.39 \pm 0.31	0.528
Apical RV SRS (s^{-1})	-1.58 \pm 0.31	-1.72 \pm 0.37	0.003*
Basal RV SRE (s^{-1})	2.10 \pm 0.67	2.18 \pm 0.55	0.380
Mid RV SRE (s^{-1})	1.68 \pm 0.40	1.86 \pm 0.41	0.001*
Apical RV SRE (s^{-1})	2.07 \pm 0.55	2.38 \pm 0.52	<0.001*
Basal RV SRA (s^{-1})	1.06 \pm 0.34	1.06 \pm 0.39	0.990
Mid RV SRA (s^{-1})	0.98 \pm 0.33	0.92 \pm 0.31	0.179
Apical RV SRA (s^{-1})	1.25 \pm 0.40	1.14 \pm 0.37	0.033*

* Denotes $P < 0.05$

Table 6.9 STE parameters and RV correlations

STE Parameter	Parameters Correlated	R Value	P Value
RV ϵ	HR	-0.021	0.755
	RVOT1	0.054	0.422
	RVOT2	0.121	0.070
	RVD1	0.075	0.265
	RVD2	0.066	0.328
	RVD3	0.111	0.098
RV SRS	HR	-0.283	<0.001*
	RVOT1	0.138	0.040*
	RVOT2	0.111	0.098
	RVD1	0.198	0.003*
	RVD2	0.209	0.002*
	RVD3	0.127	0.059
RV SRE	HR	0.110	0.102
	RVOT1	-0.102	0.129
	RVOT2	-0.231	<0.001*
	RVD1	-0.237	<0.001*
	RVD2	-0.191	0.004*
	RVD3	-0.181	0.007*

* Denotes $P < 0.05$

No differences were observed in basal and mid RV ϵ and basal and mid RV SRS between groups (Table 6.8), however, apical RV ϵ and RV SRS were lower in SA ($P = 0.016$, $P = 0.003$ respectively). There was no difference in the RV ϵ gradient from apex to base between groups. There was no difference in basal RV SRE however mid and apical RV SRE were lower in SA ($P = 0.001$, $P < 0.001$). No differences were observed in basal and mid RV SRA between groups but apical RV SRA was lower in JA ($P = 0.033$).

6.3.3 Left Atrium

LA data is presented in Table 6.10. LA volumes (LAvoles, LAvolpreA and LAvoled) were larger in SA ($P < 0.001$), however, the corresponding indexed parameters were not different between groups. The absolute LAvolres and LAvolboo were larger in SA ($P < 0.001$) whilst there was no difference in the absolute LAvolcon between SA and JA. The functional conduit / booster (con:boo) ratio was lower ($P < 0.001$) in SA.

Table 6.10 Left Atrial Parameters

	Senior Mean \pm SD (Range)	Junior Mean \pm SD (Range)	P Value
LAvoles (ml)	76 \pm 16 (36 - 118)	64 \pm 14 (35 - 99)	<0.001*
LAvoles (ml/(m²)^{1.5})	23 \pm 5 (11 - 37)	22 \pm 4 (12 - 34)	0.192
LAvolpreA (ml)	46 \pm 12 (22 - 85)	38 \pm 11 (17 - 75)	<0.001*
LAvolpreA (ml/(m²)^{1.5})	14 \pm 3 (7 - 27)	13 \pm 3 (7 - 25)	0.072
LAvoled (ml)	30 \pm 9 (11 - 69)	25 \pm 8 (12 - 55)	<0.001*
LAvoled (ml/(m²)^{1.5})	9 \pm 3 (4 - 22)	9 \pm 3 (5 - 18)	0.443
LAvolres(ml)	46 \pm 11 (20 - 73)	38 \pm 10 (17 - 64)	<0.001*
LAvolcon(ml)	46 \pm 16 (9 - 89)	46 \pm 13 (18 - 77)	0.885
LAvolboo(ml)	16 \pm 5 (6 - 30)	13 \pm 6 (5 - 31)	<0.001*
Con:Boo Ratio	3.15 \pm 1.52 (0.44 - 8)	4.24 \pm 2.06 (1.11 - 11.80)	<0.001*

* Denotes $P < 0.05$

6.3.4 Right Atrium

RA data is presented in Table 6.11. Absolute and indexed RA area were larger in SA ($P < 0.001$ and $P = 0.008$ respectively). RAvoles, RAvolpreA and RAvoled were all larger in SA ($P < 0.001$) as were the corresponding indexed volumes ($P = 0.005$, $P = 0.004$, $P = 0.006$ respectively). Absolute RAvolres and RAvolboo volumes were larger in SA ($P < 0.001$) whilst there was no difference in absolute RAvolcon between SA and JA. Con:Boo ratio was lower ($P = 0.004$) in SA.

Table 6.11 Right Atrial Parameters

	Senior Mean \pm SD (Range)	Junior Mean \pm SD (Range)	P Value
RAa(cm²)	22 \pm 4 (13 - 29)	19 \pm 3 (12 - 27)	<0.001*
RAa Index (cm²/m²)	10 \pm 1 (6 - 13)	9 \pm 1 (6 - 13)	0.008*
RAvoles (ml)	73 \pm 18 (33 - 121)	59 \pm 14 (31 - 101)	<0.001*
RAvoles Index (ml/(m²)^{1.5})	22 \pm 5 (11 - 35)	21 \pm 5 (10 - 33)	0.005*
RAvolpreA (ml)	49 \pm 13 (25 - 92)	38 \pm 11 (18 - 67)	<0.001*
RAvolpreA Index (ml/(m²)^{1.5})	15 \pm 4 (6 - 27)	13 \pm 4 (7 - 23)	0.004*
RAvoled (ml)	35 \pm 10 (15 - 75)	27 \pm 8 (13 - 47)	<0.001*
RAvoled Index (ml/(m²)^{1.5})	10 \pm 3 (5 - 22)	9 \pm 3 (5 - 17)	0.006*
RAvolres (ml)	39 \pm 11 (13 - 77)	32 \pm 9 (13-56)	<0.001*
RAvolcon (ml)	53 \pm 17 (5 - 96)	52 \pm 13 (25 - 97)	0.765
RAvolboo(ml)	14 \pm 5 (5 - 30)	12 \pm 5 (3 - 26)	<0.001*
Con:Boo Ratio	4.32 \pm 2.65 (0.17 - 16.20)	5.57 \pm 3.91 (1 - 28.67)	0.004*

* Denotes $P < 0.05$

6.4 Discussion

The main findings of this study are 1) SA have slightly higher RWT and LV mass index whilst differences in absolute LV and LA are largely removed when scaled for BSA, 2) SA have lower early diastolic functional indices alongside lower longitudinal SRS 3) SA have larger RVOT, independent of BSA, with lower global RV ϵ , SRS and SRE and 4) SA have larger LA but this is related to BSA whilst a larger RA in SA is independent of BSA. SA have functionally larger booster volumes in both atria.

6.4.1 Left Heart

BSA has been reported to be the strongest determinant of cardiac dimensions (Spirito *et al.*, 1994, Pelliccia *et al.*, 2012) and appropriate allometric scaling allows comparisons between populations (George *et al.*, 2001). Whilst absolute 2D LV and LA parameters are larger in senior RFL athletes, scaling removed many of these differences. That aside, LV mass index, RWT and mean apical wall thickness remained larger in SA. It has previously been demonstrated that LV mass increases strongly as children reach pubertal age and subsequently declines during adult life (Cain *et al.*, 2007). In view of this, the findings from the current study are likely indicative of training longevity and highlight the extent of physiological adaptation across the age range. Also it is worth noting that adaptation may also have a maturity and hormonal aspect. Similar to findings elsewhere (Utomi *et al.*, 2014), it is important to note that RFL athletes, irrespective of age, largely present with normal LV geometry with none of the athletes presenting with concentric hypertrophy.

Conventional measures of LV systolic function are similar between sedentary young individuals, junior athletes, sedentary older individuals and master athletes (Makan *et al.*, 2005, Sharma *et al.*, 2002). This study supports these findings with similar EF and

S' between groups and in addition, global LV ϵ across all functional planes were also similar between RFL groups. Myocardial SR is a measure of the rate of deformation and has been shown to be more sensitive to discrete changes in regional and global function making it an effective tool in the evaluation of sub-clinical myocardial disease (Marwick, 2006). This study demonstrated lower global and regional longitudinal SRS in SA which, in part, can be explained by absolute cavity size and HR and may represent a normal physiological adaptation to exercise. The relationship between ϵ (rate and absolute value), structure and EF/stroke volume has been studied elsewhere (MacIver and Townsend, 2008). The authors' demonstrated lower contraction is required in the presence of thicker myocardial walls when maintaining overall EF without compensatory increases in circumferential function. The finding of lower SRS in SA alongside a higher RWT and/or apical wall thickness and no differences in circumferential SRS likely highlight this phenomenon. This is further supported by a predominance of lower SRS in the mid to apical segments.

LV twist in a non-athletic population has been reported to increase from early in life with advancing age, commonly due to greater apical rotation (Notomi et al., 2006, Van Dalen *et al.*, 2008, Kaku *et al.*, 2014). The SA in the current study do not present with this normal ageing pattern and hence we can speculate that as apical rotation is similar in both groups that this may be a physiological adaptation that occurs early in an athletes training history which is maintained across the athletes age range. A lower LV twist at rest may represent a shear strain 'reserve' capacity which during exercise could act to enhance both ejection and diastolic filling (Nottin *et al.*, 2008, Weiner *et al.*, 2015) and is an important factor in both young and older athletes. Whether this finding in JA is training or age related is difficult to elucidate from the current study.

LV diastolic function has been reported to be 'supernormal' (Claessens *et al.*, 2001, D'Ascenzi *et al.*, 2011) or normal in the elite athlete (Pluim *et al.*, 2000, Sharma *et al.*, 2002), however, the impact of the athletes' age has not been studied. It is apparent that diastolic function adapts with advancing age, however this is not significant until the 5th or 6th decade (Caballero *et al.*, 2015). Our data highlights significantly higher indices of diastolic function in JA. These global indices of diastolic function were supported by higher global and regional longitudinal SRE and to a lesser extent regional circumferential and radial SRE. In addition, LA volume data highlights higher relative conduit volume in JA. Collectively these data suggest that JA have superior resting early diastolic function. As already established, the absolute LV size is smaller in JA compared to SA related to body size. This difference in body size appears to be exaggerated in the RFL population and therefore this may offer some explanation to the exaggerated changes in diastolic function. In view of this, it is sensible to consider the female heart which is smaller than the male heart primarily due to body size (Lang *et al.*, 2015, Giraldeau *et al.*, 2015). The female heart also presents with higher indices of early diastolic function and relative contribution (E/A) (Caballero *et al.*, 2015). We can speculate that a smaller ventricle can relax faster providing a greater LV pressure decline and consequently a higher LA-LV pressure gradient resulting in greater early contribution to diastolic filling. In addition, the larger ventricle in SA may be equipped with a diastolic reserve that allows greater relaxation at times when higher stroke volumes are required during exercise. In combination these two mechanisms are driven by longevity of training and absolute chamber size.

6.4.2 Right Heart

The RVOT is larger in SA, independent of BSA and therefore appears to be sensitive to chronic athletic training in RFL athletes. This may have value as a marker of normal physiological adaptation in this population. This is somewhat contradictory to previous studies where inflow dilatation has been shown to be more prevalent in endurance athletes (Oxborough *et al.*, 2012a). This disparity may well reflect the mixed training stimulus of RFL athletes. It is important to note an enlarged RVOT further exacerbates the differential diagnosis from ARVC and, therefore, careful assessment of RV function is key (Marcus *et al.*, 2010, Oxborough *et al.*, 2012a, Zaidi *et al.*, 2013).

Despite normal conventional indices of RV function (TAPSE and RVFAC), the current study demonstrates that SA have lower global RV ϵ SRS and SRE than JA. Multilinear regression suggests that a reduction in RV mechanics is related, in part, to RV morphology and slower HR and is further supported by a reduction in diastolic RV TDI (RV E' index, RV E'/A' ratio). Careful examination of regional RV mechanics suggests that the global differences are primarily driven by lower apical systolic and early diastolic function. Despite lower apical RV ϵ in SA, there is no difference in the apex to basal RV ϵ gradient suggesting there is a maintenance of the physiological nature of RV function. An RV ϵ gradient is a normal phenomenon (Marwick, 2006) and represents the dominance of deep longitudinal layers of RV myofibres with a base to apex alignment (Levy *et al.*, 2014). Reduced apical ϵ in the presence of a normal base to apex gradient in SA is an important echocardiographic finding and alterations in the gradient may therefore be indicative of some underlying pathology. Lower global RV ϵ values have been previously reported in elite endurance athletes due to reduction in basal function (Teske *et al.*, 2009b), a finding that was

reproduced in a subsequent study but with the additional finding of increased function in the apical segment ϵ (La Gerche *et al.*, 2012). Reduced basal RV ϵ was attributed to RV geometry, HR and a resting reserve (Teske *et al.*, 2009, La Gerche *et al.*, 2012). Other recent studies reported no difference in resting RV ϵ parameters (Oxborough *et al.*, 2012a, Pagourelas *et al.*, 2013), global or regional compared to controls (Utomi *et al.*, 2015). The reduction of apical RV ϵ in SA is therefore in contrast to previous studies. The presence of crisscross oblique fibres in the apical interventricular septum (IVS) contribute to RVOT morphology (Cho *et al.*, 2009) and as the distal/apical free wall is continuous with the IVS any disproportionate adaptation in RVOT morphology might contribute to changes in RV ϵ in the apical region. This theory is supported by the regional heterogeneity of LV longitudinal apical ϵ where RV fibres transcend (Cho *et al.*, 2009).

To the author's knowledge there are no previous data on age or training related effects in RA in adolescent athletes, however, a study of pre-adolescent athletes reported larger baseline indexed RA dimensions compared to controls (D'Ascenzi *et al.*, 2016c). The authors reported that endurance training produces an additive increase in bi-atrial size associated with preserved bi-atrial function (D'Ascenzi *et al.*, 2016c). In contrast to the LA, after indexing, all RA area and volume parameters were larger in SA, suggesting that the RA is also sensitive to chronic adaptation and more sensitive to chronic training than the LA. Similarly in the RA there is an increased con:boo ratio in JA again suggesting an increased contribution to diastole from the early diastolic phase, supported by increased RV SRE and RV E' index and a reduced reliance on atrial contraction.

6.4.3 Implications

It is clear that scaling for body size is an important factor in the echocardiographic interpretation of the AH but it is evident from this study that body size does not account for all of the difference between junior and senior athletes. This is especially apparent in the right heart as scaling of the RVOT and RA did not remove the differences observed between groups. Essentially RV adaptation appears to be affected more by training and training longevity and it is therefore important to take into account both the type and amount of athletic activity when performing echocardiographic assessment of athletes with very careful assessment of right ventricular structure and function. The addition of functional RV ϵ imaging may aid diagnosis in athletes, particularly where there is absence of normal RV geometry. There is some effect from HR in this study, however, this only accounts for a small percentage of the variance observed. This study supports the need for further research and subsequent development of sport specific, normative echocardiographic parameters for both junior and senior athletes.

6.5 Limitations

Due to the cross-sectional nature of the study we cannot elude to the timing of cardiac remodelling. This study was focused on male elite RFL players and therefore these findings cannot be extrapolated to the wider athletic populations.

6.6 Conclusion

There is a predominance for normal LV geometry in all RFL athletes irrespective of age with normal LV systolic function. Early diastolic function and longitudinal SRS is enhanced in JA athletes and likely reflects a combination of age, cavity size and HR. Increased RVOT dimensions are observed in SA and whilst RV systolic functional

parameters are normal in both groups, global RV ϵ is lower in SA specifically related to the apical segments. Atrial dimensions are larger in SA however scaling for body size does not account for the increased RA in SA. The right heart of RFL athletes appears to be influenced more than the left by chronic training.

Chapter 7

Cardiac Structure and Function in the Elite Senior Rugby League Athlete during the Competitive Season

7.1 Introduction

Cardiac adaptation due to chronic athletic training has been previously described and it is widely accepted that modifications in chamber size, wall thickness and cardiac mass are commonly observed (Pluim *et al.*, 2000, Utomi *et al.*, 2013, D'Ascenzi *et al.*, 2015, McClean *et al.*, 2015, D'Ascenzi *et al.*, 2013, D'Ascenzi *et al.*, 2017a, D'Andrea *et al.*, 2013, Oxborough *et al.*, 2012a). Much of the data reported in the literature has been derived from cross sectional studies with limited echocardiographic longitudinal studies relating to dynamic cardiac adaptation over time or due to varying training intensities (D'Ascenzi *et al.*, 2015a, Baggish *et al.*, 2008a, Fagard *et al.*, 1983, Abergel *et al.*, 2004, Csajági *et al.*, 2015, Weiner *et al.*, 2015, D'Ascenzi *et al.*, 2014). In addition to the cross sectional studies contained in chapters 4 to 6 it is also pertinent to perform a longitudinal cardiac study of the RFL athlete across the competitive season.

From the literature, a structured exercise training programme in non-elite athletes has been observed to induce biventricular dilatation and increased diastolic function in endurance athletes and concentric left ventricular hypertrophy with diminished diastolic function in strength athletes (Baggish *et al.*, 2008a). Cardiac adaptation within the competitive season has been reported in cyclists with decreased LV wall thickness and a slight decrease in LV function observed in the rest season (Fagard *et al.*, 1983) with LV cavity dilatation also observed in elite cyclists over a period of years (Abergel *et al.*, 2004). In elite male soccer players an increased LV mass was observed within the competitive season with concomitant regression reported with detraining (D'Ascenzi *et al.*, 2015a, Cabanelas *et al.*, 2012).

Longitudinal echocardiographic studies involving myocardial ϵ imaging by STE are also limited (Weiner *et al.*, 2015, Weiner *et al.*, 2010, Baggish *et al.*, 2008b, Spence *et al.*, 2011). Spence *et al.* (2011) reported no change in longitudinal ϵ in untrained subjects following a 6 month endurance and resistance training programme whereas increases in longitudinal, radial and circumferential ϵ was observed in competitive rowers following 90 days endurance training (Baggish *et al.*, 2008b). An acute increase in twist mechanics was observed after 90 days training in university rowers (Weiner *et al.*, 2010) followed by a regression in twist after 39 months (Weiner *et al.*, 2015). The limited number of studies is further complicated by the heterogeneous training status of participants.

There are no specific guidelines as to when in the competitive season PCS should be undertaken and therefore an understanding of the impact of seasonal variation on conventional and novel indices of physiological cardiac adaptation would be beneficial. The RFL competitive season runs over 9 months with defined variations in training type and intensity throughout. These athletes may present for PCS at any time during the season and therefore this athlete demographic serves as an ideal sample to assess the impact of seasonal variation.

The aim of this study is to assess cardiac structure and function of the elite RFL athlete at clearly defined stages of the competitive season using standard 2D echocardiography and STE.

7.2 Methods

7.2.1 Study population and design

Following ethics approval by the ethics committee of Liverpool John Moores University, 20 elite senior RFL athletes were recruited from a single Super-League

club. RFL athletes were aged 23 ± 4 years (range 18 - 31) and provided full written informed consent to participate in the study. Athletes had a training history of 13.3 ± 3.6 years and were all participating in a structured training protocol as defined by the club. Training schedules varied between pre-season (Period of training before competitive season start) and in-season (competitive season). During a typical pre-season week, the athletes on average were taking part in 5 field training sessions (skills and conditioning) each of 70 minutes duration, 4 gym sessions (resistance) each of 60 minutes duration and 2 'wrestle' sessions each of 40 minutes duration. During a typical in-season week, athletes were taking part in 3 field sessions each of 45 minutes duration and 2 gym sessions each of 40 minutes duration and competitive game play. Depending on athlete selection and or substitution, up to 80 minutes (full game duration) are spent in competitive RFL gameplay per week. Athletes not selected for competition instead perform 2 training sessions (1 gym session of 40 minutes and 1 field session of 40 minutes duration).

After a detailed explanation of the testing protocol participants completed a medical questionnaire to document any cardiovascular symptoms, family history of SCD or other cardiovascular history. All participants abstained from exercise training or recreational activity for at least 6 hours prior to the investigation. They were allowed to take food and water *ad libitum* but were restricted from alcohol consumption 24 hours prior. A longitudinal study was employed and data was acquired in a resting state during four separate testing sessions at specific time points across the season; 1) pre-season (Training period before the start of the competitive season. Data was collected at the end of this period) 2) mid-season (Middle of competitive season) 3) end-season (End of competitive season) and 4) end-season break (End of the off-season. Data was collected on athlete return to training after the season break). All

clinical data were analysed and reported by a Sports Cardiologist and further evaluation if necessary excluded underlying cardiac disease allowing all participants to be included in the study. The subsequent testing sessions were carried out using an identical protocol. Individual training data was also collected retrospectively across the season to allow for changes in training load to be compared with any changes in cardiac structure and function. Training load was calculated by training session duration (minutes) multiplied by athletes' rating of perceived exertion (RPE) for that session using the Borg category ratio scale (CR10) with rating ranges from 0-10 (Borg 1982). Load was expressed as an arbitrary unit (AU) and mean athlete daily training load data for each seasonal time point was calculated.

7.2.2 Procedures

A routine standard anthropometric assessment included height (Seca 217, Hannover, Germany) and body mass (Seca supra 719, Hannover, Germany) measurements with BSA calculated as previously described (Mosteller 1987). BP was assessed with an automated sphygmomanometer (Dinamap 300, GE Medical systems, USA). A resting 12-Lead ECG was recorded (CardioExpress SL6, Spacelabs Healthcare, Washington US). All echocardiographic acquisition and analysis was undertaken as described in chapter 3. Mean apical wall thickness was also determined from two further LV wall measurements taken at the anterior and posterior apex in a modified PSAX LV apical image.

7.2.3 Statistical Analysis and Standardisation of STE data

Study data were collected and managed using REDCAP electronic data capture tools hosted at Liverpool John Moores University (Harris *et al.*, 2009). All echocardiographic data were presented as mean \pm SD and ranges. Statistical analyses

were performed using commercially available software package SPSS Version 23.0 for Windows (SPSS, Illinois, USA). Variables were analysed across the four time points using one-way ANOVA with post-hoc Bonferroni assessment. A $P < 0.05$ was considered statistically significant.

A standardised temporal assessment was performed for global STE parameters where significance between time points was observed. The data was processed using cubic spline interpolation which interpolated the data to 300 points in both systole and diastole resulting in a total of 600 points per cardiac cycle (Burns *et al.*, 2010b, Van Dalen *et al.* 2009, Khoo *et al.*, 2011). To account for inter or intra individual differences in heart rate, the data were normalised to the percentage of systolic and diastolic duration. The average data were defined by 5% increments across systole and diastole.

7.3 Results

There were no differences ($P > 0.05$) in heart rate or other athlete demographic parameters across the competitive season (Table 7.1). Average daily training workload is also presented in Table 7.1. There was a significant increase in workload between pre-season and both mid and end-season ($P < 0.001$) with no differences between mid- and end-season ($P > 0.05$).

Table 7.1 Demographics

	Pre-Season Mean \pm SD (Range)	Mid-Season Mean \pm SD (Range)	End-Season Mean \pm SD (Range)	Post Season Break Mean \pm SD (Range)
Age (Years)	23 \pm 4 (18 - 31)	23 \pm 4 (18 - 31)	24 \pm 4 (18 - 31)	24 \pm 4 (18 - 32)
Height (m)	1.84 \pm 0.06 (1.70 - 1.97)			
Weight (Kg)	98 \pm 9 (83 - 116)	98 \pm 8.7 (84 - 116)	99 \pm 9 (82 - 116)	99 \pm 9 (83 - 115)
BSA (m²)	2.23 \pm 0.13 (1.98 - 2.52)	2.24 \pm 0.13 (1.99 - 2.52)	2.24 \pm 0.13 (1.98 - 2.52)	2.25 \pm 0.13 (1.98 - 2.51)
Systolic BP (mmHg)	132 \pm 8 (117 - 155)	135 \pm 9 (114 - 147)	133 \pm 11 (117 - 156)	132 \pm 8 (116 - 146)
Diastolic BP (mmHg)	69 \pm 8 (56 - 81)	73 \pm 6 (62 - 83)	75 \pm 7 (64 - 88)	72 \pm 6 (64 - 89)
HR (beats.min⁻¹)	55 \pm 9 (42 - 70)	55 \pm 6 (42 - 62)	56 \pm 7 (46 - 70)	60 \pm 8 (46 - 78)
Average Daily Workload (AU)	715 \pm 264* \dagger (83 - 1316)	323 \pm 232* (63 - 767)	320 \pm 242 \dagger (63 - 744)	N/A

* denotes significant difference ($P > 0.05$) between pre-season and mid-season. \dagger denotes significant difference between pre-season and end-season.

7.3.1 Left Ventricle

There were no differences ($P > 0.05$) in standard 2D echocardiographic LV structural parameters across the season (Table 7.2). With exception of transmitral A wave velocity being significantly lower ($P = 0.028$) at end season compared to following post season break, there were no differences in any of the standard functional indices.

Table 7.2 Seasonal echocardiographic parameters of the left ventricle

	Pre-Season Mean ± SD (Range)	Mid-Season Mean ± SD (Range)	End-Season Mean ± SD (Range)	Post Season Break Mean ± SD (Range)
LVIDd (mm)	57 ± 3 (50 - 62)	57 ± 2 (52 - 60)	56 ± 3 (50 - 61)	56 ± 3 (51 - 61)
LVIDd index (mm/(m²)^{0.5})	38 ± 2 (34 - 41)	38 ± 1 (35 - 40)	38 ± 2 (33 - 40)	37 ± 2 (34 - 40)
LVIDs (mm)	39 ± 3 (34 - 44)	39 ± 2 (34 - 41)	38 ± 2 (33 - 42)	39 ± 3 (32 - 43)
LVIDs index (mm/(m²)^{0.5})	26 ± 2 (23 - 29)	26 ± 1 (23 - 29)	26 ± 2 (22 - 30)	26 ± 2 (21 - 31)
MWT (mm)	9 ± 1 (8 - 10)			
MWT index (mm/(m²)^{0.5})	6.0 ± 0.4 (5.3 - 6.7)	5.9 ± 0.4 (5.2 - 6.7)	5.9 ± 0.4 (5.3 - 6.7)	5.9 ± 0.4 (5.1 - 6.5)
Max WT (mm)	10 ± 1 (9 - 11)	9 ± 1 (9 - 11)	9 ± 1 (8 - 11)	10 ± 1 (8 - 11)
Max WT index (mm/(m²)^{0.5})	6.4 ± 0.4 (5.9 - 7.3)	6.2 ± 0.4 (5.7 - 7.3)	6.2 ± 0.4 (5.3 - 7.2)	6.3 ± 0.5 (5.1 - 7.2)
RWT	0.32 ± 0.03 (0.26 - 0.37)	0.32 ± 0.03 (0.25 - 0.37)	0.32 ± 0.03 (0.27 - 0.40)	0.32 ± 0.04 (0.26 - 0.38)
Mean Apical Wall Thickness (mm)	5.8 ± 0.5 (5 - 6.5)	6.0 ± 0.5 (5 - 7)	5.7 ± 0.5 (5 - 6.5)	5.8 ± 0.6 (5 - 6.5)
Mean Apical Wall Thickness Index (mm/(m²)^{0.5})	3.9 ± 0.3 (3.2 - 4.4)	4.0 ± 0.3 (3.4 - 4.7)	3.8 ± 0.3 (3.3 - 4.4)	3.9 ± 0.4 (3.2 - 4.5)
LV Mass (g)	195 ± 28 (146 - 253)	192 ± 24 (135 - 226)	194 ± 22 (140 - 226)	188 ± 18 (159 - 226)
LV Mass index (g/(m²)^{2.7})	38 ± 5 (29 - 48)	37 ± 5 (27 - 44)	38 ± 5 (28 - 45)	37 ± 4 (31 - 46)
LV mass index (g/m²)	87 ± 10 (68 - 106)	86 ± 9 (64 - 99)	87 ± 8 (65 - 97)	84 ± 8 (75 - 107)
LV Length (mm)	93 ± 4 (83 - 102)	95 ± 4 (86 - 102)	95 ± 4 (89 - 105)	96 ± 3 (87 - 103)
LV Length Index (mm/(m²)^{0.5})	63 ± 3 (55 - 67)	63 ± 3 (58 - 68)	64 ± 3 (59 - 68)	64 ± 2 (60 - 68)
LVEDV (ml)	141 ± 21 (101 - 179)	140 ± 22 (104 - 184)	146 ± 19 (113 - 179)	148 ± 19 (115 - 181)
LVEDV (ml/(m²)^{1.5})	42 ± 6 (30 - 57)	42 ± 6 (33 - 54)	44 ± 5 (35 - 56)	44 ± 5 (35 - 58)
LVESV (ml)	61 ± 14 (44 - 87)	61 ± 11 (44 - 79)	65 ± 9 (49 - 82)	65 ± 11 (48 - 85)
LVESV (ml/(m²)^{1.5})	18 ± 4 (11 - 28)	18 ± 3 (14 - 26)	19 ± 3 (13 - 28)	19 ± 3 (15 - 27)
SV (ml)	80 ± 12 (57 - 104)	79 ± 13 (54 - 112)	81 ± 13 (57 - 112)	83 ± 13 (67 - 122)

EF (%)	57 ± 5 (48 - 67)	57 ± 4 (51 - 67)	55 ± 4 (49 - 63)	56 ± 4 (48 - 67)
E Velocity (m/s)	0.83 ± 0.12 (0.52 - 1)	0.78 ± 0.11 (0.55 - 0.92)	0.79 ± 0.14 (0.58 - 1.01)	0.82 ± 0.15 (0.46 - 1.08)
A Velocity (m/s)	0.40 ± 0.07 (0.32 - 0.55)	0.36 ± 0.08 (0.22 - 0.56)	0.35 ± 0.07 § (0.20 - 0.50)	0.43 ± 0.13 § (0.25 - 0.81)
E:A Ratio	2.15 ± 0.46 (1.37 - 2.78)	2.24 ± 0.61 (1.45 - 3.82)	2.34 ± 0.60 (1.33 - 3.65)	2.02 ± 0.61 (0.85 - 3.16)
Medial S' (cm/s)	9 ± 1 (8 - 11)	9 ± 1 (8 - 12)	9 ± 1 (7 - 12)	9 ± 1 (7 - 11)
Medial E' (cm/s)	13 ± 2 (10 - 18)	13 ± 1 (10 - 15)	14 ± 3 (10 - 18)	14 ± 2 (10 - 18)
Medial A' (cm/s)	7 ± 1 (4 - 9)	7 ± 2 (4 - 12)	7 ± 1 (3 - 9)	7 ± 2 (4 - 11)
Lateral S' (cm/s)	12 ± 2 (9 - 17)	11 ± 2 (8 - 14)	11 ± 2 (8 - 15)	12 ± 2 (8 - 15)
Lateral E' (cm/s)	19 ± 3 (11 - 25)	19 ± 3 (12 - 24)	19 ± 3 (14 - 24)	18 ± 3 (14 - 25)
Lateral A' (cm/s)	6 ± 1 (4 - 9)	6 ± 2 (3 - 10)	6 ± 2 (4 - 10)	6 ± 1 (4 - 9)
Average S' (cm/s)	10 ± 1 (9 - 14)	10 ± 1 (8 - 12)	10 ± 1 (8 - 14)	10 ± 1 (9 - 13)
Average E' (cm/s)	16 ± 2 (12 - 20)	16 ± 2 (13 - 19)	17 ± 2 (13 - 21)	16 ± 2 (13 - 19)
Average A' (cm/s)	7 ± 1 (4 - 9)	6 ± 2 (4 - 11)	6 ± 1 (4 - 9)	7 ± 1 (5 - 10)
Average S' index ((cm/s)/cm)	1.10 ± 0.12 (0.96 - 1.41)	1.03 ± 0.13 (0.82 - 1.28)	1.06 ± 0.14 (0.77 - 1.36)	1.09 ± 0.15 (0.89 - 1.38)
Average E' Index ((cm/s)/cm)	1.74 ± 0.22 (1.29 - 2.22)	1.65 ± 0.21 (1.37 - 2.09)	1.74 ± 0.24 (1.37 - 2.13)	1.66 ± 0.19 (1.38 - 1.98)
Average A' index ((cm/s)/cm)	0.70 ± 0.11 (0.42 - 0.89)	0.68 ± 0.20 (0.36 - 1.22)	0.67 ± 0.15 (0.41 - 0.93)	0.71 ± 0.13 (0.46 - 1.01)
Average E/E'	5 ± 1 (4 - 6)	5 ± 1 (4 - 7)	5 ± 1 (4 - 6)	5 ± 1 (3 - 7)

§ = denotes $P < 0.05$ between end season and post break

STE parameters are presented in table 7.3. No differences were observed during the season for LV global ϵ and SR across all three planes of contraction ($P > 0.05$). Apical rotation and derived twist were higher in pre-season compared to mid-season ($P = 0.004$ and $P = 0.027$), end season ($P = 0.002$ and $P = 0.0009$) and post break ($P = 0.019$ and $P = 0.017$) (Figure 7.1).

Table 7.3 Global Left ventricular ϵ , SR and Twist

	Pre-Season Mean \pm SD (Range)	Mid-Season Mean \pm SD (Range)	End-Season Mean \pm SD (Range)	Post Season Break Mean \pm SD (Range)
LV Longitudinal				
Global ϵ (%)	-19.2 \pm 2.2 (-16.3 to -23.7)	-19.5 \pm 1.3 (-16.5 to -21.4)	-19.4 \pm 1.4 (-16.0 to -21.6)	-19.4 \pm 1.2 (-17.5 to -21.6)
Time to Peak ϵ (s)	0.37 \pm 0.03 (0.32 - 0.43)	0.37 \pm 0.03 (0.33 - 0.41)	0.38 \pm 0.02 (0.33 - 0.41)	0.37 \pm 0.03 (0.33 - 0.44)
SRS (s^{-1})	-0.94 \pm 0.13 (-0.72 to -1.31)	-0.96 \pm 0.10 (-0.81 to -1.19)	-0.93 \pm 0.08 (-0.80 to -1.12)	-0.94 \pm 0.09 (-0.69 to -1.12)
SRE (s^{-1})	1.36 \pm 0.18 (1.01 - 1.63)	1.43 \pm 0.14 (1.20 - 1.71)	1.44 \pm 0.14 (1.11 - 1.66)	1.40 \pm 0.15 (1.09 - 1.62)
SRA (s^{-1})	0.56 \pm 0.10 (0.37 - 0.80)	0.58 \pm 0.14 (0.36 - 0.93)	0.55 \pm 0.09 (0.36 - 0.75)	0.59 \pm 0.09 (0.41 - 0.79)
LV Circumferential				
Global ϵ (%)	-19.1 \pm 2.0 (-16.6 to -23.3)	-18.3 \pm 1.4 (-16.1 to -21.2)	-18.1 \pm 2.1 (-14.4 to -21.4)	-17.5 \pm 2.09 (-14.0 to -20.4)
Time to Peak ϵ (s)	0.37 \pm 0.02 (0.31 - 0.40)	0.37 \pm 0.03 (0.32 - 0.42)	0.39 \pm 0.04 (0.33 - 0.48)	0.38 \pm 0.03 (0.32 - 0.44)
SRS (s^{-1})	-1.08 \pm 0.13 (-0.90 to -1.34)	-1.04 \pm 0.13 (-0.84 to -1.41)	-1.01 \pm 0.11 (-0.82 to -1.23)	-0.98 \pm 0.13 (-0.78 to -1.19)
SRE (s^{-1})	1.56 \pm 0.31 (0.86 - 2.34)	1.46 \pm 0.24 (1.02 - 1.94)	1.42 \pm 0.19 (0.98 - 1.72)	1.36 \pm 0.23 (0.97 - 1.95)
SRA (s^{-1})	0.44 \pm 0.14 (0.29 - 0.77)	0.38 \pm 0.11 (0.22 - 0.72)	0.37 \pm 0.11 (0.19 - 0.61)	0.40 \pm 0.12 (0.18 - 0.59)
LV Radial				
Global ϵ (%)	46.5 \pm 12.8 (27.1 - 70.2)	49.7 \pm 10.3 (34.6 - 68.4)	51.5 \pm 11.5 (31.7 - 76.7)	45.6 \pm 10.9 (28.3 - 75.0)
Time to Peak ϵ (s)	0.41 \pm 0.03 (0.34 - 0.48)	0.42 \pm 0.03 (0.36 - 0.47)	0.42 \pm 0.04 (0.35 - 0.49)	0.41 \pm 0.04 (0.36 - 0.49)
SRS (s^{-1})	1.51 \pm 0.23 (1.11 - 1.98)	1.55 \pm 0.24 (1.06 - 2.05)	1.60 \pm 0.26 (1.29 - 2.40)	1.54 \pm 0.22 (1.22 - 1.97)
SRE (s^{-1})	-2.05 \pm 0.61 (-0.99 to -4.08)	-2.04 \pm 0.33 (-1.46 to -2.86)	-2.08 \pm 0.47 (-1.29 to -2.96)	-1.97 \pm 0.33 (-1.41 to -2.59)
SRA (s^{-1})	-0.85 \pm 0.26 (-0.53 to -1.30)	-0.96 \pm 0.42 (-1.74 to -0.17)	-0.93 \pm 0.36 (-0.42 to -1.92)	-0.90 \pm 0.25 (-0.47 to -1.50)
LV Rotation				
Basal rotation ($^{\circ}$)	-7.08 \pm 3.05 (-0.29 to -11.7)	-6.81 \pm 2.50 (-3.18 to -13.42)	-6.78 \pm 3.22 (-0.08 to -13.75)	-6.29 \pm 1.82 (-2.97 to -8.61)
Apical rotation ($^{\circ}$)	9.83 \pm 3.95 *†‡ (3.35 - 16.79)	6.13 \pm 2.84 * (1.88 - 11.59)	5.84 \pm 3.15 † (0.79 - 11.52)	6.60 \pm 3.07 ‡ (2.09 - 13.98)
Twist ($^{\circ}$)	16.55 \pm 4.71 *†‡ (6.49 - 22.63)	12.62 \pm 3.97 * (3.66 - 19.9)	12.12 \pm 4.53 † (5.55 - 19.51)	12.35 \pm 3.45 ‡ (7.38 - 19.43)

* denotes $P < 0.05$ between pre-season and mid-season, † denotes $P < 0.05$ between pre-season and end season, ‡ denotes $P < 0.05$ between pre-season and post break.

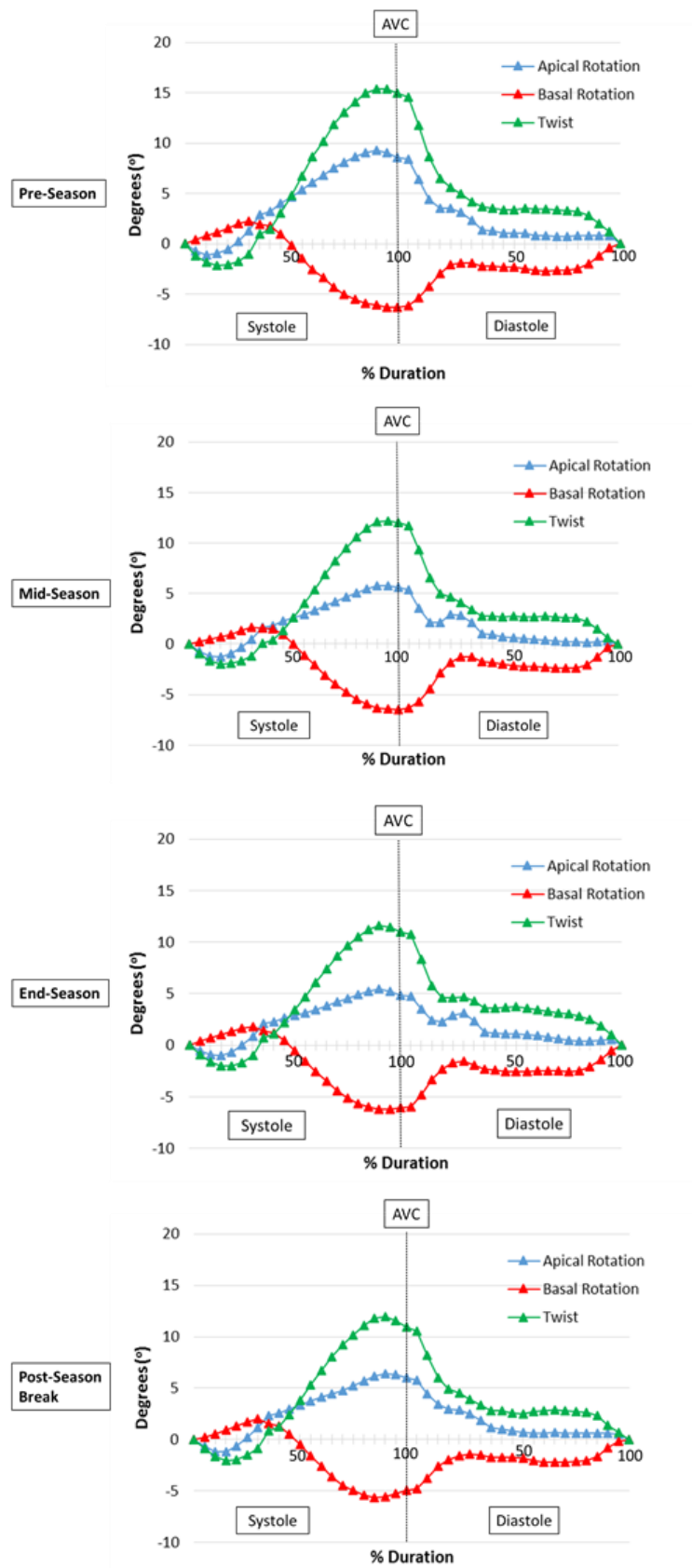


Figure 7.1 Cardiac rotation and twist during the RFL season

Regional ε and SR are presented in Tables 7.4-7.6 with most of the segments demonstrating no differences throughout the competitive season however isolated differences were observed. Longitudinal apical posterior ε was lower at pre-season compared to mid-season ($P = 0.038$) with post break being lower than mid-season ($P = 0.037$). Longitudinal basal infero-septal SRE is lower between pre-season compared to end season ($P < 0.001$) and post break ($P = 0.010$). Basal circumferential infero-septal SRS was higher at pre-season compared to mid-season ($P = 0.019$) and at post season break ($P = 0.003$). Mid radial inferior and infero-septal ε was higher in end season compared to post break ($P = 0.023$ and $P = 0.038$ respectively).

Table 7.4 Regional Longitudinal ϵ and SR

	Pre-Season Mean \pm SD	Mid-Season Mean \pm SD	End-Season Mean \pm SD	Post Season Break Mean \pm SD
Longitudinal ϵ				
Basal Infero-septal ϵ (%)	-18.7 \pm 2.5	-18.6 \pm 2.3	-16.8 \pm 2.5	-17.6 \pm 1.8
Mid Infero-septal ϵ (%)	-18.5 \pm 1.5	-18.2 \pm 2.3	-17.9 \pm 2.2	-18.1 \pm 2.3
Apical Infero-septal ϵ (%)	-22.3 \pm 3.7	-22.2 \pm 3.0	-23.6 \pm 3.6	-22.9 \pm 3.2
Apical Lateral ϵ (%)	-20.7 \pm 4.3	-20.6 \pm 3.0	-22.1 \pm 3.6	-21.2 \pm 4.0
Mid Lateral ϵ (%)	-18.1 \pm 3.9	-18.4 \pm 2.0	-18.1 \pm 2.1	-18.3 \pm 2.2
Basal Lateral ϵ (%)	-18.4 \pm 4.4	-19.1 \pm 2.5	-17.5 \pm 1.8	-19.2 \pm 2.4
Basal Inferior ϵ (%)	-21.5 \pm 2.5	-20.6 \pm 2.7	-20.7 \pm 3.5	-20.5 \pm 3.6
Mid Inferior ϵ (%)	-19.7 \pm 3.3	-20.1 \pm 2.5	-19.9 \pm 2.8	-20.2 \pm 2.9
Apical Inferior ϵ (%)	-23.0 \pm 3.5	-24.1 \pm 2.9	-24.0 \pm 2.4	-23.6 \pm 3.1
Apical Anterior ϵ (%)	-20.8 \pm 4.3	-22.7 \pm 4.1	-21.8 \pm 3.9	-21.8 \pm 3.4
Mid Anterior ϵ (%)	-19.4 \pm 3.0	-19.9 \pm 2.3	-19.2 \pm 2.8	-20.8 \pm 2.5
Basal Anterior ϵ (%)	-19.4 \pm 3.2	-18.5 \pm 2.8	-18.1 \pm 2.1	-19.7 \pm 2.6
Basal Posterior ϵ (%)	-19.6 \pm 4.2	-18.8 \pm 2.7	-19.3 \pm 2.1	-18.9 \pm 2.4
Mid Posterior ϵ (%)	-18.3 \pm 4.0	-18.0 \pm 2.1	-18.2 \pm 2.1	-17.8 \pm 1.8
Apical Posterior ϵ (%)	-19.5 \pm 4.3 *	-22.7 \pm 4.0 * ∞	-21.9 \pm 3.2	-19.5 \pm 2.6 ∞
Apical Antero-septal ϵ (%)	-22.4 \pm 5.8	-24.4 \pm 4.7	-23.5 \pm 4.1	-22.1 \pm 3.9
Mid Antero-septal ϵ (%)	-20.2 \pm 3.9	-19.9 \pm 2.2	-19.6 \pm 2.3	-19.9 \pm 2.4
Basal Antero-septal ϵ (%)	-16.3 \pm 4.0	-16.2 \pm 2.1	-16.2 \pm 1.6	-16.7 \pm 2.9
Longitudinal SRS				
Basal Infero-septal SRS (s^{-1})	-1.00 \pm 0.14	-1.00 \pm 0.18	-0.95 \pm 0.31	-0.98 \pm 0.17
Mid Infero-septal SRS (s^{-1})	-0.94 \pm 0.09	-0.93 \pm 0.11	-0.91 \pm 0.09	-0.93 \pm 0.12
Apical Infero-septal SRS (s^{-1})	-1.32 \pm 0.32	-1.29 \pm 0.21	-1.30 \pm 0.19	-1.34 \pm 0.24
Apical Lateral SRS (s^{-1})	-1.29 \pm 0.35	-1.18 \pm 0.16	-1.19 \pm 0.17	-1.25 \pm 0.26
Mid Lateral SRS (s^{-1})	-0.98 \pm 0.26	-0.96 \pm 0.18	-0.93 \pm 0.15	-0.98 \pm 0.10
Basal Lateral SRS (s^{-1})	-1.30 \pm 0.35	-1.21 \pm 0.24	-1.23 \pm 0.24	-1.25 \pm 0.23
Basal Inferior SRS (s^{-1})	-1.30 \pm 0.22	-1.26 \pm 0.25	-1.27 \pm 0.30	-1.18 \pm 0.25
Mid Inferior SRS (s^{-1})	-1.02 \pm 0.21	-1.08 \pm 0.19	-1.07 \pm 0.18	-1.03 \pm 0.15
Apical Inferior SRS (s^{-1})	-1.32 \pm 0.23	-1.45 \pm 0.38	-1.40 \pm 0.20	-1.37 \pm 0.29
Apical Anterior SRS (s^{-1})	-1.25 \pm 0.22	-1.32 \pm 0.38	-1.29 \pm 0.29	-1.22 \pm 0.29
Mid Anterior SRS (s^{-1})	-1.02 \pm 0.23	-0.96 \pm 0.11	-0.96 \pm 0.16	-1.00 \pm 0.21
Basal Anterior SRS (s^{-1})	-1.08 \pm 0.31	-0.99 \pm 0.14	-0.98 \pm 0.20	-1.02 \pm 0.26
Basal Posterior SRS (s^{-1})	-1.40 \pm 0.36	-1.37 \pm 0.33	-1.45 \pm 0.23	-1.38 \pm 0.24
Mid Posterior SRS (s^{-1})	-1.00 \pm 0.25	-1.02 \pm 0.18	-1.04 \pm 0.16	-1.00 \pm 0.17
Apical Posterior SRS (s^{-1})	-1.19 \pm 0.21	-1.29 \pm 0.30	-1.24 \pm 0.20	-1.10 \pm 0.18
Apical Antero-septal SRS (s^{-1})	-1.18 \pm 0.24	-1.29 \pm 0.28	-1.27 \pm 0.23	-1.28 \pm 0.25
Mid Antero-septal SRS (s^{-1})	-0.98 \pm 0.21	-1.02 \pm 0.18	-0.92 \pm 0.16	-1.01 \pm 0.21
Basal Antero-septal SRS (s^{-1})	-0.89 \pm 0.19	-0.92 \pm 0.21	-0.89 \pm 0.16	-0.93 \pm 0.21
Longitudinal SRE				

Basal Infero-septal SRE (s ⁻¹)	1.74 ± 0.43 ‡‡	1.49 ± 0.28	1.23 ± 0.30 †	1.40 ± 0.29 ‡
Mid Infero-septal SRE (s ⁻¹)	1.52 ± 0.36	1.53 ± 0.41	1.40 ± 0.25	1.42 ± 0.31
Apical Infero-septal SRE (s ⁻¹)	2.31 ± 0.65	2.39 ± 0.75	2.49 ± 0.65	2.34 ± 0.74
Apical Lateral SRE (s ⁻¹)	1.95 ± 0.68	2.10 ± 0.60	2.24 ± 0.56	2.18 ± 0.72
Mid Lateral SRE (s ⁻¹)	1.47 ± 0.41	1.46 ± 0.28	1.42 ± 0.30	1.55 ± 0.27
Basal Lateral SRE (s ⁻¹)	1.80 ± 0.52	1.83 ± 0.50	1.82 ± 0.48	1.81 ± 0.48
Basal Inferior SRE (s ⁻¹)	1.87 ± 0.48	1.79 ± 0.58	1.92 ± 0.40	1.60 ± 0.50
Mid Inferior SRE (s ⁻¹)	1.33 ± 0.22	1.39 ± 0.19	1.33 ± 0.20	1.34 ± 0.28
Apical Inferior SRE (s ⁻¹)	2.11 ± 0.69	2.27 ± 0.55	2.19 ± 0.47	2.14 ± 0.65
Apical Anterior SRE (s ⁻¹)	1.99 ± 0.66	2.12 ± 0.51	2.07 ± 0.53	1.97 ± 0.60
Mid Anterior SRE (s ⁻¹)	1.43 ± 0.32	1.40 ± 0.27	1.51 ± 0.35	1.58 ± 0.27
Basal Anterior SRE (s ⁻¹)	1.51 ± 0.40	1.48 ± 0.34	1.58 ± 0.42	1.49 ± 0.40
Basal Posterior SRE (s ⁻¹)	1.92 ± 0.56	1.69 ± 0.50	1.85 ± 0.61	1.71 ± 0.49
Mid Posterior SRE (s ⁻¹)	1.34 ± 0.33	1.35 ± 0.38	1.34 ± 0.30	1.23 ± 0.31
Apical Posterior SRE (s ⁻¹)	2.29 ± 0.63	2.55 ± 0.52	2.38 ± 0.57	2.24 ± 0.53
Apical Antero-septal SRE (s ⁻¹)	2.66 ± 0.87	2.87 ± 0.81	2.65 ± 0.57	2.61 ± 0.85
Mid Antero-septal SRE (s ⁻¹)	1.74 ± 0.44	1.67 ± 0.37	1.64 ± 0.38	1.70 ± 0.34
Basal Antero-septal SRE (s ⁻¹)	0.99 ± 0.29	1.10 ± 0.20	1.14 ± 0.29	1.06 ± 0.28
Longitudinal SRA				
Basal Infero-septal SRA (s ⁻¹)	0.81 ± 0.25	0.79 ± 0.32	0.68 ± 0.31	0.80 ± 0.25
Mid Infero-septal SRA (s ⁻¹)	0.65 ± 0.17	0.63 ± 0.25	0.60 ± 0.14	0.68 ± 0.15
Apical Infero-septal SRA (s ⁻¹)	0.82 ± 0.24	0.78 ± 0.17	0.73 ± 0.39	0.87 ± 0.20
Apical Lateral SRA (s ⁻¹)	0.73 ± 0.22	0.68 ± 0.21	0.71 ± 0.27	0.75 ± 0.18
Mid Lateral SRA (s ⁻¹)	0.57 ± 0.15	0.54 ± 0.21	0.55 ± 0.16	0.59 ± 0.19
Basal Lateral SRA (s ⁻¹)	0.71 ± 0.29	0.75 ± 0.31	0.64 ± 0.21	0.78 ± 0.32
Basal Inferior SRA (s ⁻¹)	0.93 ± 0.29	0.92 ± 0.31	0.90 ± 0.36	0.89 ± 0.32
Mid Inferior SRA (s ⁻¹)	0.63 ± 0.19	0.66 ± 0.26	0.65 ± 0.18	0.66 ± 0.19
Apical Inferior SRA (s ⁻¹)	0.64 ± 0.22	0.73 ± 0.33	0.64 ± 0.17	0.71 ± 0.27
Apical Anterior SRA (s ⁻¹)	0.50 ± 0.19	0.57 ± 0.25	0.52 ± 0.18	0.48 ± 0.25
Mid Anterior SRA (s ⁻¹)	0.56 ± 0.18	0.60 ± 0.23	0.50 ± 0.21	0.62 ± 0.16
Basal Anterior SRA (s ⁻¹)	0.87 ± 0.39	0.76 ± 0.30	0.66 ± 0.33	0.90 ± 0.41
Basal Posterior SRA (s ⁻¹)	0.81 ± 0.28	0.68 ± 0.22	0.72 ± 0.31	0.79 ± 0.28
Mid Posterior SRA (s ⁻¹)	0.67 ± 0.30	0.60 ± 0.23	0.59 ± 0.20	0.62 ± 0.18
Apical Posterior SRA (s ⁻¹)	0.71 ± 0.30	0.80 ± 0.36	0.73 ± 0.19	0.69 ± 0.27
Apical Antero-septal SRA (s ⁻¹)	0.71 ± 0.32	0.82 ± 0.36	0.78 ± 0.24	0.70 ± 0.29
Mid Antero-septal SRA (s ⁻¹)	0.65 ± 0.21	0.66 ± 0.19	0.64 ± 0.18	0.69 ± 0.16
Basal Antero-septal SRA (s ⁻¹)	0.47 ± 0.24	0.51 ± 0.23	0.51 ± 0.16	0.56 ± 0.20

* denotes $P < 0.05$ between pre-season and mid-season; † denotes $P < 0.05$ between pre-season and end season; ‡ denotes $P < 0.05$ between pre-season and post break; ∞ denotes $P < 0.05$ between mid-season and post break.

Table 7.5 Regional Circumferential ϵ and SR

	Pre-Season Mean\pmSD	Mid-Season Mean\pmSD	End-Season Mean\pmSD	Post Season Break Mean\pmSD
Circumferential ϵ				
Basal Antero-septal ϵ (%)	-23.0 \pm 4.7	-22.0 \pm 4.4	-19.3 \pm 10.9	-20.4 \pm 4.6
Basal Anterior ϵ (%)	-20.6 \pm 6.1	-20.2 \pm 6.1	-18.5 \pm 6.8	-16.6 \pm 5.2
Basal Lateral ϵ (%)	-14.5 \pm 6.6	-16.6 \pm 4.8	-13.8 \pm 5.1	-16.8 \pm 6.4
Basal Posterior ϵ (%)	-15.8 \pm 5.1	-16.9 \pm 6.3	-16.6 \pm 5.3	-20.1 \pm 5.5
Basal Inferior ϵ (%)	-19.0 \pm 4.6	-17.1 \pm 4.6	-19.5 \pm 5.1	-16.7 \pm 3.9
Basal Infero-septal ϵ (%)	-20.9 \pm 5.2	-18.5 \pm 3.6	-20.8 \pm 4.5	-17.8 \pm 4.8
Mid Antero-septal ϵ (%)	-23.4 \pm 4.1	-22.4 \pm 3.0	-22.3 \pm 4.7	-21.0 \pm 3.9
Mid Anterior ϵ (%)	-23.7 \pm 5.1	-23.2 \pm 3.2	-20.8 \pm 3.9	-20.4 \pm 3.9
Mid Lateral ϵ (%)	-19.5 \pm 4.3	-19.2 \pm 4.6	-16.1 \pm 3.8	-17.1 \pm 4.4
Mid Posterior ϵ (%)	-16.8 \pm 5.9	-15.0 \pm 4.4	-15.3 \pm 5.2	-15.4 \pm 6.6
Mid Inferior ϵ (%)	-17.7 \pm 4.1	-16.2 \pm 3.1	-17.8 \pm 5.1	-16.8 \pm 4.6
Mid Infero-septal ϵ (%)	-20.0 \pm 4.7	-19.3 \pm 4.0	-20.9 \pm 5.4	-19.8 \pm 5.1
Circumferential SRS				
Basal Antero-septal SRS (s^{-1})	-1.58 \pm 0.34	-1.52 \pm 0.37	-1.44 \pm 0.29	-1.39 \pm 0.39
Basal Anterior SRS (s^{-1})	-1.46 \pm 0.39	-1.60 \pm 0.61	-1.32 \pm 0.45	-1.27 \pm 0.38
Basal Lateral SRS (s^{-1})	-1.11 \pm 0.41	-1.23 \pm 0.25	-1.06 \pm 0.39	-1.20 \pm 0.41
Basal Posterior SRS (s^{-1})	-1.29 \pm 0.29	-1.44 \pm 0.51	-1.18 \pm 0.33	-1.48 \pm 0.47
Basal Inferior SRS (s^{-1})	-1.45 \pm 0.27	-1.38 \pm 0.34	-1.39 \pm 0.29	-1.30 \pm 0.22
Basal Infero-septal SRS (s^{-1})	-1.55 \pm 0.26 * \ddagger	-1.32 \pm 0.22 *	-1.42 \pm 0.24	-1.27 \pm 0.23
Mid Antero-septal SRS (s^{-1})	-1.46 \pm 0.31	-1.45 \pm 0.28	-1.38 \pm 0.37	-1.35 \pm 0.24
Mid Anterior SRS (s^{-1})	-1.57 \pm 0.43	-1.56 \pm 0.31	-1.36 \pm 0.40	-1.37 \pm 0.35
Mid Lateral SRS (s^{-1})	-1.43 \pm 0.41	-1.37 \pm 0.37	-1.21 \pm 0.33	-1.21 \pm 0.26
Mid Posterior SRS (s^{-1})	-1.25 \pm 0.43	-1.28 \pm 0.49	-1.25 \pm 0.41	-1.31 \pm 0.45
Mid Inferior SRS (s^{-1})	-1.20 \pm 0.35	-1.11 \pm 0.27	-1.25 \pm 0.32	-1.20 \pm 0.34
Mid Infero-septal SRS (s^{-1})	-1.31 \pm 0.28	-1.25 \pm 0.29	-1.33 \pm 0.32	-1.30 \pm 0.35
Circumferential SRE				
Basal Antero-septal SRE (s^{-1})	1.95 \pm 0.47	1.75 \pm 0.52	1.85 \pm 0.42	1.63 \pm 0.65
Basal Anterior SRE (s^{-1})	1.96 \pm 0.50	1.80 \pm 0.64	1.75 \pm 0.69	1.48 \pm 0.56
Basal Lateral SRE (s^{-1})	1.89 \pm 0.97	1.92 \pm 0.58	1.78 \pm 0.60	2.15 \pm 0.68
Basal Posterior SRE (s^{-1})	1.96 \pm 0.94	2.24 \pm 0.93	2.17 \pm 0.88	2.49 \pm 0.82
Basal Inferior SRE (s^{-1})	1.85 \pm 0.61	1.77 \pm 0.78	1.87 \pm 0.68	1.65 \pm 0.51
Basal Infero-septal SRE (s^{-1})	1.73 \pm 0.54	1.48 \pm 0.33	1.76 \pm 0.42	1.48 \pm 0.52
Mid Antero-septal SRE (s^{-1})	1.90 \pm 0.36	1.69 \pm 0.40	1.78 \pm 0.50	1.63 \pm 0.49
Mid Anterior SRE (s^{-1})	1.89 \pm 0.47	1.97 \pm 0.39	1.75 \pm 0.52	1.69 \pm 0.38
Mid Lateral SRE (s^{-1})	1.80 \pm 0.63	1.87 \pm 0.50	1.59 \pm 0.49	1.61 \pm 0.69
Mid Posterior SRE (s^{-1})	2.14 \pm 0.66	1.91 \pm 0.64	1.84 \pm 0.64	1.74 \pm 0.66
Mid Inferior SRE (s^{-1})	2.03 \pm 0.65	1.68 \pm 0.45	1.65 \pm 0.63	1.59 \pm 0.45
Mid Infero-septal SRE (s^{-1})	1.81 \pm 0.43	1.63 \pm 0.59	1.64 \pm 0.40	1.71 \pm 0.66

Circumferential SRA				
Basal Antero-septal SRA (s ⁻¹)	0.54 ± 0.20	0.54 ± 0.28	0.52 ± 0.27	0.52 ± 0.19
Basal Anterior SRA (s ⁻¹)	0.51 ± 0.25	0.55 ± 0.33	0.49 ± 0.28	0.57 ± 0.32
Basal Lateral SRA (s ⁻¹)	0.43 ± 0.21	0.53 ± 0.32	0.43 ± 0.20	0.54 ± 0.27
Basal Posterior SRA (s ⁻¹)	0.51 ± 0.23	0.56 ± 0.37	0.59 ± 0.40	0.52 ± 0.33
Basal Inferior SRA (s ⁻¹)	0.47 ± 0.24	0.46 ± 0.27	0.51 ± 0.30	0.55 ± 0.33
Basal Infero-septal SRA (s ⁻¹)	0.54 ± 0.37	0.44 ± 0.20	0.49 ± 0.26	0.46 ± 0.25
Mid Antero-septal SRA (s ⁻¹)	0.58 ± 0.30	0.52 ± 0.21	0.57 ± 0.32	0.61 ± 0.23
Mid Anterior SRA (s ⁻¹)	0.70 ± 0.34	0.65 ± 0.24	0.53 ± 0.22	0.64 ± 0.22
Mid Lateral SRA (s ⁻¹)	0.69 ± 0.28	0.55 ± 0.32	0.52 ± 0.18	0.59 ± 0.23
Mid Posterior SRA (s ⁻¹)	0.58 ± 0.30	0.55 ± 0.22	0.50 ± 0.32	0.57 ± 0.31
Mid Inferior SRA (s ⁻¹)	0.67 ± 0.40	0.62 ± 0.20	0.54 ± 0.36	0.58 ± 0.37
Mid Infero-septal SRA (s ⁻¹)	0.63 ± 0.28	0.56 ± 0.28	0.61 ± 0.28	0.51 ± 0.23

* denotes P < 0.05 between pre-season and mid-season; † denotes P < 0.05 between pre-season and post-season break

Table 7.6 Regional Radial ϵ and SR

	Pre-Season Mean \pm SD	Mid-Season Mean \pm SD	End-Season Mean \pm SD	Post Season Break Mean \pm SD
Radial ϵ				
Basal Antero-septal ϵ (%)	49.6 \pm 18.5	41.0 \pm 12.1	46.9 \pm 13.7	42.0 \pm 16.9
Basal Anterior ϵ (%)	49.8 \pm 16.0	47.3 \pm 14.7	48.0 \pm 14.5	44.7 \pm 17.0
Basal Lateral ϵ (%)	46.6 \pm 20.5	52.2 \pm 17.3	49.0 \pm 16.7	50.8 \pm 18.8
Basal Posterior ϵ (%)	43.4 \pm 20.5	52.6 \pm 15.8	49.3 \pm 18.8	54.1 \pm 21.4
Basal Inferior ϵ (%)	40.6 \pm 16.1	47.4 \pm 13.4	47.8 \pm 18.3	51.4 \pm 22.7
Basal Infero-septal ϵ (%)	40.8 \pm 13.6	40.8 \pm 11.9	45.9 \pm 16.3	45.3 \pm 21.2
Mid Antero-septal ϵ (%)	48.2 \pm 13.0	49.1 \pm 11.8	52.1 \pm 19.2	42.0 \pm 14.1
Mid Anterior ϵ (%)	52.1 \pm 16.6	54.0 \pm 11.8	56.0 \pm 17.8	46.7 \pm 9.2
Mid Lateral ϵ (%)	54.1 \pm 17.5	57.7 \pm 15.1	59.7 \pm 17.3	49.5 \pm 9.2
Mid Posterior ϵ (%)	53.5 \pm 18.1	58.0 \pm 16.3	61.1 \pm 17.6	48.0 \pm 10.4
Mid Inferior ϵ (%)	49.7 \pm 17.0	53.4 \pm 15.6	57.2 \pm 16.1 §	42.8 \pm 11.9 §
Mid Infero-septal ϵ (%)	46.6 \pm 14.2	48.6 \pm 14.2	52.6 \pm 16.1 §	39.1 \pm 16.2 §
Radial SRS				
Basal Antero-septal SRS (s^{-1})	2.00 \pm 0.41	1.68 \pm 0.32	1.84 \pm 0.70	1.71 \pm 0.41
Basal Anterior SRS (s^{-1})	1.81 \pm 0.39	1.71 \pm 0.26	1.81 \pm 0.46	1.76 \pm 0.36
Basal Lateral SRS (s^{-1})	1.83 \pm 0.56	1.83 \pm 0.28	1.82 \pm 0.38	1.87 \pm 0.44
Basal Posterior SRS (s^{-1})	1.79 \pm 0.62	1.92 \pm 0.28	1.85 \pm 0.39	1.99 \pm 0.43
Basal Inferior SRS (s^{-1})	1.86 \pm 0.48	1.92 \pm 0.34	1.88 \pm 0.39	2.05 \pm 0.46
Basal Infero-septal SRS (s^{-1})	1.97 \pm 0.43	1.76 \pm 0.39	1.89 \pm 0.42	1.90 \pm 0.41
Mid Antero-septal SRS (s^{-1})	1.76 \pm 0.34	1.67 \pm 0.33	1.69 \pm 0.37	1.55 \pm 0.33
Mid Anterior SRS (s^{-1})	1.88 \pm 0.37	1.78 \pm 0.45	1.80 \pm 0.33	1.65 \pm 0.29
Mid Lateral SRS (s^{-1})	1.91 \pm 0.42	1.81 \pm 0.30	1.94 \pm 0.42	1.80 \pm 0.37
Mid Posterior SRS (s^{-1})	1.84 \pm 0.44	1.86 \pm 0.27	1.93 \pm 0.41	1.76 \pm 0.36
Mid Inferior SRS (s^{-1})	1.79 \pm 0.37	1.90 \pm 0.30	1.95 \pm 0.41	1.67 \pm 0.34
Mid Infero-septal SRS (s^{-1})	1.76 \pm 0.28	1.79 \pm 0.35	1.83 \pm 0.39	1.61 \pm 0.37
Radial SRE				
Basal Antero-septal SRE (s^{-1})	-2.01 \pm 0.52	-1.83 \pm 0.46	-1.90 \pm 0.45	-1.86 \pm 0.78
Basal Anterior SRE (s^{-1})	-2.16 \pm 0.50	-2.07 \pm 0.45	-2.04 \pm 0.47	-2.00 \pm 0.61
Basal Lateral SRE (s^{-1})	-2.22 \pm 0.65	-2.41 \pm 0.89	-2.09 \pm 0.65	-2.07 \pm 0.74
Basal Posterior SRE (s^{-1})	-2.12 \pm 0.70	-2.38 \pm 0.99	-2.04 \pm 0.63	-2.00 \pm 0.68
Basal Inferior SRE (s^{-1})	-2.08 \pm 0.78	-2.13 \pm 0.78	-1.92 \pm 0.58	-1.78 \pm 0.57
Basal Infero-septal SRE (s^{-1})	-1.94 \pm 0.67	-1.84 \pm 0.48	-1.80 \pm 0.56	-1.76 \pm 0.44
Mid Antero-septal SRE (s^{-1})	-2.13 \pm 0.57	-2.00 \pm 0.56	-2.17 \pm 0.51	-2.03 \pm 0.82
Mid Anterior SRE (s^{-1})	-2.09 \pm 1.19	-2.16 \pm 0.69	-2.32 \pm 0.71	-2.18 \pm 0.77
Mid Lateral SRE (s^{-1})	-2.37 \pm 0.83	-2.35 \pm 0.83	-2.57 \pm 1.07	-2.38 \pm 0.63
Mid Posterior SRE (s^{-1})	-2.34 \pm 1.01	-2.39 \pm 0.76	-2.53 \pm 1.08	-2.39 \pm 0.58
Mid Inferior SRE (s^{-1})	-2.32 \pm 1.02	-2.30 \pm 0.62	-2.44 \pm 0.91	-2.30 \pm 0.64
Mid Infero-septal SRE (s^{-1})	-2.16 \pm 0.84	-2.04 \pm 0.50	-2.20 \pm 0.68	-1.98 \pm 0.72

Radial SRA				
Basal Antero-septal SRA (s ⁻¹)	-0.92 ± 0.38	-1.04 ± 0.47	-1.04 ± 0.49	-0.95 ± 0.41
Basal Anterior SRA (s ⁻¹)	-0.80 ± 0.34	-1.06 ± 0.52	-0.95 ± 0.45	-0.84 ± 0.36
Basal Lateral SRA (s ⁻¹)	-0.78 ± 0.35	-1.08 ± 0.64	-0.88 ± 0.43	-0.84 ± 0.37
Basal Posterior SRA (s ⁻¹)	-0.81 ± 0.39	-1.04 ± 0.68	-0.85 ± 0.38	-0.88 ± 0.38
Basal Inferior SRA (s ⁻¹)	-0.90 ± 0.36	-1.04 ± 0.54	-0.90 ± 0.36	-1.00 ± 0.43
Basal Infero-septal SRA (s ⁻¹)	-0.96 ± 0.32	-1.01 ± 0.45	-1.00 ± 0.38	-1.05 ± 0.50
Mid Antero-septal SRA (s ⁻¹)	-0.86 ± 0.40	-0.81 ± 0.43	-0.76 ± 0.45	-0.78 ± 0.29
Mid Anterior SRA (s ⁻¹)	-0.87 ± 0.47	-0.88 ± 0.35	-0.82 ± 0.36	-0.85 ± 0.29
Mid Lateral SRA (s ⁻¹)	-0.96 ± 0.43	-1.04 ± 0.38	-1.01 ± 0.45	-0.95 ± 0.30
Mid Posterior SRA (s ⁻¹)	-1.01 ± 0.38	-1.14 ± 0.47	-1.16 ± 0.55	-1.00 ± 0.33
Mid Inferior SRA (s ⁻¹)	-1.00 ± 0.41	-1.09 ± 0.50	-1.16 ± 0.55	-1.01 ± 0.36
Mid Infero-septal SRA (s ⁻¹)	-0.92 ± 0.50	-0.97 ± 0.44	-0.99 ± 0.49	-0.89 ± 0.30

§ denotes $P < 0.05$ between end season and post season break

7.3.2 Right Ventricle and Atria

Standard 2D echocardiographic RV data is shown in Table 7.7. No differences were observed across the season for any structural or functional RV parameters ($P > 0.05$).

Table 7.7 Echocardiographic parameters of the Right ventricle

	Pre-Season Mean ± SD (Range)	Mid-Season Mean ± SD (Range)	End-Season Mean ± SD (Range)	Post Season Break Mean ± SD (Range)
RVOT_{plax} (mm)	33 ± 3 (28 - 41)	34 ± 4 (27 - 42)	33 ± 3 (29 - 40)	33 ± 3 (27 - 42)
RVOT₁ (mm)	34 ± 3 (28 - 42)	34 ± 3 (27 - 40)	35 ± 3 (28 - 42)	35 ± 3 (27 - 41)
RVOT₂ (mm)	28 ± 3 (23 - 35)	27 ± 2 (24 - 33)	27±2 (21-30)	27 ± 2 (22 - 31)
RVD₁ (mm)	47 ± 4 (39 - 58)	48 ± 4 (41 - 54)	48 ± 3 (41 - 52)	46 ± 3 (40 - 52)
RVD₂ (mm)	37 ± 3 (31 - 45)	37 ± 3 (32 - 42)	36 ± 3 (30 - 44)	35 ± 2 (32 - 40)
RVD₃ (mm)	91 ± 6 (83 - 102)	93 ± 4 (87 - 101)	92 ± 5 (82 - 102)	92 ± 6 (83 - 103)
RVDa (cm²)	30 ± 3 (23 - 37)	29 ± 3 (24 - 36)	29 ± 3 (23 - 32)	30 ± 3 (23 - 36)
RVSa (cm²)	17 ± 2 (14 - 20)	16 ± 2 (13 - 21)	16 ± 2 (11 - 19)	17 ± 2 (13 - 20)
TAPSE (mm)	23 ± 2 (19 - 27)	23 ± 3 (19 - 29)	24 ± 3 (20 - 28)	24 ± 3 (20 - 29)
RV:LV Ratio	0.89 ± 0.06 (0.77 - 1.00)	0.90 ± 0.07 (0.75 - 1.00)	0.90 ± 0.05 (0.78 - 1.00)	0.89 ± 0.06 (0.78 - 1.00)
RVFAC (%)	45 ± 5 (38 - 53)	44 ± 5 (36 - 54)	44 ± 4 (36 - 54)	43 ± 5 (36 - 52)
RVOT_{PLAX} (mm/(m²)^{0.5})	22 ± 2 (19 - 27)	22 ± 2 (18 - 28)	22 ± 2 (19 - 26)	22 ± 2 (18 - 27)
RVOT₁ (mm/(m²)^{0.5})	23 ± 2 (19 - 28)	23 ± 2 (18 - 26)	23 ± 2 (19 - 28)	23 ± 2 (18 - 27)
RVOT₂ (mm/(m²)^{0.5})	19 ± 2 (16 - 24)	18 ± 1 (16 - 21)	18 ± 2 (14 - 20)	18 ± 2 (14 - 21)
RVD₁ (mm/(m²)^{0.5})	32 ± 3 (26 - 38)	32 ± 3 (27 - 37)	32 ± 2 (28 - 37)	31 ± 2 (27 - 35)
RVD₂ (mm/(m²)^{0.5})	24 ± 2 (21 - 30)	25 ± 2 (21 - 28)	24 ± 2 (20 - 30)	24 ± 1 (21 - 26)
RVD₃ (mm/(m²)^{0.5})	61 ± 4 (55 - 70)	62 ± 3 (56 - 66)	61 ± 3 (54 - 67)	61 ± 3 (56 - 67)
RVDa Index (cm²/m²)	13 ± 2 (11 - 16)	13 ± 1 (11 - 16)	13 ± 1 (11 - 15)	13 ± 1 (10 - 15)
RVSa Index (cm²/m²)	7 ± 1 (6 - 9)	7 ± 1 (6 - 9)	7 ± 1 (5 - 9)	8 ± 1 (6 - 9)
RV S' (cm/s)	13 ± 2 (11 - 17)	14 ± 2 (11 - 17)	14 ± 2 (11 - 17)	14 ± 2 (12 - 18)
RV E' (cm/s)	15 ± 3 (9 - 21)	16 ± 3 (12 - 23)	16 ± 3 (12 - 25)	17 ± 4 (11 - 28)
RV A' (cm/s)	9 ± 2 (6 - 15)	9 ± 3 (4 - 15)	10 ± 2 (6 - 14)	10 ± 2 (7 - 13)
RV E'/A' (cm/s)	1.68 ± 0.49 (1.11 - 2.83)	1.86 ± 0.75 (1.07 - 4)	1.66 ± 0.39 (1.25 - 2.78)	1.78 ± 0.58 (0.85 - 3.11)

RV S' index ((cm/s)/cm)	1.46 ± 0.21 (1.09 - 1.98)	1.48 ± 0.16 (1.20 - 1.82)	1.54 ± 0.20 (1.26 - 1.89)	1.56 ± 0.15 (1.25 - 1.83)
RV E' index ((cm/s)/cm)	1.63 ± 0.35 (1.02 - 2.38)	1.71 ± 0.32 (1.22 - 2.47)	1.75 ± 0.39 (1.43 - 3.01)	1.82 ± 0.43 (1.22 - 3.15)
RV A' index ((cm/s)/cm)	1.02 ± 0.27 (0.59 - 1.51)	1.01 ± 0.29 (0.45 - 1.58)	1.08 ± 0.22 (0.63 - 1.52)	1.07 ± 0.18 (0.73 - 1.44)

In addition, there were no significant differences for global (Table 7.8) and regional (Table 7.9) RV ϵ and SR ($P > 0.05$).

Table 7.8 Global and Regional RV ϵ and SR

	Pre-Season Mean ± SD (Range)	Mid-Season Mean ± SD (Range)	End-Season Mean ± SD (Range)	Post Season Break Mean ± SD (Range)
RV ϵ (%)	-26.4 ± 3.4 (-21.0 to -34.2)	-27.4 ± 2.82 (-21.6 to -32.3)	-26.9 ± 2.70 (-21.6 to -30.9)	-27.9 ± 2.61 (-24.3 to -33.0)
Time to Peak RV ϵ (s)	0.38 ± 0.03 (0.33 - 0.43)	0.38 ± 0.03 (0.33 - 0.44)	0.39 ± 0.02 (0.35 - 0.43)	0.38 ± 0.03 (0.33 - 0.45)
RVSRS (s⁻¹)	-1.31 ± 0.19 (-0.86 to -1.67)	-1.36 ± 0.18 (-1.10 to -1.85)	-1.33 ± 0.16 (-0.99 to -1.69)	-1.36 ± 0.17 (-1.09 to -1.89)
RVSRE (s⁻¹)	1.59 ± 0.32 (1.08 - 2.28)	1.56 ± 0.31 (0.95 - 2.02)	1.56 ± 0.29 (1.07 - 2.19)	1.60 ± 0.33 (1.11 - 2.42)
RVSRA (s⁻¹)	0.80 ± 0.18 (0.49 - 1.20)	0.85 ± 0.18 (0.43 - 1.16)	0.83 ± 0.25 (0.34 - 1.31)	0.88 ± 0.27 (0.40 - 1.50)

Table 7.9 RV Longitudinal Regional Strain and strain Rate

	Pre- Season Mean ± SD (Range)	Mid- Season Mean ± SD (Range)	End- Season Mean ± SD (Range)	Post Season Break Mean ± SD (Range)
Basal RVϵ (%)	-25.0 ± 5.7	-25.8 ± 4.5	-25.0 ± 4.5	-25.1 ± 3.9
Mid RVϵ (%)	-25.9 ± 4.0	-27.3 ± 2.9	-26.6 ± 2.9	-28.0 ± 2.8
Apical RVϵ (%)	-28.7 ± 5.3	-30.0 ± 4.0	-29.9 ± 3.2	-30.8 ± 3.3
Apex to Base ϵ gradient (%)	-3.7	-4.2	-4.9	-5.8
Basal RVSRS (s⁻¹)	-1.53 ± 0.42	-1.51 ± 0.29	-1.48 ± 0.24	-1.49 ± 0.30
Mid RVSRS (s⁻¹)	-1.29 ± 0.26	-1.39 ± 0.22	-1.34 ± 0.21	-1.39 ± 0.19
Apical RVSRS (s⁻¹)	-1.56 ± 0.23	-1.55 ± 0.30	-1.69 ± 0.35	-1.56 ± 0.27
Basal RVSRE (s⁻¹)	2.07 ± 0.55	2.02 ± 0.63	2.14 ± 0.41	2.01 ± 0.48
Mid RVSRE (s⁻¹)	1.58 ± 0.36	1.69 ± 0.43	1.71 ± 0.38	1.80 ± 0.40
Apical RVSRE (s⁻¹)	2.07 ± 0.53	2.06 ± 0.42	2.08 ± 0.38	2.25 ± 0.56
Basal RVSRA (s⁻¹)	1.00 ± 0.27	1.03 ± 0.35	1.02 ± 0.39	1.14 ± 0.51
Mid RVSRA (s⁻¹)	0.84 ± 0.20	0.87 ± 0.22	0.90 ± 0.28	0.94 ± 0.26
Apical RVSRA (s⁻¹)	1.05 ± 0.31	1.16 ± 0.42	1.15 ± 1.29	1.17 ± 0.34

There were no differences ($P > 0.05$) in the left and right atrial parameters at any of the seasonal data collection points (Tables 7.10 and 7.11).

Table 7.10 Echocardiographic parameters of the left atrium

	Pre-Season Mean \pm SD (Range)	Mid- Season Mean \pm SD (Range)	End- Season Mean \pm SD (Range)	Post Season Break Mean \pm SD (Range)
LAd (mm)	39 \pm 3 (33 - 45)	38 \pm 2 (32 - 42)	39 \pm 3 (31 - 44)	38 \pm 3 (33 - 43)
LAd (mm/(m²)^{0.5})	26 \pm 2 (23 - 30)	26 \pm 1 (23 - 29)	26 \pm 2 (21 - 29)	26 \pm 1 (23 - 27)
LAVoles (ml)	62 \pm 11 (45 - 80)	63 \pm 13 (42 - 83)	66 \pm 12 (48 - 90)	66 \pm 11 (44 - 87)
LAVoles (ml/(m²)^{1.5})	19 \pm 4 (14 - 25)	19 \pm 4 (13 - 27)	20 \pm 3 (15 - 25)	19 \pm 3 (14 - 25)
LAVolpreA (ml)	38 \pm 7 (26 - 54)	40 \pm 8 (25 - 51)	41 \pm 7 (23 - 57)	40 \pm 8 (26 - 51)
LAVolpreA ml/(m²)^{1.5})	11 \pm 2 (8 - 17)	12 \pm 2 (8 - 16)	12 \pm 2 (7 - 15)	12 \pm 2 (8 - 17)
LAVoled (ml)	26 \pm 6 (15 - 35)	27 \pm 7 (16 - 39)	28 \pm 5 (19 - 41)	27 \pm 6 (16 - 37)
LAVoled (ml/(m²)^{1.5})	8 \pm 2 (4 - 12)	8 \pm 2 (5 - 12)	8 \pm 1 (6 - 10)	8 \pm 1 (5 - 10)
LAVolres (ml)	37 \pm 8 (24 - 49)	36 \pm 9 (23 - 57)	38 \pm 10 (26 - 56)	39 \pm 8 (25 - 56)
LAVolcon (ml)	43 \pm 12 (13 - 62)	44 \pm 15 (17 - 68)	43 \pm 13 (23 - 69)	44 \pm 11 (24 - 72)
LAVolboo (ml)	12 \pm 3 (9 - 22)	13 \pm 4 (8 - 25)	13 \pm 4 (4 - 18)	13 \pm 4 (7 - 20)

Table 7.11 Echocardiographic parameters of the right atrium

	Pre-Season Mean \pm SD (Range)	Mid- Season Mean \pm SD (Range)	End- Season Mean \pm SD (Range)	Post Season Break Mean \pm SD (Range)
RAa (cm²)	21 \pm 2 (17 - 24)	19 \pm 2 (15 - 22)	20 \pm 2 (15 - 24)	20 \pm 3 (15 - 25)
RAa Index (cm²/m²)	9 \pm 1 (7 - 11)	9 \pm 1 (6 - 10)	9 \pm 1 (7 - 10)	9 \pm 1 (7 - 12)
RAvoles (ml)	67 \pm 10 (48 - 82)	59 \pm 12 (34 - 81)	68 \pm 13 (39 - 94)	65 \pm 13 (36 - 91)
RAvoles Index (ml/(m²)^{1.5})	20 \pm 3 (14 - 27)	18 \pm 4 (9 - 24)	20 \pm 4 (12 - 27)	19 \pm 4 (11 - 28)
RAvolpreA (ml)	45 \pm 9 (30 - 62)	42 \pm 10 (24 - 65)	44 \pm 9 (26 - 65)	42 \pm 11 (20 - 64)
RAvolpreA (ml/(m²)^{1.5})	14 \pm 3 (10 - 19)	12 \pm 3 (6 - 18)	13 \pm 2 (8 - 18)	12 \pm 3 (6 - 20)
RAvoled (ml)	33 \pm 9 (20 - 49)	30 \pm 8 (17 - 43)	33 \pm 7 (20 - 46)	31 \pm 8 (16 - 48)
RAvoled Index (ml/(m²)^{1.5})	10 \pm 3 (5 - 14)	9 \pm 2 (4 - 13)	10 \pm 2 (6 - 13)	9 \pm 2 (5 - 14)
RAvolres (ml)	34 \pm 7 (22 - 47)	29 \pm 8 (17 - 45)	34 \pm 9 (19 - 48)	34 \pm 8 (20 - 48)
RAvolcon (ml)	46 \pm 11 (24 - 74)	50 \pm 15 (19 - 83)	47 \pm 13 (23 - 67)	49 \pm 16 (25 - 93)
RAvolboo (ml)	13 \pm 5 (5 - 22)	12 \pm 4 (7 - 25)	11 \pm 4 (4 - 19)	11 \pm 5 (4 - 22)

7.4 Discussion

The main findings of this study were 1) a lack of any structural differences from all of the cardiac chambers during the competitive RFL season and 2) in addition to sporadic and isolated regional functional differences there were clear differences in apical rotation and twist with higher values observed at the pre-season data collection point.

7.4.1 Cardiac Structure

In this group of chronically trained RFL athletes there was no variation in biventricular structure across the season despite significant differences in training workload. This is in contrast to previous longitudinal studies in cyclists where a reduction in LV wall thickness was observed in the resting season (Fagard *et al.*, 1983) and an increased LVIDd with reduced LV wall thickness associated with participation in successive Tours de France (Abergel *et al.*, 2004). The explanation for this may lie with the strong association between LV structural remodelling and training induced alterations in fat free mass (FFM) (Whalley *et al.*, 2004, Cabanelas *et al.*, 2013, D'Ascenzi, *et al.*, 2015a). The link between body composition and LV size is well established (Batterham *et al.*, 1999) and raises an important point when considering 'short-term' training adaptation. i.e. the RFL athletes in our study, although undergoing variable seasonal training loads, did not demonstrate any changes in body composition. Furthermore, we did not demonstrate any changes in LA volume in contrast to D'Ascenzi *et al.* (2015c) whom demonstrated LA seasonal changes that were independently associated to LV mass index. This association to a scaled index further highlights the potential compounding effects of body size.

Few studies have focused on RV adaptation across the season however RV dilatation has been reported in endurance athletes (university rowers) after 90 days of training when compared to baseline assessment (Baggish *et al.*, 2008a). The athletes in this study were non-elite rowers and included both male and female rowers with females having lower absolute baseline RV dimensions than RFL athletes. In support of this, Baggish *et al.*, 2010 found greater physiological RV adaptation in elite compared to sub-elite rowers Baggish *et al.* (2010). Based on this we can speculate that the RFL athletes in this study had greater baseline adaptation and long-term remodelling which

would require a greater magnitude of training stimulus to cause ‘short-term’ adaptation. A recent longitudinal RV study (D’Ascenzi *et al.*, 2016b) in basketball and volleyball players also revealed increases in RV size during the competitive season, however baseline absolute RV dimensions were lower in these athletes compared to RFL athletes. These data are more difficult to interpret within the context of our findings although it is important to note that absolute training volume was not defined within these studies. We can therefore speculate that the seasonal variation in training stimulus was potentially greater in these particular sporting disciplines, which when considering implications for PPS, warrants further exploration.

7.4.2 Cardiac Function

Seasonal variation in LV function was observed in the RFL athlete with changes predominantly related to pre-season. There were no differences in standard systolic functional parameters which is in contrast to reports of seasonal and chronic reductions in LV systolic function in competitive cyclists (Fagard *et al.*, 1983, Abergel *et al.*, 2004). No changes in global LV ϵ and SR were observed in RFL athletes across the season despite mixed results of previously reported longitudinal studies (D’Ascenzi *et al.*, 2015b, Baggish *et al.*, 2010, Weiner *et al.*, 2015, Baggish *et al.*, 2008b, Weiner *et al.*, 2010). In a study of athletes (soccer, basketball and volleyball) involved in an 18 week training study only a mild increase in global longitudinal LV ϵ was observed despite significant increases in LV mass, LVIDd and systolic volume (D’Ascenzi *et al.*, 2015b). Whilst LVEF remained unchanged following endurance training in rowers, increases in peak LV systolic TDI and radial and longitudinal ϵ were observed with a base to apex gradient. Circumferential ϵ increased in LV free wall but decreased in regions adjacent to RV possibly secondary to RV adaptation (Baggish *et al.*, 2008b). Again we can speculate that there were significant differences in training stimulus

between studies allowing for the contrasting results. These studies however, present systolic functional adaptation that would not have been detected by conventional echocardiography alone (Baggish *et al.*, 2008b) thus highlighting the potential for STE in PCS. STE provided evidence of regional mechanical heterogeneity in RFL athletes with the infero-septal region being commonly involved. The majority of differences were observed at pre-season which is also associated with the highest training workload leading to the speculation of an acute adaptive training effect on these regions after a short training break subsequently followed by pre-season training. However, due to lack of structural changes it is difficult to speculate on potential mechanisms for these observations and the possibility of sporadic regional differences being related to type 1 statistical error also has to be considered.

Significant functional differences in systolic rotation and twist have been observed in RFL athletes during the competitive season. Apical rotation and twist were higher at the pre-season time-point compared to mid-season, end-season and post-break and this increase at pre-season also corresponds to the highest seasonal workload. Increases in apical rotation and twist observed at the end of the pre-season may be explained by a deconditioning effect occurring over the season break where there was no structured training period, immediately followed by acute and high intensity training in pre-season where the daily workload was more than double than that seen at mid and end-season time points. Twist may be sensitive to deconditioning / acute training effects and following the initial increase in apical rotation and twist there was regression of these parameters in RFL athletes across the rest of the season. This data represents both seasonal acute and chronic responses to training within a previously chronically trained groups of elite athletes.

From cross sectional studies, lower apical rotation and LV twist have been reported in chronically trained cyclists (Nottin *et al.*, 2008) and RFL athletes (chapter 4 / Forsythe *et al.*, 2018) compared to controls. This has been proposed to be a normal physiological adaptive response of the myocardium to training providing a potential mechanism for a contractile reserve (Nottin *et al.*, 2008). Similar longitudinal findings to the current study have been reported in rowers following acute and chronic training. Following a 90 day training phase there was an increase in LV mass, peak apical systolic rotation and peak systolic twist but after 39 months despite further increases in LV mass there was a regression in twist (Weiner *et al.*, 2015). The authors therefore reported a phasic training response with increased LV cavity size and systolic twist in the acute phase followed by increased wall thickness and a regression of twist after chronic training (Weiner *et al.*, 2015). The phasic phenomenon reported by Weiner *et al.*, (2015) was observed in non-elite athletes and was associated with LV structural changes whilst despite a similar pattern of twist mechanics in elite RFL athletes there were no associated changes in LV structure. In contrast, LV rotation and twist measurements did not change in national and international soccer, basketball and volleyball players who were assessed pre and post 18 weeks of intensive training (D'Ascenzi *et al.*, 2015b) however acute and chronic training phases were not defined in this study.

Variable reports of diastolic function from longitudinal studies exist, ranging from increases in diastolic function in endurance athletes (Baggish *et al.*, 2008a, Weiner *et al.*, 2015) to decreases in strength athletes (Baggish *et al.*, 2008a) to no significant difference in soccer players (Cabanelas *et al.*, 2013). In the current study, trans-mitral late diastolic velocity was significantly increased, but within normal limits, after post-season break compared to end of season which may be related to a detraining effect

on the atrial contribution to LV filling however the velocity was not significantly different between post-season break and pre-season. A relationship between the change in systolic twist and presumably the subsequent diastolic untwist, to the observed changes in trans-mitral late diastolic velocity cannot be excluded, although a potential mechanism remains difficult to ascertain.

No seasonal changes in RV function were observed in RFL athletes by either standard echocardiography or STE. Increased RV systolic (RVFAC and TDI) and diastolic function (TDI) was reported in university rowers after 90 days of training when compared to baseline assessment (Baggish *et al.*, 2008a) and enhanced RV systolic ϵ was reported in an elite group of rowers compared to sub-elite after 3 months (Baggish *et al.*, 2010). Similarity to the current study has been observed in basketball and volleyball players as global RV function did not change over the competitive season however, in contrast a significant increase in regional apical RV ϵ was observed from pre-season to end-season (D'Ascenzi *et al.*, 2016b).

Variation between this and previous seasonal and longitudinal studies may be related to training schedules, duration and intensity of training, sporting disciplines and athletes of differing competitive levels. Functional seasonal variation reported by STE data in RFL athletes indicates potential acute and chronic adaptation in LV cardiac mechanics. The acute training response in pre-season appears to produce the greatest effect on seasonal cardiac variation in RFL athletes with intense acute exercise following a short period of deconditioning in the post-season break. Further investigation is needed to ascertain if the acute increase in twist after a period of deconditioning and subsequent regression across the season does indicate a true myocardial exercise reserve. In-exercise echocardiographic studies measuring both functional 2D and STE parameters and their response to exercise at seasonal time

points, could provide key evidence for mechanisms of exercise adaptation in RFL athletes. The mechanical changes recorded by STE in this study would not have been recorded in serial cardiac assessments of these athletes by conventional 2D echocardiography alone. Given that prolonged LV twist time has been reported in cardiomyopathies (Pacileo *et al.*, 2011) this study indicates the potential clinical benefit of twist and therefore untwist in differential diagnosis, not only by the use of peak values but also through a temporal assessment.

7.5 Limitations

A small sample size was used and only RFL athletes were included in the study therefore this data may not be representative of athletes of other sporting disciplines or gender. Observations and assessment was across one competitive season and future studies should focus on longer term follow up. In-exercise echocardiographic studies of RFL athletes may help to validate the functional changes identified by STE.

7.6 Conclusion

No structural cardiac changes as measured by standard echocardiographic methods were observed across the competitive RFL season however, significant functional changes in the LV were detected with the use of STE. Standard 2D echocardiographic assessment of the elite RFL athlete does not appear to be affected by seasonal variation in training load which is reassuring for PCS of RFL athletes. Although STE is not routinely used in PCS, the utilisation of the technique in this study has revealed significant functional seasonal alterations which would otherwise go undetected during PCS. Findings have helped to elucidate potential mechanisms of normal, functional cardiac adaptation to exercise in RFL athletes and therefore STE is likely

to provide additional information to aid PCS especially in the role of differential diagnosis.

Chapter 8

General Discussion

8.1 Aims of Thesis

The work in this thesis facilitated the completion of a number of objectives in elite, male RFL athletes: 1) to establish left ventricular structural and functional indices using TTE and STE and mathematically model the structural-functional relationship; 2) to determine structural and functional indices of the right heart using TTE and STE; 3) to provide a comparative and holistic structural and functional assessment of all cardiac chambers in the junior and senior athletes using TTE and STE; and 4) to assess variation in structural and functional indices across the competitive season using TTE and STE.

8.2 Brief Summary of Findings

Chapter 4 characterised the LV phenotype of the RFL athlete. Absolute and scaled values of LV chamber size and wall thickness were greater than controls. There was a predominance of normal LV geometry in senior RFL athletes and mathematical modelling highlighted the interaction of divergent effects of LVIDd and MWT on LV function to maintain a normal LVEF. Global systolic function was also normal when assessed by STE, however lower indexed TDI and global SR were also observed in athletes. Significant regional variation in ϵ and SR was apparent and likely part of normal physiological adaptation. Apical rotation and twist parameters were lower in athletes which may serve as an important adaptive process in the AH of elite RFL athletes. Chapter 5 investigated the right heart of the RFL athlete. Absolute measures of RV size were greater in athletes, a finding which persisted after scaling for body size with exception of just one parameter, RVD₂. The increase in RV size is important as it creates an overlap with ARVC criteria making PCS more challenging. Despite structural remodelling RV function in the RFL athlete is normal as assessed by

RVFAC and RV longitudinal ϵ . Similarly to the LV, lower RV TDI index and SR was observed in athletes. All absolute and indexed RA parameters were larger in athletes. Guidelines suggest that PCS should be undertaken between the ages of 14-35 years and hence chapter 6 focused on comparing the heart of senior and junior RFL athletes. Increased RWT and LV mass index were observed in SA whilst differences in absolute LV and LA dimensions were largely removed when scaled for BSA. LV systolic function was normal irrespective of age. SA had slightly lower longitudinal SRS and early diastolic functional indices. RVOT remained larger in seniors even after scaling for BSA. RV function was normal irrespective of age with a slightly lower RV longitudinal ϵ observed in seniors, related to the apical segment, as well as lower SRS and SRE. The RA was larger in seniors after scaling and both atria had larger functional booster volumes. The right heart therefore appears more sensitive to chronic training in RFL athletes.

As there are no strict guidelines as to when PCS should be undertaken within the competitive sporting season, chapter 7 studied seasonal variation cardiac structure and function. No structural changes were observed across the season and significant functional changes were limited to higher apical rotation and twist at pre-season. Results are reassuring particularly for the application of standard echocardiography in the PCS setting. The study highlighted some potentially important physiological adaptations in LV rotation that might be missed with standard echocardiography but may aid PCS in borderline 'grey area' cases

8.3 Overarching Issues and Implications for PCS

8.3.1 *The Structural-Functional Relationship*

Studies within this thesis have confirmed a predominance of normal LV geometry in the elite RFL athlete which is supported by a recent study of endurance and resistance athletes (Utomi *et al.*, 2014). This is an important finding in a mixed training sporting discipline consisting of moderate static and moderate dynamic components (Levine *et al.*, 2015) and covers the observed differences in LV size and wall thickness between RFL athletes and controls, as well as senior athletes and junior athletes. Normal LV geometry remained constant throughout the competitive RFL season as did all structural echocardiographic parameters. A lack of concentric hypertrophy in resistance athletes has been reported recently (Utomi *et al.*, 2014) and none of the athletes, in any of the studies, presented with concentric hypertrophy which is important given the degree of resistance training that is undertaken by these athletes. In terms of PCS, the structural results from this thesis suggest that very few RFL athletes will present with abnormal LV geometry and those that do require careful consideration for a differential diagnosis. As in any population some cardiac parameters in athletes will fall at or above/below expected normal adult range limits but any RFL athlete presenting with concentric hypertrophy should be considered 'red flag' and the athlete should undergo thorough cardiac investigation by a consultant sports cardiologist.

LV systolic function in RFL athletes as measured by EF is normal in both junior and senior age groups and across the competitive season. This is mirrored by a normal global ϵ in all cardiac planes and hence a reduction in LV ϵ is not associated with normal physiological adaptation. Despite an increase in LV volume and wall thickness

in athletes compared to controls, EF and ϵ were not different and mathematical modelling in chapter 3 examined this relationship. Normal LV EF may not always equal normal systolic function highlighted by recent studies of pathological hypertension in patients diagnosed with heart failure with normal ejection fraction (HFNEF) (MacIver and Townsend, 2008). These patients may have by definition normal EF but there is a paradox of reduced longitudinal, circumferential and radial ϵ but normal absolute radial thickening and therefore normal EF which has been explained by the increased diastolic wall thickness (MacIver, 2011, MacIver and Dayer, 2012). Mathematical modelling in pathological LVH has shown that the terms EF and LV function are not synonymous and in the context of concentric LVH, normal absolute radial thickening results in a normal EF with the illusion of normal pump function (MacIver and Dayer, 2012) but in fact mechanical ϵ is reduced. For the first time a mathematical model has been applied to physiological adaptation and in this model normal EF is maintained by the divergent effects of LVIDd and MWT on LV function but in contrast to the pathological model, ϵ is also normal. An increase in LVIDd alone would be likely to cause a decrease in EF and ϵ and an increase in MWT alone would be more likely to cause an increase in EF and ϵ but their interaction reflects a normal EF. STE can provide additional functional information during PCS for identification of pathological or physiological remodelling in athletes even when systolic function as measured by EF is normal. Whilst no differences in LV ϵ were observed, lower SR's were observed in athletes compared to controls with evidence of significant regional heterogeneity in ϵ and SR. This likely reflects normal physiological adaptation in RFL athletes and in borderline PCS cases it may be necessary to assess regional wall function so knowledge of normative regional data is pertinent.

Marked differences in LV twist and rotational parameters are a prominent themes of this thesis, both in the cross-sectional and longitudinal studies. This suggests the importance of these parameters in the normal physiological adaptation of the LV to training undertaken in RFL athletes. As apical rotation and twist are lower in RFL athletes compared to controls and with prolonged LV twist duration reported in cardiomyopathies (Pacileo *et al.*, 2011), studies in this thesis indicate the potential clinical benefit of twist and potentially untwist in differential diagnosis in PCS, not only by the use of peak values but also through a temporal assessment. Lower twist In RFL athletes' was associated with normal EF or ϵ which is likely to be more representative of a physiological response to training similar to that previously described by Zocalo *et al.* (2008). The authors suggested that a lower twist is needed to maintain resting cardiac output in athletes but in response to periods of increased cardiovascular demand there is an enhanced myocardial (or twist) reserve . Twist has been shown to correlate with wall thickness (chapter 4) and although twist was not included in the mathematical model it may be part of the process of LV adaptation allowing for maintenance of normal systolic function.

RFL athletes have a larger RV than controls, even after scaling for body size (with the exception of RVD₂). Endurance training has been found to have the biggest effect on chamber dimensions (Utomi *et al.*, 2015) and in this respect the right heart of the RFL appears to be more in keeping with balanced (LV/RV) eccentric hypertrophy and more akin to adaptation observed in endurance athletes with a prominent dynamic exercise stimulus leading to adaptation. A disproportionate increase in afterload has been reported on the RV compared to the LV during endurance exercise (La Gerche *et al.*, 2011) due to a greater relative increase in pulmonary vascular resistance and pulmonary arterial pressure which affects the pressure volume relationships within the

RV cavity elevating RV wall stress (La Gerche *et al.*, 2011). La Gerche *et al.* (2011) reported a comparison on RV and LV wall stress and identified a disproportionate stroke work in the RV as a result of comparatively greater wall stress. In response to the increased afterload the thinner walled RV cavity may be less able to cope with the demand to generate greater force than the LV resulting in RV dilatation to offset the increase pressure load. The increased RV size in many RFL athletes allows significant overlap with current structural criteria for ARVC (Marcus *et al.*, 2010) thus creating a diagnostic dilemma. A thorough assessment of RV function, however, including the use of STE in these athletes will help to reduce the grey area as abnormal global and/or regional function in association with a dilated RV is characteristic of ARVC.

RV function is normal in RFL athletes irrespective of age. RV SR is, however, lower in athletes compared to controls likely reflecting normal physiological adaptation. The RV ϵ gradient is normal in RFL athletes and could be an important parameter for use in differential diagnosis as any change in the gradient should be thoroughly investigated for potential RV dysfunction and pathology. Whilst RFL athletes may present with increased RV size, functional assessment is key and STE provides further corroborative functional data with the added advantage of assessing regional as well as global function. Therefore in the RFL athlete an increased RV size with normal function is more likely to be representative of normal physiological adaptation.

8.3.2 *The Impact of Athlete Age*

In the left heart, structural differences are largely removed when scaled for BSA but SA have higher RWT and LV mass index even after scaling. LV systolic function is normal irrespective of age, however, SA have slightly lower longitudinal SRS and early diastolic functional indices. Regional heterogeneity of LV ϵ and SR was also observed between senior and junior athletes and may reflect differences in normal physiological training adaptation with training longevity.

In the right heart, many structural differences remain after scaling for body size. The RVOT and RA are larger in SA suggesting that the effect of training adaptation in the right heart is largely independent of body size and more susceptible to remodelling in response to chronic training than the left heart. In terms of PCS and differential diagnosis, RV function is normal irrespective of age. The use of STE has provided further functional information regarding RV cardiac mechanics and the relationship to athlete age. SA have a normal but slightly lower RV longitudinal ϵ , related mainly to the apical segment, as well as lower SRS and SRE which is likely due to a chronic training response.

As cardiac differences between age groups cannot be solely accounted for by body size alone, the evidence from this thesis suggests that diagnostic accuracy of PCS could be improved if echocardiography guidelines were developed according to athlete age. STE provides further corroborative imaging in these groups and has revealed mechanical changes likely reflecting adaptation in response to training longevity. The normative, holistic cardiac parameters for age group athletes presented in this thesis could contribute to PCS echocardiography guidelines in the future.

8.3.3 *The Impact of Seasonal Variation*

The majority of PCS is performed during pre-season in RFL athletes, however, PCS can occur at any time throughout the season, especially when athletes move between clubs. Standard 2D echocardiographic assessment of the elite RFL athlete does not appear to be affected by seasonal variation in training load in senior athletes which is reassuring for PCS. The utilisation of STE has identified significant LV functional changes across the season which may be related to changes in training load and would have been missed by serial 2D echocardiography alone. The benefits of this additional data are two-fold; 1) STE provides further insight into potential mechanisms of cardiac adaptation in the RFL athlete; and 2) STE provides another potentially corroborative parameter for diagnostic differentiation during PCS.

In chapter 4 RFL athletes were found to have lower apical rotation and twist compared to controls and further information about these parameters in RFL athletes in relation to training were revealed in chapter 7. The increase in apical rotation and twist in pre-season suggests a response to acute exercise training as this came after a short period of deconditioning. Increases in the same rotational parameters have been previously found, following a short duration longitudinal study in rowers (Weiner *et al.*, 2010). Following pre-season, a regression of these parameters followed throughout the remainder of the RFL season which may be reflective of an adaptive response to a chronic exercise training load, perhaps by increasing the twist reserve capacity. Both acute and chronic changes in twist would suggest that it is one of the most sensitive parameters to athletic adaptation in RFL athletes. These results also imply that even in chronically trained athletes, with years of training history, both acute and chronic seasonal adaptation still occurs at a mechanical level. The acute and chronic twist response observed in RFL athletes is similar to that reported in rowers were the authors

referred to the changes as a ‘phasic phenomenon’ (Weiner *et al.*, 2015). A schematic representing the changes in twist in the RFL athlete is presented in figure 8.1 combining the results of findings from the cross sectional study (chapter 4) and the longitudinal study (chapter 7). The measurement of STE and twist allows another potential discriminatory measure for differential diagnosis during PCS.

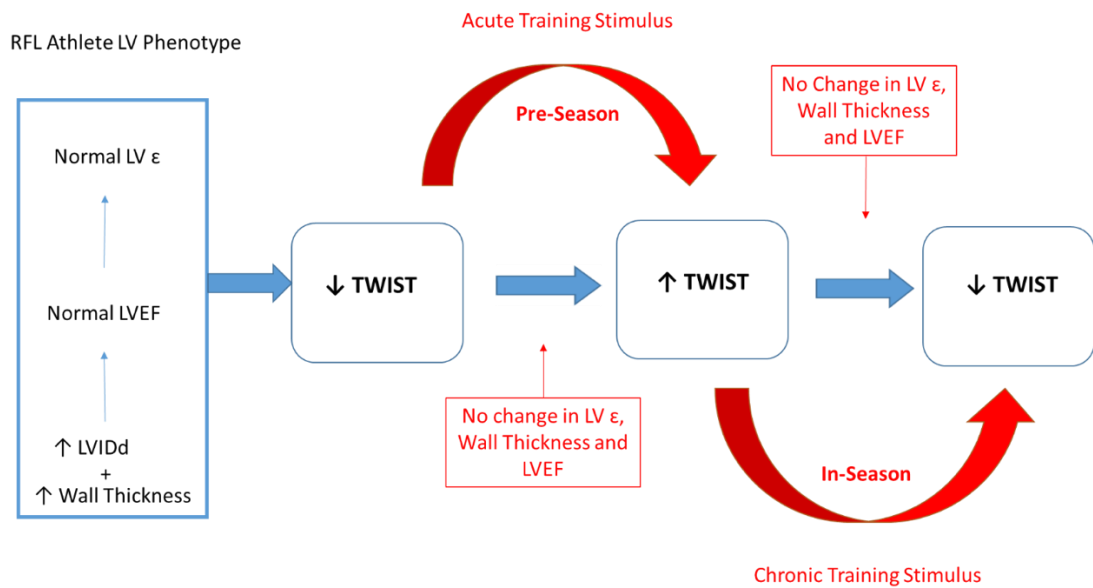


Figure 8.1 Twist in the RFL athlete in response to training stimulus

8.4 Future Research

This thesis focussed solely on RFL athletes but similar comprehensive echocardiographic studies should be performed in athletes of other sporting disciplines to generate population specific normative data which will provide valuable information for PCS. As well as sporting discipline it is known that other factors are involved in cardiac adaptation and athlete gender and ethnicity should also be considered.

In-exercise echocardiography may help to decide whether or not physiological changes observed in SR and twist represent a true contractile reserve. As twist appears to be an important factor in cardiac adaptation in RFL athletes it would be appropriate for further research to explore twist and untwist parameters in athletes and cardiomyopathy patients to determine potential benefits of this parameter in PCS.

8.5 Conclusions

The use of standard and novel echocardiographic techniques produced further understanding of the normal physiological adaptation of the AH in RFL athletes which may lead to improvements in PCS of this athlete group. Biventricular function is normal in the RFL athlete irrespective of age or seasonal time point and there is a predominance for normal LV geometry. The right heart is more sensitive to chronic training than the left with increased RV size in a large percentage of RFL athletes creating an overlap with structural ARVC criteria. A thorough functional assessment including STE however, suggests normal functional parameters and a process of physiological remodelling in these athletes.

The normative echocardiographic parameters presented in this thesis are likely to improve the efficacy of echocardiography in PCS of RFL athletes and the use of STE in addition to standard echocardiography has allowed for the establishment of a comprehensive echocardiographic dataset. STE used together with standard structural and functional echocardiographic parameters may aid in the differentiation of AH from HCM, DCM and ARVC. STE has the potential to detect cardiac dysfunction at an early stage and to corroborate conventional findings, increasing the sensitivity and specificity of the technique.

References

- Abergel, E., Chatellier, G., Hagege, A. A., Oblak, A., Linhart, A., Ducardonnet, A. and Menard, J. 2004. Serial left ventricular adaptations in world-class professional cyclists: Implications for disease screening and follow-up. *Journal of the American College of Cardiology*, 44, 144–149.
- Abraham, T.P., Dimaano, V.L. and Liang, H.Y. 2007. Role of tissue Doppler and strain echocardiography in current clinical practice. *Circulation*, 116, 2597–2609.
- Ammar, K. A., Paterick, T. E., Khandheria, B. K., Jan, M. F., Kramer, C., Umland, M. M., Tercius, A. J., Baratta, L. and Tajik, A. J. 2012. Myocardial mechanics: Understanding and applying three-dimensional speckle tracking echocardiography in clinical practice. *Echocardiography*, 29, 861–872.
- Amundsen, B.H., Helle-Valle, T., Edvardsen, T., Torp, H., Crosby, J., Lyseggen, E., Stoylen, A., Ihlen, H., Lima, J.A., Smiseth, O.A. and Slordahl, S.A. 2006. Noninvasive myocardial strain measurement by speckle tracking echocardiography: Validation against sonomicrometry and tagged magnetic resonance imaging. *Journal of the American College of Cardiology*, 47, 789–793.
- Andersen, N. H., Terkelsen, C. J., Sloth, E. and Poulsen, S. H. 2004. Influence of preload alterations on parameters of systolic left ventricular long-axis function: A doppler tissue study, *Journal of the American Society of Echocardiography*, 17, 941–947.
- Anderson, J. B., Grenier, M., Edwards, N. M., Madsen, N. L., Czosek, R. J., Spar, D. S., Barnes, A., Pratt, J., King, E. and Knilans, T. K. 2014. Usefulness of combined history, physical examination, electrocardiogram, and limited echocardiogram in screening adolescent athletes for risk for sudden cardiac death', *American Journal of Cardiology*, 114, 1763–1767.
- Arbab-Zadeh, A., Perhonen, M., Howden, E., Peshock, R. M., Zhang, R., Adams-Huet, B., Haykowsky, M. J. and Levine, B. D. 2014. Cardiac remodeling in response to 1 year of intensive endurance training. *Circulation*, 130, 2152–2161.
- Ashikaga, H., van der Spoel, T. I. G., Coppola, B. A. and Omens, J. H. 2009. Transmural Myocardial Mechanics During Isovolumic Contraction. *JACC: Cardiovascular Imaging*, 2, 202–211.
- Baggish, A. L., Wang, F., Weiner, R. B., Elinoff, J. M., Tournoux, F., Boland, A., Picard, M. H., Hutter Jr., A. M. and Wood, M. J. 2008a. Training-specific changes in cardiac structure and function: a prospective and longitudinal assessment of competitive athletes. *Journal of Applied Physiology*, 104, 1121–1128.
- Baggish, A. L., Yared, K., Wang, F., Weiner, R. B., Jr, A. M. H., Picard, M. H. and Wood, M. J. 2008b. The impact of endurance exercise training on left ventricular systolic mechanics. *American Journal of Physiology - Heart and Circulatory Physiology*, 295, H1109–H1116.

- Baggish, A. L., Yared, K., Weiner, R. B., Wang, F., Demes, R., Picard, M. H., Hagerman, F. and Wood, M. J. 2010. Differences in cardiac parameters among elite rowers and subelite rowers. *Medicine and Science in Sports and Exercise*, 42, 1215–1220.
- Baggish, A. L. and Wood, M. J. 2011. Athlete's heart and cardiovascular care of the athlete: Scientific and clinical update. *Circulation*, 123, 2723–2735.
- Banks, L., Sasson, Z., Busato, M. and Goodman, J. M. 2010. Impaired left and right ventricular function following prolonged exercise in young athletes : influence of exercise intensity and responses to dobutamine stress. *Journal of Applied Physiology*, 108, 112–119.
- Basavarajaiah, S., Wilson, M., Whyte, G., Shah, A., McKenna, W. and Sharma, S. 2008. Prevalence of Hypertrophic Cardiomyopathy in Highly Trained Athletes. Relevance to Pre-Participation Screening. *Journal of the American College of Cardiology*, 51, 1033–1039.
- Basso, C., Corrado, D., Marcus, F. I., Nava, A. and Thiene, G. 2009. Arrhythmogenic right ventricular cardiomyopathy', *The Lancet*, 373, 1289–1300.
- Basso, C., Maron, B. J., Corrado, D. and Thiene, G. 2000. Clinical profile of congenital coronary artery anomalies with origin from the wrong aortic sinus leading to sudden death in young competitive athletes. *Journal of the American College of Cardiology*, 35, 1493–1501.
- Batterham, A. M., George, K. P., Whyte, G., Sharma, S. and McKenna, W. 1999. Scaling cardiac structural data by body dimensions: a review of theory, practice, and problems. *International journal of sports medicine*, 20, 495–502.
- Batterham, A., Shave, R., Oxborough, D., Whyte, G. and George, K. 2008. Longitudinal plane colour tissue-Doppler myocardial velocities and their association with left ventricular length, volume, and mass in humans. *European Journal of Echocardiography*, 9, 542–546.
- Bauce, B., Frigo, G., Benini, G., Michieli, P., Basso, C., Folino, A.F., Rigato, I., Mazzotti, E., Daliento, L., Thiene, G., Nava, A. 2010. Differences and similarities between arrhythmogenic right ventricular cardiomyopathy and athlete's heart adaptations. *British Journal of Sports Medicine*, 44, 148-154.
- Beaumont, A., Grace, F., Richards, J., Hough, J., Oxborough, D. and Sculthorpe, N. 2017. Left Ventricular Speckle Tracking-Derived Cardiac Strain and Cardiac Twist Mechanics in Athletes: A Systematic Review and Meta-Analysis of Controlled Studies. *Sports Medicine*, 47, 1145-1170.
- Behar, V., Adam, D., Lysyansky, P., Friedman, Z. 2004. The combined effect of nonlinear filtration and window size on the accuracy of tissue displacement estimation using detected echo signals. *Ultrasonics*, 41, 743-753.
- Biering-Sørensen, T., Biering-Sørensen, S. R., Olsen, F. J., Sengeløv, M., Jørgensen, P. G., Mogelvang, R., Shah, A. M. and Jensen, J. S. 2017. Global Longitudinal Strain by Echocardiography Predicts Long-Term Risk of Cardiovascular Morbidity and Mortality in a Low-Risk General Population: The Copenhagen City Heart Study. *Circulation: Cardiovascular Imaging*, doi: 10.1161/CIRCIMAGING.116.005521.

- Borg, G.A.V. 1982. Psychophysical bases of perceived exertion', *Medicine and Science in Sports and Exercise*, 14, 377-381.
- Brown, B., Somauroo, J., Green, D. J., Wilson, M., Drezner, J., George, K. and Oxborough, D. 2017). The complex phenotype of the Athlete's heart: Implications for preparticipation screening. *Exercise and Sport Sciences Reviews*, 45, 96–104.
- Buckberg, G. and Hoffman, J. I. E. 2014. Right ventricular architecture responsible for mechanical performance: Unifying role of ventricular septum. *Journal of Thoracic and Cardiovascular Surgery*, 148, 3166–3171.
- Buckberg, G., Mahajan, A., Saleh, S., Hoffman, J. I. E. and Coghlan, C. 2008. Structure and function relationships of the helical ventricular myocardial band. *Journal of Thoracic and Cardiovascular Surgery*, 136, 578-589.
- Burns, A. T., La Gerche, A., D'hooge, J., Macisaac, A. I. and Prior, D. L. 2010a. Left ventricular strain and strain rate: Characterization of the effect of load in human subjects', *European Journal of Echocardiography*, 11, 283–289.
- Burns, A. T., Gerche, A. La, Prior, D. L. and MacIsaac, A. I. 2010b. Left ventricular torsion parameters are affected by acute changes in load. *Echocardiography*, 27, 407–414.
- Butz, T., Van Buuren, F., Mellwig, K. P., Langer, C., Plehn, G., Meissner, A., Trappe, H. J., Horstkotte, D. and Faber, L. 2011. Two-dimensional strain analysis of the global and regional myocardial function for the differentiation of pathologic and physiologic left ventricular hypertrophy: A study in athletes and in patients with hypertrophic cardiomyopathy', *International Journal of Cardiovascular Imaging*, 27, 91–100.
- Caballero, L., Kou, S., Dulgheru, R., Gonjilashvili, N., Athanassopoulos, G. D., Barone, D., Baroni, M., Cardim, N., De Diego, J. J. G., Oliva, M. J., Hagendorff, A., Hristova, K., Lopez, T., Magne, J., Martinez, C., De La Morena, G., Popescu, B. A., Penicka, M., Ozyigit, T., Carbonero, J. D. R., Salustri, A., Van De Veire, N., Von Bardeleben, R. S., Vinereanu, D., Voigt, J. U., Zamorano, J. L., Bernard, A., Donal, E., Lang, R. M., Badano, L. P. and Lancellotti, P. 2015. Echocardiographic reference ranges for normal cardiac Doppler data: Results from the NORRE Study. *European Heart Journal Cardiovascular Imaging*, 16, 1031–1041.
- Cabanelas, N., Freitas, S. and Goncalves, S. 2013. Morphological and functional changes in athlete's heart during the competitive season. *Revista Portuguesa de Cardiologia*, 32, 291-296.
- Cain, P. A., Ahl, R., Hedstrom, E., Ugander, M., Allansdotter-Johnsson, A., Friberg, P., Marild, S. and Arheden, H. 2007. Physiological determinants of the variation in left ventricular mass from early adolescence to late adulthood in healthy subjects. *Clinical Physiology and Functional Imaging*, 27, 254–262.
- Calvo, N., Brugada, J., Sitges, M. and Mont, L. 2012. Atrial fibrillation and atrial flutter in athletes', *British Journal of Sports Medicine*, 46, i37–i43.
- Cappelli, F., Toncelli, L., Cappelli, B., De Luca, A., Stefani, L., Maffulli, N. and Galanti, G. 2010. Adaptive or maladaptive hypertrophy, different spatial

distribution of myocardial contraction. *Clinical Physiology and Functional Imaging*, 30, 6-12.

- Caselli, S., Montesanti, D., Autore, C., Di Paolo, F. M., Pisicchio, C., Squeo, M. R., Musumeci, B., Spataro, A., Pandian, N. G. and Pelliccia, A. 2015. Patterns of left ventricular longitudinal strain and strain rate in olympic athletes. *Journal of the American Society of Echocardiography*, 28, 245–253.
- Chandra, N., Bastiaenen, R., Papadakis, M. and Sharma, S. 2013. Sudden cardiac death in young athletes: Practical challenges and diagnostic dilemmas. *Journal of the American College of Cardiology*, 61, 1027–1040.
- Cho, E. J., Jiamsripong, P., Calleja, A. M., Alharthi, M. S., McMahon, E. M., Khandheria, B. K. and Belohlavek, M. 2009. Right ventricular free wall circumferential strain reflects graded elevation in acute right ventricular afterload. *American journal of physiology-Heart and circulatory physiology*, 296, H413-20.
- Claessens, P. J. M., Claessens, C. W. F., Claessens, M. M. M., Claessens, M. C. F. and Claessens, J. E. J. 2001. Supernormal left ventricular diastolic function in triathletes. *Texas Heart Institute journal*, 28, 102–10.
- Corrado, D., Basso, C., Thiene, G., McKenna, W.J., Davies, M.J., Fontaliran, F., Nava, A., Silvestri, F., Blomstrom-Lundqvist, C., Wlodarska, E.K., Fontaine, G. and Camerini, F. 1997. Spectrum of clinicopathologic manifestations of arrhythmogenic right ventricular cardiomyopathy/dysplasia: a multicenter study. *Journal of the American College of Cardiology*, 30, 1512-1520.
- Corrado, D., Basso, C., Rizzoli, G., Schiavon, M. and Thiene, G. 2003. Does Sports Activity Enhance the Risk of Sudden Death in Adolescents and Young Adults?’, *Journal of the American College of Cardiology*, 42, 1959–1963.
- Corrado, D., Pelliccia, A., Bjørnstad, H. H., Vanhees, L., Biffi, A., Borjesson, M., Panhuyzen-Goedkoop, N., Deligiannis, A., Solberg, E., Dugmore, D., Mellwig, K. P., Assanelli, D., Delise, P., Van-Buuren, F., Anastasakis, A., Heidbuchel, H., Hoffmann, E., Fagard, R., Priori, S. G., Basso, C., Arbustini, E., Blomstrom-Lundqvist, C., McKenna, W. J. and Thiene, G. 2005. Cardiovascular pre-participation screening of young competitive athletes for prevention of sudden death: Proposal for a common European protocol - Consensus Statement of the Study Group of Sport Cardiology of the Working Group of Cardiac Rehabilitation and Exercise Physiology and the Working group of myocardial and pericardial diseases of the European Society of Cardiology, *European Heart Journal*, 26, 516–524.
- Corrado, D., Basso, C., Schiavon, M., Pelliccia, A. and Thiene, G. 2008. Pre-Participation Screening of Young Competitive Athletes for Prevention of Sudden Cardiac Death. *Journal of the American College of Cardiology*, 52, 1981–1989.
- Covell, J. W. 2008. Tissue Structure and Ventricular Wall Mechanics. *Circulation*, 118, 699–701.
- Csajági, E., Szauder, I., Major, Z. and Pavlik, G. 2015. Left Ventricular Morphology in Different Periods of the Training Season in Elite Young Swimmers.

Pediatric Exercise Science, 27, 185–191.

- D'Andrea, A., Limongelli, G., Caso, P., Sarubbi, B., Della Pietra, A., Brancaccio, P., Cice, G., Scherillo, M., Limongelli, F. and Calabrò, R. 2002. Association between left ventricular structure and cardiac performance during effort in two morphological forms of athlete's heart', *International Journal of Cardiology*, 86, 177–184.
- D'Andrea, A., Scarafile, R., Riegler, L., Salerno, G., Gravino, R., Cocchia, R., Castaldo, F., Allocca, F., Limongelli, G., Di Salvo, G., Cuomo, S., Pacileo, G., Caso, P., Russo, M. G. and Calabrò, R. 2009. Right atrial size and deformation in patients with dilated cardiomyopathy undergoing cardiac resynchronization therapy. *European Journal of Heart Failure*, 11, 1169–1177.
- D'Andrea, A., Riegler, L., Golia, E., Cocchia, R., Scarafile, R., Salerno, G., Pezzullo, E., Nunziata, L., Citro, R., Cuomo, S., Caso, P., Di Salvo, G., Cittadini, A., Russo, M. G., Calabrò, R. and Bossone, E. 2013. Range of right heart measurements in top-level athletes: The training impact. *International Journal of Cardiology*, 164, 48–57.
- D'Ascenzi, F., Cameli, M., Zacã, V., Lisi, M., Santoro, A., Causarano, A. and Mondillo, S. 2011. Supernormal diastolic function and role of left atrial myocardial deformation analysis by 2D speckle tracking echocardiography in elite soccer players. *Echocardiography*, 28, 320–326.
- D'Ascenzi, F., Cameli, M., Lisi, M., Zacà, V., Natali, B., Malandrino, A., Benincasa, S., Catanese, S., Causarano, A. and Mondillo, S. 2012. Left atrial remodelling in competitive adolescent soccer players. *International Journal of Sports Medicine*, 33, 795–801.
- D'Ascenzi, F., Cameli, M., Padeletti, M., Lisi, M., Zacà, V., Natali, B., Malandrino, A., Alvino, F., Morelli, M., Vassallo, G. M., Meniconi, C., Bonifazi, M., Causarano, A. and Mondillo, S. 2013. Characterization of right atrial function and dimension in top-level athletes: A speckle tracking study. *International Journal of Cardiovascular Imaging*, 29, 87–94.
- D'Ascenzi, F., Pelliccia, A., Natali, B. M., Zaca, V., Cameli, M., Alvino, F., Malandrino, A., Palmitesta, P., Zorzi, A., Corrado, D., Bonifazi, M. and Mondillo, S. 2014. Morphological and functional adaptation of left and right atria induced by training in highly trained female athletes. *Circulation: Cardiovascular Imaging*, 7, 222–229.
- D'Ascenzi, F., Pelliccia, A., Cameli, M., Lisi, M., Natali, B. M., Focardi, M., Giorgi, A., D'Urbano, G., Causarano, A., Bonifazi, M. and Mondillo, S. 2015a. Dynamic changes in left ventricular mass and in fat-free mass in top-level athletes during the competitive season. *European journal of preventive cardiology*, 22, 127–34.
- D'Ascenzi, F., Pelliccia, A., Alvino, F., Solari, M., Loffreno, A., Cameli, M., Focardi, M., Bonifazi, M. and Mondillo, S. 2015b. Effects of training on LV strain in competitive athletes. *Heart*, 22, 1834–1839.
- D'Ascenzi, F., Pelliccia, A., Natali, B. M., Cameli, M., Lisi, M., Focardi, M., Padeletti, M., Palmitesta, P., Corrado, D., Bonifazi, M., Mondillo, S. and Henein, M.

- 2015c. Training-induced dynamic changes in left atrial reservoir, conduit, and active volumes in professional soccer players. *European Journal of Applied Physiology*. 115, 1715–1723.
- D’Ascenzi, F., Caselli, S., Solari, M., Pelliccia, A., Cameli, M., Focardi, M., Padeletti, M., Corrado, D., Bonifazi, M. and Mondillo, S. 2016a. Novel echocardiographic techniques for the evaluation of athletes’ heart: A focus on speckle-tracking echocardiography. *European Journal of Preventive Cardiology*, 23, 437–446.
- D’Ascenzi, F., Pelliccia, A., Corrado, D., Cameli, M., Curci, V., Alvino, F., Natali, B. M., Focardi, M., Bonifazi, M. and Mondillo, S. 2016b. Right ventricular remodelling induced by exercise training in competitive athletes. *European Heart Journal Cardiovascular Imaging*, 17, 301–307.
- D’Ascenzi, F., Solari, M., Anselmi, F., Maffei, S., Focardi, M., Bonifazi, M., Mondillo, S. and Henein, M. 2016c. Atrial chamber remodelling in healthy pre-adolescent athletes engaged in endurance sports: A study with a longitudinal design. The CHILD study. *International Journal of Cardiology*, 223, 325–330.
- D’Ascenzi, F., Pelliccia, A., Solari, M., Piu, P., Loiacono, F., Anselmi, F., Caselli, S., Focardi, M., Bonifazi, M. and Mondillo, S. 2017a. Normative Reference Values of Right Heart in Competitive Athletes: A Systematic Review and Meta-Analysis. *Journal of the American Society of Echocardiography*, 30, 845–858.
- D’Ascenzi, F., Pisicchio, C., Caselli, S., Di Paolo, F. M., Spataro, A. and Pelliccia, A. 2017b. RV Remodeling in Olympic Athletes. *JACC: Cardiovascular Imaging*, 10, 385–393.
- D’Ascenzi, F., Pelliccia, A., Valentini, F., Malandrino, A., Natali, B. M., Barbati, R., Focardi, M., Bonifazi, M. and Mondillo, S. 2017c. Training-induced right ventricular remodelling in pre-adolescent endurance athletes: The athlete’s heart in children. *International Journal of Cardiology*, 236, 270–275.
- D’Hooge, J., Heimdal, A., Jamal F., Kukulski, T., Bijnens, B., Rademakers, F., Hatle, L., Suetens, P. and Sutherland, G.R. 2000. Regional strain and strain rate measurements by cardiac ultrasound: Principles, implementation and limitations. *European Journal of Echocardiography*, 1, 154-170.
- Daniels, S. R., Kimball, T. R., Morrison, J. a, Khoury, P. and Meyer, R. A. 1995. Indexing left ventricular mass to account for differences in body size in children and adolescents without cardiovascular disease. *The American journal of cardiology*, 76, 699–701.
- De Luca, A., Stefani, L., Pedrizzetti, G., Pedri, S. and Galanti, G. 2011. The effect of exercise training on left ventricular function in young elite athletes. *Cardiovascular Ultrasound*, 9, 27.
- Dodge, H. T. and Baxley, W. A. 1969. Left ventricular volume and mass and their significance in heart disease. *The American Journal of Cardiology*, 23, 528–537.
- Donal, E., Rozoy, T., Kervio, G., Schnell, F., Mabo, P. and Carré, F. 2011.

- Comparison of the heart function adaptation in trained and sedentary men after 50 and before 35 years of age. *American Journal of Cardiology*, 108, 1029–1037.
- Doucende, G., Schuster, I., Rupp, T., Startun, A., Dazat, M., Obert, P. and Nottin, S. 2010. Kinetics of left ventricular strains and torsion during incremental exercise in healthy subjects: The key role of torsional mechanics for systolic-diastolic coupling. *Circulation: Cardiovascular Imaging*, 3, 586–594.
- Elliott, P. M., Anastakis, A., Borger, M. A., Borggrefe, M., Cecchi, F., Charron, P., Hagege, A. A., Lafont, A., Limongelli, G., Mahrholdt, H., McKenna, W. J., Mogensen, J., Nihoyannopoulos, P., Nistri, S., Piepe, P. G., Pieske, B., Rapezzi, C., Rutten, F. H., Tillmanns, C., Watkins, H., O'Mahony, C., Zamorano, J. L., Achenbach, S., Baumgartner, H., Bax, J. J., Bueno, H., Dean, V., Deaton, C., Erol, C., Fagard, R., Ferrari, R., Hasdai, D., Hoes, A. W., Kirchhof, P., Knuuti, J., Kolh, P., Lancellotti, P., Linhart, A., Nihoyannopoulos, P., Piepoli, M. F., Ponikowski, P., Sirnes, P. A., Tamargo, J. L., Tendera, M., Torbicki, A., Wijns, W., Windecker, S., Hasdai, D., Ponikowski, P., Achenbach, S., Alfonso, F., Basso, C., Cardim, N. M., Gimeno, J. R., Heymans, S., Holm, P. J., Keren, A., Kirchhof, P., Kolh, P., Lionis, C., Muneretto, C., Priori, S., Salvador, M. J., Wolpert, C. and Zamorano, J. L. 2014. 2014 ESC guidelines on diagnosis and management of hypertrophic cardiomyopathy: The task force for the diagnosis and management of hypertrophic cardiomyopathy of the European Society of Cardiology (ESC). *European Heart Journal*, 35, 2733–2779.
- Esch, B. T. and Warburton, D. E. R. 2009. Left ventricular torsion and recoil: implications for exercise performance and cardiovascular disease. *Journal of applied physiology*, 106, 362–369.
- Esposito, R., Galderisi, M., Schiano-Lomoriello, V., Santoro, A., De Palma, D., Ippolito, R., Muscariello, R., Santoro, C., Guerra, G., Cameli, M., Mondillo, S. and De Simone, G. 2014. Nonsymmetric myocardial contribution to supranormal right ventricular function in the athletes' heart: combined assessment by speckle tracking and real time three-dimensional echocardiography. *Echocardiography*, 31, 996-1004.
- Fagard, R., Aubert, A., Lysens, R., Staessen, J., Vanhees, L. and Amery, A. 1983. Noninvasive assessment of seasonal variations in cardiac structure and function in cyclists. *Circulation*, 67, 896–901.
- Finocchiaro, G., Dhutia, H., D'Silva, A., Malhotra, A., Steriotis, A., Millar, L., Prakash, K., Narain, R., Papadakis, M., Sharma, R. and Sharma, S. 2017. Effect of Sex and Sporting Discipline on LV Adaptation to Exercise. *JACC: Cardiovascular Imaging*, 10, 965-972.
- Finocchiaro, G., Papadakis, M., Robertus, J. L., Dhutia, H., Steriotis, A. K., Tome, M., Mellor, G., Merghani, A., Malhotra, A., Behr, E., Sharma, S. and Sheppard, M. N. 2016. Etiology of Sudden Death in Sports Insights from a United Kingdom Regional Registry. *Journal of the American College of Cardiology*, 67, 2108–2115.
- Florescu, M., Stoicescu, C., Magda, S., Petcu, I., Radu, M., Palombo, C., Cinteza, M.,

- Lichiardopol, R., and Vinereanu, D. 2010. 'Supranormal' cardiac function in athletes related to better arterial and endothelial function. *Echocardiography*, 27, 659-667.
- Forsythe, L., MacIver, D. H., Johnson, C., George, K., Somauroo, J., Papadakis, M., Brown, B., Qasem, M. and Oxborough, D. 2018. The relationship between left ventricular structure and function in the elite rugby football league athlete as determined by conventional echocardiography and myocardial strain imaging. *International Journal of Cardiology*, 261, 211–217.
- Galderisi, M., Lomoriello, V.S., Santoro, A., Esposito, R., Olibet, M., Raia, R., Di Minno, M.N., Guerra, G., Mele, D. and Lombardi, G. 2010. Differences of myocardial systolic deformation and correlates of diastolic function in competitive rowers and young hypertensives: a speckle tracking echocardiography study. *Journal of the American Society of Echocardiography*, 23, 1190-1198.
- Gati, S., Chandra, N., Bennett, R. L., Reed, M., Kervio, G., Panoulas, V. F., Ghani, S., Sheikh, N., Zaidi, A., Wilson, M., Wilson, M., Papadakis, M., Carré, F. and Sharma, S. 2013. Increased left ventricular trabeculation in highly trained athletes: do we need more stringent criteria for the diagnosis of left ventricular non-compaction in athletes?. *Heart (British Cardiac Society)*, 99, 401–8.
- Gemayel, C., Pelliccia, A. and Thompson P.D. 2001. Arrhythmogenic Right Ventricular Cardiomyopathy. *Journal of the American College of Cardiology*, 38, 1773-1781.
- George, K. P., Naylor, L. H., Whyte, G. P., Shave, R. E., Oxborough, D. and Green, D. J. 2010. Diastolic function in healthy humans: Non-invasive assessment and the impact of acute and chronic exercise. *European Journal of Applied Physiology*, 108, 1–14.
- George, K., Sharma, S., Batterham, A., Whyte, G. and McKenna, W. 2001. Allometric analysis of the association between cardiac dimensions and body size variables in 464 junior athletes. *Clinical Science*, 100, 47-54..
- Giraldeau, G., Kobayashi, Y., Finocchiaro, G., Wheeler, M., Perez, M., Kuznetsova, T., Lord, R., George, K. P., Oxborough, D., Schnittger, I., Froelicher, V., Liang, D., Ashley, E. and Haddad, F. 2015. Gender Differences in Ventricular Remodeling and Function in College Athletes, Insights from Lean Body Mass Scaling and Deformation Imaging. *American Journal of Cardiology*, 116, 1610–1616.
- Greenbaum, R.A., Siew, Y.H., Gibson, D.G., Becker, A.E. and Anderson, R.H. 1981. Left Ventricular fibre architecture in man. *British Heart Journal*, 45, 248-263.
- Harmon, K. G., Drezner, J. A., Wilson, M. G. and Sharma, S. 2014. Incidence of Sudden Cardiac Death in Athletes. *Heart*, 100,1227-1234.
- Harmon, K. G., Zigman, M. and Drezner, J. A. 2015. The effectiveness of screening history, physical exam, and ECG to detect potentially lethal cardiac disorders in athletes: A systematic review/meta-analysis. *Journal of Electrocardiology*, 48, 329–338.
- Harris, P. A., Taylor, R., Thielke, R., Payne, J., Gonzalez, N. and Conde, J. G. 2009.

- Research electronic data capture (REDCap)-A metadata-driven methodology and workflow process for providing translational research informatics support. *Journal of Biomedical Informatics*, 42, 377–381.
- Haykowsky, M. J., Quinney, H. A., Gillis, R. and Thompson, C. R. 2000a. Left ventricular morphology in junior and master resistance trained athletes. *Medicine and science in sports and exercise*, 32, 349–52.
- Haykowsky, M., Humen, D., Teo, K., Quinney, A., Souster, M., Bell, G. and Taylor, D. 2000b. Effects of 16 weeks of resistance training on left ventricular morphology and systolic function in healthy men >60 years of age. *American Journal of Cardiology*, 85, 1002–1006.
- Hawkowsky, M., Taylor, D., Teo, K., Quinney, A. and Humen, D. 2001. Left ventricular wall stress during leg-press exercise performed with a brief valsalva maneuver. *Chest*, 119, 150-154.
- Heimdal, A., Stoylen, A., Torp, H., Skjaerpe T. 1998. Real time strain rate imaging of the left ventricle by ultrasound. *Journal of the American Society of Echocardiography*, 11, 1013-1019.
- Hein, I. A. and O'Brien, W. D. 1993. Current Time-Domain Methods for Assessing Tissue Motion by Analysis from Reflected Ultrasound Echoes - A Review. *IEEE Transactions on Ultrasonics, Ferroelectrics, and Frequency Control*, 40, 84–102.
- Helle-Valle, T., Crosby, J., Edvardsen, T., Lyseggen, E., Amundsen, B.H., Smith, H.J., Rosen, B.D., Lima, J.A., Torp, H., Ihlen, H. and Smiseth, O.A. 2005. New noninvasive method for assessment of left ventricular rotation: speckle tracking echocardiography. *Circulation*, 112, 3149-3156.
- Ho, S. Y. and Nihoyannopoulos, P. 2006. Anatomy, echocardiography, and normal right ventricular dimensions', *Heart*, 92, supplement 1, 2–14.
- Johnson, C., Forsythe, L., Somauroo, J., Papadakis, M., George, K. and Oxborough, D. 2018. Cardiac structure and function in elite Native Hawaiian and Pacific Islander Rugby Football League athletes: an exploratory study. *International Journal of Cardiovascular Imaging*, 34, 725-534.
- Kaku, K., Takeuchi, M., Tsang, W., Takigiku, K., Yasukochi, S., Patel, A. R., Mor-Avi, V., Lang, R. M. and Otsuji, Y. 2014. Age-related normal range of left ventricular strain and torsion using three-dimensional speckle-tracking echocardiography. *Journal of the American Society of Echocardiography*, 27, 55–64.
- Kansal, M. M., Lester, S. J., Surapaneni, P., Sengupta, P. P., Appleton, C. P., Ommen, S. R., Ressler, S. W. and Hurst, R. T. 2011. Usefulness of two-dimensional and speckle tracking echocardiography in “gray zone” left ventricular hypertrophy to differentiate professional football player’s heart from hypertrophic cardiomyopathy. *American Journal of Cardiology*, 108, 1322–1326.
- Khoo, N. S., Smallhorn, J. F., Kaneko, S., Myers, K., Kutty, S. and Tham, E. B. 2011. Novel insights into RV adaptation and function in hypoplastic left heart syndrome between the first 2 stages of surgical palliation. *JACC: Cardiovascular Imaging*, 4, 128–137.

- King, G., Almontaser, I., Murphy, R. T., La Gerche, A., Mahoney, N., Bennet, K., Clarke, J. and Brown, A. 2013. Reduced right ventricular myocardial strain in the elite athlete may not be a consequence of myocardial damage. “cream masquerades as skimmed milk”. *Echocardiography*, 30, 929–935.
- Kinoshita, N., Onishi, S., Yamamoto, S., Yamada, K., Oguma, Y., Katsukawa, F. and Yamazaki, H. 2003. Unusual left ventricular dilatation without functional or biochemical impairment in normotensive extremely overweight Japanese professional sumo wrestlers. *American Journal of Cardiology*, 91, 699–703.
- Kocica, M.J., Corno, A.F., Carreras-Costa, F., Ballester-Rodes, M., Moghbel, M.C., Cueva, C.N., Lackovic, V., Kanjuh, V.I. and Torrent-Guas, F. 2006. The helical ventricular myocardial band: global, three-dimensional, functional architecture of the ventricular myocardium. *European Journal of Cardiothoracic Surgery*, 29, Supplement 1, S21-S40.
- Korinek, J., Kjaergaard, J., Sengupta, P. P., Yoshifuku, S., McMahon, E. M., Cha, S. S., Khandheria, B. K. and Belohlavek, M. 2007. High Spatial Resolution Speckle Tracking Improves Accuracy of 2-Dimensional Strain Measurements: An Update on a New Method in Functional Echocardiography. *Journal of the American Society of Echocardiography*, 20, 165–170.
- Korinek, J., Wang, J., Sengupta, P. P., Miyazaki, C., Kjaergaard, J., McMahon, E., Abraham, T. P. and Belohlavek, M. 2005. Two-dimensional strain-A Doppler-independent ultrasound method for quantitation of regional deformation: Validation in vitro and in vivo. *Journal of the American Society of Echocardiography*, 18, 1247–1253.
- Kovacs, A., Apor, A., Nagy, A., Vago, H., Toth, A., Kovats, T., Sax, B., Szeplaki, B., Becker, D. and Merkely, B. 2014. Left Ventricular Untwisting in Athlete 's Heart : Key Role in Early Diastolic Filling ? *International Journal of Sports Medicine*, 35, 259–264.
- La Gerche, A., Heidbüchel, H., Burns, A. T., Mooney, D. J., Taylor, A. J., Pflugler, H. B., Inder, W. J., MacIsaac, A. I. and Prior, D. L. 2011. Disproportionate exercise load and remodeling of the athlete's right ventricle. *Medicine and Science in Sports and Exercise*, 43, 974–981.
- La Gerche, A., Burns, A. T., D'Hooge, J., MacIsaac, A. I., Heidbüchel, H. and Prior, D. L. 2012. Exercise strain rate imaging demonstrates normal right ventricular contractile reserve and clarifies ambiguous resting measures in endurance athletes. *Journal of the American Society of Echocardiography*, 25, 253–262.
- La Gerche, A., Baggish, A. L., Knuuti, J., Prior, D. L., Sharma, S., Heidbüchel, H. and Thompson, P. D. 2013. Cardiac imaging and stress testing asymptomatic athletes to identify those at risk of sudden cardiac death', *JACC: Cardiovascular Imaging*, 6, 993–1007.
- La Gerche, A. and Schmied, C. M. 2013. Atrial fibrillation in athletes and the interplay between exercise and health. *European Heart Journal*, 34, 3599–3602.
- Lang, R. M., Badano, L. P., Mor-Avi, V., Afilalo, J., Armstrong, A., Ernande, L., Flachskampf, F. a., Foster, E., Goldstein, S. a., Kuznetsova, T., Lancellotti, P., Muraru, D., Picard, M. H., Rietzschel, E. R., Rudski, L., Spencer, K. T., Tsang,

- W. and Voigt, J.-U. 2015. Recommendations for Cardiac Chamber Quantification by Echocardiography in Adults: An Update from the American Society of Echocardiography and the European Association of Cardiovascular Imaging', *Journal of the American Society of Echocardiography*, 28, 1–39.
- Lavie, C. J., Patel, D. A., Milani, R. V., Ventura, H. O., Shah, S. and Gilliland, Y. 2014. Impact of Echocardiographic Left Ventricular Geometry on Clinical Prognosis. *Progress in Cardiovascular Diseases*, 57, 3–9.
- Lavie, C. J. and Harmon, K. G. 2016. Routine ECG Screening of Young Athletes: Can This Strategy Ever Be Cost Effective? *Journal of the American College of Cardiology*, 68, 712–714.
- Leitman, M., Lysyansky, P., Sidenko, S., Shir, V., Peleg, E., Binenbaum, M., Kaluski, E., Krakover, R., Vered, Z. 2004. Two-dimensional strain - a novel software for real-time quantitative echocardiographic assessment of myocardial function. *Journal of the American Society of Echocardiography*, 17, 1021-1029.
- Levine, B. D., Baggish, A. L., Kovacs, R. J., Link, M. S., Maron, M. S. and Mitchell, J. H. 2015. Eligibility and Disqualification Recommendations for Competitive Athletes with Cardiovascular Abnormalities: Task Force 1: Classification of Sports: Dynamic, Static, and Impact: A Scientific Statement from the American Heart Association and American College of Cardiology. *Journal of the American College of Cardiology*, 66, 2350–2355.
- Levy, P. T., Sanchez Mejia, A. A., Machefsky, A., Fowler, S., Holland, M. R. and Singh, G. K. 2014. Normal ranges of right ventricular systolic and diastolic strain measures in children: A systematic review and meta-analysis', *Journal of the American Society of Echocardiography*, 27, 549–560
- MacIver, D. H. and Townsend, M. 2008. A novel mechanism of heart failure with normal ejection fraction. *Heart*, 94, 446–449.
- MacIver, D. H. 2011. A new method for quantification of left ventricular systolic function using a corrected ejection fraction. *European Journal of Echocardiography*, 12, 228–234.
- MacIver, D. H. and Dayer, M. J. 2012. An alternative approach to understanding the pathophysiological mechanisms of chronic heart failure. *International Journal of Cardiology*, 154, 102–110.
- Maciver, D. H., Adeniran, I. and Zhang, H. 2015. Left ventricular ejection fraction is determined by both global myocardial strain and wall thickness. *International Journal of Cardiology. Heart and Vasculature*, 7, 113–8.
- MacIver, D. H. and Clark, A. L. 2016. Contractile Dysfunction in Sarcomeric Hypertrophic Cardiomyopathy. *Journal of Cardiac Failure*, 22, 31–737.
- Makan, J., Sharma, S., Firoozi, S., Whyte, G., Jackson, P. G. and McKenna, W. J. 2005. Physiological upper limits of ventricular cavity size in highly trained adolescent athletes. *Heart (British Cardiac Society)*, 91, 495–9.
- Marcus, F. I., McKenna, W. J., Sherrill, D., Basso, C., Bauce, B., Bluemke, D. A., Calkins, H., Corrado, D., Cox, M. G. P. J., Daubert, J. P., Fontaine, G., Gear,

- K., Hauer, R., Nava, A., Picard, M. H., Protonotarios, N., Saffitz, J. E., Yoerger Sanborn, D. M., Steinberg, J. S., Tandri, H., Thiene, G., Towbin, J. A., Tsatsopoulou, A., Wichter, T. and Zareba, W. 2010. Diagnosis of arrhythmogenic right ventricular cardiomyopathy/Dysplasia: Proposed modification of the task force criteria. *Circulation*, 121, 1533–1541.
- Marijon, E., Tafflet, M., Celermajer, D. S., Dumas, F., Perier, M. C., Mustafic, H., Toussaint, J. F., Desnos, M., Rieu, M., Benameur, N., Le Heuzey, J. Y., Empana, J. P. and Jouven, X. 2011. Sports-related sudden death in the general population. *Circulation*, 124, 672–681.
- Maron, B.J., Gardin, J.M., Flack, J.M., Gidding, S.S., Kurosaki, T.T. and Bild D.E. 1995. Prevalence of hypertrophic cardiomyopathy in a general population of young adults: Echocardiographic analysis of 4111 subjects in the CARDIA study. *Circulation*, 92, 785–789.
- Maron, B. J. 2002. Hypertrophic cardiomyopathy. *Circulation*, 106, 2419–2421.
- Maron, B. J. 2003. Sudden Death in Young Athletes'. *New England Journal of Medicine*, 349, 1064–1075.
- Maron, B. J. and Pelliccia, A. 2006. The heart of trained athletes: Cardiac remodeling and the risks of sports, including sudden death. *Circulation*, 114, 1633–1644.
- Maron, B. J., Thompson, P. D., Ackerman, M. J., Balady, G., Berger, S., Cohen, D., Dimeff, R., Douglas, P. S., Glover, D. W., Hutter, A. M., Krauss, M. D., Maron, M. S., Mitten, M. J., Roberts, W. O. and Puffer, J. C. 2007. Recommendations and considerations related to preparticipation screening for cardiovascular abnormalities in competitive athletes: 2007 Update: A scientific statement from the American Heart Association council on nutrition, physical activity, and metabolism. *Circulation*, 115, 1643–1655.
- Maron, B. J., Levine, B. D., Washington, R. L., Baggish, A. L., Kovacs, R. J. and Maron, M. S. 2015. Eligibility and Disqualification Recommendations for Competitive Athletes with Cardiovascular Abnormalities: Task Force 2: Preparticipation Screening for Cardiovascular Disease in Competitive Athletes: A Scientific Statement from the American Heart Association. *Journal of the American College of Cardiology*, 66, 2356–2361.
- Marwick, T. H. 2006. Measurement of strain and strain rate by echocardiography: Ready for prime time? *Journal of the American College of Cardiology*, 47, 1313–1327.
- Marwick, T. H., Leano, R. L., Brown, J., Sun, J. P., Hoffmann, R., Lysyansky, P., Becker, M. and Thomas, J. D. 2009. Myocardial Strain Measurement With 2-Dimensional Speckle-Tracking Echocardiography. Definition of Normal Range', *JACC: Cardiovascular Imaging*, 2, 80–84.
- McClellan, G., George, K., Lord, R., Utomi, V., Jones, N., Somauroo, J., Fletcher, S. and Oxborough, D. 2015. Chronic adaptation of atrial structure and function in elite male athletes. *European Heart Journal Cardiovascular Imaging*, 16, 417–422.
- McClellan, G., Riding, N.R., Ardern, C.L., Farooq, A., Pieles, G. E., Watt, V., Adamuz, C., George, K.P., Oxborough, D.L. and Wilson, M.G. 2017. Electrical and

structural adaptations of the paediatric athlete's heart: a systematic review with meta-analysis. *Br J Sports Med*, doi: 10.1136/bjsports-2016-097052.

- Merghani, A., Narain, R. and Sharma, S. 2013. Sudden cardiac death : detecting the warning signs. *Clinical Medicine*, 13, 614–617.
- Mirsky, I. and Parmley, W.W. 1973. Assessment of passive elastic stiffness for isolated heart muscle and the intact heart. *Circulation Research*, 33, 233-243.
- Mitchell, J. H., Haskell, W., Snell, P. and Van Camp, S. P. 2005. Task force 8: Classification of sports. *Journal of the American College of Cardiology*, 45, 1364–1367.
- Modesto, K.M. et al., 2006. Two-dimensional acoustic pattern derived strain parameters closely correlate with one-dimensional tissue Doppler derived strain measurements. *European Journal of Echocardiography*, 7, 315–321.
- Mont, L., Pelliccia, A., Sharma, S., Biffi, A., Borjesson, M., Brugada, J., Carré, F., Guasch, E., Heidbuchel, H., La Gerche, A., Lampert, R., McKenna, W., Papadakis, M., Priori, S. G., Scanavacca, M., Thompson, P., Sticherling, C., Viskin, S., Wilson, M. and Corrado, D. 2017. Pre-participation cardiovascular evaluation for athletic participants to prevent sudden death: Position paper from the EHRA and the EACPR, Q2 Q3 branches of the ESC. Endorsed by APHRS, HRS, and SOLAECE. *Europace*, 19, 139-163.
- Mor-Avi, V., Lang, R. M., Badano, L. P., Belohlavek, M., Cardim, N. M., Derumeaux, G., Galderisi, M., Marwick, T., Nagueh, S. F., Sengupta, P. P., Sicari, R., Smiseth, O. a, Smulevitz, B., Takeuchi, M., Thomas, J. D., Vannan, M., Voigt, J.-U. and Zamorano, J. L. 2011. Current and evolving echocardiographic techniques for the quantitative evaluation of cardiac mechanics: ASE/EAE consensus statement on methodology and indications endorsed by the Japanese Society of Echocardiography. *Journal of the American Society of Echocardiography*, 24, 277–313.
- Morganroth, J., Maron, B.J., Henry, W.L. and Epstein, S.E. 1975. Comparative left ventricular dimensions in trained athletes. *Annals of Internal Medicine*, 82, 521-524.
- Mosteller, R.D. 1987. Simplified calculation of body surface area. *New England Journal of Medicine*, 317, p1098.
- Müller, H., Burri, H. and Lerch, R. 2008. Evaluation of right atrial size in patients with atrial arrhythmias: Comparison of 2D versus real time 3D echocardiography. *Echocardiography*, 25, 617–623.
- Nagashima, J., Musha, H., Takada, H. and Murayama, M. 2003. New Upper Limit of Physiologic Cardiac Hypertrophy in Japanese Participants in the 100-km Ultramarathon. *Journal of the American College of Cardiology*, 42, 1617–1623.
- Nagueh, S. F., Smiseth, O. A., Appleton, C. P., Byrd, B. F., Dokainish, H., Edvardsen, T., Flachskampf, F. A., Gillebert, T. C., Klein, A. L., Lancellotti, P., Marino, P., Oh, J. K., Popescu, B. A. and Waggoner, A. D. 2016. Recommendations for the Evaluation of Left Ventricular Diastolic Function by Echocardiography: An Update from the American Society of

- Echocardiography and the European Association of Cardiovascular Imaging. *Journal of the American Society of Echocardiography*, 29, 277–314.
- Nesto, R.W. and Kowalchuk, G.J. 1987. The Ischemic cascade: temporal sequence of hemodynamic, electrocardiographic and symptomatic expressions of ischemia. *American Journal of Cardiology*, 59, 23C-30C.
- Notomi, Y., Lysyansky, P., Setser, R. M., Shiota, T., Popović, Z. B., Martin-Miklovic, M. G., Weaver, J. A., Oryszak, S. J., Greenberg, N. L., White, R. D. and Thomas, J. D. 2005. Measurement of ventricular torsion by two-dimensional ultrasound speckle tracking imaging. *Journal of the American College of Cardiology*, 45, 2034–2041.
- Notomi, Y., Srinath, G., Shiota, T., Martin-Miklovic, M., Beachler, L., Howell, K., Oryszak, S.J., Deserranno, D.G., Freed, A.D., Greenberg, N.L., Younoszai, A. and Thomas, J.D. 2006. Maturation and adaptive modulation of left ventricular torsional biomechanics: Doppler tissue imaging observation from infancy to adulthood. *Circulation*, 113, 2534-2541.
- Nottin, S., Doucende, G., Schuster-Beck, I., Dautat, M. and Obert, P. 2008. Alteration in left ventricular normal and shear strains evaluated by 2D-strain echocardiography in the athlete's heart. *The Journal of Physiology*, 586, 4721–4733.
- Nottin, S., Doucende, G., Schuster, I., Tanguy, S., Dautat, M. and Obert, P. 2009. Alteration in left ventricular strains and torsional mechanics after ultralong duration exercise in athletes. *Circulation: Cardiovascular Imaging*, 2, 323–330.
- O'Keefe, J. H., Lavie, C. J. and Guazzi, M. 2015. Part 1: Potential Dangers of Extreme Endurance Exercise: How Much Is Too Much? Part 2: Screening of School-Age Athletes. *Progress in Cardiovascular Diseases*, 57, 396–405.
- Ogawa, K., Hozumi, T., Sugioka, K., Iwata, S., Otsuka, R., Takagi, Y., Yoshitani, H., Yoshiyama, M. and Yoshikawa, J. 2009. Automated assessment of left atrial function from time-left atrial volume curves using a novel speckle tracking imaging method. *Journal of the American Society of Echocardiography*, 22, 63-69.
- Okada, M., Tanaka, H., Matsumoto, K., Ryo, K., Kawai, H. and Hirata, K.I. 2012. Subclinical myocardial dysfunction in patients with reverse-remodeled dilated cardiomyopathy. *Journal of the American Society of Echocardiography*, 25, 726-732.
- Oktay, A. A., Lavie, C. J., Milani, R. V., Ventura, H. O., Gilliland, Y. E., Shah, S. and Cash, M. E. 2016. Current Perspectives on Left Ventricular Geometry in Systemic Hypertension. *Progress in Cardiovascular Diseases*, 59, 235–246.
- Oxborough, D., Sharma, S., Shave, R., Whyte, G., Birch, K., Artis, N., Batterham, A. M. and George, K. 2012a. The right ventricle of the endurance athlete: The relationship between morphology and deformation. *Journal of the American Society of Echocardiography*, 25, 263–271.
- Oxborough, D., George, K. and Birch, K. M. 2012b. Intraobserver reliability of two-dimensional ultrasound derived strain imaging in the assessment of the left

ventricle, right ventricle, and left atrium of healthy human hearts. *Echocardiography*, 29, 793–802.

- Oxborough, D., Heemels, A., Somauroo, J., McClean, G., Mistry, P., Lord, R., Utomi, V., Jones, N., Thijssen, D., Sharma, S., Osborne, R., Sculthorpe, N. and George, K. 2016. Left and right ventricular longitudinal strain-volume/area relationships in elite athletes. *International Journal of Cardiovascular Imaging*, 32, 199–1211.
- Oxborough, D., Augustine, D., Gati, S., George, K., Harkness, A., Mathew, T., Papadakis, M., Ring, L., Robinson, S., Sandoval, J., Sarwar, R., Sharma, S., Sharma, V., Sheikh, N., Somauroo, J., Stout, M., Willis, J. and Zaidi, A. 2018. A guideline update for the practice of echocardiography in the cardiac screening of sports participants: a joint policy statement from the British Society of Echocardiography and Cardiac Risk in the Young. *Echo research and practice*, 5, G1–G10.
- Pacileo, G., Baldini, L., Limongelli, G., Di Salvo, G., Iacomino, M., Capogrosso, C., Rea, A., D'Andrea, A., Russo, M. G. and Calabrò, R. 2011. Prolonged left ventricular twist in cardiomyopathies: A potential link between systolic and diastolic dysfunction. *European Journal of Echocardiography*, 12, 841–849.
- Pagourelias, E. D., Kouidi, E., Efthimiadis, G. K., Deligiannis, A., Geleris, P. and Vassilikos, V. 2013. Right atrial and ventricular adaptations to training in male caucasian athletes: An echocardiographic study. *Journal of the American Society of Echocardiography*, 26, 1344–1352.
- Papadakis, M., Carre, F., Kervio, G., Rawlins, J., Panoulas, V. F., Chandra, N., Basavarajiah, S., Carby, L., Fonseca, T. and Sharma, S. 2011. The prevalence, distribution, and clinical outcomes of electrocardiographic repolarization patterns in male athletes of African/Afro-Caribbean origin. *European Heart Journal*, 32, 2304–2313.
- Park, S.J., Miyazaki, C., Bruce C.J., Ommen, S., Miller, F.A. and Oh J.K. 2008. Left ventricular torsion by two-dimensional speckle tracking echocardiography in patients with diastolic dysfunction and normal ejection fraction. *Journal of the American Society of Echocardiography*, 21, 1129–1137.
- Pelliccia, A., Maron, B.J., Spataro, A., Proschan, M.A. and Spirito P. 1991. The upper limit of physiological hypertrophy in highly trained elite athletes. *New England Journal of Medicine*, 324, 295–301.
- Pelliccia, A., Culasso, F., Di Paolo, F.M. and Maron, B.J. 1999. Physiologic left ventricular cavity dilatation in elite athletes. *Annals of Internal Medicine*, 130, 23–31.
- Pelliccia, A., Maron, B. J., Di Paolo, F. M., Biffi, A., Quattrini, F. M., Pisicchio, C., Roselli, A., Caselli, S. and Culasso, F. 2005. Prevalence and clinical significance of left atrial remodeling in competitive athletes. *Journal of the American College of Cardiology*, 46, 690–696.
- Pelliccia, A., Maron, M. S. and Maron, B. J. 2012. Assessment of Left Ventricular Hypertrophy in a Trained Athlete: Differential Diagnosis of Physiologic Athlete's Heart From Pathologic Hypertrophy. *Progress in Cardiovascular*

- Pelliccia, A., Caselli, S., Sharma, S., Basso, C., Bax, J. J., Corrado, D., D'Andrea, A., D'Ascenzi, F., Di Paolo, F. M., Edvardsen, T., Gati, S., Galderisi, M., Heidbuchel, H., Nchimi, A., Nieman, K., Papadakis, M., Pisicchio, C., Schmied, C., Popescu, B. A., Habib, G., Grobbee, D. and Lancellotti, P. 2017. European Association of Preventive Cardiology (EAPC) and European Association of Cardiovascular Imaging (EACVI) joint position statement: recommendations for the indication and interpretation of cardiovascular imaging in the evaluation of the athlete's heart, *European Heart Journal*, doi: 10.1093/eurheartj/ehx532.
- Pinto, Y. M., Elliott, P. M., Arbustini, E., Adler, Y., Anastasakis, A., Böhm, M., Duboc, D., Gimeno, J., De Groote, P., Imazio, M., Heymans, S., Klingel, K., Komajda, M., Limongelli, G., Linhart, A., Mogensen, J., Moon, J., Pieper, P. G., Seferovic, P. M., Schueler, S., Zamorano, J. L., Caforio, A. L. P. and Charron, P. 2016. Proposal for a revised definition of dilated cardiomyopathy, hypokinetic non-dilated cardiomyopathy, and its implications for clinical practice: A position statement of the ESC working group on myocardial and pericardial diseases. *European Heart Journal*, 37, 1850–1858.
- Pirat, B., Khoury, D.S., Hartley, C.J., Tiller, L., Rao, L., Schulz, D.G., Nagueh, S.F., Zoghbi, W.A. 2008. A novel feature-tracking echocardiographic method for the quantification of regional myocardial function: Validation in an animal model of ischaemia-re-perfusion. *Journal of the American College of Cardiology*, 51, 651-659.
- Plana, J. C., Galderisi, M., Barac, A., Ewer, M. S., Ky, B., Scherrer-Crosbie, M., Ganame, J., Sebag, I. A., Agler, D. A., Badano, L. P., Banchs, J., Cardinale, D., Carver, J., Cerqueira, M., DeCara, J. M., Edvardsen, T., Flamm, S. D., Force, T., Griffin, B. P., Jerusalem, G., Liu, J. E., Magalhães, A., Marwick, T., Sanchez, L. Y., Sicari, R., Villarraga, H. R. and Lancellotti, P. 2014. Expert consensus for multimodality imaging evaluation of adult patients during and after cancer therapy: A report from the American Society of Echocardiography and the European Association of Cardiovascular Imaging. *European Heart Journal Cardiovascular Imaging*, 15,1063–1093.
- Pluim, B. M., Zwinderman, A. H., van der Laarse, A. and van der Wall, E. E. 2000. The Athlete's Heart: A Meta-Analysis of Cardiac Structure and Function. *Circulation*, 101, 336–344.
- Popović, Z. B., Sun, J. P., Yamada, H., Drinko, J., Mauer, K., Greenberg, N. L., Cheng, Y., Moravec, C. S., Penn, M. S., Mazgalev, T. N. and Thomas, J. D. 2005. Differences in left ventricular long-axis function from mice to humans follow allometric scaling to ventricular size. *The Journal of Physiology*, 568, 255–265.
- Qasem, M., Utomi, V., George, K., Somauroo, J., Zaidi, A., Forsythe, L., Bhattacharyya, S., Lloyd, G., Rana, B., Ring, L., Robinson, S., Senior, R., Sheikh, N., Sitali, M., Sandoval, J., Steeds, R., Stout, M., Willis, J. and Oxborough, D. 2016. A Meta-Analysis for the Echocardiographic Assessment of Right Ventricular Structure and Function in ARVC. *Echo Research and Practice*, 3, 95-104.

- Qasem, M., George, K., Somauroo, J., Forsythe, L., Brown, B. and Oxborough, D. 2018. Influence of different dynamic sporting disciplines on right ventricular Structure and function in elite male athletes. *The International Journal of Cardiovascular Imaging*, doi: 10.1007/s10554-018-1316-2.
- Quiñones, M. a, Otto, C. M., Stoddard, M., Waggoner, A. and Zoghbi, W. A. 2002. Recommendations for quantification of Doppler echocardiography: a report from the Doppler Quantification Task Force of the Nomenclature and Standards Committee of the American Society of Echocardiography. *Journal of the American Society of Echocardiography: official publication of the American Society of Echocardiography*, 15, 167–184.
- Reisner, S.A, Lysyansky, P., Agmon, Y., Mutlak, D., Lessick, J., Friedman Z. 2004. Global longitudinal strain: a novel index of left ventricular systolic function. *Journal of the American Society of Echocardiography*, 17, 630-633.
- Richand, V., Lafitte, S., Reant, P., Serri, K., Lafitte, M., Brette, S., Kerouani, A., Chalabi, H., Dos Santos, P., Douard, H. and Roudaut, R. 2007. An Ultrasound Speckle Tracking (Two-Dimensional Strain) Analysis of Myocardial Deformation in Professional Soccer Players Compared With Healthy Subjects and Hypertrophic Cardiomyopathy. *American Journal of Cardiology*, 100, 128–132.
- Riding, N. R., Sharma, S., Salah, O., Khalil, N., Carré, F., George, K. P., Hamilton, B., Chalabi, H., Whyte, G. P. and Wilson, M. G. 2015. Systematic echocardiography is not efficacious when screening an ethnically diverse cohort of athletes in West Asia. *European Journal of Preventive Cardiology*, 22, 263–270.
- Roca, G.Q., Campbell, P., Claggett, B., Solomon, S. D. and Shah, A. M. 2015. Right Atrial Function in Pulmonary Arterial Hypertension. *Circulation: Cardiovascular Imaging*, doi: 10.1161/CIRCIMAGING.115.003521.
- Rodrigues, J. C. L., Rohan, S., Dastidar, A. G., Trickey, A., Szantho, G., Ratcliffe, L. E. K., Burchell, A. E., Hart, E. C., Bucciarelli-Ducci, C., Hamilton, M. C. K., Nightingale, A. K., Paton, J. F. R., Manghat, N. E. and MacIver, D. H. 2016. The Relationship Between Left Ventricular Wall Thickness, Myocardial Shortening, and Ejection Fraction in Hypertensive Heart Disease: Insights From Cardiac Magnetic Resonance Imaging. *The Journal of Clinical Hypertension*, 18, 1119–1127.
- Rudski, L. G., Lai, W. W., Afilalo, J., Hua, L., Handschumacher, M. D., Chandrasekaran, K., Solomon, S. D., Louie, E. K. and Schiller, N. B. 2010. Guidelines for the Echocardiographic Assessment of the Right Heart in Adults: A Report from the American Society of Echocardiography. *Journal of the American Society of Echocardiography*, 23, 685–713.
- Rushmer, R.F., Crystal, D.K. and Wagner C. 1953. The functional anatomy of ventricular contraction. *Circulation Research*, 1, 162-170.
- Sallin, E.A. 1969. Fiber orientation and ejection fraction in the human left ventricle. *Biophysical Journal*, 9, 954-964.
- Santoro, A., Alvino, F., Antonelli, G., Caputo, M., Padeletti, M., Lisi, M. and

- Mondillo, S. 2014a. Endurance and strength athlete's heart: Analysis of myocardial deformation by speckle tracking echocardiography. *Journal of Cardiovascular Ultrasound*, 22, 196–204.
- Santoro, A., Alvino, F., Antonelli, G., Zacà, V., Benincasa, S., Lunghetti, S. and Mondillo, S. 2014b. Left ventricular twisting modifications in patients with left ventricular concentric hypertrophy at increasing after-load conditions. *Echocardiography*, 31, 1265–1273.
- Santoro, A., Alvino, F., Antonelli, G., Cassano, F. E., De Vito, R., Cameli, M. and Mondillo, S. 2015. Age related diastolic function in amateur athletes. *International Journal of Cardiovascular Imaging*, 31, 567–573.
- Scharhag, J., Schneider, G., Urhausen, A., Rochette, V., Kramann, B. and Kindermann, W. 2002. Athlete's heart: Right and left ventricular mass and function in male endurance athletes and untrained individuals determined by magnetic resonance imaging. *Journal of the American College of Cardiology*, 40, 1856–1863.
- Schmied, C. and Borjesson, M. (2014) 'Sudden cardiac death in athletes. *Journal of Internal Medicine*, 275, 93–103.
- Sengupta, P. P., Khandheria, B. K., Korinek, J., Wang, J., Jahangir, A., Seward, J. B. and Belohlavek, M. 2006b. Apex-to-base dispersion in regional timing of left ventricular shortening and lengthening', *Journal of the American College of Cardiology*, 47, 163–172.
- Sengupta, P. P., Korinek, J., Belohlavek, M., Narula, J., Vannan, M. A., Jahangir, A. and Khandheria, B. K. 2006a. Left Ventricular Structure and Function. Basic Science for Cardiac Imaging. *Journal of the American College of Cardiology*, 48, 1988–2001.
- Sengupta, P. P., Tajik, A. J., Chandrasekaran, K. and Khandheria, B. K. 2008. Twist Mechanics of the Left Ventricle. Principles and Application', *JACC: Cardiovascular Imaging*, 1, 366–376.
- Sharma, S., Whyte, G., Elliott, P., Padula, M., Kaushal, R., Mahon, N. and McKenna, W. J. 1999. Electrocardiographic changes in 1000 highly trained junior elite athletes. *British Journal of Sports Medicine*, 33,319–324.
- Sharma, S., Maron, B. J., Whyte, G., Firoozi, S., Elliott, P. M., McKenna, W. J. 2002. Physiologic limits of left ventricular hypertrophy in elite junior athletes relevance to differential diagnosis of athlete's heart and hypertrophic cardiomyopathy. *Journal of the American College of Cardiology*, 40, 1431-1436.
- Sharma, S. 2003. Physiological Society Symposium – The Athlete's Heart Athlete's heart – effect of age , sex , ethnicity and sporting Experimental Physiology : Regular physical training is associated with several physiological and biochemical adaptations which enable. *Experimental Physiology*, 88, 665–669.
- Sharma, S., Drezner, J. A., Baggish, A., Papadakis, M., Wilson, M. G., Prutkin, J. M., La Gerche, A., Ackerman, M. J., Borjesson, M., Salerno, J. C., Asif, I. M., Owens, D. S., Chung, E. H., Emery, M. S., Froelicher, V. F., Heidbuchel, H., Adamuz, C., Asplund, C. A., Cohen, G., Harmon, K. G., Marek, J. C., Molossi,

- S., Niebauer, J., Pelto, H. F., Perez, M. V., Riding, N. R., Saarel, T., Schmied, C. M., Shipon, D. M., Stein, R., Vetter, V. L., Pelliccia, A. and Corrado, D. 2017. International Recommendations for Electrocardiographic Interpretation in Athletes', *Journal of the American College of Cardiology*, 69, 1057–1075.
- Sheikh, N., Papadakis, M., Carre, F., Kervio, G., Panoulas, V. F., Ghani, S., Zaidi, A., Gati, S., Rawlins, J., Wilson, M. G. and Sharma, S. 2013. Cardiac adaptation to exercise in adolescent athletes of African ethnicity: an emergent elite athletic population. *British journal of sports medicine*, 47, 585–592.
- Sheikh, N., Papadakis, M., Ghani, S., Zaidi, A., Gati, S., Adami, P. E., Carré, F., Schnell, F., Wilson, M., Avila, P., McKenna, W. and Sharma, S. 2014. Comparison of electrocardiographic criteria for the detection of cardiac abnormalities in elite black and white athletes. *Circulation*, 129, 1637–1649.
- Sheikh, N., Papadakis, M., Schnell, F., Panoulas, V., Malhotra, A., Wilson, M., Carré, F. and Sharma, S. 2015. Clinical profile of athletes with hypertrophic cardiomyopathy. *Circulation: Cardiovascular Imaging*, doi: 10.1161/CIRCIMAGING.114.003454.
- Sheppard, M. N. 2012. Aetiology of sudden cardiac death in sport: a histopathologist's perspective. *British Journal of Sports Medicine*, 46 (Supplement 1) i15–i21..
- Simsek, Z., Hakan Tas, M., Degirmenci, H., Gokhan Yazici, A., Ipek, E., Duman, H., Gundogdu, F., Karakelleoglu, S. and Senocak, H. 2013. Speckle tracking echocardiographic analysis of left ventricular systolic and diastolic functions of young elite athletes with eccentric and concentric type of cardiac remodeling. *Echocardiography*, 30, 1202–1208.
- Smiseth, O. A., Torp, H., Opdahl, A., Haugaa, K. H. and Urheim, S. 2016. Myocardial strain imaging: How useful is it in clinical decision making? *European Heart Journal*, 37, 1196–1207b.
- Soullier, C., Obert, P., Doucende, G., Nottin, S., Cade, S., Perez-Martin, A., Messner-Pellenc, P. and Schuster, I. 2012. Exercise response in hypertrophic cardiomyopathy: Blunted left ventricular deformational and twisting reserve with altered systolic-diastolic coupling. *Circulation: Cardiovascular Imaging*, 5, 324–332.
- Spence, A. L., Naylor, L. H., Carter, H. H., Buck, C. L., Dembo, L., Murray, C. P., Watson, P., Oxborough, D., George, K. P. and Green, D. J. 2011. A prospective randomised longitudinal MRI study of left ventricular adaptation to endurance and resistance exercise training in humans. *Journal of Physiology*, 589, 5443–52.
- Spirito, P., Pelliccia, A., Proschan, M. A., Granata, M., Spataro, A., Bellone, P., Caselli, G., Biffi, A., Vecchio, C. and Maron, B. J. 1994. Morphology of the 'athlete's heart' assessed by echocardiography in 947 elite athletes representing 27 sports. *American Journal of Cardiology*, 74, 802–806.
- Stefani, L., Pedrizzetti, G., De Luca, A., Mercuri, R., Innocenti, G. and Galanti, G. 2009. Real-time evaluation of longitudinal peak systolic strain (speckle tracking measurement) in left and right ventricles of athletes. *Cardiovascular Ultrasound*, doi: 10.1186/1476-7120-7-17.

- Stöhr, E. J., McDonnell, B., Thompson, J., Stone, K., Bull, T., Houston, R., Cockcroft, J. and Shave, R. 2012. Left ventricular mechanics in humans with high aerobic fitness: adaptation independent of structural remodelling, arterial haemodynamics and heart rate. *The Journal of physiology*, 590, 2107–2119.
- Stokke, T. M., Hasselberg, N. E., Smedsrud, M. K., Sarvari, S. I., Haugaa, K. H., Smiseth, O. A., Edvardsen, T. and Remme, E. W. 2017. Geometry as a Confounder When Assessing Ventricular Systolic Function: Comparison Between Ejection Fraction and Strain. *Journal of the American College of Cardiology*, 70, 942–954.
- Sutherland, G.R., Di Salvo, G., Claus, P., D'Hooge, J., Bijnens, B. 2004. Strain and strain rate imaging: a new clinical approach to quantifying regional myocardial function. *Journal of the American Society of Echocardiography*, 17, 788-802.
- Szauder, I., Kovács, A. and Pavlik, G. 2015. Comparison of left ventricular mechanics in runners versus bodybuilders using speckle tracking echocardiography', *Cardiovascular Ultrasound*, 13, 1–7.
- Taber, L.A., Yang, M. and Podszus, W.W. 1996. Mechanics of ventricular torsion. *Journal of Biomechanics*, 29, 745-752.
- Teske, A.J., De Boeck, B.W.L., Olimulder, M., Prakken, N.H., Doevendans, P.A. and Cramer, M.J. 2008. Echocardiographic assessment of regional right ventricular function: a head-to-head comparison between 2-dimensional and tissue Doppler-derived strain analysis. *Journal of the American Society of Echocardiography*, 21, 275-283.
- Teske, A. J., Cox, M. G., De Boeck, B. W., Doevendans, P. A., Hauer, R. N. and Cramer, M. J. 2009a Echocardiographic Tissue Deformation Imaging Quantifies Abnormal Regional Right Ventricular Function in Arrhythmogenic Right Ventricular Dysplasia/Cardiomyopathy', *Journal of the American Society of Echocardiography*, 920–927.
- Teske, A. J., Prakken, N. H., De Boeck, B. W., Velthuis, B. K., Martens, E. P., Doevendans, P. A. and Cramer, M. J. 2009b. Echocardiographic tissue deformation imaging of right ventricular systolic function in endurance athletes. *European Heart Journal*, 969–977.
- Tops, L. F., Delgado, V., Marsan, N. A. and Bax, J. J. 2017. Myocardial strain to detect subtle left ventricular systolic dysfunction. *European Journal of Heart Failure*, 19, 307-313.
- Torrent-Guasp, F., Buckberg, G. D., Clemente, C., Cox, J. L., Coghlan, H. C. and Gharib, M. 2001. The structure and function of the helical heart and its buttress wrapping. I. The normal macroscopic structure of the heart', *Seminars in Thoracic and Cardiovascular Surgery*, 13, 301–319.
- Turagam, M. K., Velagapudi, P. and Kocheril, A. G. 2012. Atrial Fibrillation in Athletes. *The American Journal of Cardiology*, 109, 296–302.
- Utomi, V., Oxborough, D., Whyte, G. P., Somauroo, J., Sharma, S., Shave, R., Atkinson, G. and George, K. 2013. Systematic review and meta-analysis of training mode, imaging modality and body size influences on the morphology and function of the male athlete's heart. *Heart (British Cardiac Society)*, 99,

1727–1733.

- Utomi, V., Oxborough, D., Ashley, E., Lord, R., Fletcher, S., Stembridge, M., Shave, R., Hoffman, M. D., Whyte, G., Somauroo, J., Sharma, S. and George, K. 2014. Predominance of normal left ventricular geometry in the male “athlete’s heart’. *Heart (British Cardiac Society)*, 100, 1264–1271.
- Utomi, V., Oxborough, D., Ashley, E., Lord, R., Fletcher, S., Stembridge, M., Shave, R., Hoffman, M. D., Whyte, G., Somauroo, J., Sharma, S. and George, K. 2015. The impact of chronic endurance and resistance training upon the right ventricular phenotype in male athletes. *European Journal of Applied Physiology*, 115, 1673-1682.
- Van Dalen, B. M., Soliman, O. I. I., Vletter, W. B., ten Cate, F. J. and Geleijnse, M. L. 2008. Age-related changes in the biomechanics of left ventricular twist measured by speckle tracking echocardiography. *American Journal of Physiology-Heart and Circulatory Physiology*, 295, H1705–H1711.
- Van Dalen, B. M., Soliman, O. I. I., Vletter, W. B., Kauer, F., Van Der Zwaan, H. B., Ten Cate, F. J. and Geleijnse, M. L. 2009. Feasibility and reproducibility of left ventricular rotation parameters measured by speckle tracking echocardiography. *European Journal of Echocardiography*, 10, 669–676.
- Vitarelli, A., Capotosto, L., Placanica, G., Caranci, F., Pergolini, M., Zardo, F., Martino, F., De Chiara, S. and Vitarelli, M. 2013. Comprehensive assessment of biventricular function and aortic stiffness in athletes with different forms of training by three-dimensional echocardiography and strain imaging. *European Heart Journal Cardiovascular Imaging*, 14, 1010–1020.
- Weiner, R. B., Hutter, A. M., Wang, F., Kim, J., Weyman, A. E., Wood, M. J., Picard, M. H. and Baggish, A. L. 2010. The impact of endurance exercise training on left ventricular torsion. *JACC. Cardiovascular imaging*, 3, 1001–1009.
- Weiner, R. B. and Baggish, A. L. 2012. Exercise-Induced Cardiac Remodeling’, *Progress in Cardiovascular Diseases*, 54, 380–386.
- Weiner, R. B., DeLuca, J. R., Wang, F., Lin, J., Wasfy, M. M., Berkstresser, B., Stöhr, E., Shave, R., Lewis, G. D., Hutter, A. M., Picard, M. H. and Baggish, A. L. 2015. Exercise-Induced Left Ventricular Remodeling Among Competitive Athletes. *Circulation: Cardiovascular Imaging*, 8, p. e003651. doi: 10.1161/CIRCIMAGING.115.003651.
- Whalley, G. A., Doughty, R. N., Gamble, G. D., Oxenham, H. C., Walsh, H. J., Reid, I. R. and Baldi, J. C. 2004. Association of fat-free mass and training status with left ventricular size and mass in endurance-trained athletes. *Journal of the American College of Cardiology*, 44, 892–896.
- Whyte, G. P., George, K., Sharma, S., Firoozi, S., Stephens, N., Senior, R. and McKenna, W. J. 2004. The upper limit of physiological cardiac hypertrophy in elite male and female athletes: the British experience. *European Journal of Applied Physiology*, 92, 592–597.
- Wigle, E.D., Sasson, Z., Henderson, M.A., Ruddy, T.D., Fulop, J., Rakowski, H., Williams, W.G. 1985. Hypertrophic cardiomyopathy: The importance of the site and extent of hypertrophy: a review. *Progress in cardiovascular diseases*,

28, 1-83.

- Wilson, M. G., Chandra, N., Papadakis, M., O'Hanlon, R., Prasad, S. K. and Sharma, S. 2011. Hypertrophic cardiomyopathy and ultra-endurance running - two incompatible entities? *Journal of cardiovascular magnetic resonance : official journal of the Society for Cardiovascular Magnetic Resonance*, 13, 77. doi: 10.1186/1532-429X-13-77.
- Wu, M. T., Tseng, W. Y. I., Su, M. Y. M., Liu, C. P., Chiou, K. R., Wedeen, V. J., Reese, T. G. and Yang, C. F. 2006. Diffusion tensor magnetic resonance imaging mapping the fiber architecture remodeling in human myocardium after infarction: Correlation with viability and wall motion. *Circulation*, 114, 1036–1045.
- Yang, H., Sun, J.P., Lever, H.M., Popovic, Z.B., Drinko, J.K., Greenberg, N.L., Shiota, T., Thomas, J.D. and Garcia, M.J. 2003. Use of strain imaging in detecting segmental dysfunction in patients with hypertrophic cardiomyopathy. *Journal of the American Society of Echocardiography*, 16, 233-239.
- Yip, G., Abraham, T., Belohlavek, M. and Khandheria, B. K. 2003. Clinical Applications of Strain Rate Imaging. *Journal of the American Society of Echocardiography*, 16, 1334–1342.
- Zaidi, A., Ghani, S., Sharma, R., Oxborough, D., Panoulas, V. F., Sheikh, N., Gati, S., Papadakis, M. and Sharma, S. 2013. Physiological right ventricular adaptation in elite athletes of African and Afro-Caribbean origin. *Circulation*, 127, 1783–92.
- Zócalo, Y., Bia, D., Armentano, R. L., Arias, L., Lopez, C., Etchart, C. and Guevara, E. 2007. Assessment of training-dependent changes in the left ventricle torsion dynamics of professional soccer players using speckle tracking echocardiography. *Conference proceedings IEEE engineering in medicine and biology society*, 2007, 2709-2712.
- Zócalo, Y., Guevara, E., Bia, D., Giacche, E., Pessana, F., Peidro, R. and Armentano, R. L. 2008. A reduction in the magnitude and velocity of left ventricular torsion may be associated with increased left ventricular efficiency: evaluation by speckle-tracking echocardiography. *Revista española de cardiología*, 61, 705–13.

Appendix 1

